

Optimización de la producción de microalgas en reactores abiertos de escala industrial

TESIS DOCTORAL

Programa de Doctorado en Biotecnología y Bioprocesos Industriales
Aplicados a la Agroalimentación y Medioambiente

Grupo de Automática, Robótica y Mecatrónica (ARM 197)

Departamento de Informática

Universidad de Almería



AUTOR

Marta Barceló Villalobos

DIRECTORES

Francisco Gabriel Acién Fernández

José Luis Guzmán Sánchez

Enero 2020, Almería

Optimization of microalgae production in industrial open reactors

DOCTORAL THESIS

Doctorate in Biotechnology and industrial bioprocesses applied to agrifood and the environment

Automation, Robotics and Mechatronics Group (ARM 197)

Department of Informatics

University of Almería



AUTHOR

Marta Barceló Villalobos

SUPERVISORS

Francisco Gabriel Acién Fernández

José Luis Guzmán Sánchez

January 2020, Almería (Spain)

Agradecimientos

Esta tesis es el fruto de un gran trabajo en equipo, un equipo de calidad humana extrema que hace que te enganches y te enamores de la ciencia desde el primer día. He tenido y tengo la gran suerte de trabajar con dos de las mejores familias que la Universidad de Almería me podría ofrecer.

Muchísimas gracias a José Luis y a Gabriel por confiar en mí desde el primer día y por hacerme sentir como en casa. Trabajar con vosotros es un privilegio que pocas personas pueden disfrutar. A vuestro lado he aprendido y aprendo cada día muchísimo tanto a nivel personal como profesional. Vuestro trabajo como directores ha sido excelente.

Gracias José Luis Guzmán por recibirme siempre con una sonrisa y por sacar siempre tiempo de dónde no lo hay. Gracias Gabriel Ación por recibirme en tu casa de las microalgas con los brazos abiertos. Gracias por contagiarme ese entusiasmo y esa energía con la que nos hablas siempre. Gracias por cuidarnos tanto. Consigues que seamos una familia de las buenas, de esas con las que puedas contar tanto en los buenos como en los malos momentos.

Gracias a Jiří Masojídek y a todo su equipo (Karolina, Tomás, Gergel y Joao) por recibirme con los brazos abiertos y haber hecho de mi estancia en República Checa un recuerdo inolvidable. Ojalá algún día podamos colaborar de nuevo.

Gracias a Ismael, sin lugar a duda, media tesis es tuya. Sin ti los ensayos de esta tesis no habrían sido posibles. Contigo aprendí lo complicado y duro que puede llegar a ser el trabajo en reactores externos. Muchas gracias por todas las veces que te has preocupado por mí.

Gracias a Alicia y a Lola por cuidarme tanto, como si fuerais mis hermanas mayores.

Gracias a Martina, mi napolitana querida. Gracias por todo el cariño demostrado y por todas las risas fuera y dentro del laboratorio.

Gracias a las chicas verdes: Cintia, Ainoa y Ana. Gracias por toda la ayuda. Por animarme en los momentos más duros y buscarme siempre una segunda lectura a todo lo que me ha ocurrido en estos años.

Gracias a los chicos: Peña y Juanjo por toda la ayuda prestada y los ratitos de risas durante el desayuno. Sois únicos.

Gracias a toda la gente que hemos tenido de estancia a lo largo de estos años, pero muy en especial a mis compañeros de piso: Luis, Mirka, Peter y Martín. Ojalá que algún día nos volvamos a ver.

Gracias a todo el equipo de la Estación Experimental “Las Palmerillas” por haberme tendido la mano siempre que ha hecho falta. Y muy en especial a Paco Bretones y a José Manuel, quienes tantísimas veces me ayudaron.

Gracias a todo el equipo ARM (Automática, Robótica y Mecatrónica) por permitirme implicarme en vuestro mundo, algo tan ajeno para una Licenciada en Ciencias Ambientales como yo.

Gracias a Paco Rodríguez y Jorge Sánchez por su paciencia y ánimos en los momentos más difíciles.

Gracias a mis compañeras de despacho: Ángeles y Wang Hui, por todos los buenos ratos que compartimos en el despacho.

Gracias a mis compañeros de despacho: Jero y Juan Diego por toda la ayuda prestada en todo lo referente a la asignatura de Automatización Industrial.

Gracias a María José, Mati y Jeza. A Almería también tengo que agradecerle el haberme puesto en vuestros caminos. Tres grandes amigas que me llevaré conmigo allá donde vaya.

Gracias a mis *Supernenas*: sois unas amigas incondicionales. A María, Elena, Antonio, Vitty y Almudena, por todo el cariño demostrado durante todos estos años.

Gracias a Daniel Algarra por el diseño gráfico del raceway y del respirómetro.

Y por supuesto, gracias a mi familia y a todos mis seres queridos. Muy en especial a mis padres, quienes me dieron la vida y me han apoyado siempre en todas las decisiones que he tomado.

Acknowledgements

This thesis is the result of great teamwork, a team of extreme human quality that makes you hook and fall in love with science from the first day. I have had and I am very lucky to work with two of the best families that the University of Almeria could offer me.

Many thanks to José Luis and Gabriel for trusting me from the first day and for making me feel as at home. Working with you is a privilege that few people can enjoy. At your side I have learned and learned every day, both personally and professionally. Your work as directors has been excellent.

Thanks to José Luis Guzmán for always receiving me with a smile and for always taking time out of where there is none. Thanks to Gabriel Acién for welcoming me to your microalgae home with open arms. Thank you for transmitting me that enthusiasm and that energy with which you always speak to us. Thanks for taking care of us so much. You get us to be such a good family, one of those you can count on in both the good times and the bad times.

Thanks to Jiří Masojídek and his team (Karolina, Tomás, Gergel and Joao) for welcoming me with open arms and for having made my stay in the Czech Republic an unforgettable memory. Hopefully one day we can collaborate again.

Thanks to Ismael, without a doubt, half thesis is yours. Without you the assays of this thesis would not be possible. With you I learned how complicated and hard the work can be in outdoor reactors. Thank you very much for all the times you have worried about me.

Thanks to Alicia and Lola for taking care of me so much, as if you were my older sisters.

Thanks to Martina, my beloved Neapolitan. Thanks for all the love shown and for all the laughter outside and inside the lab.

Thanks to the green girls: Cintia, Ainoa and Ana. Thanks for all the help. For encouraging me in the hardest moments and always seek a second reading of everything that has happened to me in these years.

Thanks to the guys: Peña and Juanjo for all the help and the little laughs during breakfast. You both are unique.

Thanks to all the people we have had during these years, but especially to my roommates: Luis, Mirka, Peter and Martín. Hopefully one day we will see each other again.

Thanks to all the team of the Experimental Station "Las Palmerillas" for having extended my a hand whenever it was needed. And especially to Paco Bretones and José Manuel, who helped me so many times.

Thanks to all the ARM team (Automatic, Robotics and Mechatronics) for allowing me to get involved in your world, something so strange to a graduate in Environmental Sciences like me.

Thanks to Paco Rodríguez and Jorge Sánchez for their patience and encouragement in the most difficult moments.

Thanks to my colleagues in the office: Ángeles and Wang Hui, for all the good times we shared in the office.

Thanks to my colleagues: Jero and Juan Diego for all the help given in everything related to the subject of Industrial Automation.

Thanks to María José, Mati and Jeza. I also have to thanks to Almeria for having put me in your ways. Three great friends that I will take with me wherever I go.

Thanks to my *Supernenas*: you are my unconditional friends. To María, Elena, Antionio, Vitty and Almudena, for all the love shown all over the years.

Thanks to Daniel Algarra for the graphical design of the raceway reactor and the respirometer equipment.

And of course, thanks to my family and all my loved ones. Very especially to my parents, who gave me the life and have always supported me in all the decisions that I have made.

A mis sobrinos, Érika y José Manuel
To my niece Érika and my nephew José Manuel

A Ramsi
To Ramsi

Summary

The doctoral thesis has been developed in the framework of the research project "Control and optimization of biomass production with microalgae as a source of renewable energy" (DPI2014-55932-C2-1-R), which is focused on the modeling and control of the combined process of microalgae production and wastewater treatment with industrial reactors. This research project is a continuation of a previous project entitled "Modelling, Control and Optimization of Photobioreactors", where significant results were obtained in the field of modelling and automatic control of microalgae production in closed tubular photobioreactors. The current project continues in the same line, with the application of modelling and control techniques for the optimal production of biomass, but now focused on open photobioreactors, which are the most used worldwide.

This thesis aims to improve the knowledge regarding to open reactors characterization, light distribution and utilization by microalgae, mass transfer and oxygen accumulation, as well as the use of control strategies to improve this technology. Both, raceway and thin-layer reactors are considered in this thesis. The information obtained from this thesis is being applied into the European Project Horizon 2020 SABANA focused to the development of microalgae based biorefineries for the improvement of agriculture and aquaculture sectors.

The experimental work has been developed at three different locations: (i) "Las Palmerillas" Experimental Station (Almería, Spain) where experiments related with the improvement of open raceway reactors was performed, (ii) "Algatech" Experimental Station (Třeboň, Czech Republic) where experiments related with the evaluation of thin-layer reactors were performed, and (iii) "IFAPA" Experimental Station (Almería, Spain) where experiments related with the modelling of thin-layer cascade reactors were carried out.

The major contributions on this thesis can be summarized such as:

1. **Characterization and improvement of open raceway reactors**

- Previous works demonstrated that dissolved oxygen accumulation affects to photosynthesis activity. This thesis demonstrates that dissolved oxygen accumulation limits the biomass productivity in raceway reactors if the mass transfer capacity is not improved. Although oxygen is desorbed to the air in the channel and the paddlewheel, this is not enough to remove the oxygen produced by photosynthesis when high biomass productivity is achieved, thus being necessary to include a sump, which adequately designed and operated, contributes to avoid oversaturation of oxygen. Therefore, the mass transfer capacity in the sump must be optimized to compensate the oxygen production rate in the system. Moreover, the influence of gas flow on the mass transfer coefficient was also determined, obtaining a calibrated empirical model. Using this model, it is possible to properly

regulate the air flow in the sump and thus, the reactor operation can be optimized. Full information is available in (Barceló-Villalobos et al., 2018).

- To improve the productivity of microalgae reactors in order to optimize the light pattern at which the cells are exposed to into the reactors must be optimized. For that, the first step is to know the real light pattern taking place in raceway reactors. This thesis demonstrates that microalgae cells are adapted to local irradiance because of the unfavourable cell movement pattern in raceway reactors. It has also been demonstrated how the light regime at which the microalgae cells are exposed to in a raceway reactor is far from the optimal one required to optimize the performance of microalgae cultures through light integration. Photosynthesis rate measurements were performed along different seasons at different daytime by using different light/dark cycles. These assays confirmed that no light integration exists at 0.15 m water depth. Moreover, it has also been confirmed that the cells are adapted to the local irradiance inside the reactor. Full information is available in (Barceló-Villalobos et al., 2019a).
- Regarding control strategies, a selective control strategy proposed previously by Pawlowski et al., 2015, has been used to control pH and dissolved oxygen simultaneously. In this control, the pH value is prioritized over the dissolved oxygen value since it has a critical influence on the process performance. This thesis demonstrates the correct functionality of this selective control approach in a semi-industrial raceway (100 m²) operated in semi-continuous mode. Furthermore, the oxygen mass transfer model already developed (Klal sump model) in the present thesis, has been validated in a simulation stage to demonstrate that it is possible to adjust the mass transfer capacity of the system close to the optimal value by controlling gas injections. It is shown that it is possible to reduce gas inflow actuations and control oxygen accumulation in the system by using a feedback control strategy. Finally, it has also been demonstrated that when the dissolved oxygen reference goes down respect to the initial reference (250% Sat), the necessary gas flow is higher (full information is available in Barceló-Villalobos et al., 2019c; Barceló-Villalobos et al., 2019d)

2. Characterization and improvement of thin-layer reactors

- It has been demonstrated that although thin-layer reactors are currently more productive than raceway reactors, their productivity can also be improved if the operating conditions are optimized close to the optimal culture values. This is the first step in optimizing and scaling-up this type of reactor for industrial applications. This thesis demonstrates the influence of variations of culture parameters (irradiance, temperature, pH and dissolved oxygen) on the performance of a microalgae culture. Different assays were done to analyse the system parameters in terms of position inside the reactor and time of the daylight cycle. Results demonstrate that average irradiance and temperature to which the cells are exposed are mainly a function of time, whereas pH and dissolved oxygen concentrations also showed relevant gradients depending on their position inside the reactor.

Furthermore, it has also been demonstrated that the existence of culture parameters gradients reduces the performance of the cultures (using two different methodologies: chlorophyll-fluorescence and net photosynthesis rate methods). Moreover, the influence of culture conditions on *Scenedesmus almeriensis* cell performance was modelled. Full information is available on (Barceló-Villalobos et al., 2019b).

- The performance of pilot scale thin-layer reactors located in Algatech (Trebón) has been also evaluated. Temperature and dissolved oxygen production have been analysed and modelled at three different pilot-scale thin-layer cascade reactors (small, medium, and large). Different assays were developed to analyse: (i) the variation of culture conditions, (ii) oxygen mass balance and (iii) model the oxygen production. Temperature is a stable parameter along the channel and through the day. On the other hand, dissolved oxygen increases along the channel through the day as it is expected by photosynthesis process. The modelling of oxygen production has been done by using light integration is here reported. Temperature and dissolved oxygen measurements were done along the thin-layer cascade reactor along the day. It was demonstrated that it is more accurately to use the integrated average irradiance parameter than the average irradiance concept, to demonstrate the effective light use into the culture. Full information is available on (Barceló-Villalobos et al., in review).

INDICE

1.	HYPOTHESIS AND OBJETIVES	3
	Objectives	4
2.	INTRODUCTION.....	7
	2.1 Relevance of microalgae	7
	2.2 Major factors determining microalgae performance	8
	2.3 Microalgae production systems	10
	2.4 Advanced control strategies	12
3.	MATERIAL AND METHODS.....	17
	3.1 Microorganism and culture conditions in reactors located at Almería (Spain).	17
	3.2 Microorganism and culture conditions in reactors located at Trebon (Czech Republic)	17
	3.3 Reactors and operational conditions.....	18
	3.3.1 Raceway reactor	18
	3.3.2 Thin layer reactor at IFAPA Experimental Station	19
	3.3.3 Thin layer at Algatech Experimental Station	20
	3.4 Reactors operation	22
	3.4.1 Operation of raceway reactor located at “Las Palmerillas” Experimental Station (Almería, Spain)	22
	3.4.2 Operation of thin-layer reactor located at “IFAPA” Experimental Station (Almería, Spain)	23
	3.4.3 Operation of thin-layer reactors located at “Algatech” Experimental Station (Czech Republic)	23
	3.5 Laboratory methods	24
	3.5.1. Determination of biomass concentration	24
	3.5.2. Optical properties of the culture	24
	3.5.3. Fluorescence chlorophylls	25
	3.5.4. Off-line measurement of net-photosynthesis rate.....	27
	3.6 Fluid dynamic	28
	3.7 Mass transfer.....	28
	3.7.1. Oxygen mass balance in a raceway reactor	29
	3.7.2. Oxygen mass balance in a thin-layer cascade reactor	31
	3.7.3. Oxygen mass balance in three thin-layer cascade reactors	32
	3.8 Modelling	33
	3.8.1 Modelling light integration by microalgae in raceway reactors	34

3.8.2	Modelling of photosynthesis rate as a function of culture conditions	35
3.8.3	Modelling oxygen production of three thin-layer reactors.....	36
3.9	Control strategies	37
3.9.1.	On/off control strategy	37
3.9.2.	Selective control strategy.....	38
3.9.3.	Feedback control strategy for the air injection flow.....	39
4.	RESULTS AND DISCUSSION	43
4.1.	Characterization and improvement of raceway reactors	43
4.1.1.	Variation of culture conditions	43
4.1.2.	Oxygen mass transfer capacity	46
4.1.3.	Light integration.....	47
4.2.	Characterization and improvement of thin-layer reactor	54
4.2.1.	Variation of culture conditions	54
4.2.2.	Oxygen mass balance.....	57
4.2.3.	Modelling the net photosynthesis rate.....	57
4.3.	Evaluation of thin-layer cascade reactor	62
4.3.1.	Variation of culture conditions	62
4.3.2.	Oxygen mass balance.....	64
4.3.3.	Modelling oxygen production.....	65
4.4.	Control strategies implementation	69
5.	CONCLUSIONS.....	77
6.	LIST OF PUBLICATIONS	83
6.1.	Articles published in JCR Journals.....	83
6.2.	Articles submitted to JCR Journals	83
6.3.	Book chapter	83
7.	LIST OF OTHER CONTRIBUTIONS.....	87
7.1.	Book chapter	87
7.2.	Articles published in books of abstracts of congress.....	87
7.3.	Oral communications in international congress	88
7.4.	Communication in international congress.....	88
7.5.	Communications in national congress.....	88
	REFERENCES	90
	APPENDIX A	96
	APPENDIX B	118

Chapter 1

HYPOTHESIS AND OBJETIVES

1. HYPOTHESIS AND OBJETIVES

Open reactors have been developed since 1950s to produce microalgae, due to its simplicity and low cost of construction. Those advantages make them useful for the biomass production in an industrial scale (Chisti, 2007). However, there still have some drawbacks to be solved to make them a competitive technology. In this sense, previous works demonstrated that improving design and operational conditions are essential to optimize the performance of these systems (Chisti, 2012; Mendoza et al., 2013a). On the other hand, open reactors are highly affected by environmental conditions which make difficult to produce biomass at outdoors conditions with large variations of light and temperature taking place during solar cycle and along the year. Moreover, dissolved oxygen and pH culture variations might affect to the performance of these reactors. In this sense, accumulation of dissolved oxygen reduces the photosynthesis rate in microalgae cultures when achieving high biomass productivity (Molina et al., 2001). Previous works demonstrated that photosynthesis process decay when the dissolved oxygen accumulation is over 250% Sat. (Pawlowski et al., 2015). All these aspects make mandatory to develop models and control strategies to control the system 24 hours 365 days a year.

Most of the previous works developed until now, consider only engineering aspects of the reactors disregarding relevant biological aspects; when the biological aspects largely influencing the biomass production capacity. Nowadays, there are physics, chemicals and biological models which represent the temporal and spatial variations in these types of systems (Fernández et al., 2012; Fernández et al., 2014a; Fernández et al., 2014b). Models are a simplified representation of a real system which allow to improve the knowledge of the process, as well as to develop adequate control strategies to allow maximizing the system performance. It is necessary to use dynamic models to estimate the influence of culture conditions on the production capacity. Thus, the main objective of the thesis is to optimize the design and operation of open photobioreactors by developing engineering-biological models suitable to be used for that purpose.

Thus, this thesis makes contributions in modelling of open reactors applied to the production of microalgae. It aims to demonstrate the effectiveness of the development and implementation of proposed models in a semi-industrial scale. For that, the first step is to determine the relevance of culture conditions prevailing in open reactors, and how it affects the biomass production. The main factors that affect to the productivity of the systems include light

utilization efficiency and dissolved oxygen concentration. As a result, this thesis provides two biological models that allows to better understand the light efficiency as well as the oxygen mass transfer in open reactors. Moreover, it gives a solution to the dissolved oxygen accumulation problem, as well as to minimize CO₂/air gas consumption, by using control strategies.

From the point of view of control, the first step to design advanced control strategies is to obtain a model that reflects properly the dynamics of the system. There are a large number of models, from those based on steady-state relationships (Rotatore et al., 1995) or lineal approximations (Berenguel, 2004; García Sánchez et al., 2003), to those based non-lineal empirical features or first principles models. The control system designs must take into consideration the dynamics of the system. So, an event-based control has been used to control both raceway and thin-layer reactors located at Almería (Spain). This type of control is especially useful in bioprocess, as has been confirmed in previous works (Beschi, et al., 2014). This type of control allows to adapt the system to the dynamic process of the system. This is one of the most important difference compared to the classical feedback control. Previous works demonstrated that the use of event-based control could improve the biomass production as well as reduce the effort in controlling the effective use of CO₂ (Pawlowski et al., 2015).

Objectives

The objective of this thesis is the development of engineering- biological models of open raceway reactors. The resulting models are suitable to be used for the optimization of design and operation of these reactors, as well as for the development of control strategies to maximize the process performance. To achieve this objective, the next tasks have been completed:

1. To determine the integration of light in open raceways and how to improve it to maximize the performance of these systems (Barceló-Villalobos et al., 2019a).
2. To determine the variation of culture parameters in open raceways, especially the existence of dissolved oxygen accumulation phenomena and its influence on the performance of the systems (Barceló-Villalobos et al., 2018).
3. To develop adequate control strategies for pH and dissolved oxygen concentration allowing to maximize the performance of the reactors, and to validate it (Barceló-Villalobos et al., 2019c; Barceló-Villalobos et al., 2019d).
4. To extend this knowledge to the case of thin-layer reactors, by analysing the influence of variation of culture parameters (light, temperature, pH, dissolved oxygen) on the performance of the cultures and how to improve it (Barceló-villalobos et al., 2019b; Alameda-García et al., in review; Barceló-Villalobos et al., in review).

Chapter 2

INTRODUCTION

2. INTRODUCTION

Microalgae are one of the most natural and efficient ways to recycle wastewater as well as produce oxygen at the same time. Its performance depends on different factors: light, temperature, pH, and dissolved oxygen accumulation. These organisms could be produced in different type of systems (open and close photobioreactors). Furthermore, advance control strategies could help to improve the productivity of these systems.

2.1 Relevance of microalgae

The overpopulation issue has been a concern issue to the scientific community since 1980. Gro Harlem Brundlandt point out: "If 7 billion people were to consume as much energy and resources as we do in the West today, we would need 10 worlds, not one, to satisfy all our needs" (Brundland, 1987). From that commission, it came out the necessity of consume sources in a sustainable way without compromising the ability of future generations to meet their own needs. The alternatives to solve the problem of overpopulation goes through saving natural sources such as: energy, water and nutrients. Thus, producing microalgae could be a solution to minimize this problem. That is because it has been considered one the most efficient technology to use wastewater (water and nutrients) in order to produce valuable biomass.

There is a large number of sectors where algae could be used. Thus, a large diversity of products could be obtained from algae, to be used in agriculture and/or pharmaceuticals industry (Pulz and Gross, 2004). Microalgae can also be used for environmental caring such as: CO₂ mitigation or wastewater treatment (Wang et al., 2008). The carbon fixed by the microalgae is incorporated into proteins, carbohydrates, lipids and so on. Microalgae have been considered as the most efficient technology to fix CO₂ in the world, but it goes further. It is well reported that microalgae can contribute to wastewater treatment as a clean and natural way. Furthermore, it allows to reduce water consumption as well as recover nutrients from wastewater, such as: phosphorus and nitrates. Due to all these reasons, the processes based on the use of microalgae are receiving a growing interest within the industrial sector worldwide (Chisti, 2008; Mata et al., 2010).

Microalgae are photoautotrophic microorganisms, which means that their energy source is light, and their carbon source is CO₂. There is a wide diversity of species catalogued and available, although only about 50 species have been studied in detail from the physiological and biochemical point of view and less than 10 that have been commercially used. These microorganisms live in complex habitats, so they must be adapted quickly to new culture

conditions producing metabolites such as: proteins, antioxidants, and so on. These culture conditions (light intensity, pH, temperature and dissolved oxygen) must be as close as possible to the optimal values to maximize the performance of open reactors, as well as to ensure efficient and stable biomass production.

2.2 Major factors determining microalgae performance

Light availability

Light is the energy input that must be optimized to ensure maximal productivities in microalgae-based systems. It must be as high as possible, but it must not be provided in excess to avoid photoinhibition process, which would damage the photosynthetic apparatus (Photosystem I and Photosystem II). Algae, as plants, can only take the Photosynthetically Active Radiation (PAR) in the range from 400 to 700 nm. Furthermore, it should be taken into consideration that algae are exposed to different irradiances inside the cultures, being a function of light intensity on the reactor surface and geometry and optical properties of the cultures. The average irradiance, I_{av} , measurement can be used as a combination of all these previous light factors (Molina-Grima et al., 1994). The average irradiance is defined as a function of external irradiance, biomass concentration, extinction coefficient of the biomass and light path of the reactor.

The photosynthesis rate is a function of irradiance at which the cells are exposed to, defined by the Photosynthesis-Irradiance curve (P-I) (Molina Grima et al., 1994; Sánchez et al., 2008). From this curve the optimal irradiance to be provided can be determined. Moreover, maximal performance of the culture when providing this irradiance can be estimated, being also useful to define the optimal operation conditions for any type of reactor.

To optimize the performance of any microalgae-based process, it is necessary to adequately describe the light integration phenomena taking place on it. The impact of light regime at which the cells are exposed to on both photosynthesis rate and photo-acclimation phenomena is still poorly understood. However, it plays an important role on the culture performance. It is well known that, depending on the mixing characteristics, algae will be exposed to certain light/dark cycles (Janssen et al., 2000), what has an impact on the photosynthesis process. Photosynthetic productivity (PO_2 , $mgO_2/L\cdot h$) is a function of light distribution and frequency (Brindley et al., 2011). Previous work developed a simplified model that allows to quantify the effect of frequency of varying light on the photosynthetic response of microalgae (Fernández-Sevilla et al., 2018).

Temperature

Temperature is one of the most difficult parameters to be controlled in outdoor photobioreactors (Chu et al., 2016; Waller et al., 2012). That is because temperature varies according to the solar radiation and environmental conditions prevailing outdoor. Furthermore, it is well known that temperature affects to the photosynthesis rate and biomass productivity, but also to the pigment content (Giannelli et al., 2015), as well as to the O₂/CO₂ solubility (Raeesossadati et al., 2014).

The influence of temperature into the performance of different microalgae has been previously studied. The optimum temperature for photosynthesis of blue-green algae (cyanobacteria) is 20 °C from June to November, and ranged at 20–30 °C during summer. A temperature between 22°C and 35°C was favourable for microalgae growth. *Chlorella vulgaris* can grow in temperatures ranging 25–30°C, but also at temperatures ranging at 30–35°C. *Scenedesmus sp.* grows in the ranges 10 to 40 °C. *Spirulina* species have the ability to grow in temperatures range from 20 to 40°C, but the temperature affected the protein and carbohydrate levels (Singh and Singh, 2015). Furthermore, results from *H. pluvialis* showed that the growth rate declined with above-optimal increases in temperature, and the final maximum cell concentration at 30.5°C reached only 35% of that attained at the optimal temperature of 20°C (Giannelli et al., 2015).

This thesis provides a preliminary study of both, the optimal and harmful effects of temperature to the photosynthetically activity of the algae. Future studies should be done to obtain a more appropriate definition and modelling of optimal temperature according to temperature dependence on growth phases (Giannelli et al., 2015).

pH

Regarding pH, this variable strongly influences the productivity of microalgae-based systems, both by affecting the optimal pH for the different microorganisms, and by influencing the availability of carbon into the culture medium. At pH values lower than the optimal one the photosynthesis rate decreases, but also for values upper than the optimal one the performance of the cells strongly reduces (Costache et al., 2013). The pH control is done by injecting CO₂. It is well known that the application of CO₂ has a direct influence on the pH value since it changes the acidity of the microalgae growth medium. The CO₂ is not solely used for pH control purposes, but also for supplying inorganic carbon to avoid carbon limitation of the photosynthesis rate.

It is well demonstrated that in outdoor cultures the pH varies along the day if it is not properly controlled. The widest range in pH variations was from 7.3 to 8.3 for *Scenedesmus almeriensis* (Costache et al., 2013). Moreover, tolerance to pH is different for each strain. Diatoms such as *Phaeodactylum* can tolerate pH values up to 10.3, whereas chlorophytes such as *Dunaliella*, are unable to grow when the pH exceeds 9.3. For cyanobacteria such as *Spirulina*,

optimal pH can be above 9.5 (Jiménez et al., 2003). In summary, for most microalgae strains, growth is optimal at pH values between 7.0 and 8.0; although for cyanobacteria, the optimal pH is in the 8.0 to 9.0 range.

To maximize biomass productivity in photobioreactors, it is essential to control pH as well as to supply carbon as a nutrient source at the same rate as that required for biomass production. On the other hand, one of the disadvantages of using CO₂ injections for controlling pH is that the production costs of the biomass production are highly increased. It has been estimated that the cost of providing CO₂ is approximately 30% of the total microalgal production system cost (Benemann, 1997). Thus, improvement of CO₂ efficiency must be taken into consideration. In this sense, control strategies play an important role (Pawlowski et al., 2014b). Previous works demonstrated that, control strategies can be used to keep the pH close to the optimal values and saving CO₂ injections at the same time (Pawlowski et al., 2015).

Dissolved oxygen concentration

This is one of the most important drawbacks that should be solved to make this technology suitable for industrial scale. It is known that when dissolved oxygen concentrations rise two times above the equilibrium with the air, the photosynthesis rate is generally inhibited (Jiménez et al., 2003;Mendoza et al., 2013b). Furthermore, it has been demonstrated that the biomass productivity increases up to double when there is an adequate oxygen removal to maintain the dissolved oxygen concentration below 200 %Sat compare to the productivity obtained when there is no oxygen removal (de Godos et al., 2014). Oxygen removal is likely to be a more critical design criterion than carbon supply due to the lower solubility of oxygen compared to CO₂. This thesis presents models and control approaches to contribute in the oxygen removal issue.

2.3 Microalgae production systems

Traditionally, photobioreactors systems have been used to produce microalgae biomass in a large scale. The variety of the existing designs allows grouping them in different categories depending on the position, gas exchange system, arrangement of the units, system for culture circulation or construction material; resulting in a large number of possibilities. The culture depth is also a very important parameter, since it directly affects to the average irradiance within the culture. The open raceways, which are the ones used in this thesis, were the first systems utilized for large production of microalgae. The principles for the design and construction of this type of reactors were reviewed in (Oswald and Golueke, 1967).

The raceway reactors were firstly designed in the 60s (Oswald and Golueke, 1967). Since then, they have been slowly improved. The basic raceway reactor configuration consists of two

loops connected to a paddlewheel which recirculates the liquid along the channels, usually at water depths between 0.2 and 0.3 m. Due to the low efficiency of the paddlewheel (below 50%), the overall surface of large raceway reactors cannot exceed 5,000 m², for which an average power consumption of 10 W/m² is required. Moreover, in a less common configuration, the raceway reactor has internal channels that create turbulences, with up to four straight channels included (Ación et al., 2017). The latest raceway designs include a sump before the paddlewheel, which is used for CO₂/air injections as well as for oxygen desorption. Usually, CO₂ injections are made on demand by using a control system.

Thin-layer cascade reactors were firstly developed in 60s at Trebon, Czech Republic. The unit are characterized by two sloped cultivation plates where the lower end of the upper plate is connected by a trough to the beginning of the lower plate, which is declined in the opposite direction. The suspension flows go into a tank from where it is circulated by a pump to the upper part of the cultivation area. The second generation of thin-Layer cascade reactors constructed at the Institute of Microbiology in Trebon (Czech Republic) were made of stainless steel (Ación et al., 2017). Furthermore, the last thin-layer generation goes further. The suspension flows go into a bubble column where it is circulated by a pump to the upper part of the reactor. The bubble column is used for oxygen desorption as well as for CO₂/air injections. One of the advantages of using these types of reactors is the efficiency of light utilization due to the short optical path ranging from 0.006 to 0.02 m. Moreover, it can be operated at high densities of biomass (25-35 g/L) (Ación et al., 2017), what prevents from contaminations.

This thesis is focused in open reactors due to their convenience respect to design and operating cost; these are cheaper than closed reactors. Raceway reactors and thin layer reactors have been analysed to improve their operational conditions to make them a suitable technology in an industrial scale.

To improve the open reactors' operational conditions, two aspects should be considered: fluid dynamics and mass transfer. The optimization of fluid dynamics is a very important aspect to be considered since it can minimize the energy consumption; therefore, it can reduce the operational cost of biomass production in an industrial scale. It allows to ensure a properly circulation of the culture, that avoids cell sedimentation as well as reducing the existence of nutrient gradients and improving the light cycle to which the cells are exposed to.

Concerning mass transfer, during the photosynthesis process microalgae consume carbon and release oxygen. Therefore, to optimize the performance of this process, two objectives should be considered: to avoid carbon limitation and, at the same time to avoid inhibition by oxygen accumulation. Both phenomena reduce cell performance and, in turn, the photosynthesis rate. These drawbacks are directly related to the reactor's mass transfer

capacity. The CO₂ mass transfer has already been improved in previous works (Duarte-santos et al., 2016). On the other hand, oxygen mass transfer is an objective still to be improved, and thus, this has been one of the pillars of the present thesis due to its importance in reactors' designs and optimal operation.

2.4 Advanced control strategies

The optimal operation of the photobioreactors needs the development of control strategies to ensure an adequate control of culture conditions along the day. This allows to maximize the productivity of the system since it is automatically controlled. Nowadays, microalgae are receiving more attention by the control community, due to the challenges appeared about the reduction cost in their production. There are few studies related to the control of culture conditions or addressed to the global optimization of these production systems from a control point of view, mainly due to the high complexity of the required models or problems associated to these systems. It is well demonstrated that the control strategies give the opportunity to optimize reactors productions (Fernández et al., 2016), specially the control design that optimized the biomass production in a global way such as the hierarchical control or multiscale strategies (Fernández et al., 2016).

Several control systems have been developed to control pH and dissolved oxygen. Most of the existing works are related to the pH control in photobioreactors, which provide promising performance results with an adequate CO₂ supply. For instance, a PID (Proportional Integral Derivative) controller plus feedforward was developed (Fernández et al., 2010), where a simplified linear model of pH evolution based on disturbances was used for control design purposes. In (Romero-García et al., 2012) a FSP (Filtered Smith Predictor) control approach was employed in real system to account for long delays in the process. The proposed control solution was able to reduce the Integral Absolute Error and the time for the solution addition in more than 25%. In these two works, significant improvements to on/off controllers were obtained. Conversely, MPC (Model Predictive Control) algorithms have been used for pH control problems with satisfactory results for real-time applications where high-quality control is desired (Lazar et al., 2007; Oblak et al., 2010; Senthil et al., 2012). The use of the Generalized Predictive Controller (GPC) can be found in Berenguel et al., (2004), where overall control performance was improved compared to the classical on/off controller. The predictive algorithm was able to capture the process dynamics and the on/off valve limitation explicitly in the constrained control problem. Thus, CO₂ injections and losses were considerably reduced compared to the commonly used on/off controllers with a promising trade-off between performance and control effort.

Regarding to the dissolved oxygen control problem, fewer works are found in the literature. Dissolved oxygen removal remains a significant challenge for the control community, despite the considerable technical advances in this field such as those reported in (Mendoza et al., 2013a; Peng et al., 2013). There was a significant lack of control solutions for controlling both variables, pH and dissolved oxygen simultaneously until (Pawlowski et al., 2015) work. In that work, event-based control strategies was successfully applied for this purpose. The main difference to the classical control approaches is that, in the event-based approach, the control system can adapt the actuation rate to the process dynamics and process disturbances (Pawlowski et al., 2011). This feature is especially useful in a bioprocess applications, as has been confirmed in several recent works (Beschi et al., 2014; Pawlowski et al., 2014a, 2014b).

Most of the previous control systems were based on black box models, thus existing a high dependence of the reactor from which the control approaches were designed for. To avoid this dependence, the control approaches could be developed based on biological models. Therefore, this thesis is focused on the development of physics/biological models which are derived from fundamental laws. Specifically, two biological models for the dissolved oxygen accumulation and the light path behaviour respectively were developed. These models are then used to design new control approaches. For example, a new control law has been proposed to optimize the dissolved oxygen accumulation problem derived from a new model based on first principles.

Chapter 3

MATERIAL AND METHODS

3. MATERIAL AND METHODS

The techniques and methodologies described below were used to achieve the objectives outlined in this thesis. They involve all the requirements for algae production as well as for optimization process: culture conditions, reactors and operational conditions, laboratory methods, fluid dynamics, mass transfer and control strategies.

3.1 Microorganism and culture conditions in reactors located at Almería (Spain).

The microalgae *Scenedesmus almeriensis* (CCAP 276/24) was used (Figure 3.1). It is an algae isolated in the facilities “Las Palmerillas” experimental station, thus being a local species adapted to environmental conditions prevailing in Almería (Spain). Moreover, it predominates against other species in open bioreactors. The inoculum for the raceway reactor was produced in a 3.0 m³ tubular photobioreactor under controlled conditions at pH =8 and at a temperature ranging from 18 to 22°C using freshwater and Mann & Myers medium prepared using fertilizers: (0.14 g·L⁻¹ KH₂(PO₄)₂, 0.18 g·L⁻¹ Mg(SO₄)₂·7H₂O, 0.9 g·L⁻¹ NaNO₃, 0.02 mL·L⁻¹ Welgro, and 0.02 g·L⁻¹ Kalentol). In addition, NaHCO₃ was provided once a week to maintain the medium’s alkalinity at the optimum 7 mM.

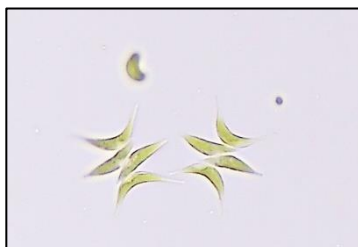


Figure 3.1. Microscope view of *Scenedesmus almeriensis*

3.2 Microorganism and culture conditions in reactors located at Trebon (Czech Republic)

The microalga *Chlorella* spp. was used (Figure 3.2). It belongs to the culture collection of the Laboratory of Algal Biotechnology at the Institute of Microbiology (Trebon, Czech Republic). The cultures were grown photoautotrophically in a mineral medium in a fed-batch regime (Doucha et al., 1995).

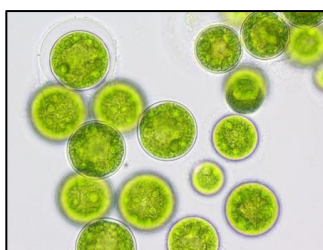


Figure 3.2. Microscope view of *Chlorella* spp.

3.3 Reactors and operational conditions

This section describes the reactors and facilities used for the results obtained in this thesis. Moreover, the operational conditions for each facility are detailed.

3.3.1 Raceway reactor

The raceway reactor used in this thesis is located at the “Las Palmerillas” Research Centre, 36° 48′N–2° 43′W, part of the Cajamar Foundation (Almería, Spain) (Figure 3.3, Figure 3.4). The reactor consists of two 50 m long channels (0.46 m high × 1 m wide), both connected by 180° bends at each end, with a 0.59 m³ sump (0.65 m long × 0.90 m wide × 1 m deep) located 1 m along one of the channels (Barceló-Villalobos et al., 2018). A paddlewheel system was used to recirculate the culture through the reactor at a regular velocity of 0.2 m·s⁻¹, although this could be increased up to 0.8 m·s⁻¹ by manipulating the frequency inverter of the engine. The pH, temperature and dissolved oxygen in the culture were measured using appropriate probes (5083 T and 5120, Crison Instruments, Barcelona, Spain), connected to an MM44 control-transmitter unit (Crison Instruments, Spain), and data acquisition software (Labview, National Instruments, USA) providing complete monitoring and control of the system. The culture pH was maintained at 8.0 by on-demand CO₂ injections whereas temperature was not controlled; this varied by ±5°C with respect to the daily mean air temperature, which, in turn, varied from 12°C in winter to 28°C in summer.

The raceway reactor was inoculated and operated in batch mode for one week, after which it was operated in continuous mode a culture depth of 0.15 m. Different dilution rates were assayed: 0.1, 0.2, 0.3, 0.4 day⁻¹. Only samples from stable conditions were used. Evaporation inside the reactor was compensated for by the daily addition of fresh medium.



Figure 3.3. General view of the raceway reactors located at the "Las Palmerillas" experimental station in Almería (Spain) working in continuous mode from May 2016 to June 2018.

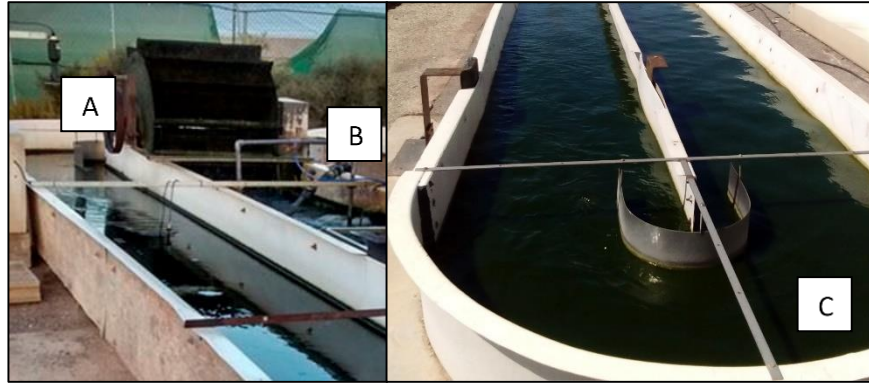


Figure 3.4. Sections of the 100 m² raceway reactor. (A) Paddlewheel, (B) Sump, (C) Loop

3.3.2 Thin layer reactor at IFAPA Experimental Station

The thin layer reactor is located at the “IFAPA” Research Centre, (Almería, Spain) (*Figure 3.5, Figure 3.6*) and it was also used in this thesis. The reactor consists of two sloped cultivation plates where the lower end of the upper plate is connected by a trough to the beginning of the lower plate, which is declined in the opposite direction. The suspension flows go into a sump from where it is circulated by a pump to the upper part of the cultivation area. The bubble column is used for mixing, degassing and mass transfer exchange.

The pH, temperature and dissolved oxygen in the culture were on-line measured using appropriate probes (5083 T and 5120, Crison, Barcelona, Spain). The gas flow rate entering the reactor was measured by a mass flow meter (PFM 725S-F01-F, SMC, Tokyo, Japan). The pH of the culture was controlled at 8.0 by on-demand injection of CO₂, controlled by the DaqDactory software. On the other hand, temperature was not controlled. Air was supplied to the reactor by a blower giving 350 mbar overpressure, through a fine bubble diffuser AFT2100 (ECOTEC, Spain) providing bubbles with a diameter smaller than 2 mm at the minimum pressure drop. The culture received continuous air injection, regardless of the CO₂ demand. The demand for carbon was supplied by the injection of pure CO₂ using an event-based pH controller at pH 8 (Pawlowski et al., 2016). The reactor was operated in semi-continuous mode at dilution rates from 0.3 day⁻¹ at a culture depth of 0.02 m. Evaporation inside the reactor was compensated for by the daily addition of fresh medium.



Figure 3.5. General view of the thin layer reactor located at the "IFAPA" experimental station in Almería (Spain) working in continuous mode since June 2018.

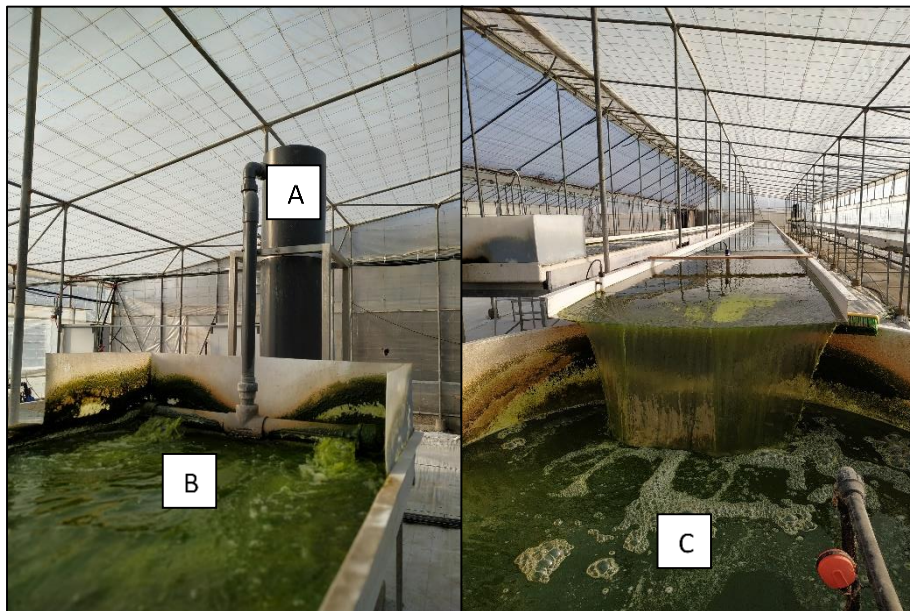


Figure 3.6. Sections of the 120 m² thin layer reactor. (A) Bubble column, (B) Plate, (C) Sump

3.3.3 Thin layer at Algatech Experimental Station

Different thin layer reactors have also been evaluated at the "Algatech" Experimental Station (Trebon, Czech Republic) (Figure 3.7) working at biomass concentrations ranging from 25-55 g/L at batch mode. Samples were taken from different equidistant positions (n=16, n=14 and n=18 respectively) at three different thin-layer cascades with different capacity (A=200 L, B=600 L, C=2200 L) at four different times (9:00, 11:00, 13:00 and 15:00 h) for 15 days.

Microalgae are grown in a smooth thin-layer cascade of 6 mm. The unit consists of two declined cultivation lanes made of glass plates in the case of small and big units and stainless steel in the case of the medium unit. All of them are supported by scaffolding. They are made up of several

parts: retention tank (degasser), inclined cultivation surface, circulation pump, CO₂ supply and a three-way valve. The end of the upper lane is connected to the beginning of the lower lane by a channel. The suspension flows go into the retention tank (degasser), from where it is pumped by a circulation pump via a riser back to the upper part of the cultivation area, being distributed by a perforated tube. Measurement and control sensors (pH, dissolved oxygen, temperature and liquid level) are mounted in the degasser and in the connecting trough. The cycle takes about 60–80 s, which can be varied by altering the pump velocity. The suspension can be harvested via a three-way valve. The whole system is controlled manually.



Figure 3.7. General view of the thin layer reactors (A=200 L, B=600 L, C=2200 L) located at the "Algatech" Experimental Station in Trebon (Czech Republic). Pictures from August 2018.

3.4 Reactors operation

The present thesis has been developed by using a Supervisory Control and Data Acquisition (SCADA) software available at the different facilities. Each SCADA allows to accomplish data acquisition requirements by collecting data from different sensors (irradiance, pH, temperature and dissolved oxygen), showing all the data through a graphical user interface, and including the implementation of adequate control strategies to optimize the reactor performance.

3.4.1 Operation of raceway reactor located at “Las Palmerillas” Experimental Station (Almería, Spain)

The operation of the raceway reactor located in “Las Palmerillas” Experimental Station was performed by using a data acquisition software developed by the Automatics, Robotics and Mechatronics research group of the University of Almeria using Labview (National Instruments) (Figure 3.8). The software allows to control the dilution rate by two methods: manually (*Manual*) or automatically (*Automático*). Firstly, it is necessary to check the volume to inject in the script screen. On the other hand, by working in the manual mode, we had to push the buttons valve of medium (VMedio1) and pump of medium (B Medio 1). The harvesting process was made by using two pumps.

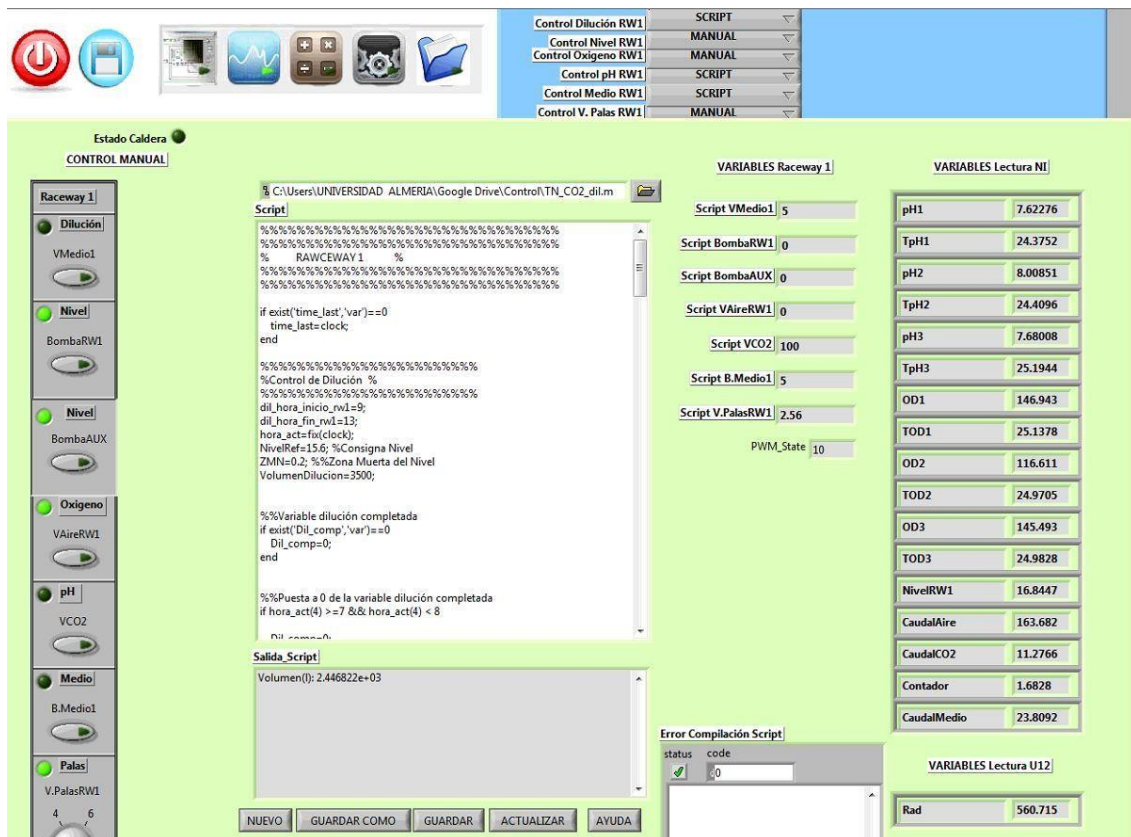


Figure 3.8. SCADA Control system architecture used in “Las Palmerillas” Experimental Station (Almería, Spain)

3.4.2 Operation of thin-layer reactor located at “IFAPA” Experimental Station (Almería, Spain)

The operation of the thin-layer reactor located at “IFAPA” Experimental Station (Figure 3.9) was performed by using a data acquisition software developed by the Biotechnology of microalgae group from University of Almeria using DaqFactory (Azeotech). The software allows to register and control all the operation parameters such as irradiance, pH, temperature and dissolved oxygen, in addition dilution rate, and compensation of water losses by evaporation. Additionally, this software allows to manipulate the composition of culture medium, and to optimize the injection of CO₂ or air into the sump to optimize the performance of the reactors.

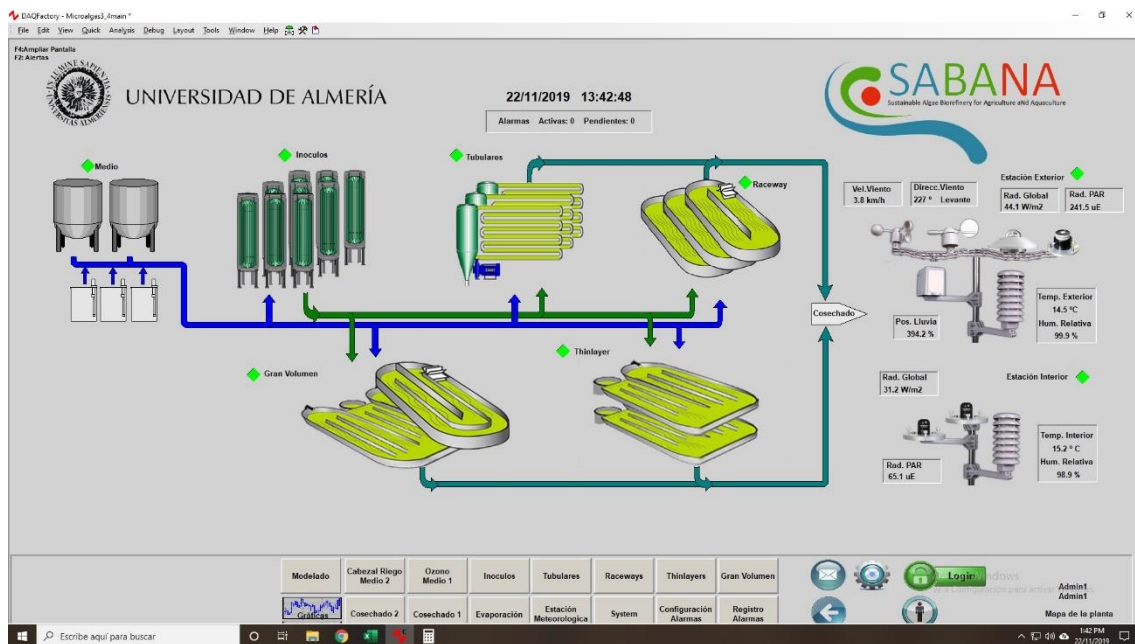


Figure 3.9. SCADA Control system architecture used in IFAPA Experimental Station (Almería, Spain)

3.4.3 Operation of thin-layer reactors located at “Algatech” Experimental Station (Czech Republic)

The operation of the three thin-layer reactors located at “Algatech” Research Centre in Trebon (Czech Republic) was performed manually.

3.5 Laboratory methods

3.5.1. Determination of biomass concentration

To quantify the biomass concentration (C_b), the dry weight of the samples was determined in a gravimetric manner. For this, filters of 90 mm diameter and 1 μm of pore diameter, previously stored in an oven at 80°C for 24 hours, were placed on a büchner funnel made of porcelain in contact with a vacuum flask connected to a vacuum pump (*Figure 3.10*).

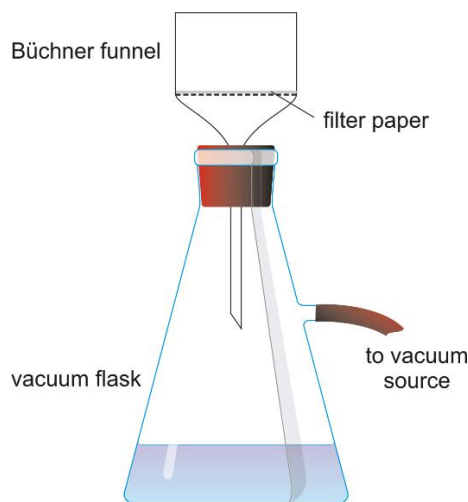


Figure 3.10. Biomass quantification method.

Samples of 50 to 250 ml of culture, depending on the biomass concentration, were filtered. The filter with the biomass is deposited again in the oven at 80 °C and after 24 hours it is weighed again. The difference between the weight of the filter with the biomass (P_f) and the filter before filtering the biomass (P_{f-b}) in grams, divided by the volume (V) filtered in litres is the dry weight of the biomass in grams per litre of culture (Equation 1).

$$C_b = \frac{(P_f - P_{f-b})}{V} \quad \text{Equation 1}$$

3.5.2. Optical properties of the culture

The spectrophotometric procedure was chosen as a rapid method of monitoring cell growth. Thus, the absorbance of the culture was used as a parameter in a spectrophotometer (GENESYS™ 10S UV-Vis, Thermo Scientific, USA) at a wavelength of 680 and 750 nm. The relationship between absorbance and biomass dry weight was determined experimentally for the different stains that had been used in the present thesis. For this issue, samples of culture were taken under different culture conditions of dilution rate, the absorbance was measured

and a dry weight of each of them was made. The obtained values were adjusted to a straight line of Abs versus Cb in the linearity interval determined for each operational condition.

3.5.3. Fluorescence chlorophylls

The stress of microalgae in the different operating conditions was studied by means of the analysis of the photosynthetic activity through the fluorescence measurements of chlorophyll (*Figure 3.11*).

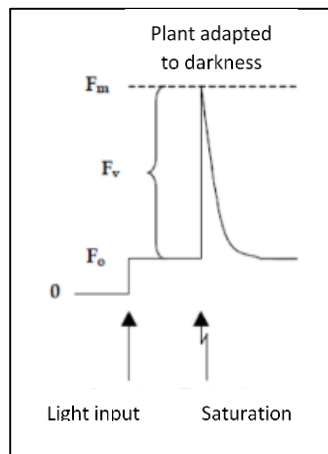


Figure 3.11. Fluorescence parameters. F_m : Maximum fluorescence in cells adapted to darkness, F_v : Variable fluorescence in cells adapted to darkness, $F_v = F_m - F_o$, F_t : Basal fluorescence in cells subjected to light.

The photosynthetic activity can be determined in a non-intrusive way under different conditions through the fluorescence of chlorophyll associated with photosystem II (Schreiber et al., 1995). When a chlorophyll molecule is excited by light, the energy absorbed can be dissipated through three processes: photochemical energy, thermal dissipation and fluorescence. The three processes compete with each other, so that the increase in the efficiency of any of them results in the decrease in the performance of others. When a cell is illuminated with light of an irradiance low enough that it does not produce a photochemical response, the cell emits a low fluorescence signal called F_o , from photosystem II. If a pulse of saturating light is applied next, the fluorescence reaches maximum values (F_m), leaving the reaction centers completely reduced. F_o : Minimum fluorescence in cells acclimated to darkness. The optimal quantum yield (F_v / F_m) indicates the maximum efficiency in the photochemical energy conversion processes of the microalgae adapted to darkness. This is an indicator of the redox state of the energy transfer system towards the electron sinks in the assimilation processes of carbon and nitrogen.

Two different devices were used depends on the use of the measurement. The daily fluorescence measurements were taken with an AquaPen-C AP-C 100 modulated amplitude

pulse fluorometer (Photon Systems Instruments, Czech Republic) (*Figure 3.12*). The microalgae was previously incubated for 15 min in the dark to ensure that all the reaction centres were closed, then a saturation pulse was emitted, determining the optimal quantum yield (F_v / F_m).



Figure 3.12. Aquapen (Photon Systems Instruments, Czech Republic)

On the other hand, the fluorescence measurements done in the thin-layer cascade reactor at different operational conditions of pH and temperature were done by using a Pulse-Amplitude-Modulation fluorometer device (Junior PAM, Walz, Effeltrich, Germany) (*Figure 3.13*). It was used to estimate the photosynthetic activity by using Rapid Light Curves of Electron Transport Rate at different light intensities (0, 25, 45, 66, 90, 125, 190, 285, 420, 625, 845, 1150, 1500 $\mu\text{E m}^{-2} \text{s}^{-1}$).

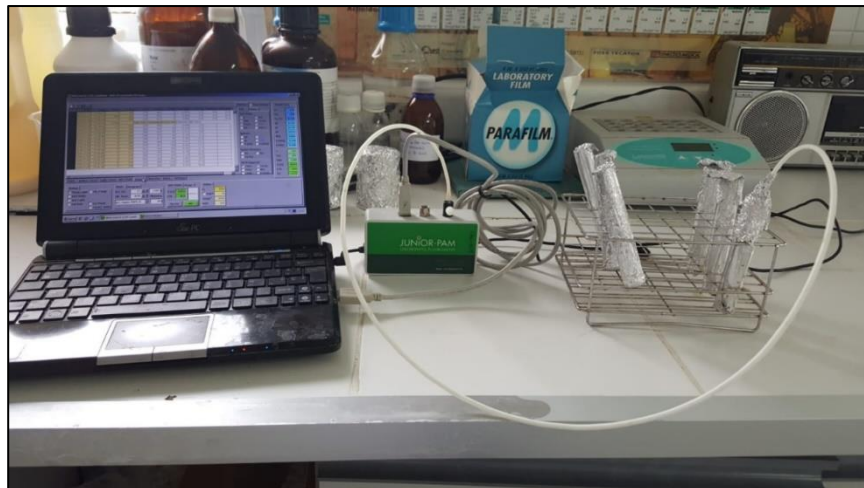


Figure 3.13. Pulse-Amplitude-Modulation fluorometer device (Junior PAM, Walz, Effeltrich, Germany)

3.5.4. Off-line measurement of net-photosynthesis rate

Photosynthesis measurements were performed in a specifically built photo-respirometer equipment. This designed equipment measures the variation of dissolved oxygen in microalgae samples under controlled conditions. The samples were placed in a 60 mL cylindrical stirred glass chamber with a diameter of 2 cm, which is illuminated using two sets of fluorescent lamps (Osram 80 W) placed at right and left of the glass chamber. The intensity of the lamps was manually regulated to obtain the desired irradiance inside the centre of the chamber once the sample was added.

The photo-respirometer is also equipped with sensors of irradiance (ULM 500, Walz, Germany), temperature (PT1000, Crison, Spain), pH (Crison 5343, Barcelona, Spain) and dissolved oxygen (Crison 5002, Barcelona, Spain) located inside of the cylindrical glass chamber, being the irradiance sensor located in the centre of the glass chamber whereas the other sensors were located close to the surface to avoid shadows into the system (*Figure 3.14*).

In order to calculate the photosynthesis rate of microalgae cultures, samples were taken and located into the cylindrical stirred glass chamber. Each sample was exposed to different light periods to measure and register the variation of dissolved oxygen under any conditions, being the oxygen production expected due to active microalgae photosynthesis. Photosynthesis rate was calculated as the sum of the slope of dissolved oxygen accumulation during light periods. Variations of dissolved oxygen were performed in the range of 70-140 %Sat, at which the oxygen mass transfer was confirmed to be negligible.

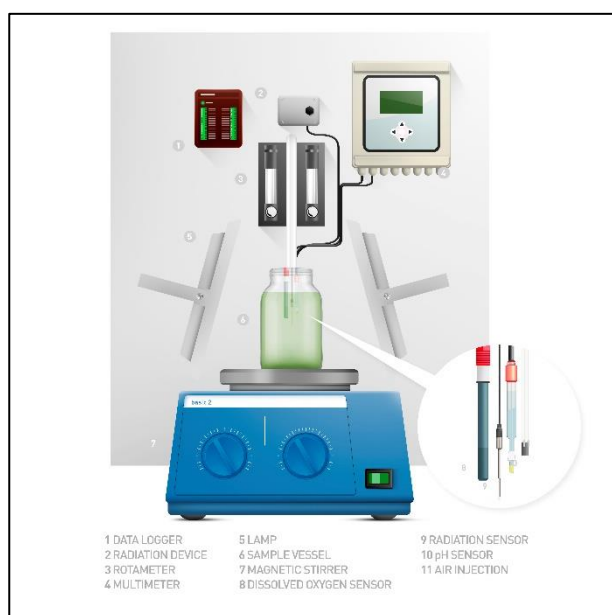


Figure 3.14. Infographic of the respirometer equipment build up by the Chemical Engineering department in the University of Almería (Spain).

3.6 Fluid dynamic

Fluid-dynamics in raceway reactors is classically defined by the Manning's equation. This equation relates the power consumption in raceway reactors as a function of the volumetric flow rate (Q), the liquid density (ρ), the Manning friction factor (n), the mean channel velocity (v), the total length of the raceway (L) and the hydraulic radius (Equation 2). Alternatively, the power consumption can be calculated as a function of the head loss in the system (ΣF) and the total liquid volume in the reactor (V) using the Bernoulli's equation (Equation 3). The head loss is a function of the reactor length (L) and the hydraulic diameter (D) (Equation 4). This is in addition to the Darcy number (f_D), which takes account of the turbulence and relative roughness. The advantage of using Bernoulli's (Equation 4) is that the head loss associated with various features (e.g. bends) can be calculated and then added to that in the channels to determine the contribution of different components to the overall head loss under different operating conditions. The head loss in a bend, or other feature, is calculated as a function of the feature's discharge coefficient (K) (Equation 5).

$$P = \frac{Q \rho g n^2 v^2 L}{R^{4/3}} \quad \text{Equation 2}$$

$$P = \frac{\Sigma F Q \rho}{V} \quad \text{Equation 3}$$

$$\Sigma F = f_D \frac{Lv^2}{2D} \quad \text{Equation 4}$$

$$\Sigma F_{\text{feature}} = K_{\text{feature}} \frac{v^2}{D} \quad \text{Equation 5}$$

Although Manning's equation has been traditionally used to design raceway reactors, it has recently been demonstrated that the Bernoulli's equation can also be applied for this type of reactors, and even provide more accurate results (Mendoza et al., 2013a).

3.7 Mass transfer

The oxygen mass transfer capacity (NO_2) is a function of mass transfer coefficient (K_{La}), the driving force (F_{iml}) and the volume of the sump (V) (Equation 6). Previous works demonstrated that the fluid dynamics (K_{La}) remains constant during the day whereas the driving force (F_{iml}) is measured as a function of the dissolved oxygen concentration (DO_2) entering the culture at the different positions (Equation 7). The difference between the dissolved oxygen

concentration in the liquid (O_2 mg/L) and that in equilibrium with the gas phase (air) (DO_2^* , mg/L) is calculated by using the Henry's law.

$$N_{O_2} = k_{lal} \cdot Fi_{ml} \cdot V \quad \text{Equation 6}$$

$$Fi_{ml} = \frac{(DO_{2\ out} - DO_2^*) - (DO_{2\ in} - DO_2^*)}{Ln \frac{(DO_{2\ out} - DO_2^*)}{(DO_{2\ in} - DO_2^*)}} \quad \text{Equation 7}$$

Previous works have already demonstrated the differences between the driving force and the mass transfer coefficient in the different parts of raceway reactors (Mendoza et al., 2013b). The mass transfer coefficient into the sump (Klal) is a function of the sump design, its geometry, the type of diffuser installed and the liquid to gas ratio inside the system. The higher this value is in the reactor the higher the system's mass transfer capacity is. This parameter is one of the most relevant when designing any raceway reactor.

3.7.1. Oxygen mass balance in a raceway reactor

Oxygen mass balances were performed to study the main phenomena taking place inside the raceway reactors. For this, the dissolved oxygen concentration was measured at three different positions (after the paddlewheel, after the sump and at the end of the loop). The oxygen mass balance allows to calculate the accumulation of dissolved oxygen as a function of oxygen production and mass transfer in each of these sections. Oxygen is produced by photosynthesis and is therefore modified as a function of the culture conditions, especially by changes in solar radiation throughout the day. In contrast, the mass transfer capacity is only a function of fluid dynamics and the driving force in the different parts of the reactor; the fluid dynamics remaining constant during the day whereas the driving force is measured as a function of the dissolved oxygen concentration in the culture at the different positions commented above along the day. Therefore, for any raceway reactor section, the following balance defines the dissolved oxygen concentration (Equation 8).

$$O_{2,inlet} + O_{2,produced} = O_{2,outlet} + O_{2,accumulation} \quad \text{Equation 8}$$

In Equation 8, $O_{2\ inlet}$ refers to the dissolved oxygen concentration measured after the paddlewheel. $O_{2\ produced}$ refers to the dissolved oxygen produced along the loop. $O_{2\ outlet}$ refers to

the dissolved oxygen concentration measured after the sump, and O_2 accumulation refers to the oxygen produced over the time.

In this work it is assumed that the sump is completely dark, because in this section less than 3% of the total volume has irradiance values above $10 \mu\text{E}\cdot\text{m}^{-2}\cdot\text{s}^{-1}$. So, no photosynthesis takes place. Furthermore, oxygen production in the paddlewheel section can be disregarded; hence the dissolved oxygen mass balance is defined by Equation 9, where PO_2 represents the oxygen production at the loop ($PO_{2,loop}$) and NO_2 represents the oxygen mass transfer capacity in each of the reactor sections ($NO_{2,loop}, NO_{2,sump}, NO_{2,paddlewheel}$).

$$PO_{2,loop} + NO_{2,loop} + NO_{2,sump} + NO_{2,paddlewheel} = O_{2,accumulation} \quad \text{Equation 9}$$

The mass transfer capacity is calculated as a function of the global mass transfer coefficient in each reactor section ($K_l a_l$), multiplied by the driving force. This means that the difference between the dissolved oxygen concentration in the liquid ($[O_2]$) and that in equilibrium with the gas phase (air) ($[O_2^*]$), which is calculated using Henry's law and the section volume (V) (Equation 10). The influence of temperature on the solubility of dissolved oxygen was included using Equation 11. In this case, the global mass transfer coefficient refers to the liquid phase, assuming that the main resistance to mass transfer takes place here.

$$NO_2 = K_l a_l ([O_2] - [O_2^*]) V \quad \text{Equation 10}$$

$$[O_2^*] = 12.408 - 0.1658 * T \quad \text{Equation 11}$$

It was reported in Mendoza et al., (2013b), that the global mass transfer coefficient in the loop of raceway reactors is very low, at 0.9 h^{-1} , as it is independently constant of the culture conditions. This coefficient can be strongly modified if the liquid velocity is greatly enhanced. However, in raceway reactors, the liquid velocity is adjusted to $0.2 \text{ m}\cdot\text{s}^{-1}$ to minimize power consumption – and for this reason, the value of 0.9 h^{-1} is acceptable as the global mass transfer coefficient in the loop. Moreover, by applying the oxygen mass balance to the loop, it is possible to obtain a “virtual oxygen production sensor” as a function of the dissolved oxygen concentration at the beginning and end of the loop, and the flow of liquid inside the reactor (Q_{liquid}); as defined by Equation 12.

$$PO_{2,loop} = Q_{liquid} ([O_2]_{outlet} - [O_2]_{inlet})_{loop} - K_l a_{l,loop} ([O_2] - [O_2^*])_{loop} V_{loop} \quad \text{Equation 12}$$

In Equation 12, PO_2 refers to oxygen production (mg/L h), Q_{liquid} is the caudal of the liquid (L/s), O_2 refers to dissolved oxygen, $K_l a_l$ refers to mass transfer coefficient (h^{-1}) and V refers to the volume (L).

In addition to this, it has been also reported in Mendoza et al., (2013b) that the global mass transfer coefficient at the paddlewheel is in the $164 h^{-1}$ range. This remains constant as it is a function of the paddlewheel configuration and the rotation speed, which stays constant despite the solar radiation and the culture conditions imposed on the reactor. Consequently, by knowing the photosynthetic production of oxygen from Equation 13 and the global mass transfer coefficient for the paddlewheel, the global mass transfer coefficient for the sump can be easily calculated using Equation 16.

$$NO_{2, sump} = O_{2, accumulation} - PO_{2, loop} - NO_{2, loop} - NO_{2, paddlewheel} \quad \text{Equation 13}$$

$$NO_{2, sump} = K_l a_{l, sump} ([O_2] - [O_2^*])_{sump} V_{sump} \quad \text{Equation 14}$$

$$K_l a_{l, sump} ([O_2] - [O_2^*])_{sump} V_{sump} = \quad \text{Equation 15}$$

$$V_{reactor} \frac{d[O_2]}{dt} - PO_{2, loop} - K_l a_{l, loop} ([O_2] - [O_2^*])_{loop} V_{loop} - K_l a_{l, paddlewheel} ([O_2] - [O_2^*])_{paddlewheel} V_{paddlewheel} \quad \text{Equation 16}$$

In this way, by using only the two dissolved oxygen probes located at the beginning and the end of the loop, it is possible to determine both the photosynthesis rate and the global mass transfer coefficient in the sump from the virtual sensors by applying the detailed equations. Given that the global mass transfer coefficient in the sump can be modified simply by varying the air gas flow, it is greatly advantageous to be able to measure this coefficient during the reactor operation. Moreover, calibration curves can be obtained to further adjust the mass transfer capacity in the sump by modifying the air flow rate.

3.7.2. Oxygen mass balance in a thin-layer cascade reactor

Oxygen mass balance was also performed to study the net oxygen production taking place in thin-layer reactors. For that aim, the dissolved oxygen concentration was measured at nine different positions in the loop of the reactor. Oxygen is produced by photosynthesis, then dissolved oxygen concentration modifies as a function of the culture conditions, especially by changes in pH, temperature and irradiance throughout the day. Therefore, for any section of the thin-layer reactor the following oxygen balance can be defined (Equation 17).

$$O_{2,inlet} + O_{2,produced} = O_{2,outlet} + O_{2,accumulation} \quad \text{Equation 17}$$

Samples were taken at different positions manually. Then, the measurements were considered as stable at each time, and net oxygen production was calculated as follows (Equation 18-Equation 20); where PO_2 represents the oxygen production.

$$O_{2,produced} = O_{2,accumulation} \quad \text{Equation 18}$$

$$O_{2,produced} = PO_2 \quad \text{Equation 19}$$

$$O_{2,accumulated} = \frac{d [O_2]}{d t} \quad \text{Equation 20}$$

The oxygen mass balance allows to calculate the oxygen production and accumulation by two methodologies, then allowing to compare them. Thus, it is possible to determine the agreement between both methods: (1) calculating the oxygen production rate by measuring the accumulation of dissolved oxygen in a closed plastic chamber of 40 mL with 2 cm depth for 5 minutes, or (2) calculating the oxygen production rate as the accumulation of dissolved oxygen along the reactor by using manual probes and considering the mass transfer capacity on the channel.

3.7.3. Oxygen mass balance in three thin-layer cascade reactors

To analyse the influence of culture conditions existing at each reactor, the oxygen mass balance was performed to study the net photosynthesis taking place in the cultures. For that objective, the dissolved oxygen concentration was measured at different positions in the loop of every reactor. Oxygen is produced by photosynthesis and is therefore modified as a function of the culture conditions, temperature and irradiance throughout the day. Therefore, for any thin layer reactor section, the following balance defines the dissolved oxygen concentration (Equation 21).

$$O_{2,inlet} + O_{2,produced} = O_{2,outlet} + O_{2,accumulation} \quad \text{Equation 21}$$

Samples were taken at different positions manually. Then, the measurements were considered as steady state, and net oxygen production was calculated as follow (Equation 22-Equation 24); where NO_2 represents the mass transfer and the mass transfer coefficient (klal) defined in Alameda-García et al., (in review) was used.

$$PO_{2,produced} = PO_{2,net} + NO_2 \quad \text{Equation 22}$$

$$PO_{2,net} = \frac{(O_{2,end} - O_{2,initial})}{Section} \times Q_{liq} \quad \text{Equation 23}$$

$$NO_2 = Fiml \times K_{lal} \quad \text{Equation 24}$$

3.8 Modelling

Modelling process requires different steps to be followed such as: experimental tests, model definition, model calibration, and model validation (Figure 3.15). Once the different experiments have been done to obtain reliable data, the second step is to filter the data to reduce the dispersion and ensure adequate data quality. Then, the model structure and parameters are defined to create the model. Afterwards, the model parameters are obtained from the calibration process by using part of the data from the experiments. Finally, the model is validated by following a cross validation procedure and using the rest of the data from the experiments. Then, the modelling process ends when the model validation successes with an adequate goodness of fitting to the real data. Otherwise, the calibration and validation processes are repeated until getting a reasonable result.

The different modelling techniques utilized in this thesis are described below.

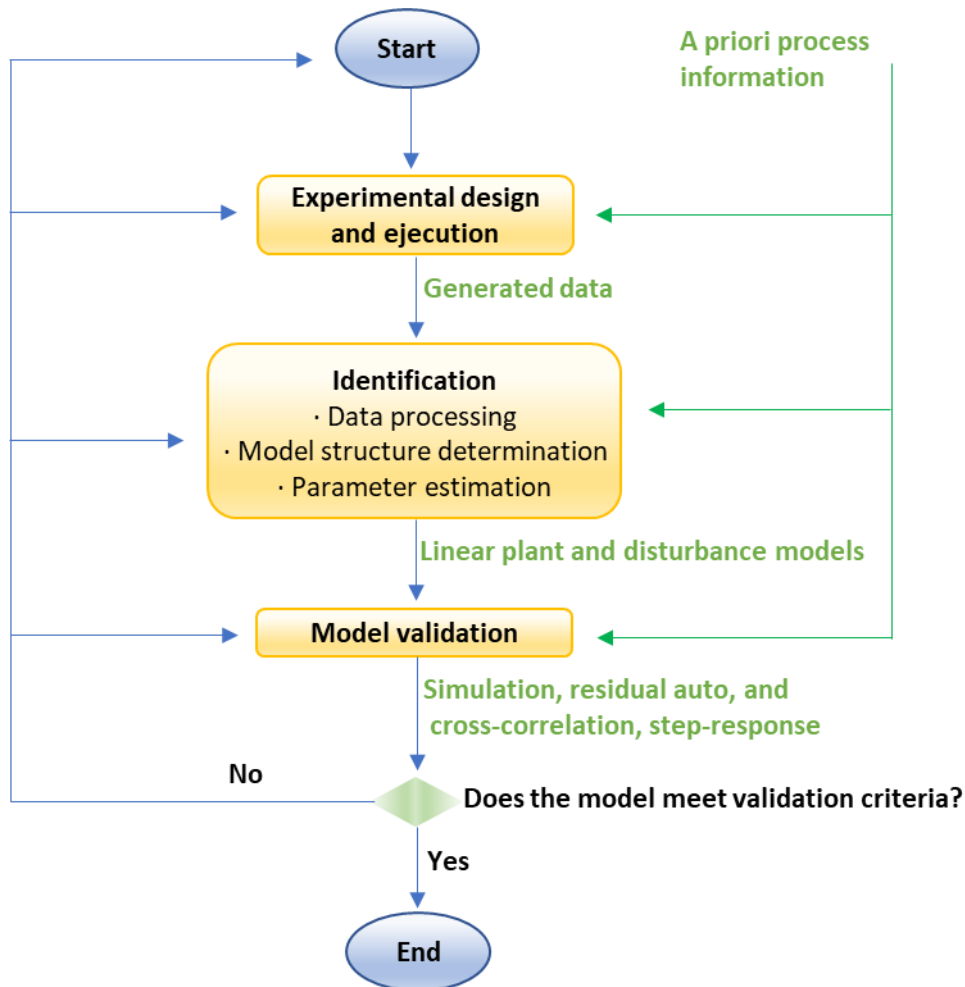


Figure 3.15. Flowchart of stages of system identification

3.8.1 Modelling light integration by microalgae in raceway reactors

This section describes the methodology used to analyse the light integration by microalgae in raceway reactors.

A total of 172 samples were taken from the raceway reactor at different times throughout the year (from February to July) and at different times of the day (8:00 h, 10:00 h, 12:00 h and 14:00 h). The photosynthesis rate (PO_2 , $\text{mg O}_2 \text{ L}^{-1} \text{ h}^{-1}$) was calculated by diluting the culture and providing the target light conditions, measuring the oxygen production over the time. The performance of the microalgae cells under continuous light conditions was evaluated first as a control stage. Following this, the performance of the cells under different light regimes was determined. In the first set of experiments, the irradiance without cells was kept at $500 \mu\text{E m}^{-2} \text{ s}^{-1}$ and the light and dark times were modified from 1 to 10 s. In the second set of experiments, the irradiance was adjusted to that existing in real outdoor reactors whereas the light and dark times were adjusted close to those experimentally determined by CFD, thus ranging from 1 to 24 s. In each experiment, the irradiance without cells (I_0), the irradiance with

cells (I), the light time, and the dark time were fixed. From these values, the different parameters were calculated. The average irradiance (I_{av}) was calculated as the light inside the jacketed vessel multiplied by the proportion of time that it was illuminated (Equation 25). The illuminated cycle proportion, Φ , was calculated as the illuminated time to total time ratio (Equation 26). The light exposure frequency, ν , was calculated as the inverse of the total cycle time (Equation 27).

$$I_{av} = I \frac{t_{light}}{t_{light} + t_{dark}} \quad \text{Equation 25}$$

$$\Phi = \frac{t_{light}}{t_{light} + t_{dark}} \quad \text{Equation 26}$$

$$\nu = \frac{1}{t_{light} + t_{dark}} \quad \text{Equation 27}$$

3.8.2 Modelling of photosynthesis rate as a function of culture conditions

In this section, photosynthesis rate was modelling according to culture conditions from in situ measurements in outdoor conditions. Different methodologies have been analysed: in situ and off-line net photosynthesis rate as well as chlorophyll-fluorescence measurements.

The existence of culture condition gradients was studied by measuring the pH, temperature and dissolved oxygen in the culture at nine different locations along the reactor length, using appropriate temperature, pH and dissolved oxygen probes (HI98198, Hanna, Spain). Measurements were carried out at different times during the daylight period to determine the variation in existing gradients throughout the day. To analyse the influence of the culture conditions existing at each reactor position on the culture performance, the net photosynthesis rate at each position was also measured. To do this, culture samples were directly taken from the reactor at the different positions and introduced into a 40 mL plastic chamber (0.02 m in depth), measuring the dissolved oxygen accumulation in this chamber over a period of 5 minutes.

In addition to the *in situ* measurements, the influence of culture conditions on the culture performance was determined offline in the laboratory, using the culture conditions (pH, temperature, dissolved oxygen and irradiance), previously found in the reactor at the different positions and times. Thus, it was possible to compare both the *in situ* experimental measurements and those determined in the laboratory under controlled conditions. Two methods were employed to evaluate the influence of culture conditions on cell performance;

the first based on the net photosynthesis rate measurements while the second involved chlorophyll-fluorescence measurements. Both are rapid methods allowing us to evaluate the culture performance in a short time. Additionally, to model the net photosynthesis rate response to changes in culture conditions, a set of experiments was performed under laboratory conditions over a wide range of pH (from 3 to 11), temperature (from 8 to 46°C), dissolved oxygen (from 0 to 400 %Sat.) and irradiance (from 100 to 2500 $\mu\text{E m}^{-2} \text{s}^{-1}$).

3.8.3 Modelling oxygen production of three thin-layer reactors

In this section, the oxygen production was modelled according to the culture conditions effects temperature and dissolved oxygen on the performance of photosynthesis activity. Firstly, temperature and dissolved oxygen gradients were analysed. Furthermore, oxygen production was modelled comparing different models.

The existence of culture conditions gradients was studied by measuring the dissolved oxygen concentration and temperature in the culture. Samples were taken from different equidistant positions (n=16 for the small reactor, n=14 for the medium, and n=18 for the large one) along each reactor, on the three different size reactors available (small=200 L, medium=600 L, large=2200 L). Measurements were done by using dissolved oxygen and temperature probes (HI98198, Hanna, Czech Republic). Measurements were carried out at different times during the daylight period (9:00, 11:00, 13:00 and 15:00 h.) to determine the variation in existing gradients throughout the day for 15 days. Oxygen production has been modelled comparing different models: Molina Grima et al., 1994 model (Equation 28), Molina Grima model including temperature effect (Equation 29), Molina Grima model including dissolved oxygen inhibition effect (Equation 30), and Molina Grima modified model (Equation 31) that uses the light frequency.

$$PO_{2(I)} = \frac{PO_{2\max} \times I^n}{I_k^n + I^n} \quad \text{Equation 28}$$

$$PO_{2(I,T)} = \frac{PO_{2\max} \times Iav^n}{I_k^n + Iav^n} \times RO2(T) \quad \text{Equation 29}$$

where RO2(T) is the cardinal temperature model from (Ippoliti et al., 2016)

$$PO_{2(I,DO2)} = \frac{PO_{2\max} \times Iav^n}{I_k^n + Iav^n} \times \left(1 - \left(\frac{DO_2}{DO_{2,\max}}\right)^m\right) \quad \text{Equation 30}$$

$$PO_{2(IavInt)} = \frac{PO_{2max} \times IavInt^n}{I_k^n + IavInt^n} \text{ where, } IavInt = \frac{Iav \times t \text{ light}}{t \text{ light} + t \text{ dark}} \quad \text{Equation 31}$$

In the previous equations, the Costache et al., 2013 parameters were used ($PO_2 \text{ max}=220$, $I_k=60$, $n=2$, $DO_2 \text{ max}= 32.09 \text{ mg/L}$, $m=5.46$). The last step was to compare each model with the experimental oxygen production (PO_2 , $\text{mg O}_2/\text{gb h}$) (Equation 32).

$$PO_{2,Experimental} = \frac{(\text{slope } DO_2) \times Qliq}{Section} \quad \text{Equation 32}$$

3.9 Control strategies

Control strategies were used to improve the operating conditions of the reactors. Two control strategies were used in the raceway reactor located at “Las Palmerillas” Experimental Station, to operate it and compare both: on/off strategy and selective control strategy. Moreover, a feedback control strategy for the air injection was used at IFAPA Experimental Station in simulation.

This thesis provides the use of different control systems to control the pH and dissolved oxygen, two very important parameters that should be controlled close to the optimal values to ensure a better production of the systems.

3.9.1. On/off control strategy

A simple feedback strategy has been used to make corrective actions based on the difference between the desired and the actual values of a variable. It can be described as follows (Equation 33):

$$U = \begin{cases} U_{max} & \text{if } e > 0, \\ U_{min} & \text{if } e < 0 \end{cases} \quad \text{Equation 33}$$

In the previous equation, the control error $e = r-y$ is the difference between the reference (or command) signal r and the output of the system y , and U is the actuation command. *Figure 3.16* shows the relation between error and control. This control law implies that maximum corrective action is always used (Åström, 2019).

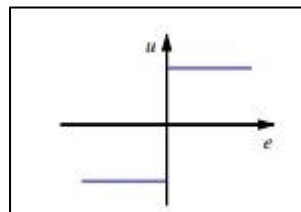


Figure 3.16. Input-output characteristics of on-off controllers

This on-off control has been used to control the pH parameter. Previous works provide promising performance results when there is an adequate CO₂ supply (Pawlowski et al., 2017).

The classical On/off controller was used by using MATLAB script as follow:

```
pH_filtrada=(sum(pH_old))/10; % pH filtered
phref_rw1=7.8; % Reference pH which depends on the strain used
ZM=0.2; % Dead zone
if pH_filtrada > phref_rw1+ZM && Rad > 50
    VCO2 =100;
else if pH_filtrada <phref_rw1-ZM;
    VCO2 = 0;
end
end
```

However, the on/off control has some drawbacks. It has not control about the amount of CO₂ injections to reduce and high pH variations are obtained (even including a dead zone). Furthermore, the valve is totally opened during the injections which may leads to increase the energy cost.

3.9.2. Selective control strategy

The event-based control strategies have been successfully applied to control pH and dissolved oxygen variables. The main difference respect to the classical control approaches is that, in the event-based approach, the control system can adapt the actuation rate to the dynamics and disturbances (Pawlowski et al., 2011). This feature is especially useful in a bioprocess application, as it has been confirmed in several recent works (Beschi et al., 2014; Pawlowski et al., 2014a, 2014b).

The selective control approach developed by (Pawlowski et al., 2015) was used. This selective event-based control scheme is shown in *Figure 3.17*, and thanks to its operation mode one can switch between the control signals provided by the pH and DO controllers. The switching between the two controllers takes place when the selective control satisfies a logical condition within the established band (control performance precision in the case of pH and a maximum limit for dissolved oxygen). It should be noted that the priority variable is the pH control, where the controller CpH tries to compensate for pH variability caused by the photosynthesis process and the CO₂ supply. When pH is within a certain range and the dissolved oxygen is close to surpassing its maximum limit, the control approach disconnects the pH control (and thus the

CO₂ injection) and switches to the dissolved oxygen control signal. In this way, the control scheme is continuously switching between both control algorithms according to the needs of both the pH and the DO control problems. Thanks to this control approach, the interaction between air injection and the deterioration in CO₂ assimilation is avoided (Pawlowski et al., 2015).

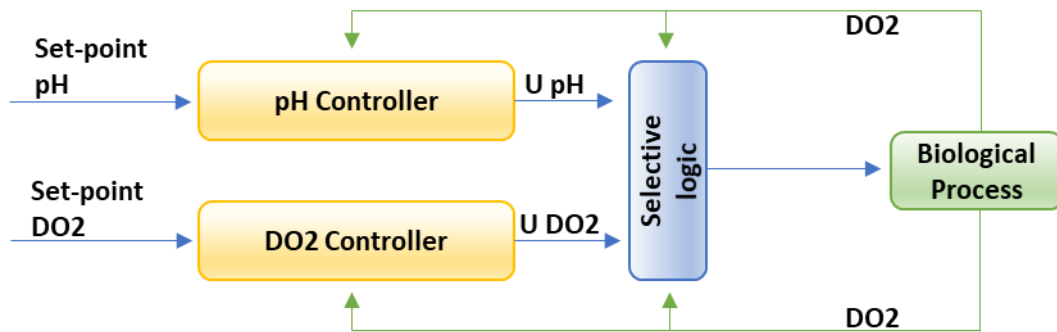


Figure 3.17. Selective control scheme for a raceway reactor (Pawlowski et al., 2015 modified).

3.9.3. Feedback control strategy for the air injection flow

A feedback control strategy with a set-point generator was developed in this thesis to regulate the air injection flow. This control approach allows to control the dissolved oxygen accumulation into the reactor by improving the mass transfer coefficient. The control strategies that have been developed until now, use a fixed air injection flow through the day. In this thesis, it is demonstrated that it is possible to save air injections actions by using a feedback control strategy, as well as, to reduce the dissolved oxygen accumulation into the reactor until values lower than the optimal dissolved oxygen imposed (usually below 250% Sat.).

The control strategy proposed in this thesis (Figure 3.18) includes two different possibilities. The first one is to set a fixed set-point for the DO₂ (that usually works at 250% Sat) and the controller opens or closes the air valve to regulate the de DO₂ by using a fixed air injection flow. This first option is the classical control approach to regulate the DO₂. On the other hand, in the second option the DO₂ set-point is estimated by using an on-line oxygen production estimation (PO₂ _{estimated}; Equation 34) and is the contribution of this thesis. Now, the set-point value is calculated by using the liquid caudal (Q_{liq}), the dissolved oxygen measurement at the loop (DO_{2Loop}) and at the sump (DO_{2Sump}). The estimation should be equal to the dissolved oxygen

desorption (NO_2 , Equation 35) to ensure lower values of dissolved oxygen than the Fixed DO_2 set-point.

$$PO_2_{estimated} = Q_{liq} \times (DO_{2Loop} - DO_{2Sump}) \quad \text{Equation 34}$$

$$NO_2 = PO_2_{estimated} \quad \text{Equation 35}$$

Then, the next step is to calculate the estimated mass transfer coefficient (Kl_{al} estimated) which is calculated at every minute (Equation 36, Equation 37). Once the estimated Kl_{al} value is obtained and the variable air gas injection set-point (L/min) is calculated at every minute by using the empirical model developed in this thesis in Barceló-Villalobos et al., (2018) (Equation 38, Equation 39). So, this air gas is injected into the system by using the proportional valve.

$$NO_2 = Kl_{al}_{estimated} \cdot (DO_{2Sump} - O_2^*) \times V \quad \text{Equation 36}$$

$$Kl_{al}_{estimated} = \frac{(PO_2_{estimated} - PO_2_{set-point})}{(DO_{2Sump} - O_2^*) \times V} \quad \text{Equation 37}$$

$$U_{gr} = \frac{Gas\ injection}{Sump\ area} \quad \text{Equation 38}$$

$$Gas\ injection = Sump\ area \times \sqrt{\frac{0.9123 \cdot Kl_{al}_{estimated}}{10379}} \quad \text{Equation 39}$$

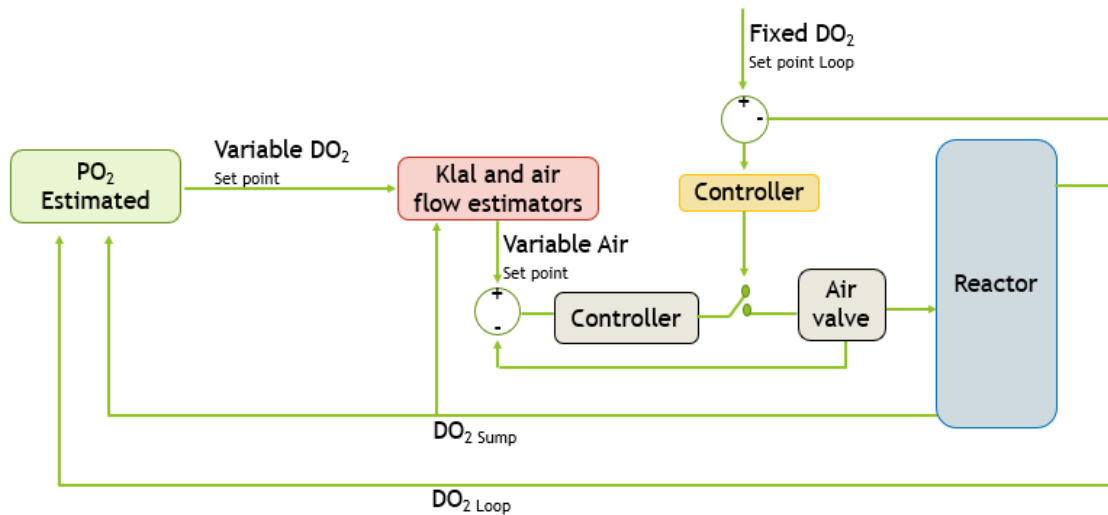


Figure 3.18. Feedback control strategy proposed to ensure optimal dissolved oxygen (DO_2) accumulation into the system

The feedback control strategy proposed has been validated in simulation by using the Fernández et al., (2016) model.

Chapter 4

RESULTS AND DISCUSSION

4. RESULTS AND DISCUSSION

Production of microalgae at a large scale requires the use of efficient photobioreactors to enhance their productivity. Two types of open reactors have been analysed: open raceway reactors and thin-layer cascade reactors, both described in the Material and Methods chapter. Some drawbacks must be solved to make this technology suitable in the future. It is well known that light integration as well as dissolved oxygen accumulation are two of the main problems that should be solved to make microalgae cultures more productive. The solutions proposed in this thesis go through the improvement of fluids dynamics, as well as, biological modelling and the development of feedback control strategies to operate the reactor automatically.

In a first step, both technologies have been characterized regarding the dynamic variations of the culture parameters (dissolved oxygen, temperature, pH and solar radiation) to identify which are the problems that should be solved to make this technology suitable for future developments. Next, the dynamics of the systems have been analysed at the different sections of the reactors (sump, loop, paddlewheel, and thin-layer's channel) to know the limitation of each one and propose new strategies to control the systems by using biological models. This is the first step to optimize and scale-up this type of reactors for industrial applications.

4.1. Characterization and improvement of raceway reactors

4.1.1. Variation of culture conditions

The variation of culture parameters in a raceway reactor has been analysed for two years. The solar irradiance on the reactors surface varies over the year ranging from 409 to 814 W/m² being the maximal value being obtained at 14:00 h in summertime. Temperature and pH are constant along the day. On the other hand, light integration and dissolved oxygen depend on the culture conditions and the solar radiation variation along the day, respectively. In terms of the culture conditions inside the reactor through a year, the mean values of pH, dissolved oxygen and temperature (*Figure 4.19*) range from 8.07 to 8.61, 146 to 220 % Sat., and 13.91 to 32.88 °C, respectively. This difference regarding temperature range is due to night cooling and daylight warming.

Regarding variation along the year, pH is a stable parameter at the set point control-imposed pH=8. Moreover, dissolved oxygen modified along the day with the solar radiation depends on the biomass concentration and the season of the year. The highest dissolved oxygen

accumulation take place during summer and spring time as expected, and the maximum value is lower than 250%Sat according to the control strategy imposed. On the other hand, the lower range is during winter. Furthermore, the highest temperature corresponds to summer whereas the lowest was in winter. Spring and autumn have similar temperature pattern.

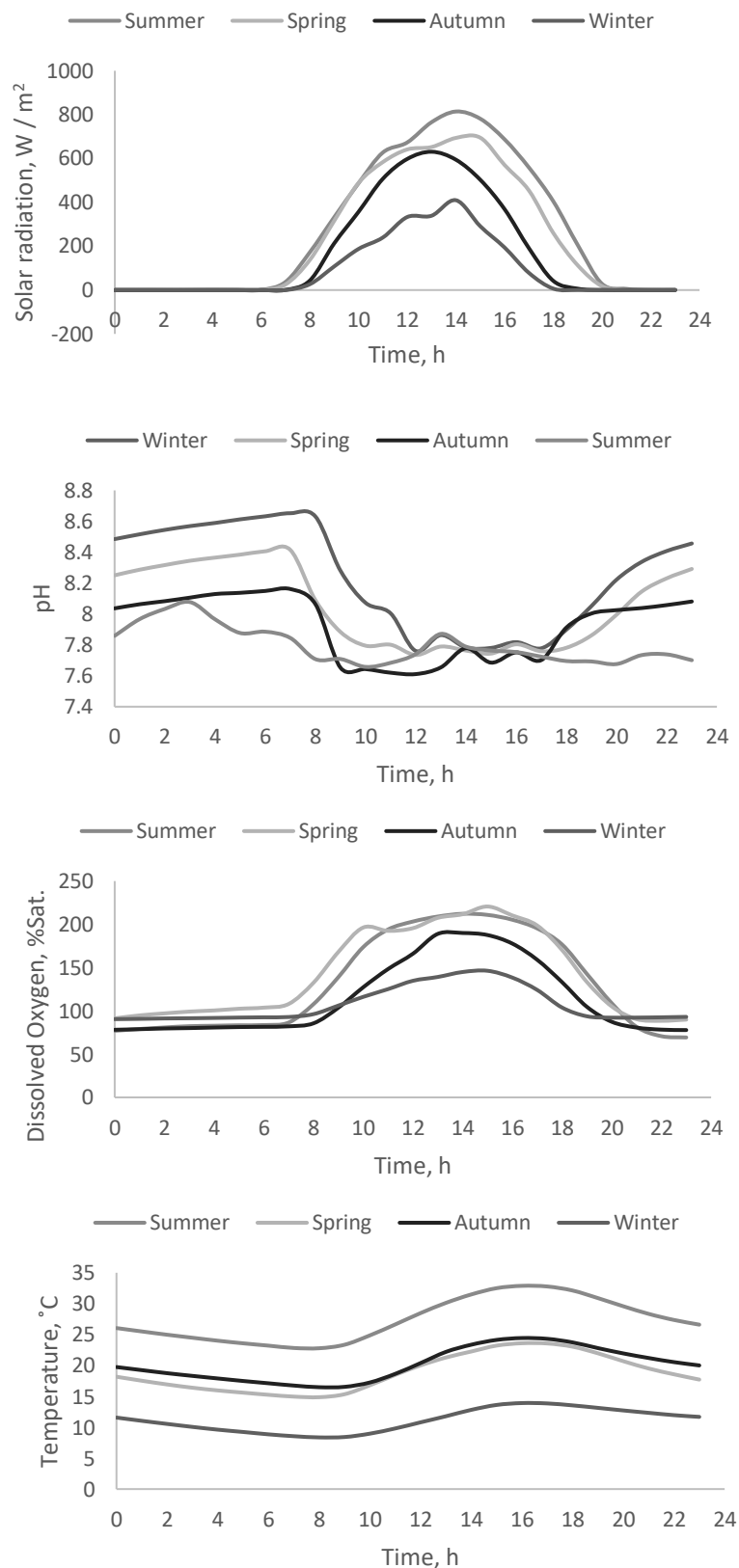


Figure 4.19. Variation of culture parameters (Solar radiation, pH, Dissolved oxygen, and Temperature) in the 100 m² raceway reactor located in the experimental station “Las Palmerillas” (Almería, Spain). Mean values from two years assays

4.1.2. Oxygen mass transfer capacity

Regarding dissolved oxygen concentration, it has been demonstrated that there is an accumulation along the day due to the high oxygen production rate, which can reach values over 6 g/min in summer time (Barceló-Villalobos et al., 2018). Previous works demonstrated that there is a negative effect of excess of dissolved oxygen concentration on the photosynthesis rate (Pawlowski et al., 2015). That is the reason for which dissolved oxygen concentration over 250 %Sat (22 mg/L) should be avoided, to make open reactors a more productive technology. Notice that this contribution is very important to define dissolved oxygen set-points in the control algorithms.

A solution to avoid dissolved oxygen accumulation has been proposed in the present thesis through the improvement of the mass transfer capacity of the system. To achieve this, the variations in the volumetric mass transfer coefficient in the sump has been studied and modelled as a function of the air flow rate (L/min), and therefore the superficial gas velocity in the sump (m/s). Moreover, the developed model has been used to estimate the mass transfer requirements in the sump as a function of the target dissolved oxygen concentration and the oxygen production rate. This would allow to automatically control the system and to reduce the oxygen accumulation significantly along the year, as a function of overall oxygen production rate at each moment.

Results presented in (Barceló-Villalobos et al., 2018) demonstrated that dissolved oxygen is accumulated in raceway reactors when no appropriate mass transfer capacity is provided. Moreover, the sump is the main section that contributes to the oxygen removal. Furthermore, it is reported that the mass transfer capacity is a relevant parameter that can be used in a control strategy. Furthermore, it has also been demonstrated that mass transfer capacity can be improved by controlling the air flow into the sump. Controlling the efficiency of these inputs, it is far enough to control the oxygen accumulation until concentrations of 15 mg/L along the year. Thus, an empirical model ($K_{La} = 10379 U_{gr}^{0.9123}$, $R^2 = 0.9772$) has been developed that relates the gas inflow with the mass transfer coefficient (h^{-1}) of the system (*Figure 4.20*) (Full information is available in Barceló-Villalobos et al., 2018). The proposed model allows to determine and optimize the mass transfer capacity in the sump for any existing raceway reactor.

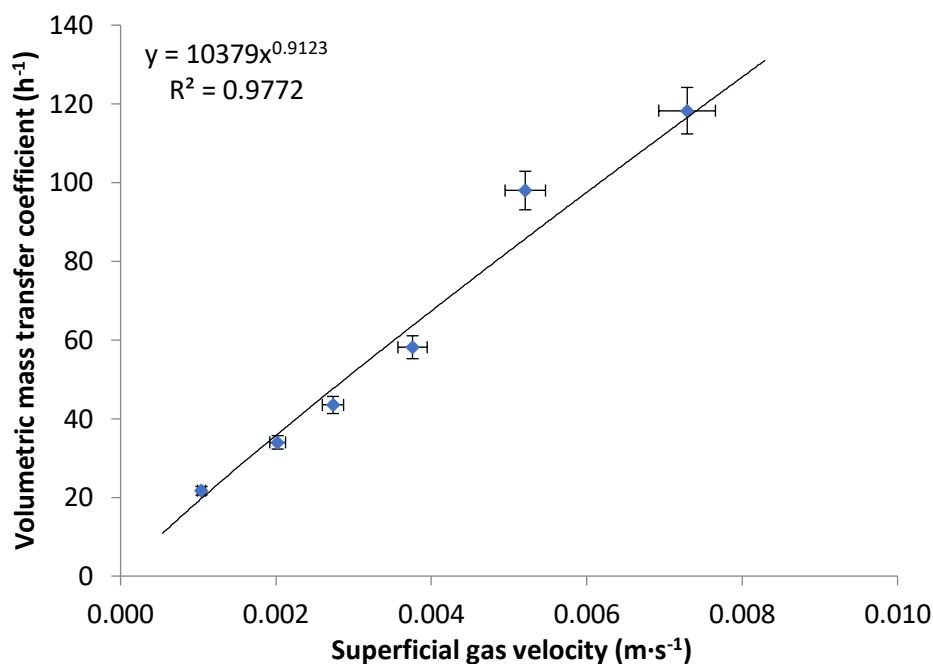


Figure 4.20. Variation in the mass transfer coefficient in the sump as a function of the air flow rate, expressed as the superficial gas velocity. Values obtained using the proposed methodology to estimate the mass transfer coefficient in raceway reactors. Data shown as mean \pm SD, $n=31$.

4.1.3. Light integration

Light gradients exist in any microalgae culture as a function of solar radiation, geometry and optical properties of the culture. Moreover, the light regime at which the cells are exposed to in any system is also a function of movement of the cells along this gradient, being defined as light history of the cells. Photosynthesis rate is a function of irradiance at which the cells are exposed to. When exposition to light is fast enough to achieve integration of light by the photosynthetic apparatus, the maximal performance is obtained. In the opposite, when the cells expend too much time at each position, local adaptation takes place and the lower performance is achieved. To determine the extension of light integration phenomena in raceway reactors is mandatory to determine how to optimize it.

For that, a simple simulation exercise was performed considering the operation of the 100 m² raceway reactor under the culture conditions imposed (Dilution rate=0.2 day⁻¹, $C_b=1.2$ g·L⁻¹). Knowing the extinction coefficient of the biomass ($K_a=0.15$ m²·g⁻¹), the light profile inside the reactor at different solar hours/irradiance could be estimated using the Lambert's law (Figure 4.21A). This was performed in a spring day in Almería (Spain) where the raceway reactor is located. The results show how the irradiance inside the reactor exponentially decreased with culture depth regardless to the solar irradiance on the reactor surface. This is because only the first 0.04 m (approximately) of the culture receives a light intensity greater than the minimum

value, of $I_c=40 \mu\text{E}/\text{m}^2\cdot\text{s}$, required for photosynthesis. Therefore, approximately 73% of the culture is in total darkness, receiving insufficient light for photosynthesis to take place. From this data, the maximal proportion of illuminated culture was calculated to be 27%. In terms of the photosynthesis rate, by considering the local irradiance at different culture depths and the hyperbolic growth model found in springtime, the variation in the photosynthesis rate with the culture depth at different solar irradiances can also be easily calculated (*Figure 4.21B*). The results show how most of the photosynthesis took place in the first 0.035 m of culture; only at a very high irradiances did photosynthesis take place at culture depths greater than 0.050 m. However, independent of the solar irradiance, there is always a large reactor volume performing respiration in complete darkness.

In most studies focusing on the flashing effect, light is represented as an oversimplified on/off signal. A better option is to represent the light pattern, assuming that the light source switches between two intensities (Demory et al., 2018). However, an even better approach is obtained when considering the light profile on the entire reactor, as demonstrated here, as well as using the complete optimal light regime history (although this requires more complex and time-consuming computing efforts) (Brindley et al., 2016).

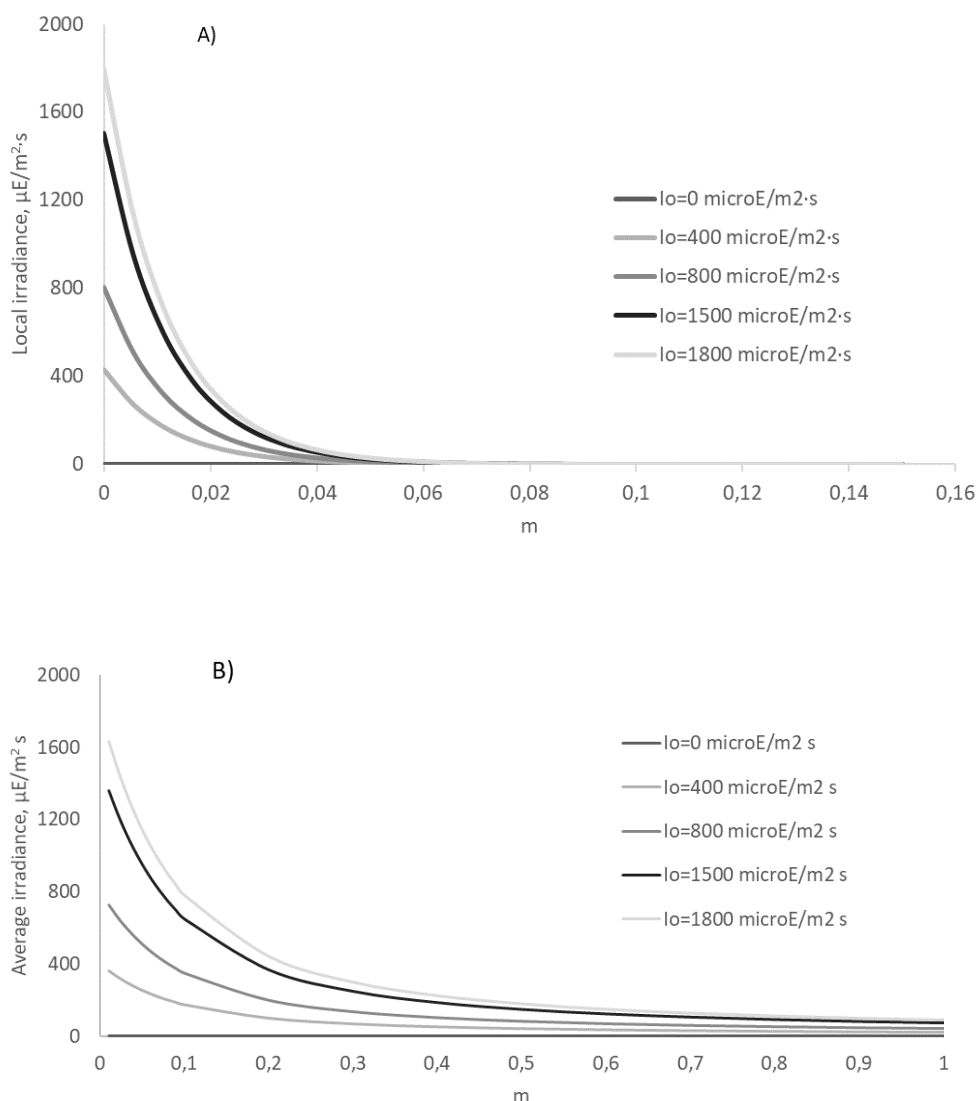


Figure 4.21. Variation in the local irradiance (A) and average irradiance (B) with the culture depth for a *Scenedesmus almeriensis* culture produced in a 100 m² raceway reactor in continuous mode at 0.2 day⁻¹.

Moreover, it has also been demonstrated that the cells are fully adapted to local irradiances which was validated in the real outdoor raceway at different seasons (winter, spring, summer) (Barceló-Villalobos et al., 2019a). In this sense, the first set of experiments was performed taking the culture from the raceway reactor and evaluating its photosynthesis rate under laboratory conditions. Outdoor conditions were simulated by providing light and dark times based on the experimental results from a raceway reactor. For this, a complete factorial experimental design was performed considering light and dark times of 1, 2, 3, 4, 5 and 10 s, and the photosynthesis rate under these conditions was determined (Figure 4.22). Based on the irradiance provided, the maximum photosynthesis rate, PO_{2io} , was calculated using the Molina-Grima hyperbolic model (Equation 40). By employing the average irradiance to which the cells were exposed to, calculated as the irradiance provided multiplied by the percentage of time by which it was provided, the theoretical maximal photosynthesis rate with full light integration (PO_{2iav}) was

determined (*Equation 41*). Conversely, the theoretical minimum photosynthesis rate, if null light integration took place, PO_{2local} , was calculated as the sum of the photosynthesis rate during light and dark periods, both calculated using the same hyperbolic model previously determined (*Equation 42*). The experimental photosynthesis rate, PO_{2exp} , must be midway between these two limit values. Results show as the higher the frequency at which the light was provided, the greater the light integration with the experimental values of the photosynthesis rate approaching the PO_{2iav} values.

$$PO_{2io} = \frac{PO_{2max} \times I_o^n}{I_k^n + I_o^n} + RO_2 \quad \text{Equation 40}$$

$$PO_{2iav} = \frac{PO_{2max} \times I_{av}^n}{I_k^n + I_{av}^n} + RO_2 \quad \text{Equation 41}$$

$$PO_{2local} = (PO_{2io} \cdot \Phi)_{light} + (RO_2 \cdot (1 - \Phi))_{dark} \quad \text{Equation 42}$$

Future works should be necessary to know the PO_{2max} , and I_k values for different strains. Furthermore, additional experiments should be done to implement this model (*Equation 42*) in the SCADA architecture and connect it to the actuators related to the culture depth operational conditions to increase the efficiency of solar radiation assimilation.

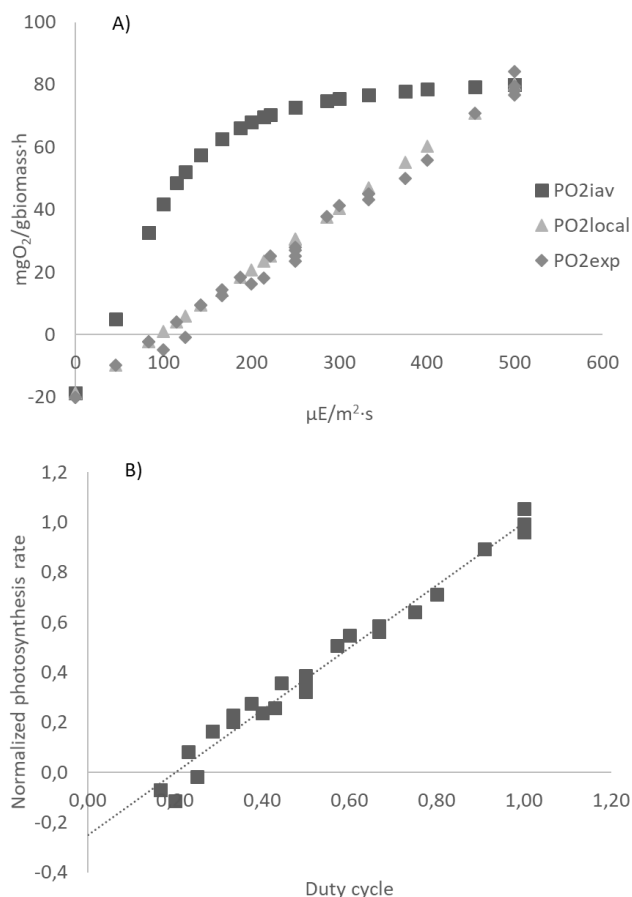


Figure 4.22. (A) Variation in the photosynthesis rate ($\text{mg O}_2/\text{g biomass h}$) of *Scenedesmus almeriensis* cultures in a raceway reactor as a function of the average irradiance ($\mu\text{E}/\text{m}^2 \text{s}^{-1}$) to which the cells were exposed, under different light/dark cycles ranging from 1 to 10 s. PO_2iav corresponds to the modelled photosynthesis rate if complete light integration takes place; whereas PO_2local corresponds to the modelled photosynthesis rate with null light integration. (B) Variation in the normalized photosynthesis rate with the duty cycle for the same experiments.

To validate this fact, a large set of experiments was performed over six months, maintaining the raceway reactor in semi-continuous mode and taking samples from the reactor to evaluate the photosynthesis rate in the laboratory, simulating the real light/dark cycles at which the cells were exposed to inside the outdoor reactor. In this case, the external irradiance provided was that found in the outdoor reactor at different daylight times, where several samples were measured each day at different hours of the day, with light times ranging from 1 to 8 s while dark times ranged from 1 to 24 s. To take into consideration the variation in culture conditions at different seasons, the performance of the cells was periodically evaluated taken directly from the reactor under continuous light. In this way, the P-I curve of the culture was obtained as a control curve. The results confirmed that the hyperbolic model is always suitable to fit the light response of the *Scenedesmus almeriensis* cells, including from real outdoor reactors in different seasons (Figure 4.23). However, the results clearly show how the behaviour was not the same for all the seasons evaluated. The cultures grown in spring performed better than those grown in summer and winter. By fitting the experimental data to the hyperbolic

model, the characteristic parameter values were calculated for the cultures obtained in each season (see *Table 1*). The values were similar to the previous ones not only in terms of the maximal photosynthesis rate and the half-saturation irradiance, but also in terms of the respiration rate and the minimum irradiance required to start photosynthesis. The major difference was for the maximum photosynthesis rate, which was notably high for the culture grown in spring; thus, indicating the adequacy of the operating conditions during this period.

To consider the variation in cell performance along the different seasons, the analysis of the influence of average irradiance and light/dark cycles on the performance of outdoor cultures was applied to the entire set of data from the six-month operation of the raceway reactor. Hence, *Figure 4.24* demonstrates a slightly better correlation in the winter time, what it is also highly acceptable for spring and summer time, especially considering the large variations in culture conditions that take place in outdoor reactors and the large number of measurements taken (up to 172). In Barbosa et al., (2003) study, the effect of a medium-frequency cycle time (10–100 s) and light fraction (0.1–1) on the growth rate and the biomass yield of the microalgae *Dunaliella tertiolecta* was studied. The biomass yield and growth rates were mainly affected by the light fraction while the cycle time had little influence (Barbosa et al., 2003).

This thesis also demonstrated that the continuous light model from Molina Grima et al. (1994) is appropriate for a raceway reactor with a biomass concentration ranging from 0.2-0.4 g/L (Barceló-Villalobos et al., 2019a) working in continuous mode at a dilution rate of 0.2 day⁻¹.

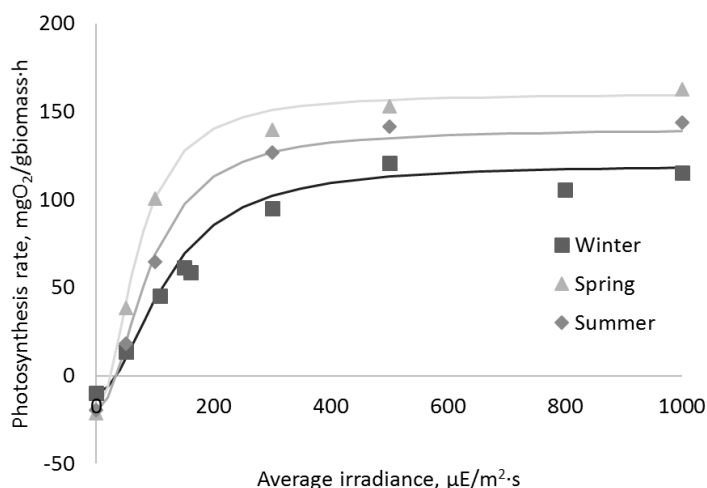


Figure 4.23. Variation in the photosynthesis rate with average irradiance for three *Scenedesmus almeriensis* samples produced in a 100 m² raceway reactor in continuous mode at 0.2 day⁻¹ for different seasons.

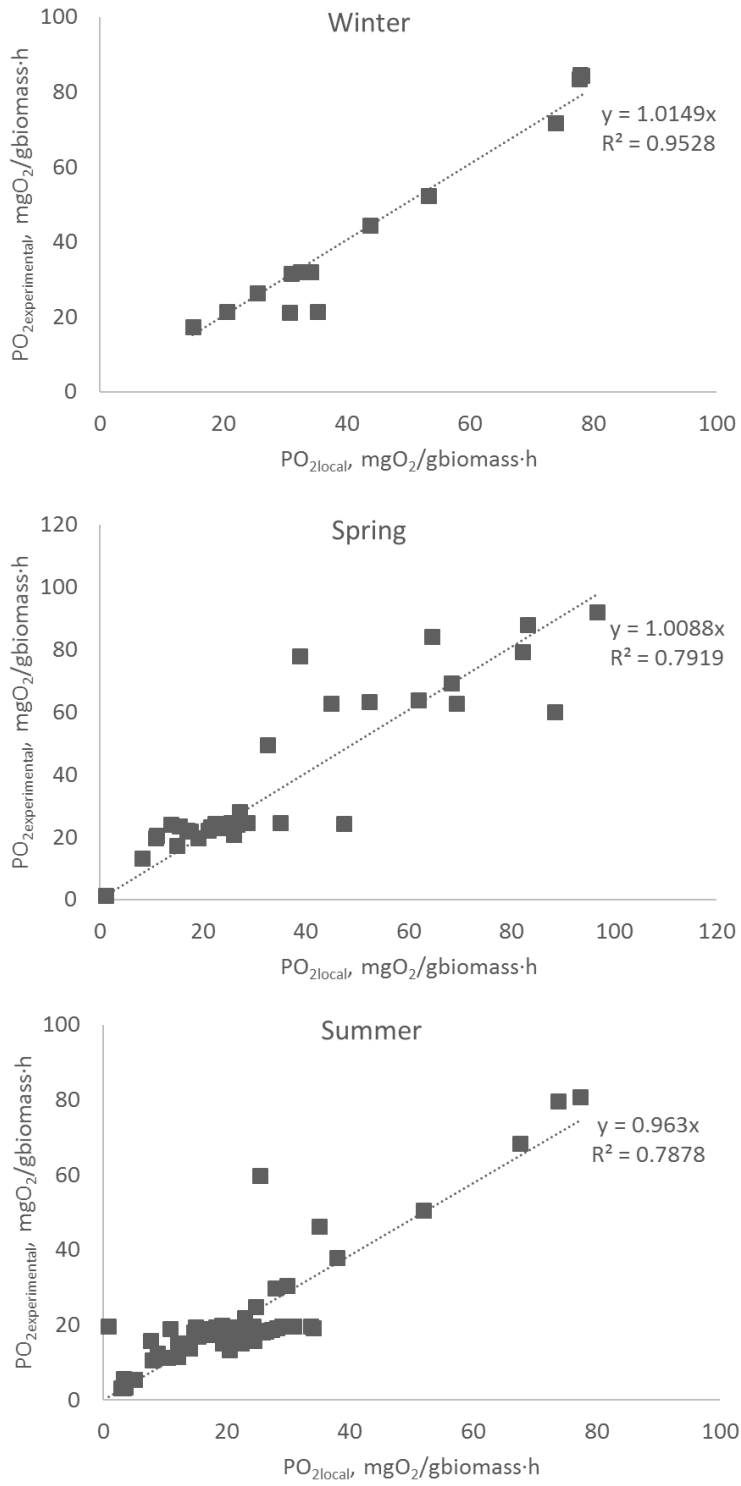


Figure 4.24. Correlation between the experimental and local photosynthesis rate of *Scenedesmus almeriensis* samples produced in a 100 m² raceway reactor in continuous mode at 0.2 day⁻¹ for different seasons.

Table 1. Characteristic parameter values of the hyperbolic model determined from the different samples studied: samples from the same reactor at different biomass concentrations; samples from the same reactor in different seasons.

Cb	PO2 max	n	lk	RO2	lc	Φ
g/L	mg O₂/gb h		μE/m² s	mg O₂/gb h	μE/m² s	%
0.1	101.3	2.01	82.2	-18.7	40.0	0.93
0.2	101.4	1.99	90.5	-18.9	43.0	0.86
0.4	63.5	2.00	61.3	-18.5	39.0	0.75
Season	PO2 max	n	lk	RO2	lc	Φ
	mg O₂/gb h		μE/m² s	mg O₂/gb h	μE/m² s	%
Winter	130.0	2.00	120.0	-10.0	35.0	0.86
Spring	180.0	2.00	70.0	-20.0	26.0	0.86
Summer	160.0	2.00	90.0	-20.0	34.0	0.86

4.2. Characterization and improvement of thin-layer reactor

Thin-layer cascade reactors have been less studied and developed than raceway reactors. Moreover, they have been demonstrated to be more efficient than raceway reactors due to the lower light path that enhances the light regime at which the cells are exposed to in this type of systems, thus achieving higher biomass productivities (Morales-Amaral et al., 2015). These reactors are usually operated at culture depths ranging from 0.006 m to 0.020 m (Masojídek et al., 2011). It is very important to know the major bottlenecks limiting the capacity of this type of reactors for its further improvement for industrial purposes.

4.2.1. Variation of culture conditions

The variation of culture conditions in thin-layer reactors was studied (Temperature, pH and dissolved oxygen) (*Figure 4.25*) (Full information available in Barceló-villalobos et al., 2019b). Results demonstrated that no gradients of temperature take place in thin-layer reactors along the channel, or they are not relevant, at least during the 80 m of the entire channel. This is due to the short residence time of the culture into the channel, when it is exposed to solar radiation.

Regarding the pH, results showed that the pH slightly increases along the channel. That means that the existence of pH gradients along the channel can be neglected or they are so small to have a large influence into the performance of the cultures. This small pH change along the channel is explained by the on-demand injection of CO₂ and the large buffer capacity of

carbonate-bicarbonate buffer existing into the culture medium, that allows to compensate the consumption of inorganic carbon by photosynthesis along the channel. However, the increase of pH with time, and moreover, the existence of pH values upper than set point of 8.0, indicates that overall CO₂ injection could be inadequate in some cases. According to these results, the CO₂ consumption by the microalgae was higher than the CO₂ transference capacity, and although pH values are not too high, the mean hourly value increases from 8.1 to 8.6.

Regarding dissolved oxygen concentration, a much larger variation with both the position and time was observed. It clearly increases with the position due to the accumulation of oxygen produced by photosynthesis along the channel, the desorption capacity on the channels being not enough to remove this oxygen. Along the day, the larger average irradiance also enhances the production of oxygen, and gradients of dissolved oxygen concentration increases. Mean values of dissolved oxygen concentration vary from 141 to 197 % but values up to 225 %Sat were experimentally determined at the end of the channel at 13:00, including in a cloudy day.

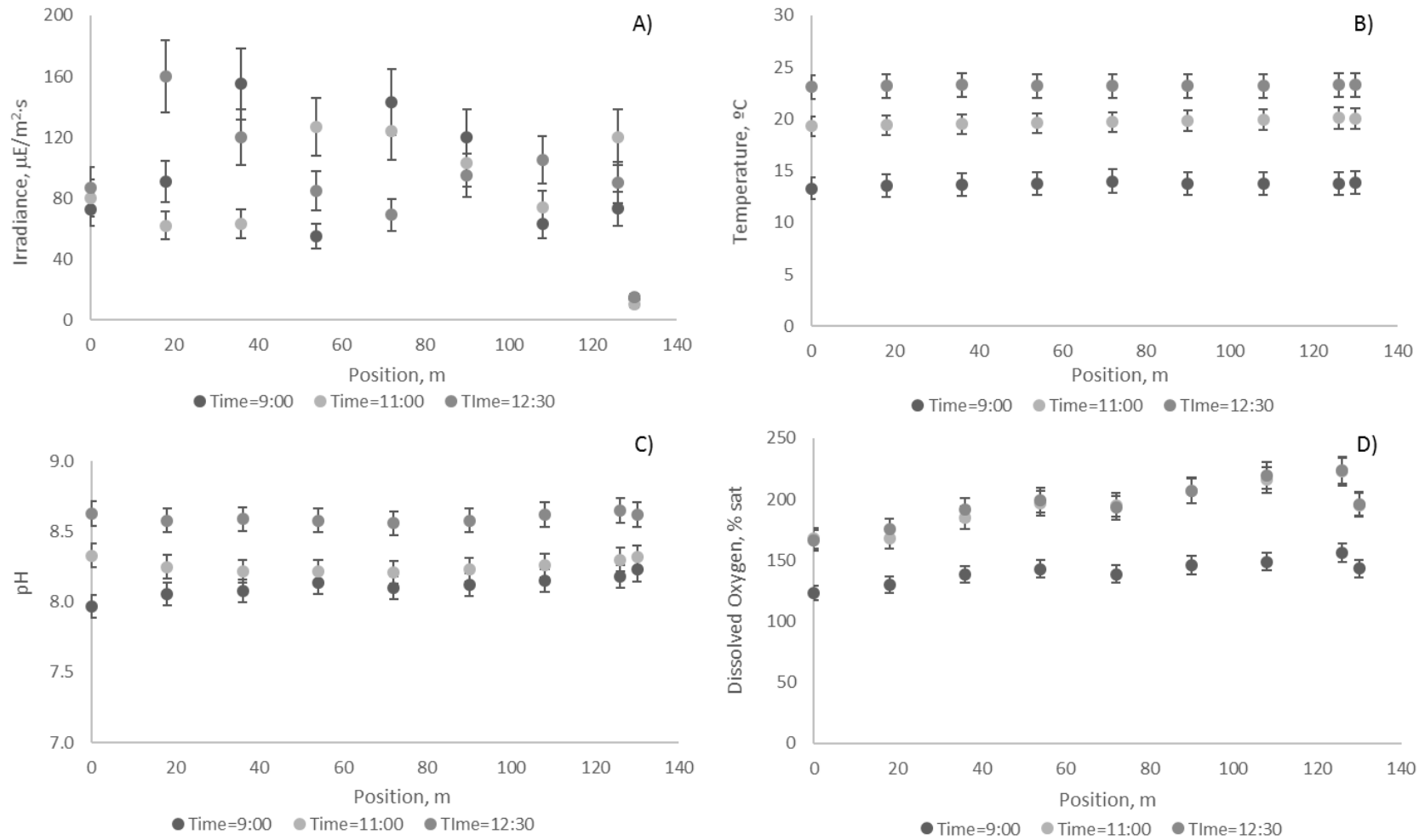


Figure 4.25. Variation in culture parameters (temperature, pH and dissolved oxygen) with the position and time of day in the thin-layer reactor operated in continuous mode at 0.3 day^{-1} at the IFAPA research centre.

4.2.2. Oxygen mass balance

This is the first time that mass transfer capacity has been determined in thin-layer cascade reactors, which highly influences on the productivity of these systems. Dissolved oxygen (mg/L) measurements were done along the channel as well as oxygen production measurements (mg/L h) along different days (n=5) by using the following equation (Equation 43). As a result, a mass transfer coefficient of 9.25 h^{-1} was calculated (Alameda-García, et al., in review). This value is higher than the mass transfer coefficient calculated before for a raceway 0.9 h^{-1} in (Mendoza et al., 2013a). That difference could be due to the different culture depths 0.15 m and 0.02 m in raceway and thin-layer cascade respectively.

$$k_{lal} = \frac{Q_{liq} \cdot (DO_{in} - DO_{out}) + \frac{d DO}{dt} \cdot V}{F_{i_{ml}} \cdot V} \quad \text{Equation 43}$$

In Equation 43, the different parameters used were: mass transfer coefficient (K_{lal}), caudal of liquid (Q_{liq}), dissolved oxygen concentration (DO), volume (V) and logarithmic mean driving force ($F_{i_{ml}}$).

4.2.3. Modelling the net photosynthesis rate

To confirm the influence of changing culture conditions on the cell performance off-line, measurements were performed in the laboratory to simulate the culture conditions prevailing outdoors. For this purpose, the net photosynthesis rate and chlorophyll-fluorescence methods were used. Regarding the net photosynthesis rate, different assays were carried out to modify the irradiance to which the cells were exposed to. Results show the Monod's type light curve response of the photosynthesis rate (*Figure 4.26*). These assays were performed under the optimal conditions of temperature (25°C), pH (8.0) and dissolved oxygen ($9 \text{ mg/L} = 100 \text{ \%Sat.}$). By fitting the experimental values to the hyperbolic model proposed by Molina et al., (Equation 44) (Molina-Grima et al., 1994), the characteristic parameter values of the model were obtained ($PO_{2,max}=380 \text{ mgO}_2/\text{L}\cdot\text{h}$, $I_k=200 \text{ }\mu\text{E}/\text{m}^2\cdot\text{s}$, $n=2$). Therefore, the curve that represents the model for the entire solar radiation range can be simulated. *Figure 4.26* shows how the model accurately represents the experimental data. Moreover, it can be concluded that a maximal photosynthesis rate of $350 \text{ mgO}_2/\text{L}\cdot\text{h}$ is achieved at the average irradiances of $500 \text{ }\mu\text{E}/\text{m}^2\cdot\text{s}$; that is because the

culture becomes saturated above this value. These assays were carried out under controlled conditions of biomass concentration of 0.2 g/L.

$$PO_2 = \frac{PO_{2,max} \cdot I_{av}^n}{I_k^n + I_{av}^n} \quad \text{Equation 44}$$

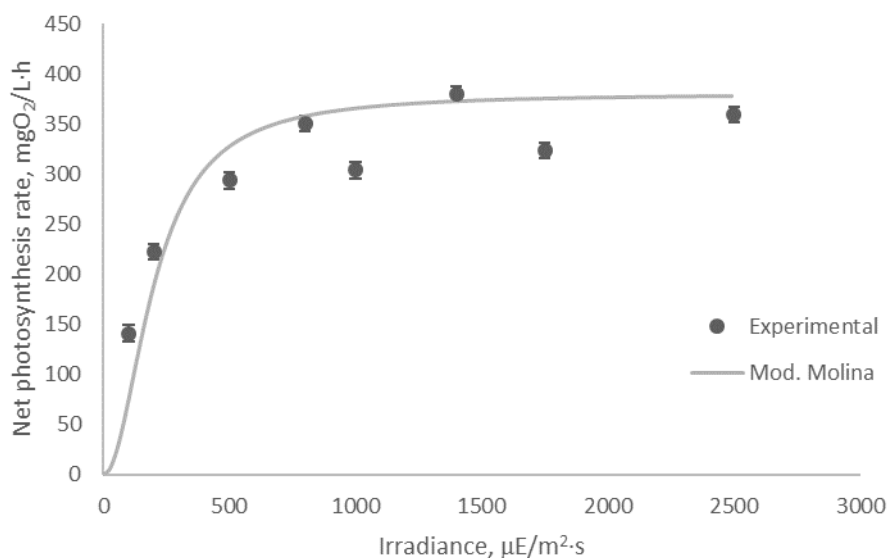


Figure 4.26. Off-line measurements of the photosynthesis rate versus the irradiance for samples directly taken from the reactor.

The net photosynthesis rate response was analysed under different culture parameters (temperature, pH and dissolved oxygen) conditions. Thus, net photosynthesis rate measurements were taken at different temperature, pH and dissolved oxygen ranges. For each set of data, the experimental photosynthesis rate values were normalized (by dividing each value between the maximum value) to better understand the values obtained and compare them with the final value obtained.

Regarding the temperature parameter, the results show that when it is below 26°C, or above 34°C, the culture performance is significantly reduced. Furthermore, at temperatures of 12°C and 46°C, the photosynthesis rate is highly neglected (*Figure 4.27A*). In the case of pH, a similar trend was observed. The net photosynthesis rate is close to the maximal value from 5.7 to 8.0; outside of this range, it is highly reduced nearing zero at pH values of 3 and 10 (*Figure 4.27B*). Regarding the influence of the dissolved oxygen concentration, a different trend was observed. The photosynthesis rate remains constant at dissolved oxygen concentrations below 15 mg/L (135 %Sat.), whereas above 20 mg/L (180 %Sat.), it nears zero (*Figure 4.27C*). These results confirm previous studies concerning the effect of culture conditions on *Scenedesmus almeriensis*, which showed that the optimal pH should be in the range of 7.0 to 9.0, and the

maximal photosynthesis activity to be at a temperature of 35 °C, reducing dramatically at temperatures above this value (Costache et al., 2013).

The experimental figures can be fitted to the different models (Equation 45-Equation 47) in order to model the influence of culture conditions on cell performance. In case of temperature and pH, to use the cardinal model is recommended (Bernard and Rémond, 2012; Ippoliti et al., 2016), whereas for dissolved oxygen, to use models that consider the inhibition by product is advised (Costache et al., 2013).

$$RO2(T) = \frac{(T - T_{max})(T - T_{min})^2}{(T_{opt} - T_{min}) \left(((T_{opt} - T_{min})(T - T_{opt})) - ((T_{opt} - T_{max})(T_{opt} + T_{min} - 2T)) \right)} \quad \text{Equation 45}$$

$$RO2(pH) = \frac{(pH - pH_{max})(pH - pH_{min})^2}{(pH_{opt} - pH_{min}) \left(((pH_{opt} - pH_{min})(pH - pH_{opt})) - ((pH_{opt} - pH_{max})(pH_{opt} + pH_{min} - 2pH)) \right)} \quad \text{Equation 46}$$

$$RO2(DO_2) = 1 - \left(\frac{DO_2}{DO_{2,max}} \right)^m \quad \text{Equation 47}$$

The different parameters used in the previous equations were: temperature (T), maximum temperature (Tmax), minimum temperature (Tmin), optimum temperature (Topt), maximum pH (pH max), minimum pH (pHmin), optimum pH (pHopt), dissolved oxygen (DO₂), maximum dissolved oxygen (DO₂ max).

In terms of the temperature, the maximum and minimum tolerable temperatures were 48°C and 7°C, respectively, while the optimal temperature was 30°C. For pH, the maximum and minimum tolerable values were 9.6 and 2.0, respectively, whereas the optimal pH was 6.8. In the case of the dissolved oxygen concentration, the maximum dissolved oxygen concentration tolerated by the culture was 25 mg/L (225 %Sat.).

Results from *in situ* net photosynthesis measurements are comparable to those obtained when evaluating the electron transfer rate of the cells in the reactor by taking chlorophyll fluorescence measurements. The data in Figure 4.28 show that temperature has a negative effect on the electron transfer rate at values of 8°C and 46°C, with no photo inhibition being observed up to 1500 μE/m² s. Regarding pH, an adverse effect was observed at values below pH 5 and above pH 8; the lowest electron transfer rate being measured at pH 3. Finally, regarding the influence of dissolved oxygen, a similar trend was observed to that of the photosynthesis rate – the electron transfer rate showed a similar trend to that of irradiance at dissolved oxygen concentrations below 150% Sat. Above this value, it is significantly reduced. The utilization of Chlorophyll-fluorescence measurements to identify adverse culture conditions in thin-layer reactors has already been reported. They are also recommended as a rapid tool for optimizing water depth in these types of reactors (Jerez et al., 2014, 2016).

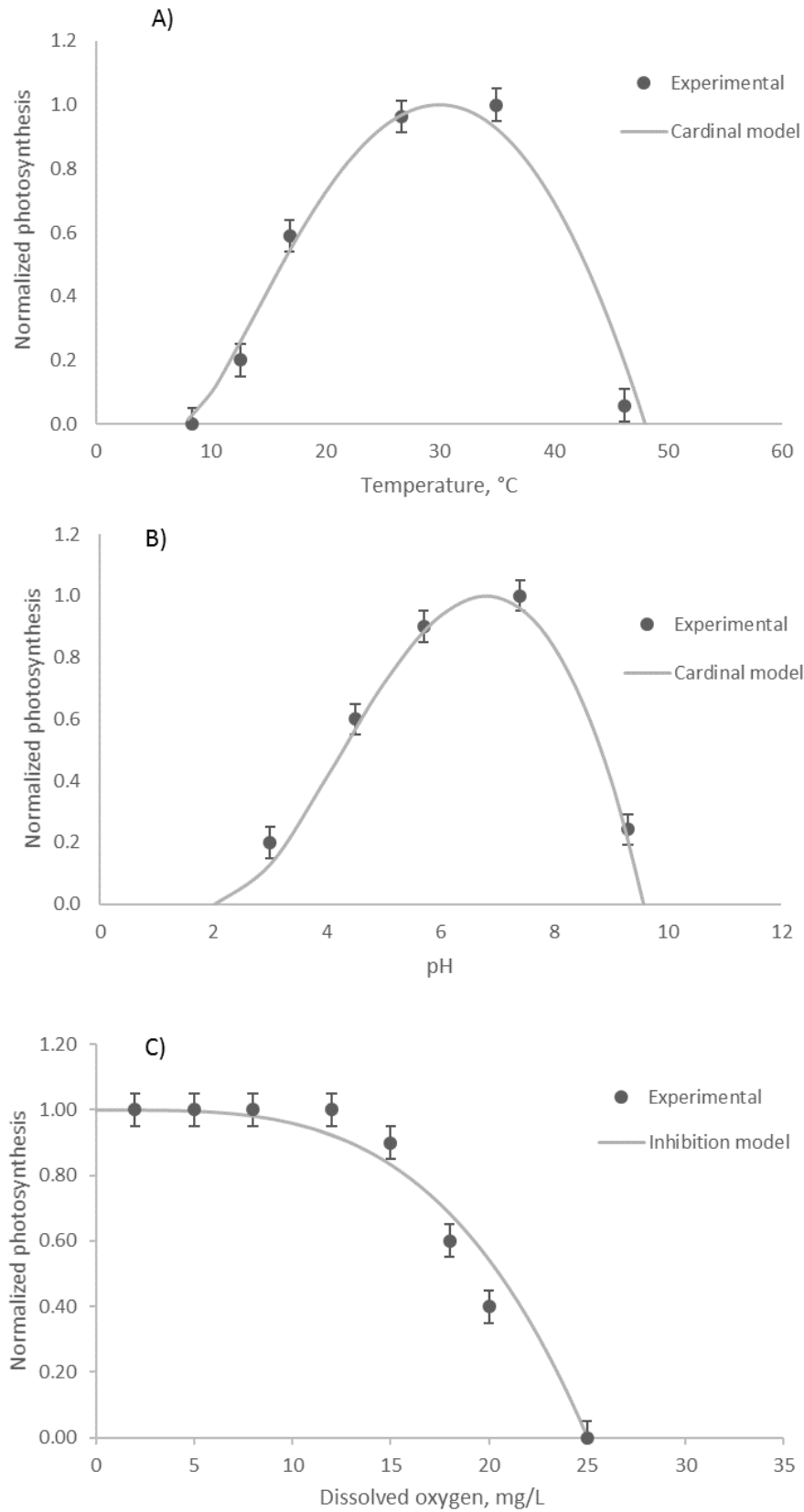


Figure 4.27. Influence of temperature (A), pH (B) and dissolved oxygen (C) on the normalized photosynthesis rate of *Scenedesmus almeriensis* at an irradiance of $200 \mu\text{E m}^{-2} \text{s}^{-1}$. Lines correspond to the proposed models (Equation 45- Equation 47).

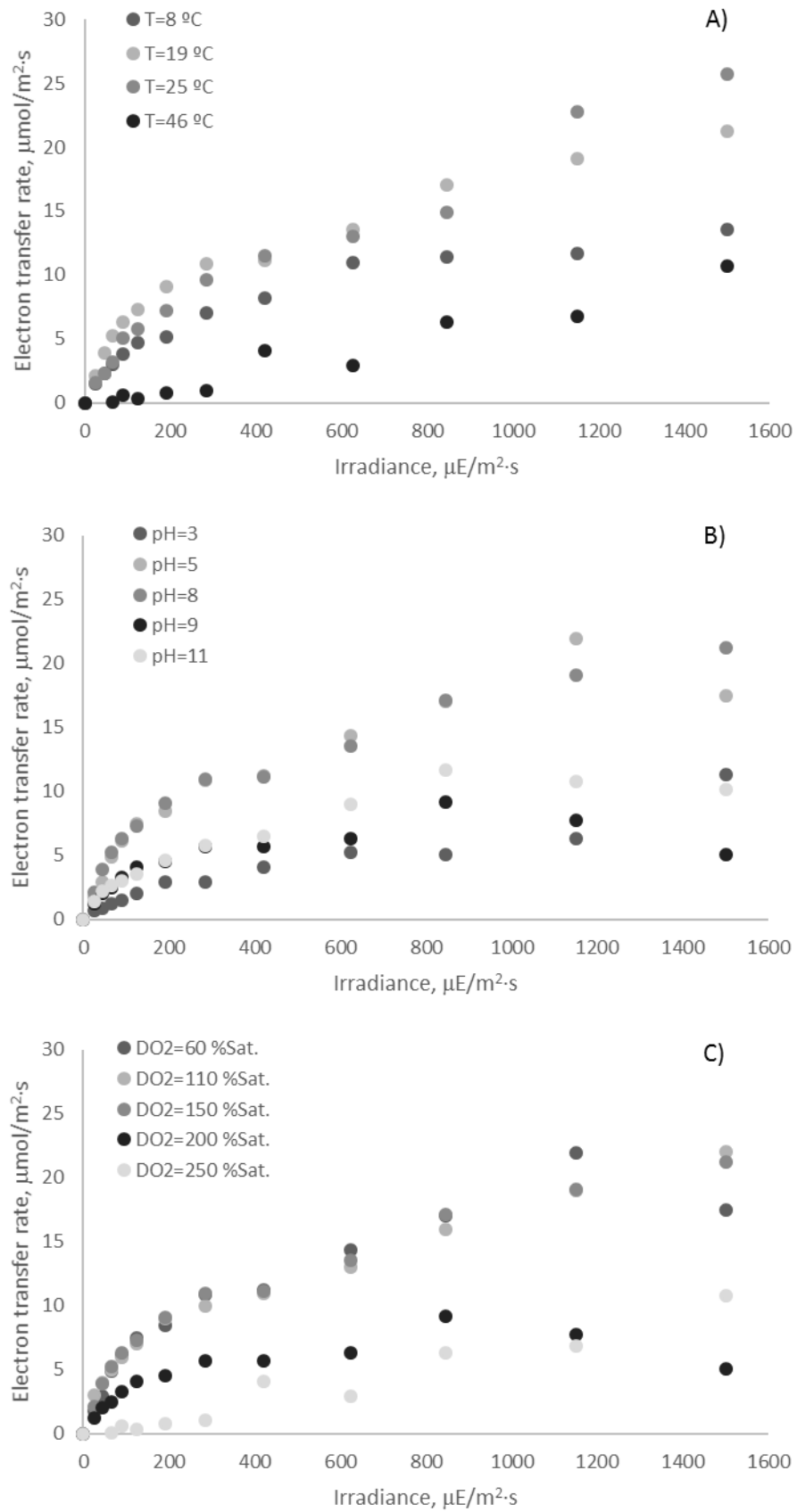


Figure 4.28. Influence of temperature (A), pH (B) and dissolved oxygen (C) on the electron transfer rate of *Scenedesmus almeriensis* cells. Data from Chlorophyll-fluorescence measurements.

4.3. Evaluation of thin-layer cascade reactor

4.3.1. Variation of culture conditions

Results from thin-layer cascade reactors already installed in Třeboň (Czech Republic) were used to validate the major achievements from thin-layer reactor being operated at IFAPA research centre (Full information available in Barceló-Villalobos et al., (in review)). Data shows (*Figure 4.29*) that the temperature is quite stable along the channel, independently of the reactor size. It ranges from 24°C to 28°C in the small unit. Moreover, it ranges from 25°C to 29°C in the medium unit; with a peak around 31°C in the turn section of the reactor. This is because of having a narrow and long channel (about 4 meters long) with no waterfalls, so the culture cannot be refresh enough. On the other hand, in the large unit the temperature ranges from 26°C to 28°C, with a peak at 30.55°C, also due to the turn section.

Concerning oxygen, results demonstrate (*Figure 4.29*) that dissolved oxygen concentration increases along the channel from 150 %Sat up to values of 400 %Sat and 344 %Sat in the small and medium units, respectively. That is because the mass transfer capacity in those reactors is not enough to desorb the oxygen produced, as well as by the high biomass concentration achieved (ranging from 30-40 g/L). On the other hand, the accumulation of dissolved oxygen in the larger unit is only up to 177 %Sat. That is due to a lower oxygen production in this reactor.

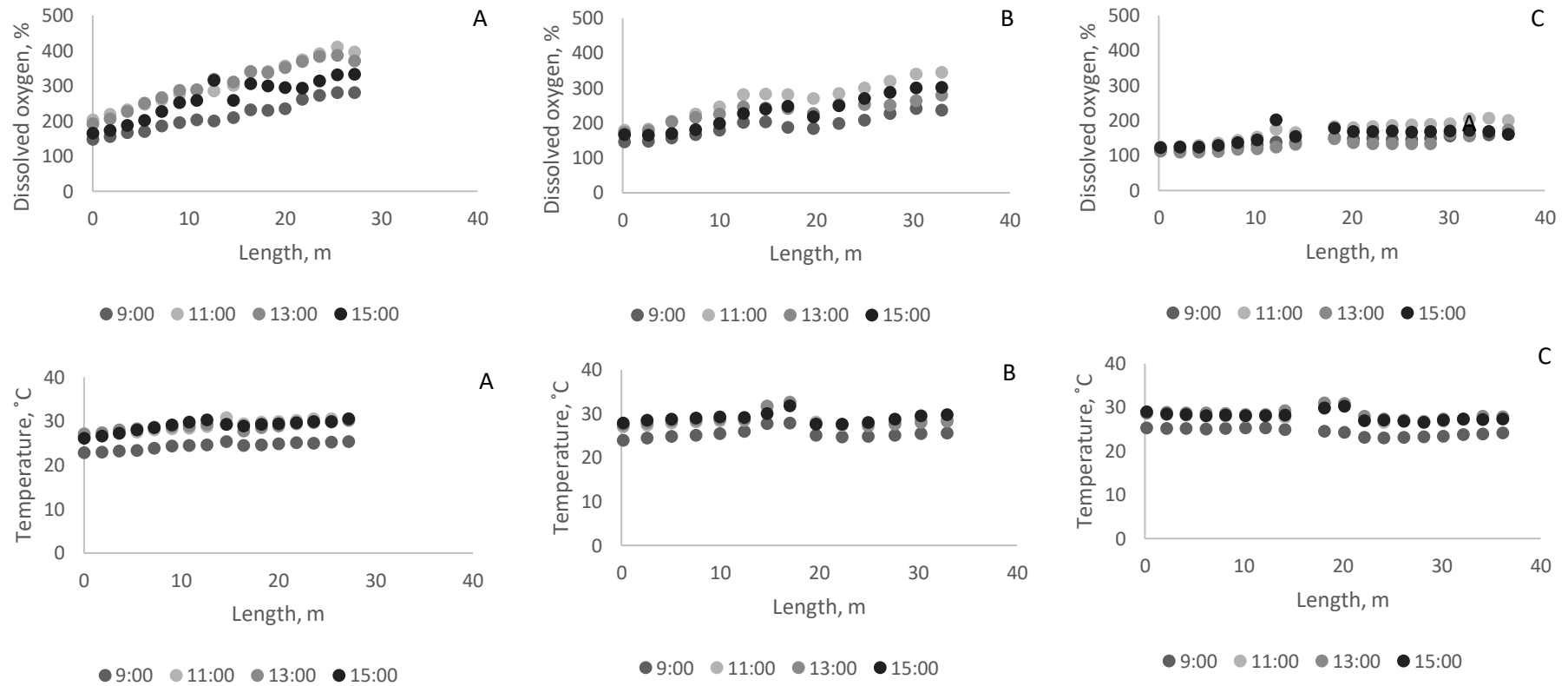


Figure 4.29. Variation of culture parameters (Dissolved oxygen and temperature) with the position and time of the day (9:00, 11:00, 13:00 and 15:00 h) in three thin-layer reactors (A=194.24 L, B=550 L and C=2200 L) operated in batch mode and located in Třeboň (Czech Republic). Mean values of 15 days.

4.3.2. Oxygen mass balance

To maintain the dissolved oxygen concentration below adverse values, it is imperative to improve the reactor design as well as the operating conditions, especially the mass transfer capacity. Previous works concluded that being able to manipulate the mass transfer capacity of raceway reactors in order to maintain the dissolved oxygen concentration below inhibitory values is a challenge (Barceló-Villalobos et al., 2018). Regarding thin-layer reactors, there still much work to do. Alameda-García, et al., (in review) demonstrated a higher mass transfer coefficient ($klal$) in thin-layer reactor's channel compare to the raceway reactor loop. This value (9.25 h^{-1}), was used to analyse mass transfer capacity in the three thin layer reactors evaluated at "Algatech" Experimental Station facilities. Results show (*Figure 4.30*) that the mass transfer capacity of each thin layer analysed is below 4% of total oxygen production ($PO_{2, \text{ produced, mg/gb h}}$). Thus, it is correct to assume that the net oxygen production ($PO_{2, \text{ net}}$) is equal to the generated oxygen production (Equation 48).

$$PO_{2, \text{ produced}} = PO_{2, \text{ net}}$$

Equation 48

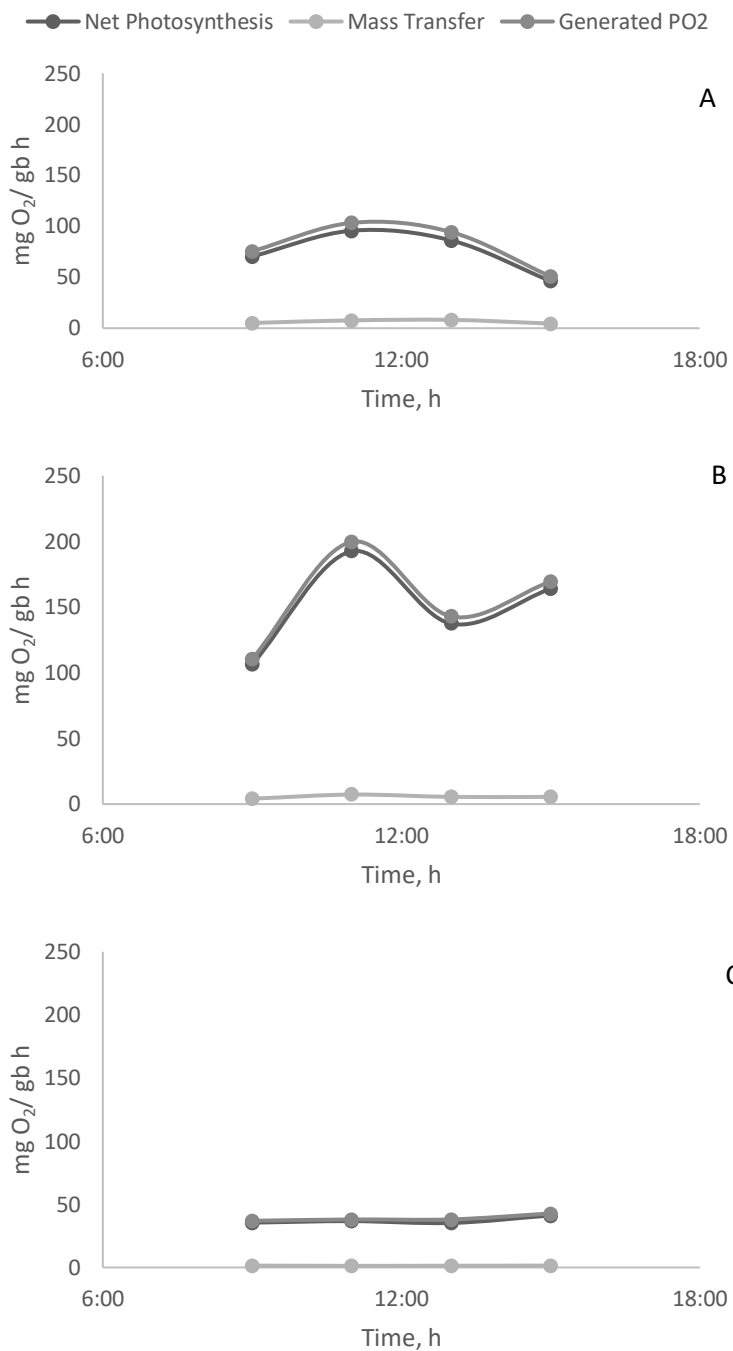


Figure 4.30. Oxygen mass balance at three thin-layer reactors (A=Small, B=Medium, C=Big) located at Třeboň (Czech Republic).

4.3.3. Modelling oxygen production

The influence of culture conditions into the performance of *Clorella sp.* cells was modelled as photosynthesis rate (PO₂, mg/gb h) according to the experimental dissolved oxygen measurements. Oxygen production (PO₂) was modelled according to dissolved oxygen concentration (DOC) and temperature variables. Dissolved oxygen effect has been included into

the model by using Costache et al., (2013) inhibition model (Equation 49). As a result, there is a very high reduction of the oxygen production (Figure 4.31). On the other hand, the temperature cardinal model proposed by Ippoliti et al., (2016) (Equation 50) has been used to analyse the temperature effect on oxygen production. It has been demonstrated that temperature values are not harmful, in this case, the values are close to the optimal values (Figure 4.31).

$$DO_2 model = \left(1 - \left(\frac{DO_2}{DO_{2,max}}\right)^m\right) \quad \text{Equation 49}$$

$$RO2(T) = \frac{(T - T_{max})(T - T_{min})^2}{(T_{opt} - T_{min}) \left((T_{opt} - T_{min})(T - T_{opt}) - (T_{opt} - T_{max})(T_{opt} + T_{min} - T) \right)} \quad \text{Equation 50}$$

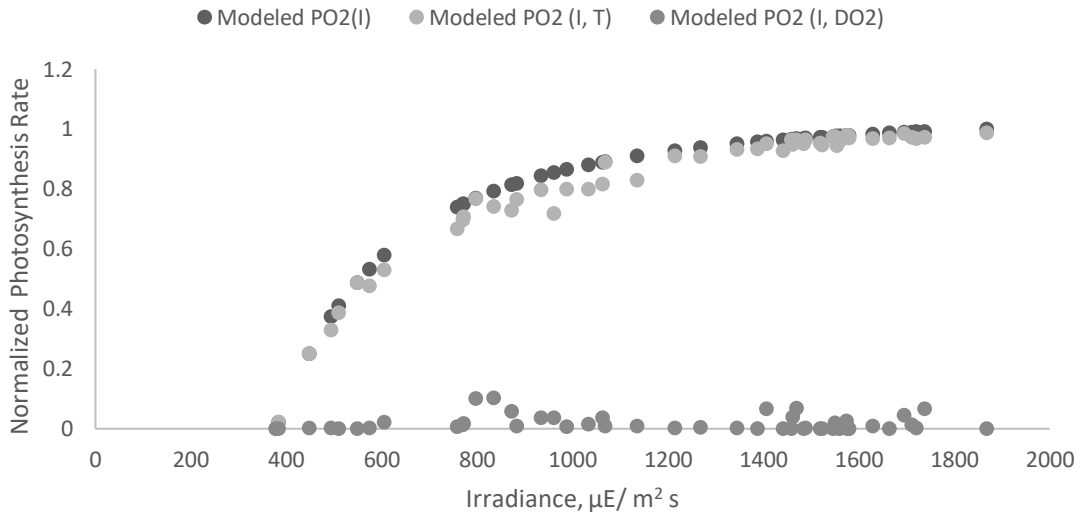


Figure 4.31. Comparison of oxygen production model (PO2 (I)) by including the temperature effect (PO2 (I, T)) and the dissolved oxygen effect (PO2 (I,DO2)).

Figure 4.32 demonstrates that, if we include the effect of temperature and optimal dissolved oxygen parameters into the oxygen production model (Modeled PO2(I_{av}, T, Optimal DO2 model); Equation 51), it is not enough to validate the experimental values of oxygen production. Thus, it might be another factor that affects to the oxygen production and it is not included into the model.

$$PO_{2(I_{av},T,DO_2)} = \frac{PO_{2,max} \times I_{av}^n}{I_k^n + I_{av}^n} \times RO2(T) \times \left(1 - \left(\frac{DO_2}{DO_{2,max}}\right)^m\right) \quad \text{Equation 51}$$

Where, DO2 was 10.8 mg/L (120% Sat.)

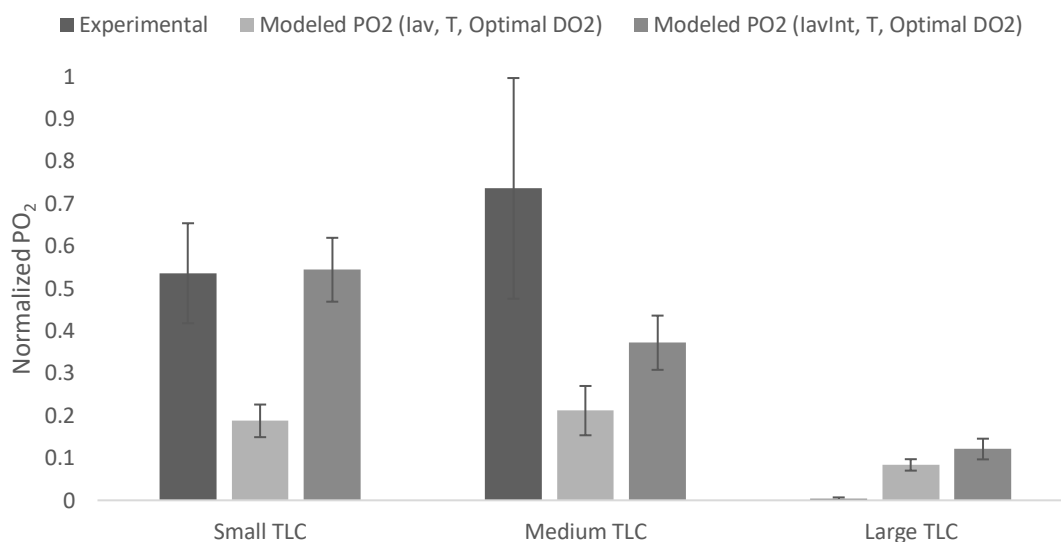


Figure 4.32. Comparison of experimental data respect to: modeled PO2 (lav, T, Optimal DO2) and modeled PO2 (lavInt, T, Optimal DO2) at three different thin-layer cascade reactors (Small, Medium and Large).

A previous work (Barceló-Villalobos et al., 2019a) demonstrated that the light penetrance into the culture depends on the location of the algae along the water depth. Thus, light/dark time and volume should be taken into consideration to better understand and model the photosynthesis rate ($\text{mg O}_2/\text{gb h}$) according to the design of the reactor.

The different sections of the reactors have different light/dark behaviour. For instance, bubble column and sink/sump/reservoir sections should be considered as dark volumes. On the other hand, the loop section should be considered as light volume. Moreover, water depth and water speed also influence into the light/dark cycling. Thus, the culture spends some time in light or dark zone. It depends on the residence time at each section of the reactor. In case of large dark time, the culture might be in respiration process due to the dark photosynthesis phase.

Three different size reactors have been analysed in this work. A small reactor with a total volume of 200 L (dark volume of 56 L and light volume of 144 L); a medium reactor, with a total volume of 600 L (dark volume of 60 L and light volume of 540 L); and a large reactor with a total volume of 2200 L (dark volume of 850 L and light volume of 1350 L).

The culture is exposed to solar radiation along the channel (48, 54 and 113 seconds at the small, medium and big reactors respectively). As higher is this time, as better the productivity of the system should be due to photosynthesis process. It might be achieved by improving the light/dark cycles in the reactor. Previous works demonstrated the improvement of productivity

of the reactors by this (Barceló-Villalobos et al., 2019a; Fernández-Sevilla et al., 2018). On the other hand, the culture is exposed to darkness in the reservoir section for values of 19, 6 and 71 seconds, at the small, medium and large reactors respectively. As longer is this time, as lower is the productivity of the system -291, 301 and 263 g O₂/m² d at the small, medium and large reactors respectively. Furthermore, there is a big influence of biomass concentration into the productivity of the system that should be considered in future works (28, 37 and 40 g/L mean values), to analyse how the biomass concentrations affects to the light path penetrance as well as to the light/dark volume.

In this work, we propose to include the light parameter as an average integrated irradiance (*IavInt*), where the light/dark time is included (Equation 31, Equation 52). That is because the light time and dark time affect to the photosynthesis and respiration process respectively. Results demonstrated that experimental data fit the PO₂ *IavInt* model (Equation 31) in a 81% of the cases (R²=0.8115). Moreover, light frequency was incorporated to the model with optimal conditions of dissolved oxygen by the inclusion of the average irradiance integration concept (*IavInt*) (Modeled PO₂ (*IavInt*, T, Optimal DO₂ Model), Equation 53).

$$IavInt = \frac{Iav \times t_{light}}{t_{light} + t_{dark}} \quad \text{Equation 52}$$

$$PO_{2(IavInt,T,DO_2)} = \frac{PO_{2,max} \times IavInt^n}{I_k^n + IavInt^n} \times RO_2(T) \times \left(1 - \left(\frac{DO_2}{DO_{2,max}}\right)^m\right) \quad \text{Equation 53}$$

As a result (Figure 4.32, Figure 4.33), the modelled data reach much better results compare to *Iav* concept. It is shown that light/dark frequency is optimal for the medium thin-layer cascade reactor (540 L light volume and 60L dark volume).

This work demonstrates that the influence of the light/dark time and volume ratio regarding the design and operation conditions of the reactor should be taken into consideration to achieve a maximal productivity of the system (Full information available in (Barceló-Villalobos, et al., under review).

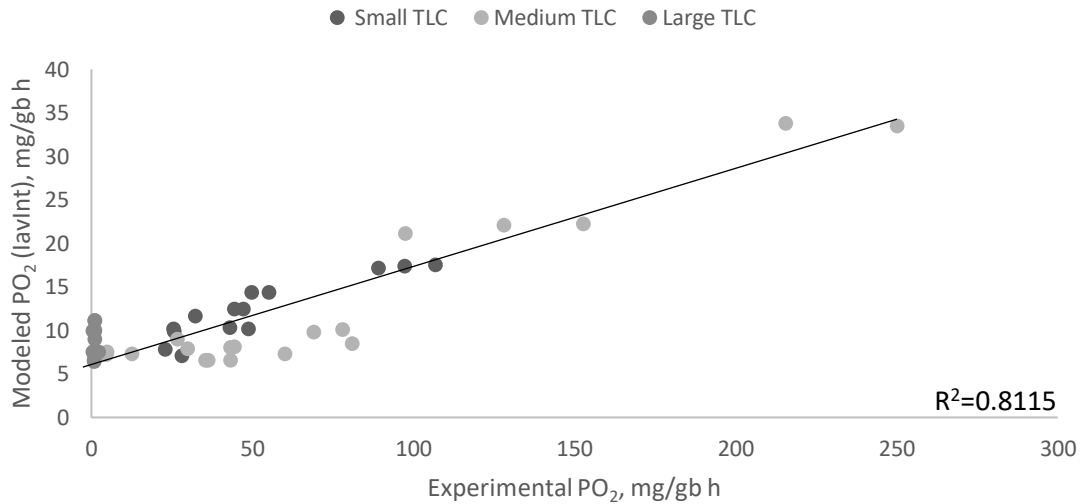


Figure 4.33. Validation of PO₂ (lavInt) model (Equation 31) at three thin-layer cascade reactors.

4.4. Control strategies implementation

Finally, this thesis provides some solutions regarding the use of control strategies to improve the efficiency of open reactors and to make this technology more competitive in the market. These control approaches were designed according to the experimental and biological models developed in this thesis. The advantage of using biological models for control design purposes is that these are useful to understand the biological behaviour of the technology. As much amount of data is being used to validate those models along the year, as much robust the model and the control strategy are. This is the main reason because the models developed in this thesis have been made by using a large set of assays all over a year, at different time seasons, to make them a powerful and robust tool for designing control strategies.

An event-based selective approach to control the operationing conditions of the reactors was used in “Las Palmerillas” and “IFAPA” Experimental Stations facilities. On the other hand, a feedback control strategy with a set-point generator has been tested in a simulation study.

The event-based selective strategy has been used to control both, pH and dissolved oxygen accumulation, around the desired set-point (pH=8.0, 250%Sat. respectively). The advantage of using this control strategy is to ensure pH control and at the same time, control dissolved oxygen accumulation below a specific set-point. *Figure 4.34* demonstrates how the selective control approach switches between CO₂ and air injections to reach these simultaneous objectives. pH is controlled around a value of 8.0, and the dissolved oxygen is always below the desired value of 250%Sat (Full information is available in Barceló-Villalobos, et al., 2019c).

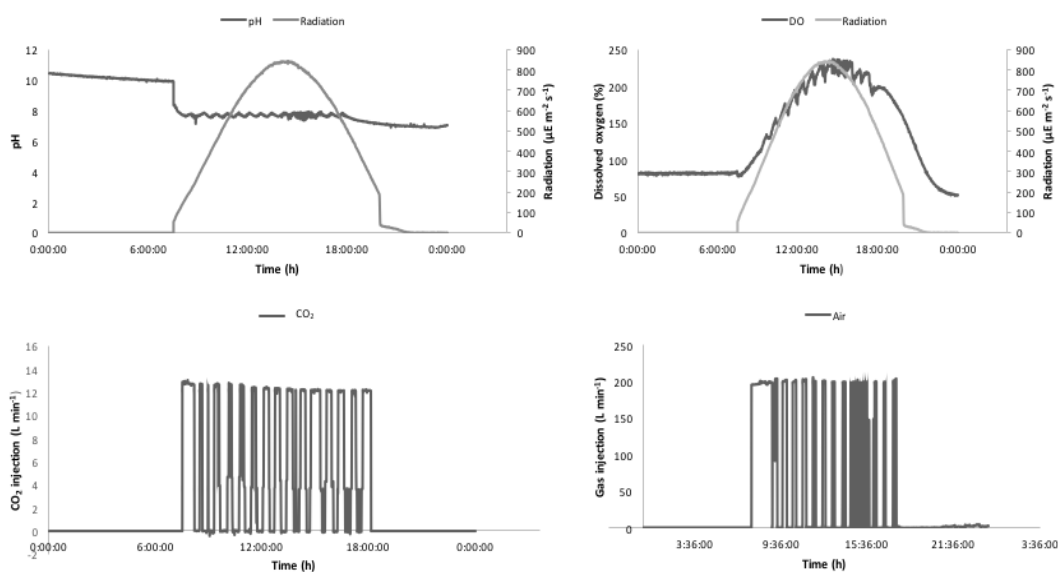


Figure 4.34. Experimental results for the raceway reactor's selective control scheme

As it was commented previously, open reactors have the big drawback of dissolved oxygen accumulation. It is well known that dissolved oxygen accumulation can affect to photosynthesis process if it is over 250 %Sat (Mendoza et al., 2013b; Pawlowski et al., 2015). This fact can be solved with a control approach as the one described before, but on the other hand, it can be reached by calculating and providing the optimal air gas injection to the reactor.

To solve that and ensure the optimal gas inflow, mass transfer coefficient control was mandatory. Thus, a feedback control strategy with a set-point generator was proposed to use the optimal air gas injection at each time. Until now, the reactor works by using a fixed air gas injection flow along the day. In this thesis, it was demonstrated that it is possible to determine the optimal air injections to the necessity of the system through a feedback control strategy. Some of the main advantages of using this strategy are: use the optimal CO₂/air injections and reduce the number of injections. Notice that these injections are adjusted to the necessity of the culture at every time. Consequently, sources of CO₂ and air as well as energy consumption are reduced.

The model presented in Fernández et al., (2016) has been improved, by including mass transfer capacity property as Barceló-Villalobos et al., (2018). The model is based on physicochemical and biological principles and predicts temperature, pH and dissolved oxygen dynamics in raceway photobioreactors, considering the transport phenomena.

Different results have been obtained from the simulation approach:

(1) The optimization of mass transfer coefficient (K_{La} , s^{-1}) allows to properly control dissolved oxygen accumulation until the set-point imposed (250% Sat.) (Figure 4.35).

(2) It is demonstrated that the mass transfer coefficient ($K_{l,a}$, s^{-1}) can be controlled as a fixed or a variable parameter. The present thesis shows that it should be controlled in a variable manner to optimize the air gas injections into the system (Figure 4.36).

(3) Furthermore, regarding air gas injections (L/min), it is possible to control it by a fixed and/or a variable manner (Figure 4.37).

(4) It is also demonstrated that it is possible to adjust the dissolved oxygen set-point to different values, depends on the requirements of the strain used in the reactor. As much higher is the value of dissolved oxygen set-point the lower mass transfer coefficient ($k_{l,a}$) is required; thus, lower amount of gas injections is required (Figure 4.38).

(5) Different mass transfer coefficients ($K_{l,a}$, s^{-1}) should be used, depends on the dissolved oxygen set-point (Figure 4.39). As lower is the dissolved oxygen set-point, the higher amount of dissolved oxygen should be desorp to the atmosphere, which means that a higher value of mass transfer coefficient ($k_{l,a}$) should be imposed.

(6) A variable control of mass transfer coefficient allows to control and save gas injections and use it efficiently. As lower is the dissolved oxygen set-point imposed, as higher is the amount of gas injections (L/min) that should be inject; which means, increasing of the production costs of the system (Figure 4.40) (Full information is available in (Barceló-Villalobos, et al.,2019)).

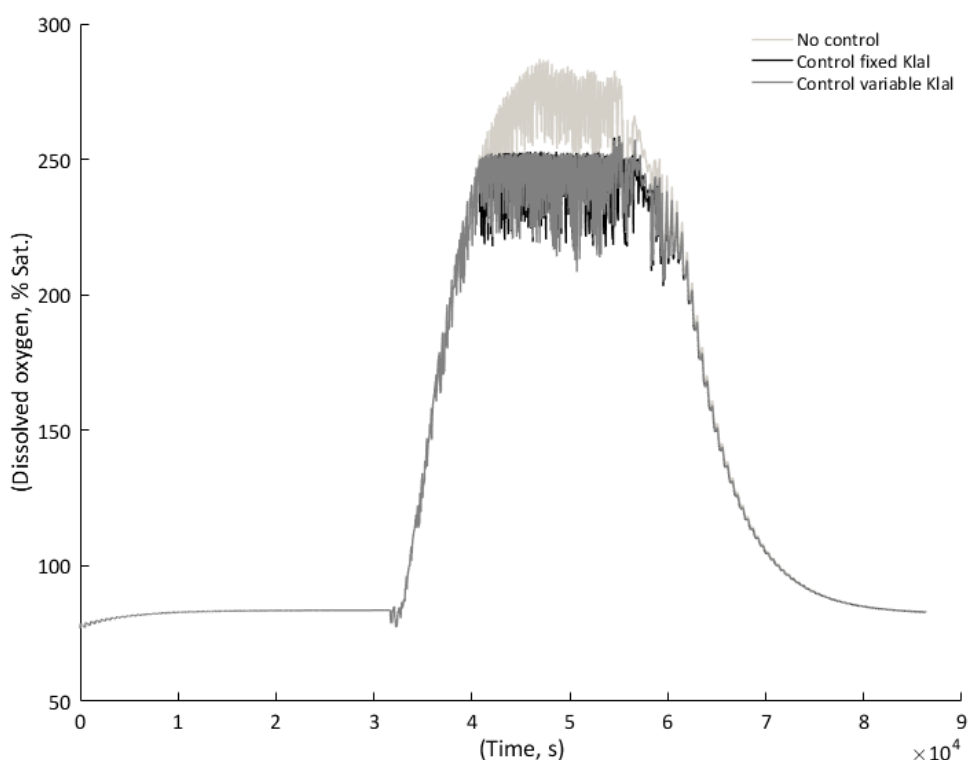


Figure 4.35. Simulation of dissolved oxygen accumulation into the culture at different control conditions.

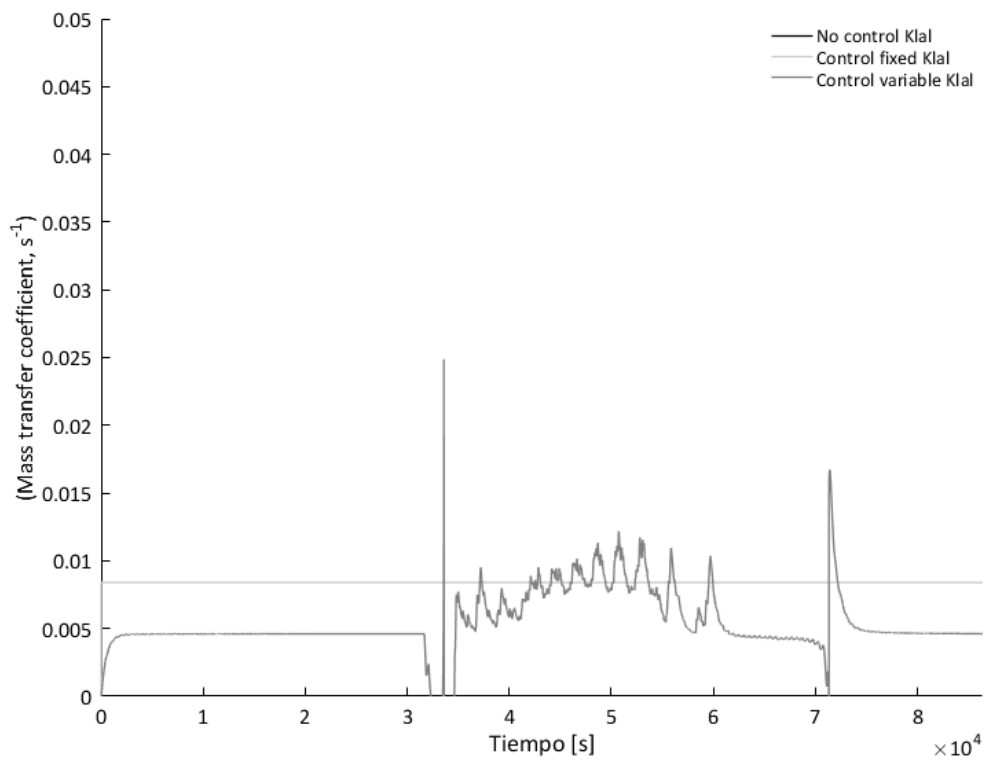


Figure 4.36. Simulation of mass transfer coefficient (s^{-1}) performance along the day. at different control conditions.

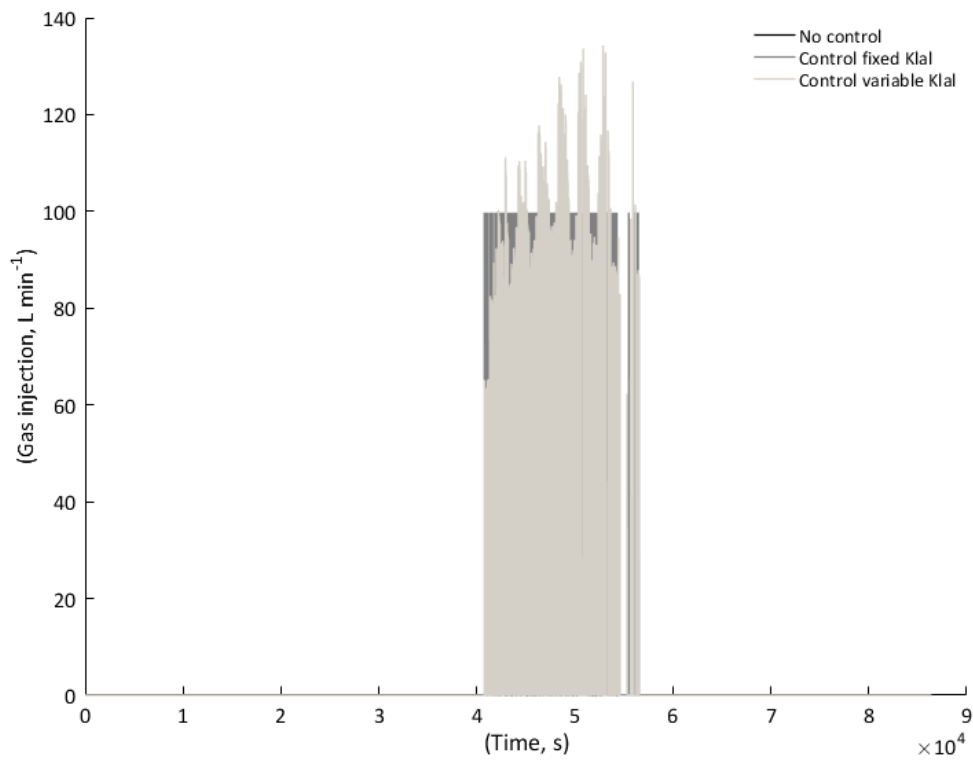


Figure 4.37. Simulation of air gas injection (L/min) into the culture at different control conditions.

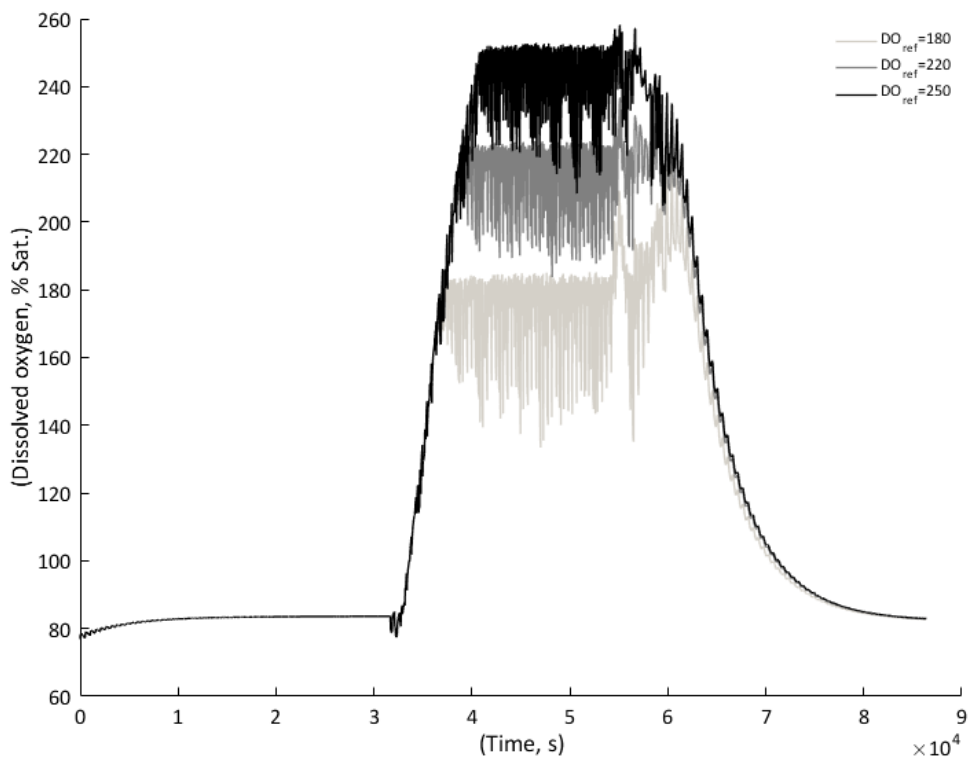


Figure 4.38. Simulation of dissolved oxygen accumulation control (% Sat.) into the culture, at different set-points

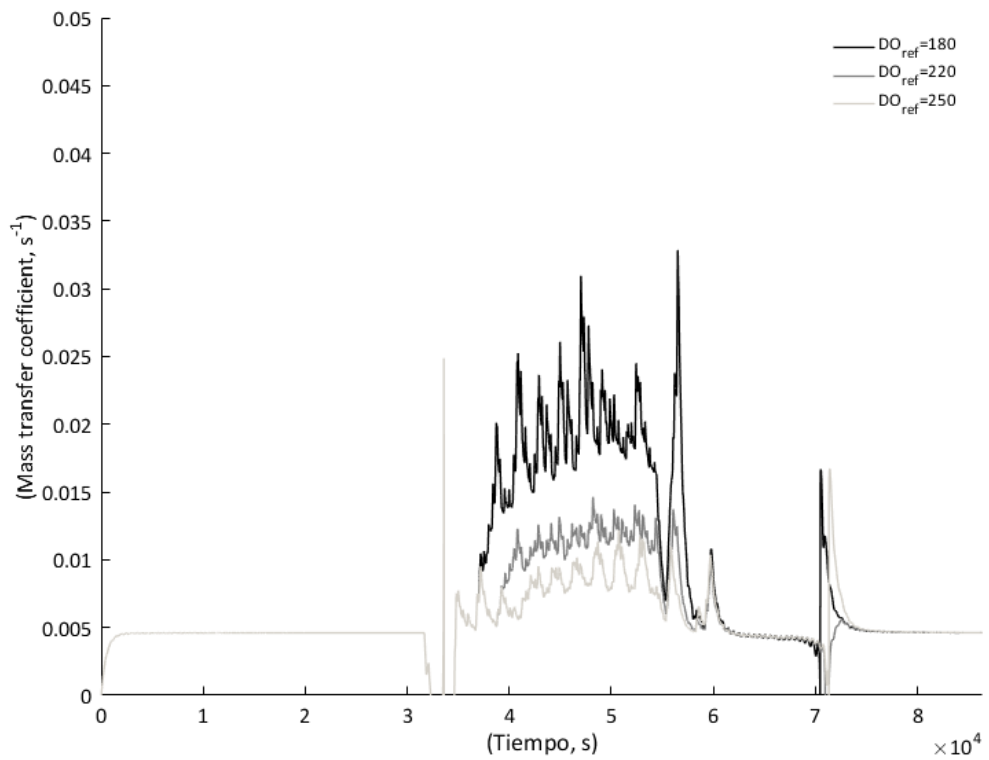


Figure 4.39. Simulation of mass transfer coefficient (s^{-1}) performance at different dissolved oxygen set-points

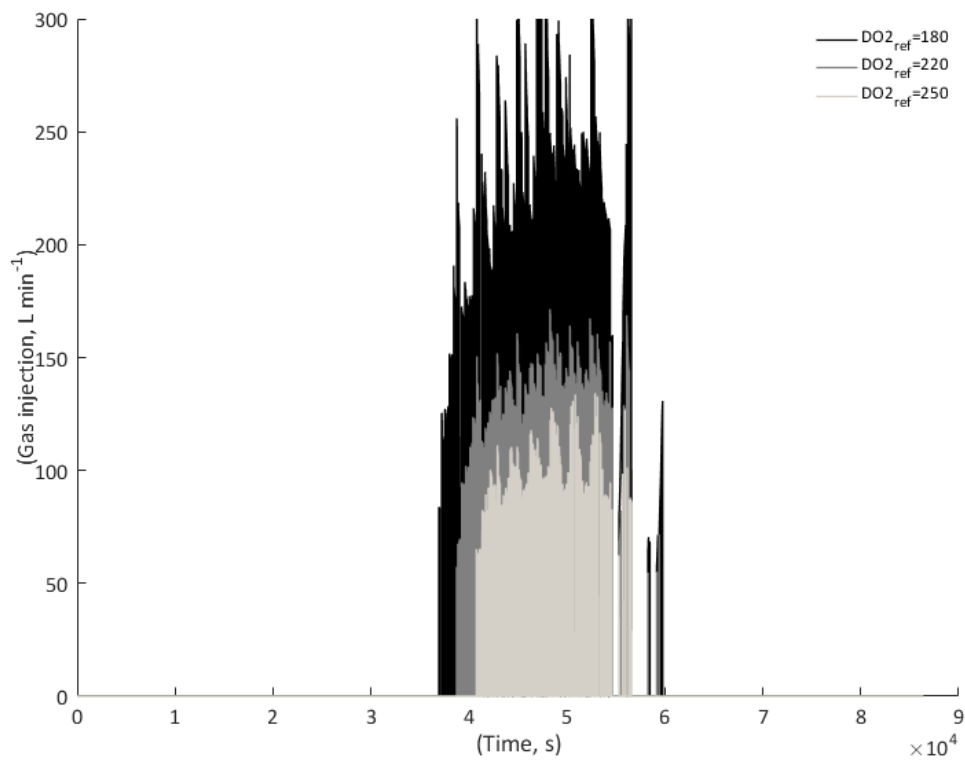


Figure 4.40. Simulation of air gas injection (L/min) into the culture at different dissolved oxygen set-points

Chapter 5

CONCLUSIONS

5. CONCLUSIONS

The main objectives of this PhD thesis are to provide biological models and control strategies for microalgae production systems in a semi-industrial scale. Previous works were focused on closed photobioreactors due to its less risk of contaminations, but these are more expensive than open reactors related to their construction and production. Thus, this thesis has been focused on two types of open reactors: raceway and thin-layer reactors.

Raceway reactors are usually characterized by a paddlewheel and a culture depth of 15 cm. On the other hand, thin-layer cascade reactors are characterized by a shallow culture depth of 4-0.6 cm. Both of these reactors have some drawbacks to be solved in order to make them a suitable technology for industrial scale: dissolved oxygen accumulation and light integration. To fulfil these drawbacks, different models and a feedback control strategy have been developed.

In a first step, both technologies have been characterized regarding the dynamic variations of the culture parameters (dissolved oxygen, temperature, pH and light integration) to identify the dynamics at the different sections of the reactors (sump, loop, paddlewheel, and thin-layer's channel) along the year. This is the first step to optimize and scale-up this type of reactors for industrial applications.

Regarding raceway reactor, this technology has been used to optimize the dissolved oxygen accumulation issue as well as to improve the knowledge of light integration.

There is an accumulation of dissolved oxygen along the day due to high oxygen production rate, which can reach values over 6 g/min in summer-time (Barceló-Villalobos et al., 2018). To solve this problem, the first step of this work was focused on mass transfer analysis to better understand the fluid-dynamics of the system along a year. Fluid-dynamics improvements were developed to achieve a better desorption of the dissolved oxygen to the atmosphere. It has been demonstrated that the mass transfer coefficient (h^{-1}) must be changed along the year (depends on the season) to achieve optimal values of dissolved oxygen concentration into the reactor (Barceló-Villalobos et al., 2018). Thus, an empirical model has been developed to determine and optimize the mass transfer capacity in the sump for any existing raceway reactor.

Regarding light integration, it is well known that light regime at which the cells are exposed into the reactor depends on both: the solar irradiance and the movement of cells along the channel. The results showed how the irradiance inside the reactor exponentially decreased along the culture depth regardless to the solar irradiance on the reactor surface (Barceló-Villalobos et al., 2019a).

This thesis demonstrated that the cells are fully adapted to local irradiances which was validated in the real outdoor raceway at different seasons (winter, spring, summer) (Barceló-Villalobos et al., 2019a). Furthermore, the continuous light model from Molina-Grima et al., (1994) is appropriate for a raceway reactor with a biomass concentration ranging from 0.2-0.4 g/L (Barceló-Villalobos et al., 2019a).

Concerning thin-layer cascade reactors, they have been less studied even though they are more efficient than raceway reactors, achieving higher biomass productivities (Morales-Amaral et al., 2015). It is shown that dissolved oxygen accumulation into the system was high due to the inefficient desorption capacity on the system to reduce it (Barceló-villalobos et al., 2019b). Thus, it was necessary to determine their mass transfer capacity (Alameda-García, L. et al., in review) to properly operate the reactor under the optimal operational conditions because it highly influences on the productivity of these systems; as previous works demonstrated (Mendoza et al., 2013).

The next step was to confirm the influence of changing the culture conditions on the cell performance. Thus, *in situ* outdoor measurements and off-line measurements in the laboratory were performed by using net photosynthesis rate and chlorophyll-fluorescence methods.

The net photosynthesis experimental data have been fitted to different models (Barceló-villalobos et al., 2019b). Moreover, results from *in situ* net photosynthesis measurements are comparable to those obtained when evaluating the electron transfer rate of the cells in the reactor by taking chlorophyll fluorescence measurements (Barceló-villalobos et al., 2019b). The utilization of Chlorophyll-fluorescence measurements to identify adverse culture conditions in thin-layer reactors has already been reported (Jerez et al., 2014, 2016).

The last step concerning biology issues was to validate the major achievements from thin-layer cascade reactors at the thin-layer cascade reactors already installed in Třeboň (Czech Republic). It has been shown that the mass transfer capacity in those reactors is not enough to desorb the oxygen produced. Moreover, the oxygen production has been modelled according to dissolved oxygen and temperature parameters effects. As a result, there is a very high reduction of the oxygen production due to dissolved oxygen over-accumulation. It also has been demonstrated that temperature values is not harmful, in this case, the values are close to the optimal values (Barceló-Villalobos et al., in review).

On the other hand, the inclusion of the temperature and optimal dissolved oxygen parameters into the oxygen production model (Modeled PO₂(I_{av}, T, Optimal DO₂ model) was not enough to validate the experimental values of oxygen production. Thus, it might be another factor that affects to the oxygen production and it is not included into the I_{av} model. Previous works demonstrated that the light penetrance into the culture depends on the location of the

algae along the water depth (Barceló-Villalobos et al., 2019a). Moreover, in this thesis, it is proposed to include the light parameter as an average integrated irradiance (I_{avInt}), where the light/dark time is added. As a result, the modelled data reach much better results compare to I_{av} concept (Barceló-Villalobos, et al., in review).

In order to optimize the production of the reactors, different control strategies (on-off control and a selective control strategy) were analysed to control pH and dissolved oxygen parameters. Moreover, a new feedback control strategy with a set-point generator was proposed and has been tested in simulation approach to control and reduce the dissolved oxygen accumulation into the system by improving its mass transfer capacity. The present thesis demonstrates that this strategy gives a solution to the dissolved oxygen accumulation drawbacks.

Firstly, on-off control was used to reduce and control pH variations. On the other hand, it has some disadvantages respect to others control strategies; the valve is totally opened during the injections which may leads to increase the energy cost and also the control performances are very poor.

Secondly, the selective control approach developed by Pawlowski et al., (2015) was used to adapt the actuation rate to the dynamics and disturbances, as it is proposed by (Pawlowski, et al., (2011)). The pH control was prioritized over the dissolved oxygen. This thesis demonstrates how the selective control approach switches between CO₂ and air injections to reach these simultaneous objectives. pH is successfully controlled around a value of 8.0, and the dissolved oxygen is always below the desired value of 250%Sat (Barceló-Villalobos et al., 2019d).

Finally, it is demonstrated that it is possible to save air injections actions by using a new feedback control strategy, as well as, to reduce the dissolved oxygen accumulation into the reactor until values lower than the optimal dissolved oxygen imposed (usually below 250% Sat.).

Future efforts should be concentrated on the optimization of the operating conditions according to the environmental conditions where the reactor is place on.

Chapter 6

LIST OF PUBLICATIONS

6. LIST OF PUBLICATIONS

During the development of this PhD thesis, the following works have been published:

6.1. Articles published in JCR Journals

- **M. Barceló-Villalobos**, J.L. Guzmán Sánchez., I. Martín Cara, J.A. Sánchez Molina, F.G. Acién Fernández. (2018) Analysis of mass transfer capacity in raceway reactors. **Algal Research** 35:91-97.
- **M. Barceló-Villalobos**, P. Fernández-del Olmo, J.L. Guzmán, J.M. Fernández-Sevilla, F.G. Acién Fernández (2019a) Evaluation of photosynthetic light integration by microalgae in a pilot-scale raceway reactor. **Bioresource Technology** 280:404-411.
- **M. Barceló-Villalobos**, C. Gómez Serrano, A. Sánchez Zurano, L. Alameda García, S. Esteve Maldonado, J. Peña, F.G. Acién Fernández (2019b) Variations of culture parameters in a pilot scale thin-layer reactor and their influence on the performance of *Scenedesmus almeriensis* culture. **Bioresource Technology Reports** 6: 190-197

6.2. Articles submitted to JCR Journals

- **M. Barceló-Villalobos**, T. Grivalský, K. Ranglová, J.L. Guzmán, J. Masojídek, F.G. Acién (in review) Photosynthetic performance of *Chlorella vulgaris* in thin-layer cascades.
- Alameda-García, L., De-Arriba, A., **Barceló-Villalobos, M.**, Gómez Serrano, C., Acién Fernández, F.G (in review) Photosynthetic performance of *Scenedesmus almeriensis* in thin-layer reactors.
- **M. Barceló-Villalobos**, A. Hoyo, E. Miranda, J.L. Guzmán, F.G. Acién (in review) A feedback control strategy for the air injection flow at raceway reactors.

6.3. Book chapter

- **M. Barceló-Villalobos**, F. Acién, J.L. Guzmán, J.M. Fernández-Sevilla, M. Berenguel, New strategies for the design and control of raceway reactors to optimize microalgae production. Chapter 18. **Handbook of Algal Technologies and Phytochemicals: Volume II Phycoremediation, Biofuels and Global Biomass Production**. CRC Press, 2019c.

Chapter 7

LIST OF OTHER CONTRIBUTIONS

7. LIST OF OTHER CONTRIBUTIONS

During the development of the present thesis, the author of this PhD has collaborated actively with other members of research group TEP-197, as well members of other research groups (national and international). These collaborations have originated the following publications:

7.1. Book chapter

Srivastava A., **Villalobos M.B.**, Singh R.K. Engineering Photosynthetic Microbes for Sustainable Bioenergy Production. Chapter 10. **Contemporary Environmental Issues and Challenges in Era of Climate Change**. Springer, 2020.

7.2. Articles published in books of abstracts of congress

- **M. Barceló-Villalobos**, J. L. Guzmán, F.G. Ación, I. Martín, J.A. Sánchez. (2016). Assessment of mass transfer coefficient in open raceways. V Minisimposio de Investigación en Ciencias Experimentales. Universidad de Almería. Libro de abstracts 1: 15
- **M. Barceló-Villalobos**, J. L. Guzmán, F.G. Ación, J.A. Sánchez. (2017). Análisis del coeficiente de transferencia de materia en reactores raceways. XXXVIII Jornadas de Automática (JA2017). 50 Aniversario del Comité Español de Automática. Universidad de Oviedo. Gijón, España. Book of abstracts 1: 534-538.
- **M. Barceló-Villalobos**, F.G. Ación, J.M. Fernández-Sevilla, J. L. Guzmán. (2017). Photosynthetic response under intermittent light in an industrial raceway reactor. VI Minisimposio de Investigación en Ciencias Experimentales. Universidad de Almería. Book of abstracts 1: 13
- **M. Barceló-Villalobos**, F. G. Ación, J.M. Fernández-Sevilla, J. L. Guzmán, F. Rodríguez. (2018). Mejora de la producción del alga *Scenedesmus almeriensis* mediante la optimización de los ciclos de luz/oscuridad. III Simposium nacional de ingeniería hortícola. I Simposium Ibérico. Sociedad española de ciencias hortícolas. 78: 269-274.
- **M. Barceló-Villalobos**, J.L. Guzmán, F.G. Ación (2019d). A feedback control strategy of dissolved oxygen in raceway reactors. 2nd IWA Conference on Algal Technologies for Wastewater Treatment and Resource Recovery. Book of abstracts 245-246.

7.3. Oral communications in international congress

M. Barceló-Villalobos, J.L. Guzmán, F.G. Acién (1st-2nd July 2019) A feedback control strategy of dissolved oxygen in raceway reactors. IWA Conference on Algal Technologies and stabilization ponds for wastewater treatment and resource recovery (IWAAlgae2019). Valladolid, España.

7.4. Communication in international congress

M. Barceló-Villalobos, J.L. Guzmán, I. Martín, J.A. Sánchez., F.G Acién (11th-13th June 2018) Analysis of mass transfer capacity in a raceway reactor. 8th International conference on Algal Biomass, Biofuels, and Bioproducts. Seattle, WA, USA.

7.5. Communications in national congress

- **M. Barceló-Villalobos**, J. L. Guzmán, F.G. Acién, I. Martín, J.A. Sánchez. (November 2016). Assessment of mass transfer coefficient in open raceways. V Minisimposio de Investigación en Ciencias Experimentales. Almería, España.
- **M. Barceló-Villalobos**, J.L Guzmán, F. G. Acién, I. Martín, J. A. Sánchez. (September 2017). Análisis del coeficiente de transferencia de materia en reactores raceways. XXXVIII Jornadas de Automática (JA2017). 50 Aniversario del Comité Español de Automática. Gijón, España.
- **M. Barceló-Villalobos**, F.G. Acién, J.M. Fernández-Sevilla, J. L. Guzmán. (November 2017). Photosynthetic response under intermittent light in an industrial raceway reactor. VI Minisimposio de Investigación en Ciencias Experimentales. Almería, España.
- **M. Barceló-Villalobos**, F. G. Acién, J.M. Fernández-Sevilla, J. L. Guzmán, F. Rodríguez. (February 2018). Mejora de la producción del alga *Scenedesmus almeriensis* mediante la optimización de los ciclos de luz/oscuridad. III Simposium nacional de ingeniería hortícola. I Simposium Ibérico. Lugo, España.

Acknowledgements

This study was supported financially by the Ministry of Economy and Competitiveness (DPI2014-55932-C2-1-R, DPI2017-84259-C2-1-R, EDARSOL (CTQ2014-57293-C3-1-R) and the European Union's Horizon 2020 Research and Innovation Program under Grant Agreement No. 727874 SABANA.

REFERENCES

- Acién, F.G., Molina, E., Reis, A., Torzillo, G., Zittelli, G.C., Sepúlveda, C., Masojídek, J., 2017. Photobioreactors for the production of microalgae, *Microalgae-Based Biofuels and Bioproducts: From Feedstock Cultivation to End-Products*.
- Alameda-García, L.; De-Arriba, A.; Barceló-Villalobos, M.; Gómez, C.; Acién, F.G., in review. Photosynthetic performance of *Scenedesmus almeriensis* in thin-layer reactors.
- Åström, K.J. Murray, R.R., 2019. *Feedback systems: An introduction for scientists and engineers*, Princeton. ed.
- Barbosa, M.J., Janssen, M., Ham, N., Tramper, J., Wijffels, R.H., 2003. Microalgae cultivation in air-lift reactors: Modeling biomass yield and growth rate as a function of mixing frequency. *Biotechnol. Bioeng.* 82, 170–179.
- Barceló-Villalobos, M., Guzmán, J.L., Martín, I., Sánchez, J.A., Acién, F.G., 2018. Analysis of mass transfer capacity in raceway reactors. *Algal Res.* 35, 91–97.
- Barceló-Villalobos, M., Olmo, P.F., Guzmán, J.L., Fernández-Sevilla, J.M., Acién, F.G., 2019a. Evaluation of photosynthetic light integration by microalgae in a pilot-scale raceway reactor. *Bioresour. Technol.* 280, 404-411
- Barceló-villalobos, M., Gómez, C., Sánchez, A., Alameda-García, L., Esteve, S., Peña, J., Acién, F.G., 2019b. Variations of culture parameters in a pilot-scale thin-layer reactor and their influence on the performance of *Scenedesmus almeriensis* culture. *Bioresour. Technol. Reports* 6, 190–197.
- Barceló-Villalobos, M., Acién, F., Guzmán, J.L., Fernández-Sevilla, J.M., Berenguel, M., 2019c. New strategies for the design and control of raceway reactors to optimize microalgae production, in: Gokare, A.; Ravishankar, A.; Ranga, R. (Ed.), *Handbook of Algal Technologies and Phytochemicals*. pp. 221–230.
- Barceló-Villalobos, M., Guzmán, J.L., Acién, F.G., 2019d. A feedback control strategy of dissolved oxygen in raceway reactors, in: *2nd IWA Conference on Algal Technologies for Wastewater Treatment and Resource Recovery*. Valladolid (Spain), pp. 245–246.
- Barceló-Villalobos, M., T. Grivalský, K. Ranglová, Masojídek, J., Guzmán, J.L., Acién, F.G., in review. Photosynthetic performance of *Chlorella vulgaris* in thin-layer cascades.
- Benemann, J.R., 1997. CO₂ mitigation with microalgae systems. *Energy Convers. Manag.* 38, 475–479.
- Berenguel, M., 2004. Model predictive control of pH in tubular photobioreactors. *J. Process*

Control 14, 377–387.

- Bernard, O., Rémond, B., 2012. Validation of a simple model accounting for light and temperature effect on microalgal growth. *Bioresour. Technol.* 123, 520–527.
- Beschi, M., Pawlowski, A., Guzmán, J.L., Berenguel, M., Visioli, A., 2014. Symmetric send-on-delta PI control of a greenhouse system., in: *Proceedings of the 19th IFAC World Congress*. Cape Town, South Africa.
- Beschi, M., Dormido, S., Sanchez, J., Visioli, A., 2012. Characterization of symmetric send-on-delta PI controllers. *J. Process Control* 22, 1930–1945.
- Brindley, C., Ación, F.G., Fernández-Sevilla, J.M., 2011. Analysis of light regime in continuous light distributions in photobioreactors. *Bioresour. Technol.* 102, 3138–3148.
- Brindley, C., Jiménez-Ruiz, N., Ación, F.G., Fernández-Sevilla, J.M., 2016. Light regime optimization in photobioreactors using a dynamic photosynthesis model. *Algal Res.* 16, 399–408.
- Brundland, G.H., 1987. *Our common future Report of the World Commission on Environment and Development*, Oxford Uni. ed. New York.
- Chisti, Y., 2012. Microalgal biotechnology: Potential and production, in: *Raceways-Based Production of Algal Crude Oil*. C. Posten, C. Walter, de Gruyter, Berlin, pp. 113–146.
- Chisti, Y., 2008. Biodiesel from microalgae beats bioethanol. *Trends Biotechnol.* 26, 126–131.
- Chisti, Y., 2007. Biodiesel from microalgae. *Biotechnol. Adv.* 25(3), 294–306.
- Chu, H., Zhao, F., Tan, X., Yang, L., Zhou, X., Zhao, J., Zhang, Y., 2016. The impact of temperature on membrane fouling in algae harvesting. *Algal J.* 16, 458–464.
- Costache, T.A., Ación, F.G., Morales, M.M., Fernández-Sevilla, J.M., Stamatini, I., Molina, E., 2013. Comprehensive model of microalgae photosynthesis rate as a function of culture conditions in photobioreactors. *Appl. Microbiol. Biotechnol.* 97, 7627–7637.
- De Godos, I., Mendoza, J.L., Ación, F.G., Molina, E., Banks, C.J., Heaven, S., Rogalla, F., 2014. Evaluation of carbon dioxide mass transfer in raceway reactors for microalgae culture using flue gases. *Bioresour. Technol.* 153, 307–314.
- Demory, D., Combe, C., Hartmann, P., Talec, A., Pruvost, E., Hamouda, R., Souillé, F., Lamare, P.O., Bristeau, M.O., Sainte-Marie, J., Rabouille, S., Mairet, F., Sciandra, A., Bernard, O., 2018. How do microalgae perceive light in a high-rate pond? Towards more realistic Lagrangian experiments. *R. Soc. Open Sci.* 5, 180523.
- Doucha J, L.K., 1995. Novel outdoor thin-layer high density microalgal culture system: productivity and operation parameters. *Algal Stud* 76, 129–147.
- Duarte-Santos, T., Mendoza-Martín, J.L., Ación, F.G., Molina, E., Vieira-Costa, J.A., 2016. *Bioresource Technology Optimization of carbon dioxide supply in raceway reactors:*

- Influence of carbon dioxide molar fraction and gas flow rate. *Bioresour. Technol.* 212, 72–81.
- Fernández-Sevilla, J.M., Brindley, C., Jiménez-Ruiz, N., Ación, F.G., 2018. A simple equation to quantify the effect of frequency of light/dark cycles on the photosynthetic response of microalgae under intermittent light. *Algal Res.* 35, 479–487.
- Fernández, I., Peña, J., Guzmán, J.L., Berenguel, M., Ación, F.G., 2010. Modelling and control issues of pH in tubular photobioreactors., in: *Proceedings of the 11th IFAC Symposium on Computer Applications in Biotechnology*. Leuven, Belgium.
- Fernández, I., Ación, F.G., Berenguel, M., Guzmán, J.L., 2014. First principles model of a tubular photobioreactor for microalgal production. *Ind. Eng. Chem. Res.* 53, 11121–11136.
- Fernández, I., Ación, F.G., Berenguel, M., Guzmán, J.L., Andrade, G.A., Pagano, D.J., 2014. A lumped parameter chemical-physical model for tubular photobioreactors. *Chem. Eng. Sci.* 112, 116–129.
- Fernández, I., Ación, F.G., Fernández, J.M., Guzmán, J.L., Magán, J.J., Berenguel, M., 2012. Dynamic model of microalgal production in tubular photobioreactors. *Bioresour. Technol.* 126, 172–181.
- Fernández, I., Ación, F.G., Guzmán, J.L., Berenguel, M., Mendoza, J.L., 2016. Dynamic model of an industrial raceway reactor for microalgae production. *Algal Res.* 17, 67–78.
- García-Sánchez, J.L., Berenguel, M., Rodríguez, F., Fernández-Sevilla, J.M., Brindley, C., Ación, F.G., 2003. Minimization of carbon losses in pilot-scale outdoor photobioreactors by model-based predictive control. *Biotechnol. Bioeng.* 84, 533–543.
- Giannelli, L., Yamada, H., Katsuda, T., Yamaji, H., 2015. Effects of temperature on the astaxanthin productivity and light harvesting characteristics of the green alga *Haematococcus pluvialis*. *J. Biosci. Bioeng.* 119, 345–350.
- Fernández, I., Berenguel, M., Guzmán, J.L., Ación, F.G., Andrade, G.A., Pagano, D.J., 2016. Hierarchical control for microalgae biomass production in photobioreactors. *Control Eng. Pract.* 54, 246–255.
- Ippoliti, D., Gómez, C., Morales-Amaral, M. M., Pistocchi, R., Fernández-Sevilla, J.M., Ación, F.G., 2016. Modeling of photosynthesis and respiration rate for *Isochrysis galbana* (T-Iso) and its influence on the production of this strain. *Bioresour. Technol.* 203, 71–79.
- Janssen, M., De Winter, M., Tramper, J., Mur, L.R., Snel, J., Wijffels, R.H., 2000. Efficiency of light utilization of *Chlamydomonas reinhardtii* under medium-duration light/dark cycles. *J. Biotechnol.* 78, 123–137.
- Jerez, C., Navarro, E., Malpartida, I., Rico, R., Masojídek, J., Abdala, R., Figueroa, F., 2014. Hydrodynamics and photosynthesis performance of *Chlorella fusca* (Chlorophyta) grown in

- a thin-layer cascade (TLC) system 22, 111–122.
- Jerez, C.G., Malapascua, J.R., Sergejevová, M., Masojídek, J., Figueroa, F.L., 2016. *Chlorella fusca* (Chlorophyta) grown in thin-layer cascades: Estimation of biomass productivity by in-vivo chlorophyll a fluorescence monitoring. *Algal Res.* 17, 21–30.
- Jiménez, C., Cossío, B.R., Labella, D., Niell, F.X., 2003. The feasibility of industrial production of *Spirulina* (*Arthrospira*) in Southern Spain. *Aquaculture* 217, 179–190.
- Lazar, C., Pintea, R., Keyser, R., 2007. Nonlinear predictive control of a pH process., in: *Proceedings of 17th European Symposium on Computer Aided Process Engineering ESCAPE17*, Bucharest, Romania.
- Masojídek, J., Kopecký, J., Giannelli, L., Torzillo, G., 2011. Productivity correlated to photobiochemical performance of *Chlorella* mass cultures grown outdoors in thin-layer cascades. *J. Ind. Microbiol. Biotechnol.* 38, 307–317.
- Mata, T.M., Martins, A.A., Caetano, N.S., 2010. Microalgae for biodiesel production and other applications: a review. *Renew. Sustain. Energy Rev.* 14(1), 217–232.
- Mendoza, J.L., Granados, M.R., De Godos, I., Ación, F.G., Molina, E., Banks, C., Heaven, S., 2013a. Fluid-dynamic characterization of real-scale raceway reactors for microalgae production. *Biomass and Bioenergy* 54, 267–275.
- Mendoza, J.L., Granados, M.R., De Godos, I., Ación, F.G., Molina, E., Heaven, S., Banks, C.J., 2013b. Oxygen transfer and evolution in microalgal culture in open raceways. *Bioresour. Technol.* 137, 188–195.
- Molina, E., García-Camacho, F., Sánchez-Pérez, J.A., Fernández-Sevilla, J.M., Ación, F.G., Contreras-Gómez, A., 1994. A mathematical model of microalgal growth in light-limited chemostat culture. *J. Chem. Technol. Biotechnol.* 61, 167–173.
- Molina, E., Fernández, J., Ación, F.G., Chisti, Y., 2001. Tubular photobioreactor design for algal cultures. *J. Biotechnol.* 92, 113–131.
- Molina, E., García-Camacho, F., Sánchez-Pérez, J.A., Fernández-Sevilla, J., Ación, F., Contreras-Gómez, A., 1994. A mathematical model of microalgal growth in light-limited chemostat culture. *J. Chem. Technol. Biotechnol.*
- Morales-Amaral, M.M., Gómez, C., Ación, F.G., Fernández-Sevilla, J.M., Molina, E., 2015. Outdoor production of *Scenedesmus* sp. in thin-layer and raceway reactors using centrate from anaerobic digestion as the sole nutrient source. *Algal Res.* 12, 99–108.
- Oblak, S., Skrjanc, I., 2010. Continuous-time Wiener-model predictive control of a pH process based on a PWL approximation. *Chem. Eng. Sci.* 65, 1720–1728.
- Oswald, W.J., Golueke, C.G., 1967. Biological transformation of solar energy, in: *Advances in Applied Microbiology*. Vol. 2. W.W. Umbreit Ed., New York, pp. 223–262.

- Pawlowski, A., Cervin, A., Guzmán, J.L., Berenguel, M., 2011. Generalized predictive control with actuator deadband for event-based approaches. *IEEE Trans. Ind. Informatics* 10(1), 523–537.
- Pawlowski, A., Guzmán, J.L., Rodríguez, F., Berenguel, M., Normey-Rico, J.E., 2011. Predictive control with disturbance forecasting for greenhouse diurnal temperature control, in: 18th World Congress of IFAC. Milan, Italy.
- Pawlowski, A., Fernández, I., Guzmán, J.L., Berenguel, M., Ación, F.G., Normey-Rico, J.E., 2014a. Event-based predictive control of pH in tubular photobioreactors. *Comput. Chem. Eng.* 65, 28–39.
- Pawlowski, A., Fernández, I., Guzmán, J.L., Berenguel, M., Ación, F.G., Dormido, S., 2016. Event-based selective control strategy for raceway reactor: A simulation study. *IFAC-Papers on line* 49, 478–483.
- Pawlowski, A., Guzman, J.L., Berenguel, M., Acien, F.G., Dormido, S., 2017. Event-based control systems for microalgae culture in industrial reactors, *Prospects and Challenges in Algal Biotechnology*.
- Pawlowski, A., Mendoza, J.L., Guzmán, J.L., Berenguel, M., Ación, F.G., Dormido, S., 2015. Selective pH and dissolved oxygen control strategy for a raceway reactor within an event-based approach. *Control Eng. Pract.* 44, 209–218.
- Pawlowski, A., Mendoza, J.L., Guzmán, J.L., Berenguel, M., Ación, F.G., Dormido, S., 2014b. Effective utilization of flue gases in raceway reactor with event-based pH control for microalgae culture. *Bioresour. Technol.* 170, 1–9.
- Peng, L., Lan, C. Q., Zhang, Z., 2013. Evolution, detrimental effects, and removal of oxygen in microalga cultures: A review. *AIChE—Environmental Prog. Sustainable Energy* 32(4), 982–988.
- Pulz, O., Gross, W., 2004. Valuable products from biotechnology of microalgae. *Appl. Microbiol. Biotechnol.* 65(6), 635–648.
- Raesossadati, M.J., Ahmadzadeh, H., McHenry, M.P., Moheimani, N.R., 2014. CO₂ bioremediation by microalgae in photobioreactors: Impacts of biomass and CO₂ concentrations, light, and temperature. *Algal Res.* 6, 78–85.
- Romero-García, J.M., Guzmán, J.L., Moreno, J.C., Ación, F.G., Fernández-Sevilla, J.M., 2012. Filtered Smith Predictor to control pH during enzymatic hydrolysis of microalgae to produce l-aminoacids concentrates. *Chem. Eng. Sci.* 82, 121–131.
- Rotatore, C., Colman, B., Kuzma, M., 1995. The active uptake of carbon-dioxide by the marine diatoms *Phaeodactylum-Tricornutum* and *Cyclotella Sp.* *Plant Cell Environ.* 18, 913–918.
- Sánchez, J.F., Fernández-Sevilla, J.M., Ación, F.G., Cerón, M.C., Pérez-Parra, J., Molina, E., 2008.

- Biomass and lutein productivity of *Scenedesmus almeriensis*: influence of irradiance, dilution rate and temperature. *Appl. Microbiol. Biotechnol* 79, 719–729.
- Schreiber U., Bilger W., N.C., 1995. Chlorophyll Fluorescence as a nonintrusive indicator for rapid assessment of in vivo photosynthesis, in: *Ecophysiology of Photosynthesis*. Springer Study Edition, pp. 49–70.
- Senthil, K.A., Zainal, A., 2012. Model predictive control (MPC) and its current issues in chemical engineering. *Chem. Eng. Commun.* 199, 472–511.
- Singh, S.P., Singh, P., 2015. Effect of temperature and light on the growth of algae species : A review. *Renew. Sustain. Energy Rev.* 50, 431–444.
- Waller, P., Ryan, R., Kacira, M., Li, P., 2012. The algae raceway integrated design for optimal temperature management. *Biomass and Bioenergy* 46, 702–709.
- Wang, Y.H., Turton, R., Semmens, K., Borisova, T., 2008. Raceway design and simulation system (RDSS): An event-based program to simulate the day-to-day operations of multiple-tank raceways. *Aquac. Eng.* 39, 59–71.

Appendix A

ARTICLES PUBLISHED IN JRC JOURNALS



Analysis of mass transfer capacity in raceway reactors

M. Barceló-Villalobos^{a,*}, J.L. Guzmán Sánchez^a, I. Martín Cara^b, J.A. Sánchez Molina^a,
F.G. Acién Fernández^b

^a Department of Informatics, Universidad de Almería, E04120 Almería, Spain

^b Department of Chemical Engineering, Universidad de Almería, E04120 Almería, Spain



ARTICLE INFO

Keywords:

Microalgae
Raceways
Mass transfer
CO₂ transfer
Oxygen desorption

ABSTRACT

In the present work, a methodology is proposed to determine the mass transfer capacity in existing microalgae raceway reactors to minimize excessive dissolved oxygen accumulation that would otherwise reduce biomass productivity. The methodology has been validated using a 100 m² raceway reactor operated in semi-continuous mode. The relevance of each raceway reactor section was evaluated as well as the oxygen transfer capacity in the sump to different air flow rates. The results confirm that dissolved oxygen accumulates in raceway reactors if no appropriate mass transfer systems are provided. Therefore, mass transfer in the sump is the main contributor to oxygen removal in these systems. The variation in the volumetric mass transfer coefficient in the sump as a function of the gas flow rate, and therefore the superficial gas velocity in the sump, has been studied and modelled. Moreover, the developed model has been used to estimate the mass transfer requirements in the sump as a function of the target dissolved oxygen concentration and the oxygen production rate. The proposed methodology allows us to determine and optimize the mass transfer capacity in the sump for any existing raceway reactor. Moreover, it is a powerful tool for the optimization of existing reactors as well as for the design optimization of new reactors.

1. Introduction

Raceway reactors have been used since the 1950s for the industrial production of microalgae. Today, > 90% of worldwide microalgae biomass production is carried out using these types of reactors [1]. The major advantage of raceway reactors is their simplicity and low construction cost. However, these reactors have certain problems related to their low productivity, high risk of contamination and poor control of growing conditions, in addition to their low mass transfer capacity. It has been demonstrated that the mass transfer capacity in these reactors is limited and must be improved to allow significantly increased biomass productivity [2]. In this regard, improvements are necessary in the fluid dynamics, the related CO₂ absorption and the oxygen desorption to enhance productivity in these systems [1–3]. Moreover, models are required that allow us to determine the mass transfer capacity and overall performance of these reactors for the scaling-up of any reactor type.

To maximize the performance of any microalgae strain, the culture conditions prevailing inside the reactor must be as close to optimal as possible for that strain. Any deviation from optimal culture conditions in outdoor cultures reduces productivity by > 50% compared to indoor

production, even when using closed tubular photobioreactors. These deviations and losses in productivity are still higher in raceway reactors where there is less control of the culture conditions [4,5]. By providing the most suitable culture conditions possible, we can increase biomass productivity, thus reducing the production costs per biomass unit as well as ensuring efficient and stable biomass production. Concerning CO₂ transfer, some works have been carried out optimizing the utilization of the supplied CO₂ to save costs; this is because CO₂ can contribute up to 30% of the total biomass production cost [6,7]. Nonetheless, much less attention has focused on dissolved oxygen accumulation in the system. It is commonly believed that oxygen is naturally desorbed to the atmosphere without the need for specific desorption systems. However, this is erroneous and the negative effect of dissolved oxygen accumulation on biomass productivity in raceway reactors has already been proven, with values surpassing 300% Sat. reported [2,9]. In this regard, to ensure that dissolved oxygen accumulation does not diminish biomass productivity in raceway reactors, it is imperative to improve the reactor design as well as the operational conditions, especially the mass transfer capacity.

Although the utilization of raceway reactors for the production of microalgae was first proposed in the 1960s, only recently has its design

* Corresponding author.

E-mail address: mbv001@ual.es (M. Barceló-Villalobos).

been revised, both from the fluid-dynamic and mass transfer capacity points of view [3,8–12]. Most of the studies focus on improving fluid dynamics to minimize power consumption, especially in biofuels production, whereas others focus on CO₂ transfer to make more efficient use of this expensive raw material. However, only a few studies have focused on oxygen removal and its improvement. Nonetheless, it was reported that reducing dissolved oxygen below 250 %Sat. by injecting flue gases as a source of CO₂ leads to an increase in biomass productivity above 30% compared to cultures operated with pure CO₂, in which dissolved oxygen increases above 300 %Sat. [3]. Thus, it was concluded that being able to manipulate the mass transfer capacity of raceway reactors in order to maintain the dissolved oxygen content below inhibitory values is a challenge.

In this paper, the mass transfer capacity of a pilot-scale raceway reactor is studied to identify the major phenomena taking place, the oxygen accumulation and the contribution of each reactor section to the mass transfer capacity of the entire reactor. The objective is to be able to fit the mass transfer capacity to that required for the productivity or photosynthesis rate of the specific biomass. To do this, a simple novel methodology has been developed using online dissolved oxygen sensors that do not disturb the reactor's normal operation; these can be used to audit any raceway reactor. The methodology has been validated and utilized to estimate the optimal operating conditions in an existing raceway reactor, making it a useful tool for improving this reactor type.

2. Materials and methods

2.1. Microorganism and culture conditions

The microalgae strain *Scenedesmus almeriensis* (CCAP 276/24) was used. Inoculum for the raceway reactor was produced in a 3.0 m³ tubular photobioreactor under controlled conditions: at pH = 8 and at a temperature ranging from 18 to 22 °C using freshwater and Mann & Myers medium prepared using fertilizers: (0.14 g·L⁻¹ K(PO₄)₂, 0.18 g·L⁻¹ Mg(SO₄)₂, 0.9 g·L⁻¹ NaNO₃, 0.02 mL·L⁻¹ Welgro, and 0.02 g·L⁻¹ Kalentol) [15]. In addition, NaHCO₃ was provided once a week to maintain the medium's alkalinity at the optimum 7 mM.

2.2. Raceway reactor design and operational conditions

The raceway reactor is located at the “Las Palmerillas” Research Centre, 36° 48'N–2° 43'W, part of the Cajamar Foundation (Almería, Spain). The reactor consists of two 50 m long channels (0.46 m high × 1 m wide), both connected by 180° bends at each end, with a

0.59 m³ sump (0.65 m long × 0.90 m wide × 1 m deep) located 1 m along one of the channels (Fig. 1) [17]. The pH, temperature and dissolved oxygen in the culture were measured at three different places along the reactor length using appropriate probes (5083 T and 5120, Crison, Barcelona, Spain), connected to an MM44 control-transmitter unit (Crison Instruments, Spain), and data acquisition software (Labview, National Instruments) providing complete monitoring and control of the installation. It was previously confirmed that no vertical or transversal gradients of pH, dissolved oxygen and biomass concentration existed, only longitudinal gradients, so the probes were located in the middle of both the culture depth and the channel. The gas flow rate entering the reactor was measured by a mass flow meter (PFM 725S-F01-F, SMC, Tokyo, Japan). The pH of the culture was controlled at 8.0 by on-demand injection of CO₂, whereas temperature was not controlled; it ranged ± 5 °C with respect to the daily mean air temperature, which varied from 12 °C in winter to 28 °C in summer. Air was supplied to the reactor from a blower providing 350 mbar overpressure, through a fine bubble diffuser AFT2100 (ECOTEC, Spain) providing bubbles with a diameter smaller than 2 mm at the minimum pressure drop; the estimated residence time of the bubbles in the sump ranged from 5 to 10 s [3]. The culture received continuous air injection, regardless of the CO₂ demand. The demand for carbon was supplied by the injection of pure CO₂ using an event-based pH controller at pH 8 [13]. The raceway reactor was inoculated and operated in batch mode for one week, after which it was operated in semi-continuous mode at 0.4 day⁻¹ at a culture depth of 0.15 m. Only data corresponding to steady-state conditions were used. Evaporation inside the reactor was compensated for by the daily addition of fresh medium.

2.3. Experimental design

To study the mass transfer capacity in the raceway reactor, experiments were performed in different seasons (spring, summer, autumn and winter) modifying the gas flow rate into the sump (0, 100, 160, 185, 200 and 350 L·min⁻¹ so the superficial gas velocity was 0.0, 0.0021, 0.0033, 0.0039, 0.0042, 0.0073 m·s⁻¹), and the L/G ratio (0.0, 18.0, 12.0, 9.7, 9, 5.1 L·L⁻¹), while the culture was operated in semi-continuous mode. In this way, we could study the oxygen produced by photosynthesis as well as that removed in the different parts of the reactor under the different culture conditions imposed (Fig. 1). These experiments allowed us to quantify the different phenomena taking place and to measure the mass transfer coefficient as a function of the culture conditions.

The reactor was operated throughout all the tests under the same

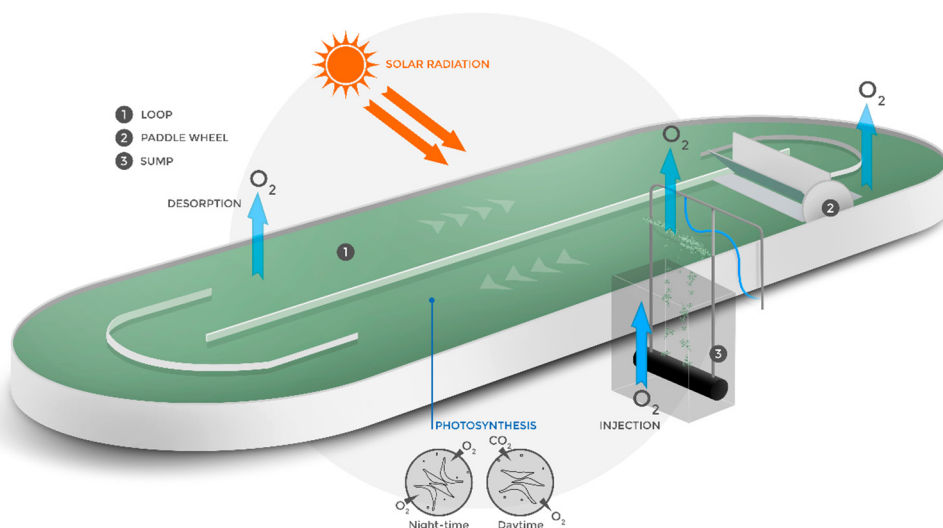


Fig. 1. Scheme of the 100 m² raceway reactor used to study this type of system and the mass transfer capacity, indicating the major phenomena taking place.

environmental conditions (solar radiation and temperature) and the same operational conditions (biomass concentration and dilution rate). The mean daily solar radiation was $600 \mu\text{E m}^{-2} \text{s}^{-1}$, the biomass concentration was 0.39 g L^{-1} and the cells did not present signs of any photosynthetic stress (Quantum Yield = 0.69). Under these conditions, the mean biomass productivity was $0.16 \text{ g L}^{-1} \text{ day}^{-1}$, equivalent to $23.4 \text{ g m}^{-2} \text{ day}^{-1}$.

2.4. Oxygen mass balance

Oxygen mass balances were performed to study the main phenomena taking place inside the reactor. For this, the dissolved oxygen concentration was measured at three different positions (after the paddlewheel, after the sump and at the end of the loop). The oxygen mass balance allows us to calculate the accumulation of dissolved oxygen as a function of oxygen production and mass transfer in each of these sections. Oxygen is produced by photosynthesis and is therefore modified as a function of the culture conditions, especially by changes in solar radiation outdoors throughout the day. In contrast, the mass transfer capacity is only a function of fluid dynamics and the driving force in the different parts of the reactor; the fluid dynamics remains constant during the day whereas the driving force is measured as a function of the dissolved oxygen concentration entering the culture at the different positions (after the paddlewheel, after the sump and at the end of the loop) throughout the day. Therefore, for any raceway reactor section, the following balance defines the dissolved oxygen concentration (Eq. (1)).

$$\text{O}_{2,\text{inlet}} + \text{O}_{2,\text{produced}} = \text{O}_{2,\text{outlet}} + \text{O}_{2,\text{accumulation}} \quad (1)$$

We consider that the sump is completely dark, because in this section < 3% of the total volume have irradiance values above $10 \mu\text{E m}^{-2} \text{s}^{-1}$, so no photosynthesis takes place. Furthermore, oxygen production in the paddlewheel section can be disregarded; hence the dissolved oxygen mass balance is defined by Eq. (2), where PO_2 represents the oxygen production and NO_2 represents the oxygen mass transfer capacity in each of the reactor sections.

$$\text{PO}_{2,\text{loop}} + \text{NO}_{2,\text{loop}} + \text{NO}_{2,\text{sump}} + \text{NO}_{2,\text{paddlewheel}} = \text{O}_{2,\text{accumulation}} \quad (2)$$

The mass transfer capacity is calculated as a function of the global mass transfer coefficient in each reactor section (K_{1a_i}), multiplied by the driving force. This means that the difference between the dissolved oxygen concentration in the liquid ($[\text{O}_2]$) and that in equilibrium with the gas phase (air) ($[\text{O}_2^*]$) is calculated using Henry's law and the section volume (V) (Eq. (3)). The influence of temperature on the solubility of dissolved oxygen was included using Eq. (4). In this case, the global mass transfer coefficient refers to the liquid phase, assuming that the main resistance to mass transfer takes place here.

$$\text{NO}_2 = K_{1a_i}([\text{O}_2] - [\text{O}_2^*])V \quad (3)$$

$$[\text{O}_2^*] = 12.408 - 0.1658 * T \quad (4)$$

It was previously reported that the global mass transfer coefficient in the loop of raceway reactors is very low, at 0.9 h^{-1} , as it is independently constant of the culture conditions [3]. This coefficient can be strongly modified if the liquid velocity is greatly enhanced. However, in raceway reactors, the liquid velocity is adjusted to 0.2 m s^{-1} to minimize power consumption — for this reason, the value of 0.9 h^{-1} is acceptable as the global mass transfer coefficient in the loop. Moreover, by applying the oxygen mass balance to the loop, it is possible to obtain a “virtual oxygen production sensor” as a function of the dissolved oxygen concentration at the beginning and end of the loop, and the flow of liquid inside the reactor (Q_{liquid}); as defined by Eq. (5).

$$\text{PO}_{2,\text{loop}} = Q_{\text{liquid}}([\text{O}_2]_{\text{outlet}} - [\text{O}_2]_{\text{inlet}})_{\text{loop}} - K_{1a_{1,\text{loop}}}([\text{O}_2] - [\text{O}_2^*])_{\text{loop}} V_{\text{loop}} \quad (5)$$

In addition to this, it has been reported that the global mass transfer

coefficient at the paddlewheel is in the 164 h^{-1} range; this remains constant as it is a function of the paddlewheel configuration and the rotation speed, which stay constant despite the solar radiation and the culture conditions imposed on the reactor [3]. Consequently, by knowing the photosynthetic production of oxygen from Eq. (5) and the global mass transfer coefficient for the paddlewheel, the global mass transfer coefficient for the sump can be easily calculated using Eq. (8).

$$\text{NO}_{2,\text{sump}} = \text{O}_{2,\text{accumulation}} - \text{PO}_{2,\text{loop}} - \text{NO}_{2,\text{loop}} - \text{NO}_{2,\text{paddlewheel}} \quad (6)$$

$$\text{NO}_{2,\text{sump}} = K_{1a_{1,\text{sump}}}([\text{O}_2] - [\text{O}_2^*])_{\text{sump}} V_{\text{sump}} \quad (7)$$

$$\begin{aligned} K_{1a_{1,\text{sump}}}([\text{O}_2] - [\text{O}_2^*])_{\text{sump}} V_{\text{sump}} &= V_{\text{reactor}} \frac{d[\text{O}_2]}{dt} - \text{PO}_{2,\text{loop}} \\ &\quad - K_{1a_{1,\text{loop}}}([\text{O}_2] - [\text{O}_2^*])_{\text{loop}} V_{\text{loop}} \\ &\quad - K_{1a_{1,\text{paddlewheel}}}([\text{O}_2] - [\text{O}_2^*])_{\text{paddlewheel}} \\ &\quad V_{\text{paddlewheel}} \end{aligned} \quad (8)$$

In this way, by using only the two dissolved oxygen probes located at the beginning and the end of the loop, it is possible to determine both the photosynthesis rate and the global mass transfer coefficient in the sump from the virtual sensors by applying the detailed equations. Given that the global mass transfer coefficient in the sump can be modified simply by modifying the air gas flow supplied, it is greatly advantageous to be able to measure this coefficient during the reactor's operation. Moreover, calibration curves can be obtained to further adjust the mass transfer capacity in the sump by modifying the air flow rate supplied to it.

2.5. Statistical analysis

The effect of the superficial gas velocity (m s^{-1}) on the volumetric mass transfer coefficient (h^{-1}) was correlated by descriptive statistics (correlation, R^2) in a total of 31 days of assays. Data from the reactors were obtained daily as a total of 1440 samples for each day. The Statistica v.7 program was used to perform the statistical analysis.

3. Results and discussion

The negative effect of dissolved oxygen accumulation on the performance of microalgae cultures has been widely reported [14,15]. Dissolved oxygen can damage the cultures or modify the metabolism if values over 250 %Sat. are reached; this is because the photosynthesis rate is exponentially reduced above this value [16,17]. In tubular photobioreactors, the loop length is limited by this phenomenon. It has also been necessary to install adequate bubble column systems to remove all the oxygen produced by photosynthesis [18,19]. In contrast, in raceway reactors, the dissolved oxygen concentration is usually disregarded even though the same phenomenon occurs. Therefore, the same criteria for design and scale-up need to be applied.

In raceway reactors, oxygen is produced by photosynthesis during the day and consumed by respiration at night, modified by the oxygen concentration equilibrium with the air, of 8.8 mg L^{-1} (20°C , 1 atm); this is therefore the driving force for the absorption/desorption of oxygen from or to the air. The results show that the dissolved oxygen concentration in the 100 m^2 raceway reactor varies throughout the day, with different values being observed at the different positions considered (Fig. 2). Also, the dissolved oxygen varied from 6.0 mg L^{-1} (70 %Sat.) at night to 18.0 mg L^{-1} (204 %Sat.) during the daylight period, under the culture conditions imposed. Moreover, these extreme measurements were obtained at the end of the channel whereas the values obtained after the paddlewheel and sump were attenuated compared to those at the end of the loop. From these figures, one can reasonably conclude that the optimal position to locate dissolved oxygen probes in raceway reactors is at the end of the channel or before the paddlewheel, as it is there that the major variations in dissolved

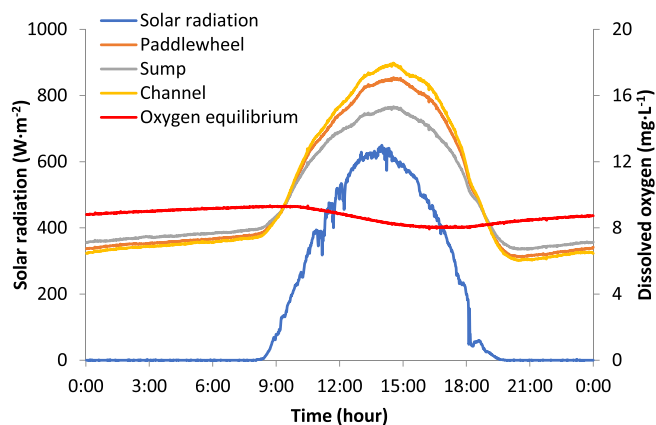


Fig. 2. Daily variation in solar radiation and dissolved oxygen concentration at the different positions in the reactor.

oxygen can be determined throughout the whole day.

Data clearly show that during the night the dissolved oxygen concentration is lower than that in equilibrium with the air, meaning a driving force exists for oxygen absorption from the air, whereas during the day the dissolved oxygen concentration is higher than that in equilibrium with the air so a driving force exists for oxygen desorption to the atmosphere. Moreover, the figures demonstrate that oxygen is consumed by the respiration process at night as well as being desorbed to the air, especially in the paddlewheel and sump, where the culture is put into intensive contact with the air (Fig. 2). One can also conclude that the respiration rate is higher than the oxygen absorption capacity in the paddlewheel and sump due to equilibrium with the air not being achieved. During the daylight period, the photosynthesis rate is higher, modified by solar radiation; thus oxygen accumulates in the culture because the reactor's mass transfer capacity is lower than the oxygen production rate resulting from photosynthesis. When analysing the dissolved oxygen values at the different locations, it is clear that the oxygen removal capacity in the paddlewheel is limited so the dissolved oxygen concentration after the paddlewheel is slightly lower than at the end of the channel. Although most of the oxygen is removed in the sump, the dissolved oxygen concentration at this point is lowest during the daylight period. The dissolved oxygen concentration after the sump decreases by 15% compared to the channel at midday (15.28 mg L^{-1} and 17.85 mg L^{-1} respectively). This is because it is a dark zone where air is continually being injected at a constant flow rate of 100 L min^{-1} . These results not only confirm that the mass transfer capacity in the sump is the most relevant but also that it is not sufficient to avoid excessive dissolved oxygen accumulation at noon ($6.38 \text{ g O}_2 \text{ min}^{-1}$). Therefore, the mass transfer capacity in the reactor must be optimized throughout the day as a function of the culture conditions.

Experimental data on the dissolved oxygen concentration in the culture can be used to estimate the oxygen production rate as well as the mass transfer capacity in the different reactor sections. Hence, using Eq. (5), the oxygen production rate in the reactor can be calculated from the dissolved oxygen concentrations at the beginning and the end of the channel; this is a more precise value than that obtained when considering the oxygen transferred in the loop. Fig. 3 shows the oxygen transfer in the loop, calculated considering a global mass transfer coefficient value of 0.9 h^{-1} [2]; this is minimal at night (below 0.37 g min^{-1}) due to the low mass transfer coefficient and the driving force during this period. Nonetheless, it is positive because the dissolved oxygen concentration in the culture is lower than that in equilibrium with the air. On the other hand, during the day, the driving force is far greater and the oxygen transfer in the loop is more relevant (-1.74 g min^{-1} at noon); this is negative (desorption) because the culture is oversaturated with oxygen produced by photosynthesis. If one only considers the variation in dissolved oxygen concentration at the

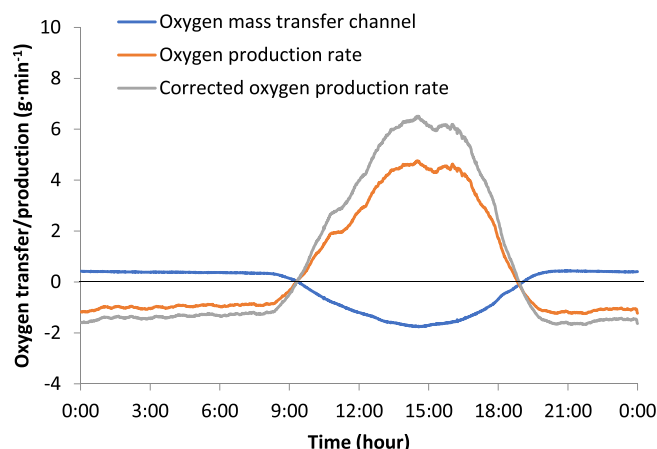


Fig. 3. Daily oxygen transfer variation in the loop and oxygen production in the reactor; estimated from data on dissolved oxygen concentration at the beginning and end of the channel using Eq. (5).

beginning and the end of the channel, a non-valid oxygen production rate is obtained; whereas by considering the oxygen transferred in the channel, the corrected oxygen production rate is a valid measurement. No large deviations in either the non-valid or the corrected oxygen production rates are observed but the net values are slightly different. According to these results, the maximum respiration rate at night was 1.45 g min^{-1} (equivalent to $5.8 \text{ mg O}_2 \text{ L}^{-1} \text{ h}^{-1}$), whereas the maximum oxygen production rate during the daylight period was 6.36 g min^{-1} (equivalent to $25.4 \text{ mg O}_2 \text{ L}^{-1} \text{ h}^{-1}$). Moreover, a net oxygen amount of 1198 g was produced during the complete daylight period. Therefore, considering a stoichiometric value of 1.33 g O_2 per gram of biomass obtained from the basic photosynthesis equation, we estimated that up to 0.9 kg of biomass would be produced in this reactor under the assayed experimental conditions. However, the net amount of biomass produced was 2.34 kg , thus indicating that the basic photosynthesis equation is not completely valid in estimating biomass production outdoors. Thus, due to the existence of other phenomena such as photorespiration, amongst others, the amount of oxygen produced per g of oxygen varies from 0.85 to $2.26 \text{ g O}_2 \text{ g}_{\text{biomass}}^{-1}$ [3].

In this way, the proposed methodology can estimate the biomass production capacity from the dissolved oxygen measurements. However, the most relevant application is the ability to determine and optimize the mass transfer requirements. Therefore, by applying a mass balance to the paddlewheel, it is possible to estimate the mass transfer in this section; while using Eq. (6), it is also possible to determine the mass transfer in the sump, thus obtaining an overall picture of the mass transfer and oxygen production in the entire reactor (Fig. 4). The results confirm that the most relevant reactor section related to mass transfer is the sump, where up to 3.30 g min^{-1} of oxygen ($335 \text{ mg O}_2 \text{ L}^{-1} \text{ h}^{-1}$) are desorbed during the daylight period, while in the channel, a maximum value of 1.75 g min^{-1} ($7 \text{ mg O}_2 \text{ L}^{-1} \text{ h}^{-1}$) was determined. In the paddlewheel, on the other hand, a maximum value of 1.50 g min^{-1} ($450 \text{ mg O}_2 \text{ L}^{-1} \text{ h}^{-1}$) is removed. By applying Eq. (8), it is possible to know not only the oxygen transfer capacity but also the global mass transfer coefficients for the paddlewheel and the sump. The results show that the global mass transfer coefficient values are stable throughout the day except at sunrise and sunset, when the driving force approaches zero and the mass transfer coefficient values cannot be determined (Fig. 5). Considering the period from 12:00 to 17:00, when the driving force is greatest, global mass transfer coefficient values of 49 and 34 h^{-1} are obtained for the paddlewheel and the sump, respectively. This paddlewheel value is lower than that previously reported, of 160 h^{-1} [2]; however, two different paddlewheel systems were used in each case indicating that, although the paddlewheel is a standard impulsion system, modifications in its design can affect the

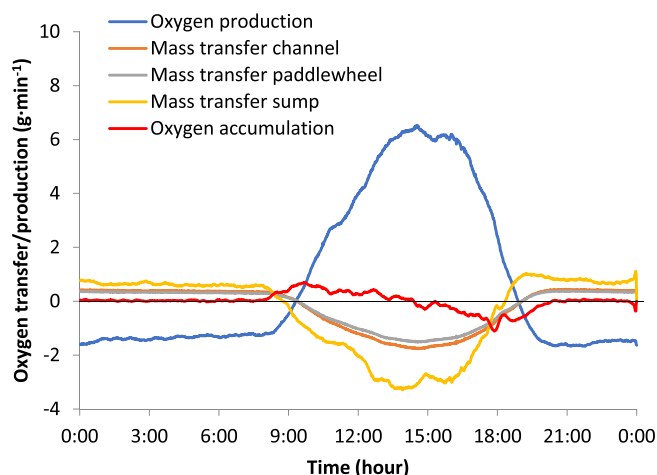


Fig. 4. Daily variation in oxygen production, oxygen transfer in each raceway reactor section and oxygen accumulation in the reactor; estimated from data on dissolved oxygen concentration at the different positions using Eq. (6).

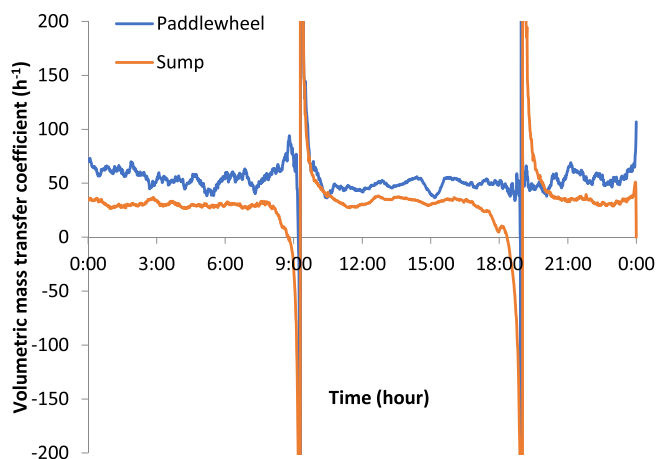


Fig. 5. Daily variation in the volumetric mass transfer coefficient in the paddlewheel and sump.

mass transfer capacity in this section of the reactor. Concerning the sump, the global mass transfer coefficient determined was 34 h^{-1} , lower than the previously reported value of 64 h^{-1} for the same air flow rate of $100 \text{ L}\cdot\text{min}^{-1}$ [2]; nonetheless, this was likewise due to modifications in the diffuser system. In any case, the results show how the proposed methodology can be used to estimate the global mass transfer coefficient value in an existing raceway reactor without disturbing the reactor's normal operation. Consequently, the proposed model can be used as a stable on-line sensor.

The utility of this methodology together with on-line sensors is the ability to measure any variation in the mass transfer capacity as a function of the operational conditions, meaning that one can make adjustments according to the system requirements. Given that liquid circulation is not normally modified during raceway reactor operation, the global mass transfer coefficients for the loop and the paddlewheel are constants; only the global mass transfer capacity in the sump can be modified according to the gas flow rate supplied. To estimate this variation, experiments were carried out on different days using the same methodology described previously, but modifying the air flow rate in the sump from 50 to $350 \text{ L}\cdot\text{min}^{-1}$. Because the air flow rate is not an intensive variable, it is a function of the total sump volume, correlating the mass transfer coefficient with an intensive variable is preferred. Consequently, different intensive variables can be used such as the power per unit of gas volume, the gas volume fraction to total

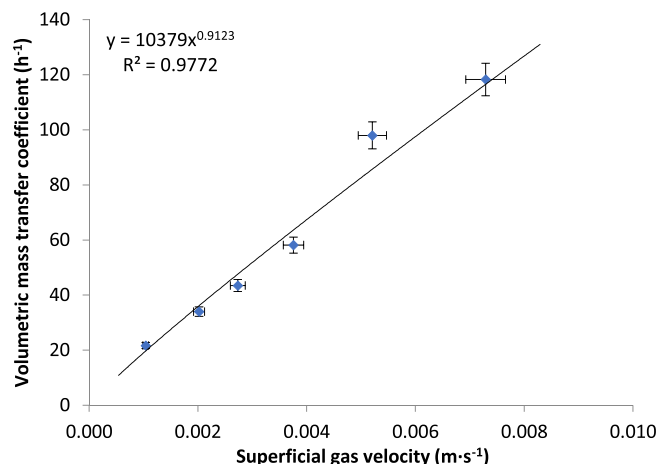


Fig. 6. Variation in the mass transfer coefficient in the sump as a function of the air flow rate, expressed as the superficial gas velocity. Values obtained using the proposed methodology to estimate the mass transfer coefficient in raceway reactors. Data shown as mean \pm SD, $n = 31$.

volume or hold-up, or the superficial gas velocity, amongst others [22]. In our case, the superficial gas velocity was selected because it is easily calculated as the ratio between the gas flow rate and the cross-sectional area of the sump, so additional measurements regarding energy consumption or gas hold-up in the system are not required. The results show that the mass transfer coefficient in the sump increased from 22 to 118 h^{-1} when the air flow rate increased from 50 to $350 \text{ L}\cdot\text{min}^{-1}$, equivalent to variations in the superficial gas velocity from 0.0010 to $0.0073 \text{ m}\cdot\text{s}^{-1}$ (Fig. 6). A potential relationship between both variables is therefore obtained, with the exponent value less than one, indicating that with the higher superficial gas velocity, the mass transfer coefficient will be saturated at its maximal value. In addition, because this exponent was close to one, it indicates that the experiments were performed at low superficial gas velocity values. Thus, in conventional mass transfer units such as bubble columns or stirred reactors, the superficial gas velocity can reach values up to $0.12 \text{ m}\cdot\text{s}^{-1}$ [23]. Microalgae reactors, on the other hand, have far lower superficial gas velocities, of up to $0.0015 \text{ m}\cdot\text{s}^{-1}$ [20,21], because microalgae cultures usually require lower mass transfer coefficients than bacteria or yeast cultures. In any case, the correlation obtained (Eq. (9)) allows us to adjust the mass transfer coefficient value by manipulating the superficial gas velocity, according to the system requirements.

$$K_{La, \text{sump}} = 10379 \cdot U_{gr}^{0.9123} \quad (9)$$

It is important to note that the supply of air imposes an additional energy consumption to liquid circulation. Thus, in raceway reactors, the energy consumption for liquid circulation ranges from 1 to $10 \text{ W}\cdot\text{m}^{-3}$; in the case of the 100 m^2 raceway reactor used, a value of $4 \text{ W}\cdot\text{m}^{-3}$ was determined, resulting in a net energy consumption of 1.9 kWh per day being measured. Air supply from 50 to $350 \text{ L}\cdot\text{min}^{-1}$ imposes an additional energy consumption ranging from 0.6 to 4.0 kWh per day if maintaining the air flow constant throughout the day, thus increasing the energy consumption from 29% to 200% . Previously, it was reported that the overall power consumption in raceway reactors increases from $4 \text{ W}\cdot\text{m}^{-3}$ (1.9 kWh per day) when no gas is supplied to the sump (only liquid circulation), up to $13 \text{ W}\cdot\text{m}^{-3}$ (6.2 kWh per day) when gas is supplied to the sump at a maximum flow rate of $200 \text{ m}^3 \cdot \text{h}^{-1}$ [2]. Because photosynthesis take place mainly during the 6 h in the middle of the daylight period, the energy consumption for aeration can be reduced to a range from 0.2 to 1.3 kWh per day; this represents between 8 and 55% of energy consumption for liquid circulation. Numerous studies have demonstrated a wide range in the mass transfer coefficient values, between 0.4 and 350 h^{-1} , for various aerated systems [26]. In

our study, the mass transfer coefficient values obtained in the sump agree with those reported previously for the same reactor [2]. They are also similar to those previously reported for other types of microalgae reactors, such as 72 h^{-1} in rectangular airlift reactors [24], 22 h^{-1} in flat-panel reactors [25], and 108 h^{-1} in the airlift section of tubular photobioreactors [27]. Nevertheless, it is important to note that in rectangular or flat-panel reactors, the entire system is aerated so the mass transfer is taking place in the entire volume of the reactor. Conversely, with raceway reactors, as with tubular photobioreactors, the mass transfer mainly takes place in the aerated zones (the sump in raceway reactors and the bubble column/airlift system in tubular reactors) — so to compare the mass transfer coefficient in any kind of system, a value that considers the total reactor volume has to be used. Doing it this way, we see that in tubular reactors, the total mass transfer coefficient decreases to 10 h^{-1} [27], whereas in the raceway that we studied, the value ranged from 1.8 to 9.6 h^{-1} , a similar range of values to those in tubular reactors. These results confirm that the behaviour of raceway and tubular photobioreactors are not so different regarding mass transfer capacity, and that both systems must be carefully designed to meet the culture requirements with regard to their mass transfer capacity, especially in terms of oxygen desorption.

Finally, to evaluate the influence of the mass transfer capacity on the dissolved oxygen concentration at the end of the channel, simulations were performed using the experimental values for the oxygen production rate and the volumetric mass transfer coefficients in the different reactor sections (Fig. 7). Data show that, if no air is supplied to the sump or if no sump exists in the reactor, the dissolved oxygen concentration in the culture can reach values up to $26 \text{ mg}\cdot\text{L}^{-1}$ (295 %Sat.) — these have been shown to dramatically reduce the performance of microalgae cultures [16,17]. When the mass transfer coefficient in the sump increases, the dissolved oxygen concentration decreases, but not in a linear fashion because the mass transfer capacity in the sump is limited. The dissolved oxygen concentration remains lower than $15 \text{ mg}\cdot\text{L}^{-1}$ (170 %Sat.) thus avoiding the negative effect of excessive concentration only when the mass transfer coefficient in the sump is higher than 50 h^{-1} ; this means that the superficial gas velocity must be higher than $0.0003 \text{ m}\cdot\text{s}^{-1}$ and the air flow rate in the sump higher than $150 \text{ L}\cdot\text{min}^{-1}$. A similar analysis can be performed when considering the variation in the oxygen production rate throughout the year, with the resultant difference in the required mass transfer capacity in the different seasons. The results show that the oxygen production rate in summer reaches values up to $6.8 \text{ g}\cdot\text{min}^{-1}$, whereas in the winter, the

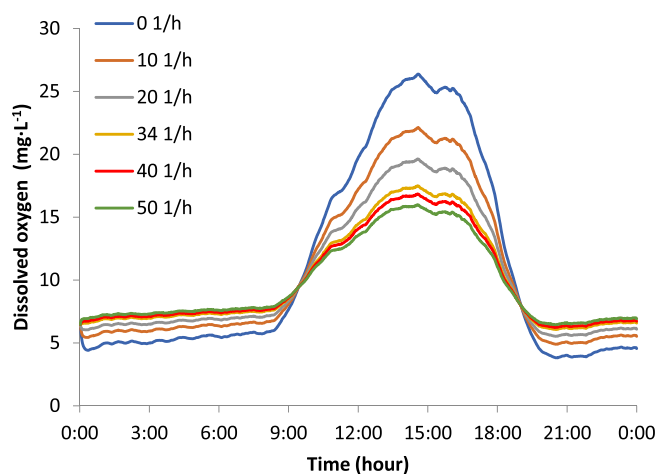


Fig. 7. Variation in the dissolved oxygen concentration at the end of the channel as a function of the volumetric mass transfer coefficient in the sump. Values obtained using experimental measurements for the oxygen production rate and simulating the mass transfer capacity in the different reactor sections according to the reported values for the volumetric mass transfer coefficients.

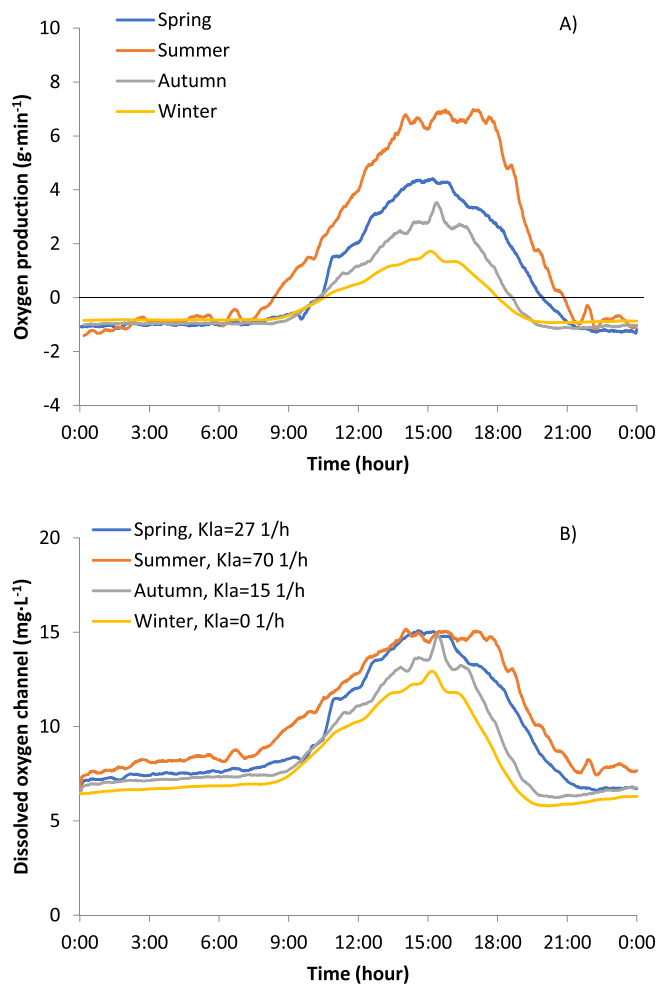


Fig. 8. (A) Daily variation in the oxygen production rate during the different seasons of the year; (B) Mass transfer coefficient values in the sump required to avoid oxygen accumulation above $15 \text{ mg}\cdot\text{L}^{-1}$ according to the methodology proposed.

maximal oxygen production rate is $1.63 \text{ g}\cdot\text{min}^{-1}$ (Fig. 8). Differences in the oxygen production rate require different mass transfer coefficient values in the sump. To avoid oxygen accumulation above $15 \text{ mg}\cdot\text{L}^{-1}$ (thus ensuring there are no adverse effects from dissolved oxygen on the culture performance), the mass transfer coefficient in the sump must be higher than 70 h^{-1} in the summer, whereas in spring, the required value drops to 27 h^{-1} and in the autumn, to 15 h^{-1} (Fig. 8). Only in winter is the oxygen production capacity so low that there is sufficient mass transfer in the channel and the paddlewheel to avoid dissolved oxygen accumulation above $15 \text{ mg}\cdot\text{L}^{-1}$; making the required mass transfer coefficient value in the sump zero.

4. Conclusions

The mass transfer capacity in raceway reactors was studied. The results confirm that dissolved oxygen accumulation can limit biomass productivity in these systems if their mass transfer capacity is not optimized. Although oxygen is desorbed to the air in the channel and the paddlewheel, the sump is the reactor section that contributes most — therefore, the mass transfer capacity in this section must be optimized according to the oxygen production rate in the system. The influence of gas flow on the mass transfer coefficient was also determined, obtaining a calibrated empirical model. Using this model, it is possible to properly regulate the air flow in the sump so that the reactor operation can be optimized. The methodology proposed allows us to determine and then

optimize the mass transfer capacity in the sump of any raceway reactor. For this reason, it is a powerful tool for the optimization of existing reactors as well as in optimizing the design of new reactors.

Nomenclature

Variable	Units	Description
PO ₂	g·min ⁻¹	Oxygen production by photosynthesis
NO ₂	g·min ⁻¹	Oxygen transfer between the culture and the air
K _{a1}	min ⁻¹	Volumetric mass transfer coefficient
[O ₂]	mg·L ⁻¹	Dissolved oxygen concentration
[O _{2e}]	mg·L ⁻¹	Dissolved oxygen concentration in equilibrium with air
V	L	Volume of the respective zone
T	°C	Temperature of the culture
Q _{liquid}	L·min ⁻¹	Liquid flow rate
U _{gr}	m·s ⁻¹	Superficial gas velocity

Acknowledgements

This study was supported financially by the Ministry of Economy and Competitiveness (DPI2014-55932-C2-1-R, DPI2017-84259-C2-1-R), EDARSOL (CTQ2014-57293-C3-1-R), and the European Union's Horizon 2020 Research and Innovation Program under Grant Agreement No. 727874 SABANA. We are most grateful for the practical assistance given by the staff of the Cajamar Foundation's "Las Palmerillas" Experimental Station. We are also grateful to Daniel Algarra Navas for his work on the graphical design of Fig. 1.

Author contributions statement

M. Barceló-Villalobos was responsible for the work and data collection, in addition to writing the manuscript. J. L. Guzmán Sánchez was responsible for data processing and contributed to the elaboration of the manuscript. I. Martín Cara was responsible for the operation of the reactors and verifying the data quality. J. A. Sánchez Molina was responsible for developing the models. F. G. Acién Fernández was responsible for the team and coordinating the work, mainly participating in the discussion regarding the results and finalizing the manuscript.

Conflict of interest statement

The authors declare no potential financial or other interests that could be perceived as influencing the outcome of the research.

Statement of informed consent, human/animal rights

"No conflicts, informed consent, human or animal rights are applicable."

Declaration of authors

All the participants share authorship of this work and agree to submit the manuscript for peer review to Algal Research.

References

- [1] J. Benemann, Microalgae for biofuels and animal feeds, *Energies* 6 (2013) 5869–5886.
- [2] J.L. Mendoza, M.R. Granados, I. de Godos, F.G. Acién, E. Molina, S. Heaven, C.J. Banks, Oxygen transfer and evolution in microalgal culture in open raceways, *Bioresour. Technol.* 137 (2013) 188–195.
- [3] S. Li, S. Luo, R. Guo, Efficiency of CO₂ fixation by microalgae in a closed raceway pond, *Bioresour. Technol.* 136 (2013) 267–272.
- [4] I. de Godos, J.L. Mendoza, F.G. Acién, E. Molina, C.J. Banks, S. Heaven, F. Rogalla, Evaluation of carbon dioxide mass transfer in raceway reactors for microalgal culture using flue gases, *Bioresour. Technol.* 153 (2014) 307–314, <https://doi.org/10.1016/j.biortech.2013.11.087>.
- [5] A. Pawlowski, I. Fernández, J.L.L. Guzmán, M. Berenguel, F.G.G. Acién, J.E.E. Normey-Rico, Event-based predictive control of pH in tubular photobioreactors, *Comput. Chem. Eng.* 65 (2014) 28–39, <https://doi.org/10.1016/j.compchemeng.2014.03.001>.
- [6] D. Ippoliti, A. González, I. Martín, J.M.F. Sevilla, R. Pistocchi, F.G. Acién, Outdoor production of *Tisochrysis lutea* in pilot-scale tubular photobioreactors, *J. Appl. Phycol.* 28 (2016) 3159–3166, <https://doi.org/10.1007/s10811-016-0856-x>.
- [7] Y. Bao, M. Liu, X. Wu, W. Cong, Z. Ning, In situ carbon supplementation in large-scale cultivations of *Spirulina platensis* in open raceway pond, *Biotechnol. Bioprocess Eng.* 17 (2012) 93–99.
- [8] E. Posadas, M.M. Morales, C. Gomez, F.G. Acién, R. Muñoz, Influence of pH and CO₂ source on the performance of microalgae-based secondary domestic wastewater treatment in outdoors pilot raceways, *Chem. Eng. J.* 265 (2015) 239–248.
- [9] C. Jiménez, B.R. Cossío, D. Labella, F.X. Niell, The feasibility of industrial production of *Spirulina (Arthrospira)* in Southern Spain, *Aquaculture* 217 (2003) 179–190, [https://doi.org/10.1016/S0044-8486\(02\)00118-7](https://doi.org/10.1016/S0044-8486(02)00118-7).
- [10] I. de Godos, J.L. Mendoza, F.G. Acién, E. Molina, C.J. Banks, S. Heaven, F. Rogalla, Evaluation of carbon dioxide mass transfer in raceway reactors for microalgal culture using flue gases, *Bioresour. Technol.* 153 (2014) 307–314, <https://doi.org/10.1016/j.biortech.2013.11.087>.
- [11] S.C. James, V. Boriah, Modeling algae growth in an open-channel raceway, *J. Comput. Biol.* 17 (2010) 895–906.
- [12] Y.H. Wang, R. Turton, K. Semmens, T. Borisova, Raceway design and simulation system (RDSS): an event-based program to simulate the day-to-day operations of multiple-tank raceways, *Aquac. Eng.* 39 (2008) 59–71, <https://doi.org/10.1016/j.aquaeng.2008.06.002>.
- [13] J.L. Mendoza, M.R. Granados, I. de Godos, F.G. Acién, E. Molina, C. Banks, S. Heaven, Fluid-dynamic characterization of real-scale raceway reactors for microalgal production, *Biomass Bioenergy* 54 (2013) 267–275, <https://doi.org/10.1016/j.biombioe.2013.03.017>.
- [14] K. Sompech, Y. Chisti, T. Srinophakun, Design of raceway ponds for producing microalgae, *Biofuels* 3 (2012) 387–397.
- [15] I. Fernández, F.G. Acién, J.M. Fernández, J.L. Guzmán, J.J. Magán, M. Berenguel, Dynamic model of microalgal production in tubular photobioreactors, *Bioresour. Technol.* 126 (2012) 172–181, <https://doi.org/10.1016/j.biortech.2012.08.087>.
- [16] A. Pawlowski, J.L. Mendoza, J.L. Guzmán, M. Berenguel, F.G. Acién, S. Dormido, Effective utilization of flue gases in raceway reactor with event-based pH control for microalgal culture, *Bioresour. Technol.* 170 (2014) 1–9, <https://doi.org/10.1016/j.biortech.2014.07.088>.
- [17] I. Fernández, F.G. Acién, J.L. Guzmán, M. Berenguel, J.L. Mendoza, Dynamic model of an industrial raceway reactor for microalgal production, *Algal Res.* 17 (2016) 67–78, <https://doi.org/10.1016/j.algal.2016.04.021>.
- [18] A.S. Mirón, A.C. Gómez, F.G. Camacho, E.M. Grima, Y. Chisti, Comparative evaluation of compact photobioreactors for large-scale monoculture of microalgae, *Prog. Ind. Microbiol.* 35 (1999) 249–270, [https://doi.org/10.1016/S0079-6352\(99\)80119-2](https://doi.org/10.1016/S0079-6352(99)80119-2).
- [19] C. Sousa, D. Valev, M.H. Vermué, R.H. Wijffels, Effect of dynamic oxygen concentrations on the growth of *Neochloris oleabundans* at sub-saturating light conditions, *Bioresour. Technol.* 142 (2013), <https://doi.org/10.1016/j.biortech.2013.05.041>.
- [20] T.A.A. Costache, F.G.A. Fernández, F.G. Acien, M.M. Morales, J.M. Fernández-Sevilla, I. Stamatin, E. Molina, Comprehensive model of microalgal photosynthesis rate as a function of culture conditions in photobioreactors, *Appl. Microbiol. Biotechnol.* 97 (2013) 7627–7637.
- [21] D. Ippoliti, C. Gómez, M.M. Morales-Amaral, R. Pistocchi, J.M.M. Fernández-Sevilla, F.G.G. Acién, Modeling of photosynthesis and respiration rate for *Isochrysis galbana* (T-Is0) and its influence on the production of this strain, *Bioresour. Technol.* 203 (2016) 71–79.
- [22] F. Garcia-Ochoa, E. Gomez, Bioreactor scale-up and oxygen transfer rate in microbial processes: an overview, *Biotechnol. Adv.* 27 (2009) 153–176, <https://doi.org/10.1016/j.biotechadv.2008.10.006>.
- [23] Y. Chisti, U.J. Jauregui-Haza, Oxygen transfer and mixing in mechanically agitated airlift bioreactors, *Biochem. Eng. J.* 10 (2002) 143–153.
- [24] X. Guo, L. Yao, Q. Huang, Aeration and mass transfer optimization in a rectangular airlift loop photobioreactor for the production of microalgae, *Bioresour. Technol.* 190 (2015) 189–195, <https://doi.org/10.1016/j.biortech.2015.04.077>.
- [25] E. Sierra, F.G. Acién, J.M. Fernández, J.L. García, C. González, E. Molina, Characterization of a flat plate photobioreactor for the production of microalgae, *Chem. Eng. J.* 138 (2008) 136–147.
- [26] A.P. Carvalho, L.A. Meireles, F.X. Malcata, Microalgal reactors: a review of enclosed system designs and performances, *Biotechnol. Prog.* 22 (2006) 1490–1506.
- [27] F. Camacho-Rubio, F.G. Acién, J.A. Sánchez-Pérez, F. García-Camacho, E. Molina-Grima, Prediction of dissolved oxygen and carbon dioxide concentration profiles in tubular photobioreactors for microalgal culture, *Biotechnol. Bioeng.* 62 (1999) 71–86, [https://doi.org/10.1002/\(SICI\)1097-0290\(199910\)62:1<71::AID-BIT9>3.0.CO;2-T](https://doi.org/10.1002/(SICI)1097-0290(199910)62:1<71::AID-BIT9>3.0.CO;2-T).



Evaluation of photosynthetic light integration by microalgae in a pilot-scale raceway reactor

M. Barceló-Villalobos^a, P. Fernández-del Olmo^c, J.L. Guzmán^a, J.M. Fernández-Sevilla^b,
F.G. Ación Fernández^{b,*}

^a Department of Informatics, Universidad de Almería, ceIA3, CIESOL, E04120 Almería, Spain

^b Department of Chemical Engineering, Universidad de Almería, Spain

^c Institute for Research in Agriculture and Fisheries, Junta de Andalucía, E04720 Almería, Spain

ARTICLE INFO

Keywords:

Microalgae
Raceway
Biomass production
Light frequency
CFD

ABSTRACT

The improvement of photosynthetic efficiency in a 100 m² raceway reactor by enhancement of light regime to which the cells are exposed is here reported. From Computational Fluid Dynamics it was calculated that the light exposure times ranged from 0.4 to 3.6 s while the exposure times to darkness were much longer, from 6 to 21 s. It was demonstrated that these times are too long for light integration, the cells fully adapting to local irradiances. This phenomenon was validated in the real outdoor raceway at different seasons. Simulations allow to confirm that if total light integration is achieved biomass productivity can increase up to 40 g/m²-day compared to 29 g/m²-day obtained considering local adaptation, which is close to the experimental value of 25 g/m²-day. This paper provides clear evidence of microalgae cell adaptation to local irradiance because of the unfavourable cell movement pattern in raceway reactors.

1. Introduction

Raceway reactors are the most extended technology for microalgae growth; more than 90% of the worldwide microalgae production is performed using this technology. The design of raceway reactors was first proposed by Oswald and Golueke in the 1960's (Oswald and Golueke, 1960). This design has recently been revised to increase microalgae production, and especially to integrate these reactors into large applications such as wastewater treatment. Therefore, the energy consumption, mixing and mass transfer of these reactors are currently the subject of research (Barceló-Villalobos et al., 2018; de Godos et al., 2014; Labatut et al., 2007; Liffman et al., 2013; Mendoza et al., 2013b). In spite of the recent improvements regarding these aspects, the overall performance of whichever microalgae culture is always limited by the light utilization efficiency; that is to say, by how the microalgae use the light impinging on the reactor surface.

In raceway reactors, as in any microalgae culture system, light gradients exist due to the light attenuation caused by the cells. According to the culture movement (vertical mixing), the cells are exposed to different light regimes as a function of the existing light gradients. The relevance of the light regime (to which the cells are exposed) on microalgae culture performance has been widely discussed,

and is still a hot topic in the microalgae biotechnology field given its importance in improving the biomass productivity of real systems (Brindley et al., 2016, 2011; Grobbelaar, 1989; Schulze et al., 2014; Ugwu et al., 2005; Vejrazka et al., 2011). Moreover, it is not only light intensity and frequency that matter - the actual "shape" of the irradiance variation pattern also influences the response of microalgae cells (Brindley et al., 2016). These authors showed that pure flashing light (neat dark/light changes represented by square-wave functions) elicit a lower photosynthetic response than other light patterns, calling into question the idea that any light regime is a mere transition from light to dark. On the basis of the photosynthesis mechanism, the time requested for reactions to take place in PSI-PSII is much lower than the time required to use the energy produced by the cells. High frequency fluctuating light (< 100 ms) has been reported to lead to higher growth rates and higher photosynthesis rates than continuous light (Matthijs et al., 1996; Nedbal et al., 1996). These values are a function of light intensity and other variables such as the strain and status of the cells, among others; thus it is a complex phenomenon. To summarize, it is generally accepted that to allow complete light integration, dark cycles at frequencies higher than 1 Hz are required (Brindley et al., 2011).

However, applying these results to large-scale reactors is difficult because the real patterns in these systems have barely been analysed.

* Corresponding author.

E-mail address: facien@ual.es (F.G. Ación Fernández).

<https://doi.org/10.1016/j.biortech.2019.02.032>

Received 11 December 2018; Received in revised form 4 February 2019; Accepted 5 February 2019

Available online 06 February 2019

0960-8524/ © 2019 Elsevier Ltd. All rights reserved.

Recently, the utilization of Computational Fluid Dynamics (CFD) tools, such as ANSYS Fluent, have allowed us to analyse the hydrodynamics in real-scale reactors (Bitog et al., 2011; Fernández-Del Olmo et al., 2017; García et al., 2012; Soman and Shastri, 2015). The studies performed to date are mainly focused on the reactor's energy consumption and on how to minimize the pressure drop caused by the liquid circulation. Other papers are focused on the elucidation of the light pattern to which the cells are exposed as a function of the design, operational and environmental parameters. There is, however, an underlying inconsistency in the literature dealing with the light integration effect in microalgae reactors. While numerous studies provide converging evidence for enhanced photosynthetic efficiency at a higher frequency of on/off signals (Perner-Nochta et al., 2007), there is no clear experimental evidence that more mixing actually enhances growth. Overall, studies that demonstrate productivity enhancement through increased mixing are scarce compared to studies restricted to the flashing effect, and they are rarely supported by experimental evidence (Demory et al., 2018). However, most of these studies have been performed on small reactors. Moreover, no clear figures were provided regarding the light regimes to which the cells were exposed in these reactors. The relevance of the reactor size must be emphasized because the circulation pattern is significantly modified according to the scale of the reactors. Consequently, when using small raceway reactors, the contribution of bends, paddlewheel and other structural elements, such as baffles, greatly modifies the liquid pattern in the channel, with these sections increasing the vertical mixing. Conversely, in large reactors, the contribution of these sections is minimal so the vertical mixing is very low (Demory et al., 2018; Mendoza et al., 2013a).

Accordingly, this paper focuses on quantifying the light utilization phenomenon taking place in real raceway reactors. For this, the light exposure times in a real pilot-scale reactor were determined and their influence on the cells' photosynthesis rate was measured under laboratory conditions. The objective was to determine if the biomass productivity of real-scale raceway reactors can be improved by enhancing the light regime to which the cells are exposed; and how it would be possible to achieve this objective. Clarifying this question is highly relevant for microalgae biotechnology, not only in terms of the potential improvements in the productivity of real production systems, but also because it would affect all the models and design tools currently used in this field.

2. Materials and methods

2.1. Microorganism, raceway reactor and culture conditions

The microalgae strain used was *Scenedesmus almeriensis* (CCAP 276/24). Inoculum for the raceway reactor was produced in a 3.0 m³ tubular photobioreactor under controlled conditions (pH 8 by on-demand CO₂ injection and a temperature ranging from 18 to 22 °C) using freshwater and Mann & Myers medium prepared with fertilizers (0.14 g·L⁻¹ KH₂PO₄, 0.18 g·L⁻¹ MgSO₄·7H₂O, 0.9 g·L⁻¹ NaNO₃, 0.02 mL·L⁻¹ Welgro, and 0.02 g·L⁻¹ Kalentol).

The raceway reactor is located at the "Las Palmerillas" Research Centre, 36° 48'N–2° 43'W, part of the Cajamar Foundation (Almería, Spain). The reactor consists of two 50 m long channels (0.46 m high × 1 m wide), both connected by 180° bends at each end, with a 0.59 m³ sump (0.65 m long × 0.90 m wide × 1 m deep) located 1 m along one of the channels (Barceló-Villalobos et al., 2018). A paddlewheel system was used to recirculate the culture through the reactor at a regular velocity of 0.2 m·s⁻¹, although this could be increased up to 0.8 m·s⁻¹ by manipulating the frequency inverter of the engine. The pH, temperature and dissolved oxygen in the culture were measured using appropriate probes (5083 T and 5120, Crison Instruments, Barcelona, Spain), connected to an MM44 control-transmitter unit (Crison Instruments, Spain), and data acquisition software (Labview, National Instruments, USA) providing complete monitoring and control of the

system. The culture's pH was maintained at 8.0 by on-demand CO₂ injection whereas temperature was not controlled – this varied by ± 5 °C with respect to the daily mean air temperature, which, in turn, varied from 12 °C in winter to 28 °C in summer. The raceway reactor was inoculated and operated in batch mode for one week, after which it was operated in semi-continuous mode at 0.2 day⁻¹ at a culture depth of 0.15 m. Only samples from steady-state conditions were used. Evaporation inside the reactor was compensated for by the daily addition of fresh medium.

2.2. CFD model

The ANSYS Meshing 12.1 pre-processor was used to generate the numerical grid for a suitable discretization of the computational domain. Hexahedral mesh was used because of its capabilities in providing a high-quality solution with fewer cells for simple geometry. To obtain the mesh-independent result, three different mesh densities (1,096,250, 1,656,875 and 2,096,875 cells) were evaluated. The optimal mesh density (1,656,875), in terms of computational time and accuracy, was implemented in the numerical analysis. In order to exclude turbulence model dependence on the results, a sensitivity study on the turbulence settings was performed on the optimal mesh. The realizable k-ε model was used. The numerical model was based on the finite-volume method. The transport equations were solved using the ANSYS FLUENT 12.1 CFD commercial software package. The flow solution procedure used was the Semi-Implicit Method for Pressure-Linked Equation (SIMPLE) routine. The momentum equations were discretized using both first and second-order upwind scheme options, and second-order upwind for the other transport equations. The convergence criterion consisted of monitoring the mass flow rate at the inlet and outlet, and the variation in velocity profiles with iteration, a reduction of several orders of magnitude in the residual errors. The results were validated by comparing them with the experimental measurements. 3D simulations were performed on a workstation with two Six-Core Intel Xeon X5650 2.66 GHz 12 MB/1333 processors, and HP 48 GB RAM (6 × 8 GB) DDR3-1333 (Hewlett Packard, USA).

2.3. Photosynthetic rate measurement

The photosynthesis rate of the microalgae samples was determined using a photo-respirometer built by the Chemical Engineering Department at the University of Almería. The system basically consists of a magnetically-stirred jacketed vessel (0.03 m diameter, 80 mL total volume), in which the pH (Crison pH5010, Spain), dissolved oxygen (Crison OD6050, Spain), temperature (Crison PT1000, Spain) and light (Walz US-SQS/L, Germany) probes are submerged; the light being provided by two LED lamps (SMD Bridgelux Pro 200W, Germany). The entire system was computer controlled. Sensors were connected to an MM44 control-transmitter unit (Crison Instruments, Spain) and data acquisition software (DAQFactory, Labjack, USA) to provide complete experiment monitoring and control. The LED lamps were controlled both in intensity and on/off period duration. The photosynthesis rate was measured by providing the requested light conditions and evaluating the oxygen accumulation rate, also providing air between cycles to always perform the measurements close to 100 %Sat; thus avoiding the influence of this variable. A minimum of three cycles were used to obtain a mean value under the conditions assayed.

2.4. Experimental design and accuracy of measurements

A total of 172 samples were taken from the raceway reactor at different times throughout the year (from February to July) and at different times of the day (8:00 h, 10:00 h, 12:00 h and 14:00 h). The photosynthesis rate (PO₂, mg L⁻¹ h⁻¹) was calculated by diluting the culture and providing the target light conditions, measuring the oxygen production over time. The performance of the microalgae cells under

continuous light conditions was evaluated first as a control stage. Following this, the performance of the cells under different light regimes was determined. In the first set of experiments, the irradiance without cells was kept at $500 \mu\text{E m}^{-2} \text{s}^{-1}$ and the light and dark times were modified from 1 to 10 s. In the second set of experiments, the irradiance was adjusted to that existing in real outdoor reactors whereas the light and dark times were adjusted close to those experimentally determined by CFD, thus ranging from 1 to 24 s. In each experiment, the irradiance without cells (I_0), the irradiance with cells (I), the light time, and the dark time were fixed. From these values, we calculated the different parameters. The average irradiance, I_{av} , was calculated as the light inside the jacketed vessel multiplied by the proportion of time that it was illuminated (Eq. (1)). The illuminated cycle proportion, Φ , was calculated as the illuminated time to total time ratio (Eq. (2)). The light exposure frequency, ν , was calculated as the inverse of the total cycle time (Eq. (3)).

$$I_{av} = I \frac{t_{light}}{t_{light} + t_{dark}} \quad (1)$$

$$\Phi = \frac{t_{light}}{t_{light} + t_{dark}} \quad (2)$$

$$\nu = \frac{1}{t_{light} + t_{dark}} \quad (3)$$

2.5. Statistical analysis

Data were processed using Microsoft Excel 2016, and the statistical analysis was performed using Statgraphics Centurion 18. Data from the outdoor reactors were obtained at steady state whereas measurements under laboratory conditions were performed in triplicate (as a minimum).

3. Results and discussion

To study the influence of the light/dark cycles taking place in a 100 m^2 raceway reactor on the performance of microalgae cells, the first step was to model the photosynthesis rate for continuous light under laboratory conditions. A classical P-I curve was obtained for the *Scenedesmus almeriensis* cells taken directly from the reactor. The curve was obtained at three different biomass concentrations, 0.1, 0.2 and 0.4 g/L, by diluting the initial culture, 1.2 g/L, with fresh culture broth to minimize the variations in culture conditions. The results show that the photosynthesis rate increased hyperbolically with the irradiance, the system behaviour being equal at biomass concentrations of 0.1–0.2 g/L whereas at 0.4 g/L, a lower photosynthesis rate was observed for the same irradiance values (Fig. 1). This can be attributed to the light gradients inside the test cultures. In spite of the small size of the glass reactor used (0.03 m diameter), light gradients always exist in microalgal cultures due to light attenuation by the cells; these are more intense when the biomass concentration in the culture is high. In diluted microalgal cultures, the cells are almost continuously exposed to light and, under such conditions, photosynthetic performance is optimal (0.1–0.2 g/L). In contrast, when intense light gradients are present (0.4 g/L), the cells remain at low irradiance for a significant amount of time and thus the photosynthesis rate is reduced.

Data from the three experiments were fitted to the hyperbolic model (Molina-Grima et al., 1996) (Eq. (4)); the model's characteristic parameter values being shown in Table 1. The results show that the maximum photosynthesis rate, PO_{2max} , was $101 \text{ mgO}_2/\text{g}_{biomass}\cdot\text{h}$ at the optimal biomass concentration of 0.1–0.2 g/L but this reduced to $63 \text{ mgO}_2/\text{g}_{biomass}\cdot\text{h}$ when using the higher biomass concentration of 0.4 g/L. Regarding the irradiance at half-saturation, I_k , a value of $82\text{--}90 \mu\text{E}/\text{m}^2\cdot\text{s}$ was obtained at the optimal biomass concentration of 0.1–0.2 g/L whereas at the higher biomass concentration of 0.4 g/L, this

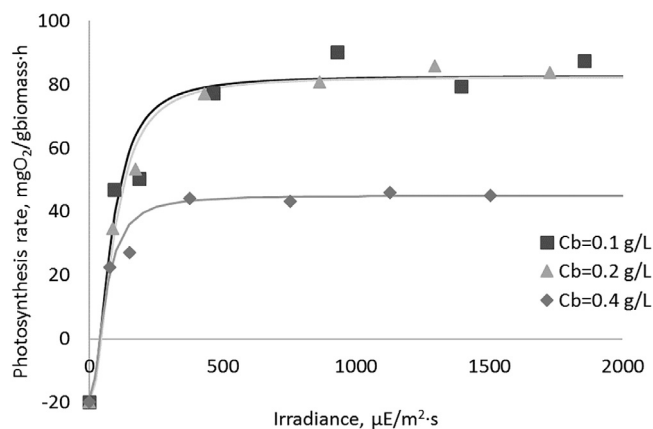


Fig. 1. Variation in the photosynthesis rate/of *Scenedesmus almeriensis* cells as a function of the average irradiance for continuous light under laboratory conditions.

Table 1

Characteristic parameter values of the hyperbolic model determined from the different samples studied: samples from the same reactor at different biomass concentrations; samples from the same reactor in different seasons.

Cb g/L	PO_{2max} $\text{mgO}_2/\text{g}_{biomass}\cdot\text{h}$	n	I_k $\mu\text{E}/\text{m}^2\cdot\text{s}$	RO_2 $\text{mgO}_2/\text{g}_{biomass}\cdot\text{h}$	I_c $\mu\text{E}/\text{m}^2\cdot\text{s}$	Φ %
0.1	101.3	2.01	82.2	-18.7	40.0	0.93
0.2	101.4	1.99	90.5	-18.9	43.0	0.86
0.4	63.5	2.00	61.3	-18.5	39.0	0.75
Season	PO_{2max} $\text{mgO}_2/\text{g}_{biomass}\cdot\text{h}$	n	I_k $\mu\text{E}/\text{m}^2\cdot\text{s}$	RO_2 $\text{mgO}_2/\text{g}_{biomass}\cdot\text{h}$	I_c $\mu\text{E}/\text{m}^2\cdot\text{s}$	Φ %
Winter	130.0	2.00	120.0	-10.0	35.0	0.86
Spring	180.0	2.00	70.0	-20.0	26.0	0.86
Summer	160.0	2.00	90.0	-20.0	34.0	0.86

value dropped to $61 \mu\text{E}/\text{m}^2\cdot\text{s}$. The value of form parameter, n , remained constant at 2.0. What is also highly relevant is that the respiration rate was the same regardless of the biomass concentration; a value of $-18 \text{ mgO}_2/\text{g}_{biomass}\cdot\text{h}$ being measured. This confirms that the respiration rate is independent of biomass concentration; it being only a function of the culture conditions under which the cells are produced. Concerning the minimum irradiance for photosynthesis, I_c , values from 39 to $43 \mu\text{E}/\text{m}^2\cdot\text{s}$ were obtained for the biomass concentrations assayed, with no tendency being observed of this characteristic parameter with regard to the biomass concentration. The maximum photosynthesis rate measured agreed with previously reported values of $270 \text{ mgO}_2/\text{g}_{biomass}\cdot\text{h}$ (Brindley et al., 2016). From these figures, the duty cycle can also be calculated (that is to say, the percentage of time at which the cells were exposed to light) as the ratio between the irradiance with the culture present, I , and the initial irradiance with water only, I_0 (Eq. (5)) - a value of 0.75 was obtained when using 0.4 g/L whereas this parameter increased to 0.86 and 0.93 when using 0.2 and 0.1 g/L, respectively. These figures anticipate the relevance of the duty cycle on culture performance - the higher this parameter is, the higher the photosynthesis rate for the same average irradiance results.

$$PO_2 = \frac{PO_{2max} \times I^n}{I_k^n + I^n} + RO_2 \quad (4)$$

$$\Phi = \frac{I}{I_0} \quad (5)$$

Once the photosynthesis model was known, the light/dark cycles existing in the 100 m^2 raceway reactor were studied, a critical parameter that needs to be defined is the minimum irradiance required for the microalgal cells to perform photosynthesis, I_c . On the basis of this

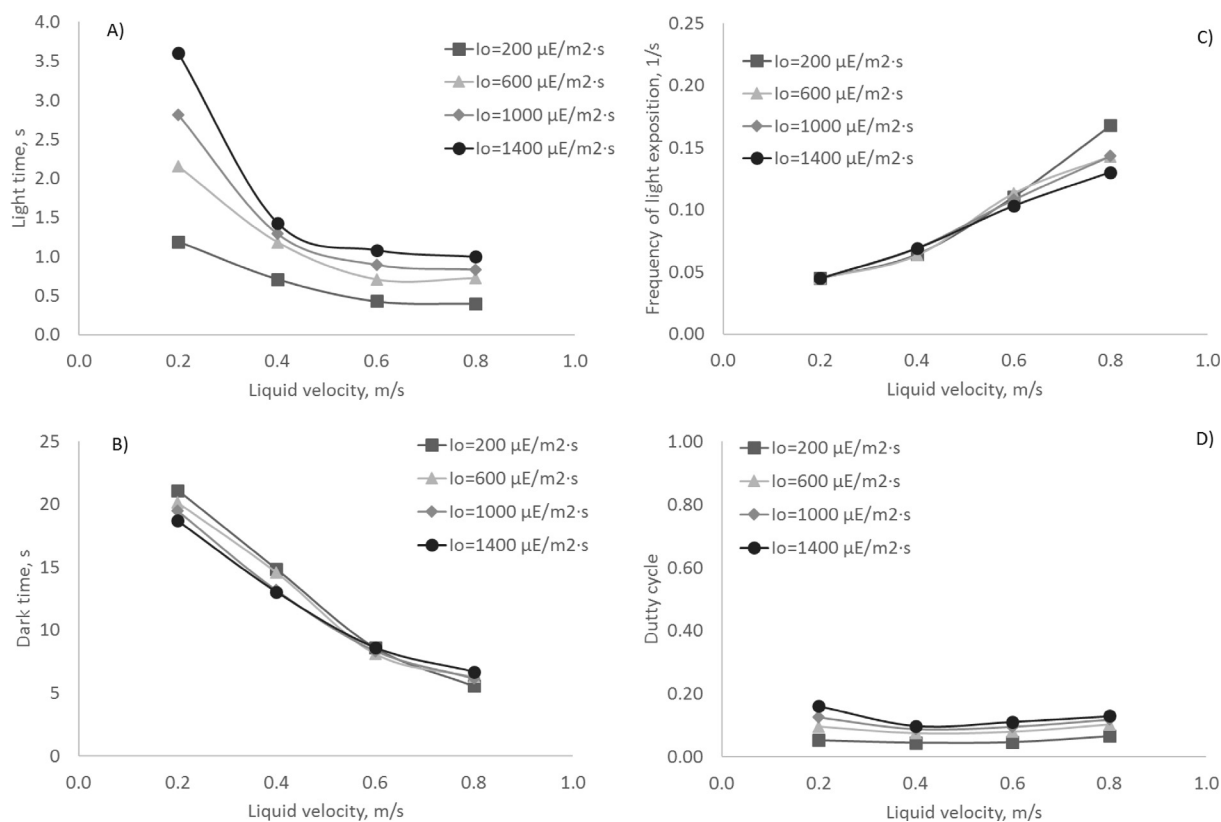


Fig. 2. Variation in the light time (A), dark time (B) and light exposure frequency (C) of *Scenedesmus almeriensis* cultures in a raceway reactor as a function of the liquid velocity/and solar irradiance/on the reactor surface. Data obtained from CFD analysis of a real raceway reactor operated in continuous mode.

value, the entire volume of any reactor can be divided into light volume (a zone where there is enough light for photosynthesis to take place) and a dark volume (a zone where no photosynthesis is possible). Considering an I_c value equal to $40 \mu\text{E}/\text{m}^2\cdot\text{s}$ (Table 1), the time that the cells spend in the illuminated volume and in the dark volume of the real raceway reactor was calculated by CFD (Fig. 2). The results show that the time the cells were exposed to light, when close to the surface of the raceway reactor, was much shorter than the time that the cells remained in the dark, inside the reactor, where maximum values of 3.6 and 28 s were obtained, respectively (Fig. 2A and B). Conversely, the minimum time the cells were exposed to light was 0.4 s compared to a minimum dark time of 5.6 s. All of these figures are mean values, obtained considering the average times for a total of 50 cells/particles moving along the raceway reactor for 50 m in a straight channel. The data show that the vertical movement of the liquid in the raceway reactor was minimal so displacement of the cells/particles from the reactor's light to dark zones was very slow, with some of them never moving between the light and dark zones; however, on average, the times calculated correspond to the expected average behaviour of a single cell. The results also show how the light time increased when increasing the solar irradiance onto the reactor surface due to deeper light penetration into the culture whereas this reduced when increasing the liquid velocity because of the higher light/dark cycle frequency taking place. Regarding the dark time, this was reduced when the solar irradiance was greater, again due to the increased light penetration into the reactor. Likewise, higher liquid velocity in the reactor brought about an increase in the light/dark transition frequency to which the cells were exposed. Analysing the data on the frequency of light exposure, one observes how this increased when the liquid velocity increased; the solar irradiance influence being minimal in spite of the maximum frequencies measured at 0.17 Hz (Fig. 2C). It has been indicated that, to maximize the performance of microalgae cultures, an approximate mixing frequency of 15 Hz is needed, which would require

an increase in liquid velocity up to 7.2 m/s in a 0.09 m tube diameter tubular photobioreactor (Brindley et al., 2016). Such a high liquid velocity would be very difficult to achieve in real reactors, and it would cause undesirable side-effects; for example, severe damage to the cells by shear-related stress phenomena (Alías et al., 2004). In raceway reactors, increasing the velocity above 0.8 m/s is almost impossible; in addition, when the velocity is increased above 0.2 m/s, the power consumption required for circulating the liquid is greatly increased (Mendoza et al., 2013a). Regarding the duty cycle, the results show how, in real raceway reactors, the proportion of time that the cells received light was very low, with maximum values of 0.16, and where no relevant variations were observed with liquid velocity or solar irradiance (Fig. 2D). Duty cycle values in the 0.05 range are typical for concentrated cultures whereas in diluted cultures, values up to 0.4 can be found; values up to 0.9 being measured only in really diluted cultures (Brindley et al., 2016). Higher duty cycle values favour light integration by the cells although this is also influenced by other variables such as the irradiance and frequency under those conditions (Brindley et al., 2011). In any case, the most relevant insight from the data obtained is that the times to which the cells are exposed to light or dark conditions are very large, especially when compared to that recommended for light integration, which is less than 1 s (Brindley et al., 2011). Therefore, in order to evaluate the performance of microalgae cells based on the light/dark variations taking place inside real raceway reactors, experiments must be performed under these conditions, thus providing light and dark periods in the range of seconds.

Consequently, the first set of experiments was performed taking culture from the raceway reactor and evaluating its photosynthesis rate under laboratory conditions yet simulating those outdoors, thus providing light and dark times based on the experimental raceway reactor results. For this, a complete factorial experimental design was performed that considered light and dark times of 1, 2, 3, 4, 5 and 10 s with the photosynthesis rate under these conditions being determined

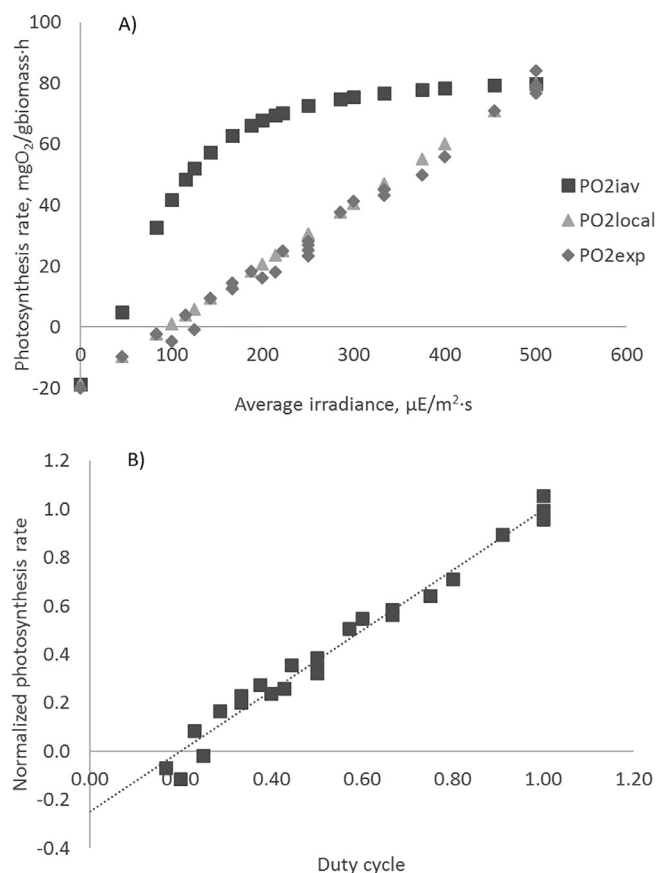


Fig. 3. (A) Variation in the photosynthesis rate (mg O₂/g biomass h) of *Scenedesmus almeriensis* cultures in a raceway reactor as a function of the average irradiance (μE/m² s) to which the cells were exposed, under different light/dark cycles ranging from 1 to 10 s. PO_{2iav} corresponds to the modelled photosynthesis rate if complete light integration takes place; whereas PO_{2local} corresponds to the modelled photosynthesis rate with null light integration. (B) Variation in the normalized photosynthesis rate with the duty cycle for the same experiments.

(Fig. 3). Based on the irradiance provided, the maximum photosynthesis rate, PO_{2io}, was calculated using the hyperbolic model previously described (Eq. (6)). By employing the average irradiance to which the cells were exposed, calculated as the irradiance provided multiplied by the percentage of time for which it was provided, the theoretical maximal photosynthesis rate with full light integration (PO_{2iav}) was determined (Eq. (7)). Conversely, the theoretical minimum photosynthesis rate, if null light integration took place, PO_{2local}, was calculated as the sum of the photosynthesis rate during light and dark periods, both calculated using the same hyperbolic model previously determined (Eq. (8)). The experimental photosynthesis rate, PO_{2exp}, must be midway between these two limit values, the higher the frequency at which the light was provided, the greater the light integration with the experimental values of the photosynthesis rate approaching the PO_{2iav} values.

$$PO_{2io} = \frac{PO_{2max} \times I_0^n}{I_k^n + I_0^n} + RO_2 \quad (6)$$

$$PO_{2iav} = \frac{PO_{2max} \times I_{av}^n}{I_k^n + I_{av}^n} + RO_2 \quad (7)$$

$$PO_{2local} = (PO_{2io} \hat{\Delta} \cdot \Phi)_{light} + (RO_2 \hat{\Delta} \cdot (1 - \Phi))_{dark} \quad (8)$$

The results show how the maximal photosynthesis rate, PO_{2iav}, increased hyperbolically with the average irradiance; as expected from the hyperbolic model used to calculate these values (Fig. 3). These

values correspond to the maximal values in the event that full light integration of the cells took place. Regarding the photosynthesis rate, if null light integration took place, PO_{2local}, values increased linearly with the average irradiance because these experiments were always performed at the same external irradiance of 500 μE/m² s using diluted cultures. Hence, the average irradiance increased linearly with the proportion of light in the illumination cycle assayed. What is more interesting is that the experimental measurements performed, PO_{2exp}, completely fitted the trend of PO_{2local}; thus indicating that light integration does not occur under long light/dark times. The results show that, only when the average irradiance was really high, did the experimental photosynthesis rate approximate the maximal one although this was because, under these conditions, the minimum dark times assayed were of 1 s. In contrast, it was also observed that, when providing long light/dark times, the minimum average irradiance required to start the photosynthesis process increased up to 100 μE/m² s. Analysing the variation in the normalized photosynthesis rate (PO_{2exp}/PO_{2iav}) with the proportion of light time in the cycle, a clear linear correlation was observed (Fig. 3B). This confirms that, at the time scale used, there is no light integration and the cells perform photosynthesis according to the irradiance that they receive during the “seconds-scale” times provided. It has been reported that, in commercial photobioreactors, medium-frequency fluctuations prevail, the behaviour being different for medium frequency fluctuations than for high frequency fluctuations (Barbosa et al., 2003). Light/dark cycles in the 6–87 s range lead to similar or lower growth rates and biomass yields on light energy compared to those obtained under continuous light of the same light intensity as that during the light period of the light/dark cycles (Janssen et al., 2000a,b, 1999). No influence of light/dark cycles in the 1–263 s range was found in terms of the volumetric productivity, specific oxygen production, or carbon dioxide fixation (Grobbelaar, 1991, 1989). On the other hand, it has been reported that maximal carbon dioxide fixation is achieved under 4 s light/dark cycles (Bosca et al., 1991) whereas maximal growth rates are achieved under light/dark cycles with a dark period of 9 and 6 s (Lee and Pirt, 1981; Merchuk et al., 1998).

To demonstrate this fact, a large set of experiments was performed over six months, maintaining the raceway reactor in continuous mode and taking samples from the reactor to evaluate the photosynthesis rate in the laboratory yet simulating the real light/dark cycles at which the cells were exposed to inside the outdoor reactor. In this case, the external irradiance provided was that found in the outdoor reactor at different daylight times, where several samples were measured each day at different hours of the day, with light times ranging from 1 to 8 s while dark times ranged from 1 to 24 s. To take into account the variation in culture conditions in different seasons, we periodically evaluated the performance of the cells taken directly from the reactor under continuous light. In this way, the P-I curve of the culture was obtained as a control curve. The results confirmed that the hyperbolic model is always suitable to fit the light response of the *Scenedesmus almeriensis* cells, including from real outdoor reactors in different seasons (Fig. 4). However, the results clearly show how the behaviour was not the same for all of the seasons evaluated. The cultures grown in spring performed better than those grown in summer and winter. By fitting the experimental data to the hyperbolic model, we calculated the characteristic parameter values for the cultures obtained in each season (Table 1). The values were similar to the previous ones not only in terms of the maximal photosynthesis rate and the half-saturation irradiance but also in terms of the respiration rate and the minimum irradiance required to start photosynthesis. The major difference was for the maximum photosynthesis rate, which was notably high for the culture grown in spring; thus indicating the adequacy of the operating conditions during this period.

To consider the variation in cell performance in the different seasons, the same analysis as previously performed to study the influence of average irradiance and light/dark cycles on the performance of

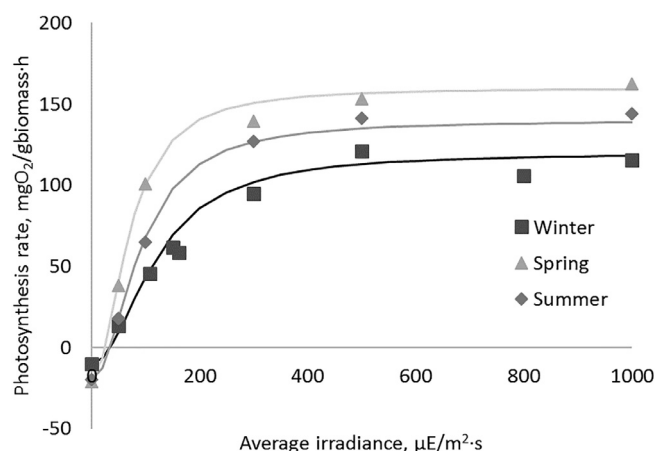


Fig. 4. Variation in the photosynthesis rate with average irradiance for three *Scenedesmus almeriensis* samples produced in a 100 m² raceway reactor in continuous mode at 0.2 day⁻¹ for different seasons.

outdoor cultures was applied to the entire set of data from the six-month operation of the raceway reactor. Because different irradiances, and different light and dark times were used, it was not possible to provide a single figure summarizing all of the results. However, the results did confirm that the behaviour of the cultures completely fitted the local irradiance available. Hence, Fig. 5 demonstrates how a linear relationship exists between the experimental photosynthesis rate determined in the laboratory simulating the light/dark cycles taking place in real raceway reactors with that predicted by the hyperbolic model and the estimated local utilization of light. The correlation is slightly better in the winter time yet it is also highly acceptable for spring and summer time, especially considering the large variations in culture conditions that take place in outdoor reactors and the large number of measurements taken (up to 172). In a previous study, the effect of a medium-frequency cycle time (10–100 s) and light fraction (0.1–1) on the growth rate and the biomass yield of the microalgae *Dunaliella tertiolecta* was studied. The biomass yield and growth rates were mainly affected by the light fraction while the cycle time had little influence (Barbosa et al., 2003).

These results have clear consequences regarding the performance and modelling of raceway reactors. The first is that, from the photosynthetic point of view, cell adaptation to average irradiance cannot be approximated in these reactors. It has been demonstrated that cells adapt to the local irradiance present at different positions inside the reactor. The second consequence is that, in raceway reactors, the light frequency to which the cells are exposed inside the culture is about 0.05 Hz, far from that required to allow light integration (1 Hz), and thus trying to optimize the light regime in raceway photobioreactors by increasing liquid velocity is unrealistic. The third is that raceway reactor productivity is limited by the phenomenon of local irradiance adaptation.

To analyse how the local irradiance adaptation phenomenon influences raceway reactor productivity, a simple simulation exercise was performed considering the operation of the 100 m² raceway reactor under the culture conditions imposed (Dilution rate = 0.2 day⁻¹, C_b = 1.2 g·L⁻¹). Knowing the extinction coefficient of the biomass (K_a = 0.15 m²·g⁻¹), the light profile inside the reactor at different solar hours/irradiances could be estimated using Lambert's law (Fig. 6A); this was performed on a spring day in Almeria (Spain) where the raceway reactor is located. The results show how irradiance inside the reactor exponentially decreased with culture depth regardless of the solar irradiance on the reactor surface; this is because only the first 0.04 m (approximately) of the culture receives a light intensity greater than the minimum value, of I_c = 40 μE/m²·s, required for photosynthesis. Therefore, approximately 73% of the culture is in total darkness,

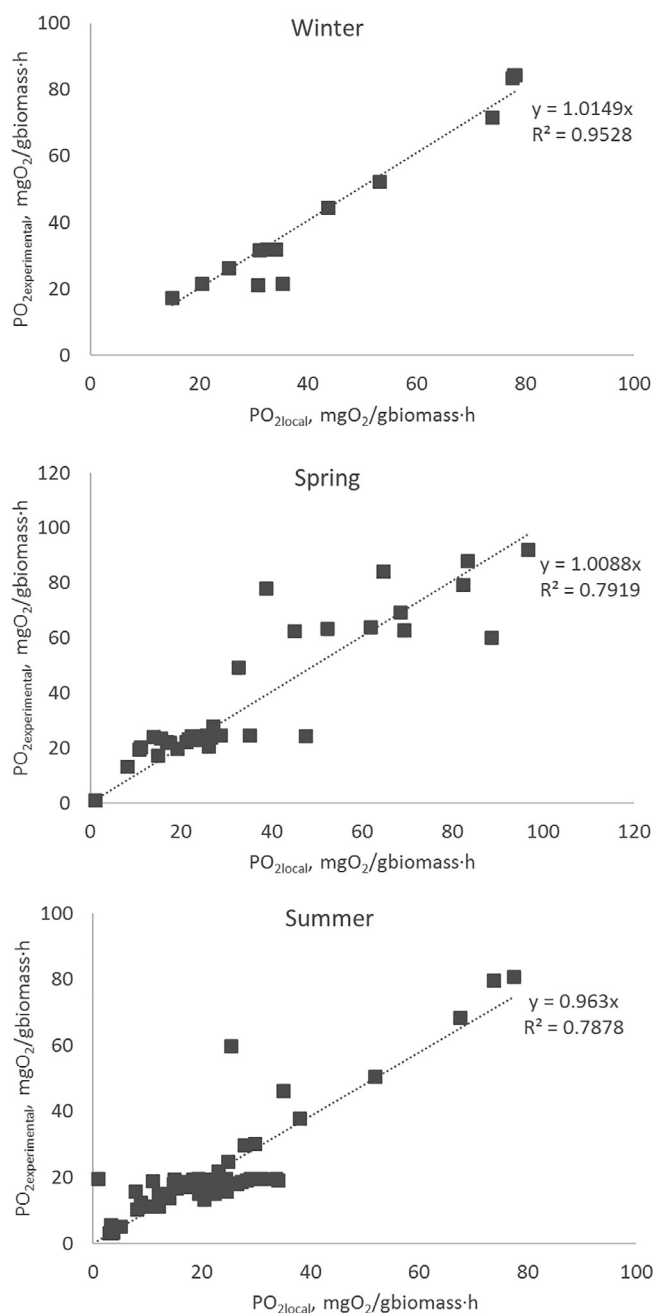


Fig. 5. Correlation between the experimental and local photosynthesis rate of *Scenedesmus almeriensis* samples produced in a 100 m² raceway reactor in continuous mode at 0.2 day⁻¹ for different seasons.

receiving insufficient light for photosynthesis to take place. From this data, the maximal proportion of illuminated culture was calculated to be 27%. In terms of the photosynthesis rate, by considering the local irradiance at different culture depths and the hyperbolic growth model found in springtime, the variation in the photosynthesis rate with the culture depth at different solar irradiances can also be easily calculated (Fig. 6B). The results show how most of the photosynthesis took place in the first 0.035 m of culture; only at really high irradiances did photosynthesis take place at culture depths greater than 0.050 m. However, independent of the solar irradiance, there is always a large reactor volume performing respiration in complete darkness. In most studies focusing on the flashing effect, light is represented as an oversimplified on/off signal. A better option is to represent the light pattern, assuming that the light source switches between two intensities (Demory et al.,

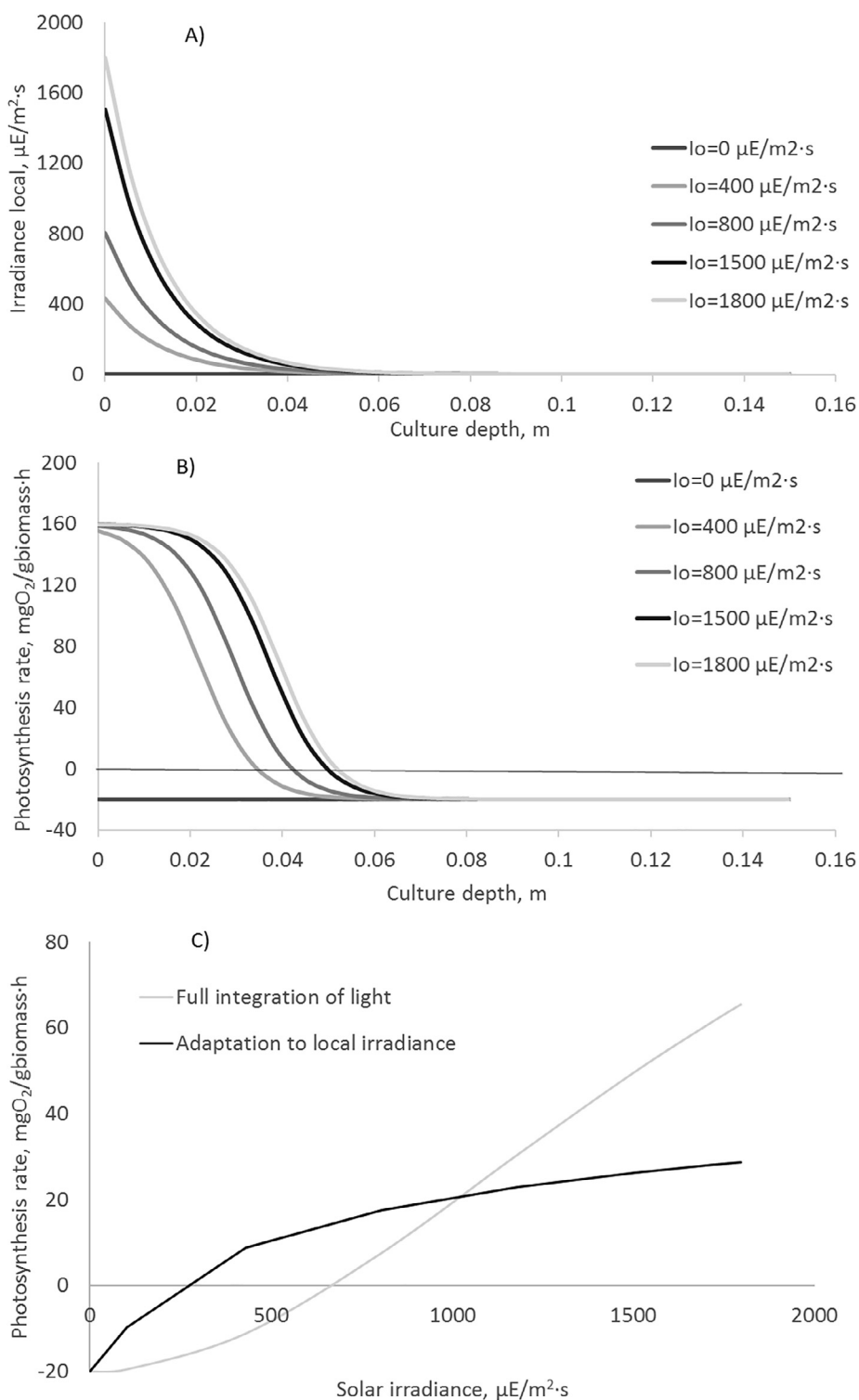


Fig. 6. Variation in the local irradiance (A) and photosynthesis rate (B) with the culture depth for a *Scenedesmus almeriensis* culture produced in a 100 m² raceway reactor in continuous mode at 0.2 day⁻¹. (C). Integrated values of the net photosynthesis rate at different solar irradiances. Data simulated on the basis of the experimental results obtained.

2018). However, an even better approach is obtained if one considers the light profile on the entire reactor, as demonstrated here, as well as using the complete optimal light regime history (although this requires more complex and time-consuming computing efforts) (Brindley et al., 2016).

To determine the net photosynthesis rate inside the reactor, the sum of all the photosynthesis rates at different culture depths must be

calculated (Fig. 6C). The data show that, if light integration takes place inside the reactor, the photosynthesis rate increases almost linearly with the solar irradiance on the reactor surface. Nonetheless, the real scenario is that the photosynthesis rate adapts to local irradiance and so the curve corresponding to this behaviour fits a hyperbolic trend. It is highly relevant that at low irradiances, the model considering local adaptation provides higher photosynthesis rates than the model

considering light integration. However, the opposite occurs at high solar irradiances when the photosynthesis rate considering light integration is much higher than when adaptation to local irradiance takes place. By integrating the photosynthesis rate in the daylight period, a daily value of $303 \text{ mgO}_2/\text{g}_{\text{biomass}}$ was obtained when considering full light integration, whereas when considering adaptation to local irradiance, the daily value was $216 \text{ mgO}_2/\text{g}_{\text{biomass}}$ (Fig. 6C). Taking into account the basic photosynthesis equation, these values are equivalent to biomass productivities of 0.23 and 0.16 g per gram, respectively; again, this is equivalent to 40 and $29 \text{ g}_{\text{biomass}}/\text{m}^2\text{day}$, respectively. Such values are quite reasonable; the $29 \text{ g}_{\text{biomass}}/\text{m}^2\text{day}$ value is very close to the $25 \text{ g}_{\text{biomass}}/\text{m}^2\text{day}$ value determined experimentally under these conditions. Our figures clearly show how modifying the light regime in raceway reactors would improve their performance by up to 40%. Nonetheless, this is really a difficult objective, especially when considering the greater energy input requirements to achieve it.

4. Conclusions

It has been demonstrated how the light regime at which the microalgae cells are exposed to in a raceway reactor is far from the optimal one required to optimize the performance of microalgae cultures through light integration. Photosynthesis rate measurements, performed at light/dark times in the range of that experimentally determined, have confirmed that no light integration exists, and that the cells are adapted to the local irradiance inside the reactor. This phenomenon has been validated with reactor samples over a complete annual cycle. The phenomena here described are fundamental to better understanding the potential and limitations of raceway reactors.

Acknowledgements

This study was supported financially by the Ministry of Economy and Competitiveness (DPI2014-55932-C2-1-R, DPI2017-84259-C2-1-R), (EDARSOL, CTQ2014-57293-C3-1-R), and the European Union's Horizon 2020 Research and Innovation Program under Grant Agreement No. 727874 SABANA. We are most grateful for the practical assistance given by the staff of the Cajamar Foundation's "Las Palmerillas" Experimental Station.

Appendix A. Supplementary data

Supplementary data to this article can be found online at <https://doi.org/10.1016/j.biortech.2019.02.032>.

References

Alías, C.B., García-Malea López, M.C., Ación Fernández, F.G., Fernández Sevilla, J.M., García Sánchez, J.L., Molina Grima, E., 2004. Influence of power supply in the feasibility of *Phaeodactylum tricoratum* cultures. *Biotechnol. Bioeng.* 87, 723–733.

Barbosa, M.J.J., Janssen, M., Ham, N., Tramper, J., Wijffels, R.H.H., 2003. Microalgae cultivation in air-lift reactors: modeling biomass yield and growth rate as a function of mixing frequency. *Biotechnol. Bioeng.* 82, 170–179.

Barceló-Villalobos, M., Guzmán Sánchez, J.L., Martín Cara, I., Sánchez Molina, J.A., Ación Fernández, F.G., 2018. Analysis of mass transfer capacity in raceway reactors. *Algal Res.* 35, 91–97.

Bitog, J.P., Lee, I., Lee, C., Kim, K., Hwang, H., Hong, S., Seo, I., Kwon, K., Mostafa, E., 2011. Application of computational fluid dynamics for modeling and designing photobioreactors for microalgae production: a review. *Comput. Electron. Agric.* 76, 131–147.

Bosca, C., Dauta, A., Marvalín, O., 1991. Intensive outdoor algal cultures: how mixing enhances the photosynthetic production rate. *Bioresour. Technol.* 38, 185–188.

Brindley, C., Fernández, F.G.A., Fernández-Sevilla, J.M., 2011. Analysis of light regime in continuous light distributions in photobioreactors. *Bioresour. Technol.* 102, 3138–3148.

Brindley, C., Jiménez-Ruiz, N., Ación, F.G., Fernández-Sevilla, J.M., 2016. Light regime optimization in photobioreactors using a dynamic photosynthesis model. *Algal Res.* 16, 399–408.

de Godos, I., Mendoza, J.L., Ación, F.G., Molina, E., Banks, C.J., Heaven, S., Rogalla, F., 2014. Evaluation of carbon dioxide mass transfer in raceway reactors for microalgae culture using flue gases. *Bioresour. Technol.* 153, 307–314.

Demory, D., Combe, C., Hartmann, P., Talec, A., Pruvost, E., Hamouda, R., Souillé, F., Lamare, P.O., Bristeau, M.O., Sainte-Marie, J., Rabouille, S., Mairet, F., Sciandra, A., Bernard, O., 2018. How do microalgae perceive light in a high-rate pond? Towards more realistic Lagrangian experiments. *R. Soc. Open Sci.* 5, 180523.

Fernández-Del Olmo, P., Fernández-Sevilla, J.M., Ación, F.G., González-Céspedes, A., López-Hernández, J.C., Magán, J.J., 2017. Modeling of biomass productivity in dense microalgal culture using computational fluid dynamics. *Acta Hort.*

García, S., Paternina, E., Pupo, O.R., Bula, A., Acuña, F., 2012. CFD simulation of multiphase flow in an airlift column photobioreactor for the cultivation of microalgae. In: *ASME 2012 6th Int. Conf. Energy Sustain. Parts A and B. American Society of Mechanical Engineers*, pp. 1253.

Grobbelaar, J.U., 1991. The influence of light/dark cycles in mixed algal cultures on their productivity. *Bioresour. Technol.* 38, 189–194.

Grobbelaar, J.U., 1989. Do light/dark cycles of medium frequency enhance phytoplankton productivity? *J. Appl. Phycol.* 1, 333–340.

Janssen, M., Bresser, L.De, Baijens, T., Tramper, J., Mur, L.R., Snel, J.F.H., Wijffels, R.H., 2000a. Scale-up aspects of photobioreactors: Effects of mixing-induced light/dark cycles. *J. Appl. Phycol.* 12, 225–237.

Janssen, M., Janssen, M., De Winter, M., Tramper, J., Mur, L.R., Snel, J., Wijffels, R.H., 2000b. Efficiency of light utilization of *Chlamydomonas reinhardtii* under medium-duration light/dark cycles. *J. Biotechnol.* 78, 123–137.

Janssen, M., Kuijpers, T.C., Veldhoen, B., Ternbach, M.B., Tramper, J., Mur, L.R., Wijffels, R.H., 1999. Specific growth rate of *Chlamydomonas reinhardtii* and *Chlorella sorokiniana* under medium duration light/dark cycles: 13–87 s. *J. Biotechnol.* 70, 323–333.

Labatut, R.A., Ebeling, J.M., Bhaskaran, R., Timmons, M.B., 2007. Hydrodynamics of a large-scale mixed-cell raceway (MCR): experimental studies. *Aquac. Eng.* 37, 132–143.

Lee, Y.-K., Pirt, S.J., 1981. Energetics of photosynthetic algal growth: influence of intermittent illumination in short (40 s) cycles. *J. Gen. Microb.* 124, 43–52.

Liffman, K., Paterson, D.A., Liovic, P., Bandopadhyay, P., 2013. Comparing the energy efficiency of different high rate algal raceway pond designs using computational fluid dynamics. *Chem. Eng. Res. Des.* 91, 221–226.

Matthijs, H., Balke, H., Van Hes, U., Kroon, B., Mur, L., Binot, R., 1996. Application of light-emitting diodes in bioreactors- flashing light effects and energy economy in algal culture (*Chlorella pyrenoidosa*). *Biotechnol. Bioeng.* 50, 98–107.

Mendoza, J.L., Granados, M.R., de Godos, I., Ación, F.G., Molina, E., Banks, C., Heaven, S., 2013a. Fluid-dynamic characterization of real-scale raceway reactors for microalgae production. *Biomass Bioenergy* 54, 267–275.

Mendoza, J.L., Granados, M.R., de Godos, I., Ación, F.G., Molina, E., Heaven, S., Banks, C.J., 2013b. Oxygen transfer and evolution in microalgal culture in open raceways. *Bioresour. Technol.* 137, 188–195.

Merchuk, J.C., Ronen, M., Giris, S., Arad, S.(Malis), 1998. Light/dark cycles in the growth of the red microalga *Porphyridium* sp. *Biotechnol. Bioeng.* 59, 705–713.

Molina-Grima, E., Sevilla, J.M.F., Pérez, J.A.S., Camacho, F.G., 1996. A study on simultaneous photolimitation and photoinhibition in dense microalgal cultures taking into account incident and averaged irradiances. *J. Biotechnol.* 45, 59–69.

Nedbal, L., Tichý, V., Xiong, F., Grobbelaar, J.U., 1996. Microscopic green algae and cyanobacteria in high-frequency intermittent light. *J. Appl. Phycol.* 8, 325–333.

Oswald, W.J., Golueke, C.G., 1960. Biological transformation of solar energy. In: W.W. Umbreit (Ed.), *Advances in Applied Microbiology*. Vol. 2. New York, pp. 223–262.

Perner-Nochta, I., Lucumi, A., Posten, C., 2007. Photoautotrophic cell and tissue culture in a tubular photobioreactor. *Eng. Life Sci.* 7, 127–135.

Schulze, P.S.C., Barreira, L.A., Pereira, H.G.C., Perales, J.A., Varela, J.C.S., 2014. Light emitting diodes (LEDs) applied to microalgal production. *Trends Biotechnol.* 32, 422–430.

Soman, A., Shastris, Y., 2015. Optimization of novel photobioreactor design using computational fluid dynamics. *Appl. Energy* 140, 246–255.

Ugwu, C.U., Ogbonna, J.C., Tanaka, H., 2005. Light/dark cyclic movement of algal culture (*Synechocystis aquatilis*) in outdoor inclined tubular photobioreactor equipped with static mixers for efficient production of biomass. *Biotechnol. Lett.* 27, 75–78.

Vejrazka, C., Janssen, M., Streefland, M., Wijffels, R.H., 2011. Photosynthetic efficiency of *Chlamydomonas reinhardtii* in flashing light. *Biotechnol. Bioeng.* 108, 2905–2913.



Variations of culture parameters in a pilot-scale thin-layer reactor and their influence on the performance of *Scenedesmus almeriensis* culture



M. Barceló-Villalobos^{a,*}, C. Gómez Serrano^b, A. Sánchez Zurano^b, L. Alameda García^b, S. Esteve Maldonado^c, J. Peña^b, F.G. Ación Fernández^b

^a Department of Informatics, Universidad de Almería, E04120 Almería, Spain

^b Department of Chemical Engineering, Universidad de Almería, E04120 Almería, Spain

^c IES AZCONA, Calle Policía José Rueda Alcaraz, 1, 04006 Almería, Spain

ARTICLE INFO

Keywords:

Thin-layer cascade
Photosynthesis
Irradiance
Gradients
Temperature
Dissolved oxygen

ABSTRACT

The variations in culture conditions (irradiance, temperature, pH and dissolved oxygen) in a thin-layer 120 m² surface reactor have been studied, both in terms of position inside the reactor and time of the daylight cycle. Results demonstrate that average irradiance and temperature to which the cells are exposed are mainly a function of time, whereas pH and dissolved oxygen concentrations also showed relevant gradients depending on their position inside the reactor. The existence of gradients has been demonstrated to reduce the culture performance, using both chlorophyll-fluorescence and net photosynthesis rate methods. Moreover, the influence of culture conditions on *Scenedesmus almeriensis* cell performance was modelled. The obtained model allows us to quantify the loss in productivity caused by inadequate culture conditions; the net photosynthesis rate being demonstrated as only 32% of the maximal achievable. This is the first step in optimizing and scaling-up this type of reactor for industrial applications.

1. Introduction

There is always a requirement for large-scale microalgae biomass production to increase the biomass productivity of outdoor cultures and to approximate it to the maximum theoretical values. To do so, three major issues have to be solved: (i) to produce robust strains capable of rapid growth and of producing large amounts of biomass under a wide range of culture conditions, (ii) to use photobioreactors capable of providing the optimal conditions required by the selected microalgae strain, and (iii) to be able to adjust the overall production system operation to the changing environmental conditions prevailing in the actual outdoor cultures, both on an hourly and seasonal basis. The production of different microalgae strains in raceway and tubular photobioreactors has been widely reported; these technologies now being the most extended worldwide for microalgae biomass production, both in low-value and high-value applications, respectively (Benemann, 2013; Grobbelaar, 2010). In the case of thin-layer reactors, their use still remains at the laboratory or pilot scale, no industrial facilities with this technology exists as yet in spite of the high productivity already reported when using these types of photobioreactors (Ación et al., 2017).

Thin-layer reactors have been developed for decades at the

laboratory of photosynthesis in Trebon, Czech Republic (Masojídek and Prášil, 2010). These reactors are characterized by their low-depth culture, which is recirculated over a flat surface by providing it with an adequate slope of 0.1 to 2%. Under these conditions, the culture depth ranges from 5 to 0.5 cm, and biomass concentration values of up to 40 g/L can be achieved (Masojídek et al., 2015). This technology has been proposed as one of the most efficient in terms of areal productivity, with values ranging from 30 to 50 g/m²·day (Masojídek et al., 2015; Morales-Amaral et al., 2015a). The largest reactor of this type was recently built and put into operation in Portugal, having a total surface area of 1500 m²; to date, no figures for this reactor are available. Data from small pilot-scale reactors, of up to 50 m², show that they have certain problems related to an inadequate mass transfer capacity and the existence of pH and temperature gradients, along with a significant accumulation of oxygen in the culture, reaching values of up to 400%Sat (Lívanský et al., 2006; Morales-Amaral et al., 2015b).

To properly optimize microalgae production in these reactors, the first step is to characterize it and then determine how the culture conditions change along the reactor length due to daily variations in environmental conditions (i.e. light and temperature). It has been widely reported that biomass productivity is influenced by temperature and pH, as well as by dissolved oxygen. The effect of temperature is

* Corresponding author.

E-mail address: mbv001@ual.es (M. Barceló-Villalobos).

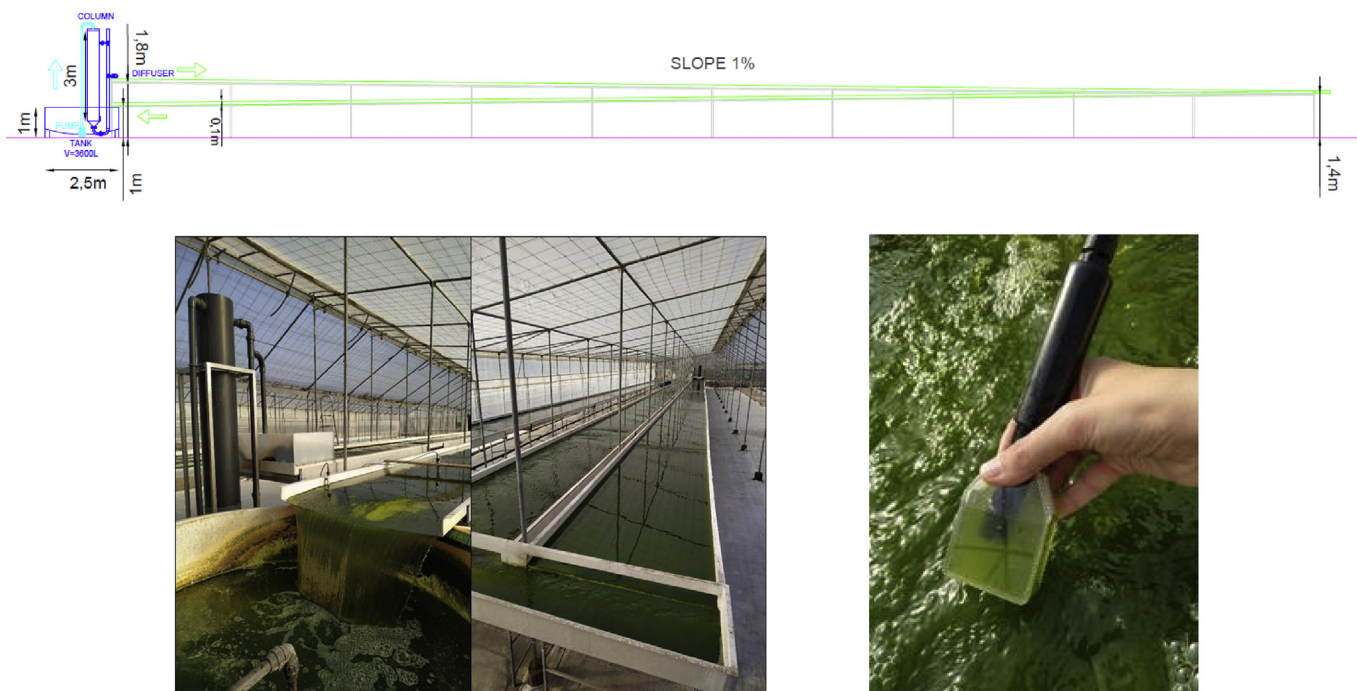


Fig. 1. Scheme of the thin-layer cascade reactor located at the IFAPA Experimental Station (Almería, Spain) (Up). Images of reactor (below-left) and the plastic chamber used to determine the net photosynthesis rate at the different positions (below-right).

analogous to any microorganism, while inadequate pH also reduces microalgae culture performance. Dissolved oxygen content is also a critical parameter in microalgae production; it is well known that it causes inhibition at concentrations above 250%Sat. (Camacho Rubio et al., 1999; de Godos et al., 2014; Mendoza et al., 2013). These effects have been previously reported in both tubular and raceway reactors, allowing us to identify the major bottlenecks for each of these reactor types; and consequently the best strategies to resolve them (de Godos et al., 2014; Ippoliti et al., 2016b; Mendoza et al., 2013). Conversely, in thin-layer cascades, the available information is far more limited, the major challenges of which still need to be identified and overcome before scaling-up this technology.

To evaluate the performance of whichever type of reactor, the usual method is to focus on overall biomass productivity. However, biomass productivity does not provide information regarding inadequate culture conditions in the different parts of the reactor or about conditions throughout the day; these measurements have to be carried out in distinct parts of the reactor. Moreover, one also needs to establish the performance of cells under these conditions so as to be able to evaluate the losses in productivity resulting from inadequate culture conditions at different reactor locations or at different points over the day. To evaluate cell performance, rapid methods such as *in situ* fluorescence of chlorophylls are effective although a more robust estimation can be obtained by evaluating the net oxygen production rate under different culture conditions (Malapascua et al., 2014). Data from cultures performance can be used to develop reliable models that are useful for optimizing the design and operation of any reactor type, including thin-layer cascade reactors (Bernard and Rémond, 2012; Costache et al., 2013; Gao et al., 2018; Ippoliti et al., 2016a).

In this paper, we study the existence of gradients for the most relevant culture parameters (temperature, pH and dissolved oxygen) in thin-layer cascade reactors; both in terms of their location in the reactor and their daily variation based on environmental conditions. Moreover, we evaluated the performance of the microalgae cells under the different conditions using chlorophyll fluorescence and oxygen production rate methods. Accordingly, the existence of adverse conditions in these types of reactors is elucidated, and the losses in productivity are

quantified. This study is the first step in optimizing and scaling-up thin-layer reactors for large-scale commercial microalgae production.

2. Materials and methods

2.1. Microorganism and culture conditions

The microalga strain *Scenedesmus almeriensis* (CCAP 276/24) was selected for its adaptability and abundant growth in outdoor reactors. The microalga was produced in a thin-layer reactor utilizing Mann & Myers medium, prepared using fertilizers: (0.14 g·L⁻¹ K(PO₄)₂, 0.18 g·L⁻¹ Mg(SO₄)₂, 0.9 g·L⁻¹ NaNO₃, 0.02 mL·L⁻¹ Welgro, and 0.02 g·L⁻¹ Kalentol) (Fernández et al., 2012). The inoculum for the reactor was produced in a tubular photobioreactor (3 m³) using the same culture medium. Tubular reactor was operated at a constant pH of 8 by the on-demand injection of CO₂, whereas temperature was controlled by passing cool water by an internal heat exchanger located into the bubble column of this tubular photobioreactor. Dissolved oxygen accumulation over 250%Sat. was avoided in the tubular photobioreactor by supplying air to the bubble column for oxygen desorption. On this way the culture was maintained below the critical values for this strain (temperature below 40 °C, dissolved oxygen below 250%Sat. (100%Sat. is equivalent to 9 mg/L)).

2.2. Thin-layer reactor design and operating conditions

The thin-layer reactor is located at the “IFAPA” Research Centre, (Almería, Spain). The reactor consists of two sloped cultivation plates, each 40 m long and 1.5 m wide, connected by a flat channel that acts as a solar collector. The culture is recirculated through this solar collector by a pump after passing through a bubble column for pH adjustment and oxygen desorption (Fig. 1)). The total surface area of the solar collector reactor is 120 m² with a water depth of 0.02 m; thus the total culture volume in this section is 2.4 m³. The sump from which the culture is recirculated has a culture volume of 0.7 m³ whereas the bubble column has a volume of 0.3 m³, making the total culture volume 3.4 m³. The reactor is operated in continuous mode by harvesting up to

1.0 m³/day of culture, replacing it with fresh medium prepared using freshwater and fertilizers; therefore, the imposed dilution rate is 0.3 day⁻¹. Water evaporation from the reactor is compensated for by the daily addition of water. The culture's pH is controlled by the on-demand injection of CO₂ into the bubble column; alternatively, air is injected to remove oxygen and avoid dissolved oxygen accumulation. The gas flow rate of both CO₂ and air entering the bubble column is measured using mass flow meters (PFM 725S-F01-F, SMC, Tokyo, Japan). Air is supplied to the reactor via a blower providing 350 mbar overpressure through a fine bubble diffuser AFT2100 (ECOTEC, Spain) capable of creating bubbles with a diameter of less than 2 mm at the minimum pressure drop. The culture's temperature was not controlled.

2.3. *In situ* measurements in the reactor

The existence of culture condition gradients was studied by measuring the pH, temperature and dissolved oxygen in the culture at nine different points along the reactor's length, using appropriate temperature, pH and dissolved oxygen probes (HI98198, Hanna, Spain). Measurements were carried out at different times during the daylight period to determine the variation in existing gradients throughout the day. To analyse the influence of the culture conditions existing at each reactor position on the culture's performance, the net photosynthesis rate at each position was also measured. To do this, culture samples were directly taken from the reactor at the different positions and introduced into a 40 mL plastic chamber (0.02 m in depth), measuring the dissolved oxygen accumulation in this chamber over a period of 5 min on which maximum accumulation of 20% sat was measured (Fig. 1).

2.4. Offline measurements in the laboratory

In addition to the *in situ* measurements, the influence of culture conditions on culture performance was determined offline in the laboratory, using the culture conditions (pH, temperature, dissolved oxygen and irradiance) previously found in the reactor at the different positions and times. Thus, it was possible to compare both the *in situ* experimental measurements and those determined in the laboratory under controlled conditions. Two methods were employed to evaluate the influence of culture conditions on cell performance; the first based on the net photosynthesis rate measurements while the second involved chlorophyll-fluorescence measurements. Both are rapid methods allowing us to evaluate the culture performance in a short time. Additionally, to modelize the net photosynthesis rate response to changes in culture conditions, a set of experiments was performed under laboratory conditions over a wide range of pH (from 3 to 11), temperature (from 8 to 46), dissolved oxygen (from 0 to 400%Sat.) and irradiance (from 100 to 2500 μE m⁻² s⁻¹).

2.4.1. Net photosynthesis rate measurements

The net photosynthesis rate was measured using specially-built photo-respirometer equipment. This equipment measures the variation in dissolved oxygen in microalgae samples under controlled conditions. The samples were placed in a stirred cylindrical glass chamber, 60 mL in volume and 2 cm in diameter, illuminated using two sets of LED lamps placed to the right and left of the glass chamber. The lamps' intensity was automatically regulated to obtain the desired irradiance inside the chamber once the sample was added. The photo-respirometer was also equipped with sensors for irradiance (ULM 500, Walz, Germany), temperature (PT1000, Crison, Spain), pH (Crison 5343, Spain) and dissolved oxygen (Crison 5002, Spain) located inside the cylindrical glass chamber; to be exact, the irradiance sensor was positioned in the centre of the glass chamber whereas the other sensors were located close to the surface to avoid shadows inside the system.

To determine the photosynthesis rate, samples from the thin-layer cascade were taken and then placed inside the stirred cylindrical glass chamber. Each sample was exposed to three-minute light periods to

measure and register the variation in dissolved oxygen under all the conditions. The photosynthesis rate was calculated from the slope of dissolved oxygen accumulation during the light periods. The variations in dissolved oxygen were evaluated in the 70–140%Sat range, for which the oxygen mass transfer was confirmed to be negligible. Irradiance was modified by adjusting the power of the LED lamps whereas the pH was modified by adding HCl or NaOH to achieve the desired values. The temperature was modified by heating/cooling the samples, whereas the dissolved oxygen concentration was modified by bubbling pure N₂/O₂ gases.

2.4.2. Chlorophyll-fluorescence measurements

A Pulse-Amplitude-Modulation fluorometer device was utilized (Junior PAM, Walz, Effeltrich, Germany) to estimate the photosynthetic activity of the microalgae cells using the Rapid Light Curves of Electron Transport Rate at different irradiances and culture conditions. Samples from the reactor were directly adjusted to the required culture conditions (temperature, pH, dissolved oxygen) and subject to irradiances from 0 to 1500 μE/m²·s (Figuerola et al., 1997). Measurements were performed in parallel with photo-respirometry experiments thus allowing us to compare the performance of both methods in order to elucidate the influence of culture conditions on photosynthetic process performance.

2.5. Biomass concentration and statistical analysis

The microalgal biomass concentration was measured using dry weight measurements. For this, 50 mL samples were filtered through a Macherey-Nagel MN 85/90 glass fibre filter, and the filters containing the algae were dried in an oven at 80 °C for 24 h. Data were analysed using the Statistica v.7 program. Data from the reactor were obtained from a total of 30 samples. Each measurement was performed in triplicate, both *in situ* and under laboratory conditions.

3. Results and discussion

3.1. *In situ* measurements in the reactor

The performance of whichever microalgae culture is a direct function of the irradiance to which the cells are exposed, in addition to how close the culture conditions are to those that are optimal for the selected microalgae, these being different for each strain. Light availability in outdoor reactors is a function of solar radiation on the reactor surface and reactor/culture parameters such as the light path, biomass concentration and biomass extinction coefficient. Therefore, to determine the average irradiance in outdoor cultures, the simplified equation proposed by Molina can be used (Eq. (1)), it providing the volumetric mean irradiance inside the reactor (Grima et al., 1994). Table 1 shows the most relevant irradiance values determined in the thin-layer reactor at different times. Because the entire solar collector is exposed to the same irradiance, the external irradiance on the reactor surface (I_o) is a unique value at each point in time. The irradiance inside the culture was measured at the centre of the culture depth at different positions; a mean value of all the experimental values being obtained, which corresponds to the entire reactor (I_{mean}). Finally, because the culture's hydraulic residence time in the solar collector is really short, only

Table 1

Hourly variation in light availability and culture parameters in the thin-layer reactor. Mean values at the different positions measured.

Time	I _o , μE/m ² ·s	I _{mean} , μE/m ² ·s	I _{av} , μE/m ² ·s	T, °C	pH	DO ₂ , %Sat.
9:00	643	97	129	13.7	8.1	141
11:00	1620	90	324	19.7	8.3	195
13:00	902	101	180	23.2	8.6	197

2 min, the biomass concentration along the channel length would be considered constant as no biomass concentration gradients exist. Accordingly, a single average irradiance value in the reactor (I_{av}) could be calculated at each point in time (Eq. (1)). The data show that the irradiance on the reactor surface varies over time from 643 to 1620 $\mu\text{E}/\text{m}^2\cdot\text{s}$; the maximal value being obtained at 11:00 h (as there was cloud at noon). Based on these values, the average irradiance to which the cells were exposed inside the reactor varied from 129 to 324 $\mu\text{E}/\text{m}^2\cdot\text{s}$ for the same period of time. These values do not agree with those determined experimentally, which ranged from 90 to 101 $\mu\text{E}/\text{m}^2\cdot\text{s}$, although they are in the same order of magnitude. This is because it is difficult to adequately measure irradiance in thin-layer reactors - small variations in the sensor position and in the culture depth have a large effect on the final values. Consequently, utilizing average irradiance values instead of experimental measurements is recommended. In terms of the culture conditions inside the reactor, the mean values of temperature, pH and dissolved oxygen ranged from 13.7 to 23.2 °C, from 8.1 to 8.6, and from 141 to 197%Sat., respectively; thus, they were in the range recommended for most microalgae strains (Table 1). It is important to note that, under these conditions, the biomass productivity measured was 11.7 $\text{g}/\text{m}^2\cdot\text{day}$, with the reactor being operated in continuous mode at 0.3 day^{-1} in winter time. This productivity was not high when compared to the 38 $\text{g}/\text{m}^2\cdot\text{day}$ previously reported in a 224 m^2 unit (Doucha et al., 2009), or the 42 $\text{g}/\text{m}^2\cdot\text{day}$ reported when using centrate from an anaerobic digester as the nutrient source in a 32 m^2 unit (Morales-Amaral et al., 2015a); although these values were obtained in summer time.

$$I_{av} = \frac{I_0}{K_a \cdot C_b \cdot p} (1 - \exp(-K_a \cdot C_b \cdot p)) \quad (1)$$

Regarding the existence of gradients along the length of the reactor, the results show that the irradiance measurement at the different positions and times had no clear tendency, the standard deviation of the measurements being high; thus, these measurements were not confiable (Fig. 2A). This is due to the significant variation in the irradiance measurements caused by small changes in the culture depth along the

reactor length, or because of the particular position where the light sensor was located. Therefore, it is recommended that the average irradiance values obtained from Eq. (1) are used. In contrast, the temperature showed a clear pattern, with no variation observed based on the position, yet it did increase with time (Fig. 2B). The culture temperature increases due to infrared radiation absorption from solar radiation - the larger the area exposed to the light (or solar radiation), the greater the increase in temperature. These figures show that, along the channel length, no temperature gradients occurred in thin-layer reactors, or they were not relevant; this is because of the short time to which the culture is exposed to solar radiation in the channel. However, during the day, the temperature increases because the energy input is greater than the output, which mainly results from evaporation. In a 220 m^2 thin-layer reactor, a temperature increase from 20 to 35 °C was previously reported during the daylight period (Doucha et al., 2009).

In the case of pH, a similar trend was observed. The pH only slightly increased along the channel length but mean values over the day clearly increased (Fig. 2C). This signifies that the existence of pH gradients along the channel length can be disregarded as they are too small to significantly influence the performance of the cultures. This small pH increase along the channel length is explained by the on-demand injection of CO_2 and the significant capacity of the carbonate-bicarbonate buffer in the culture medium, which compensates for the inorganic carbon consumption caused by photosynthesis along the channel length. However, the increase in pH over time, and moreover the existence of pH values above the set point of 8.0, indicates that overall CO_2 injection was inadequate. According to these figures, the CO_2 consumed by the microalgae was higher than the CO_2 transference capacity, and although pH values were not too high, the mean hourly values increased from 8.1 to 8.6 (Table 1). The control of pH in thin-layer reactors has been already reported as a major factor determining the efficiency of these systems; and especially the efficiency of CO_2 utilization (Lívanský and Doucha, 1996). The carbon supply is widely used to control and maintain pH close to the optimal value, which is important for ensuring optimal operating conditions inside the reactor; hence, the control of pH in thin-layer reactors must be carefully

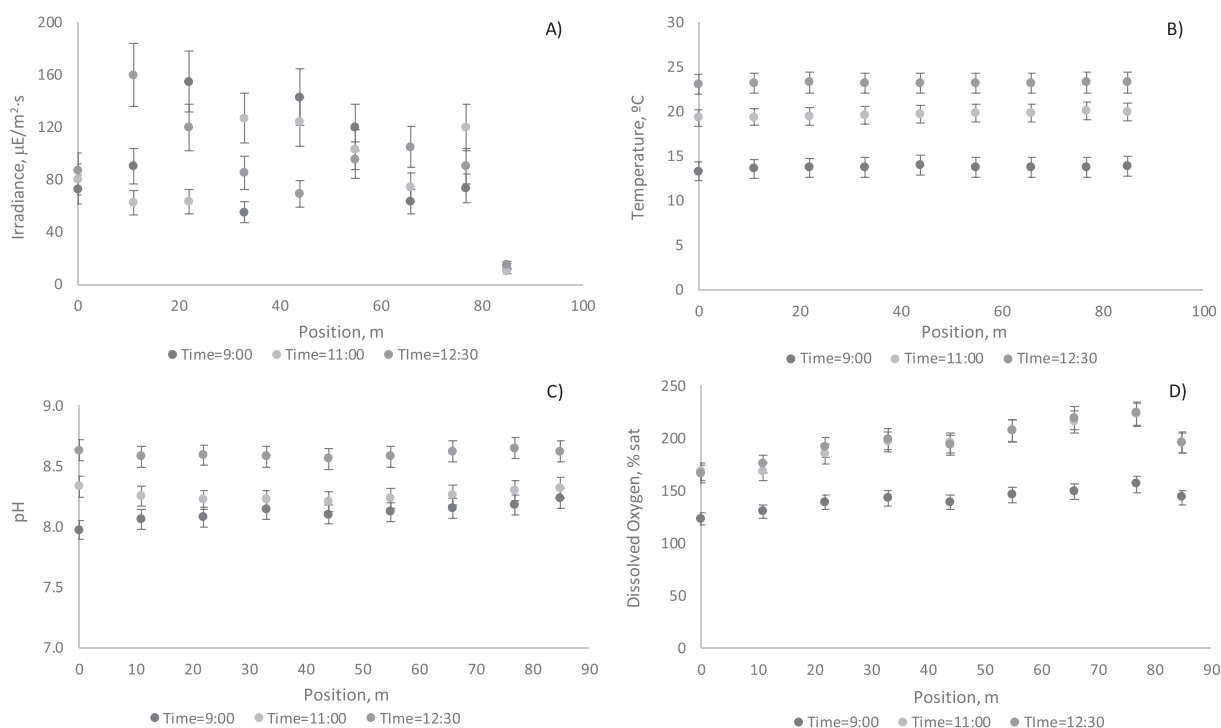


Fig. 2. Variation in culture parameters (temperature, pH and dissolved oxygen) with the position and time of day in the thin-layer reactor operated in continuous mode at 0.3 day^{-1} at the IFAPA research centre.

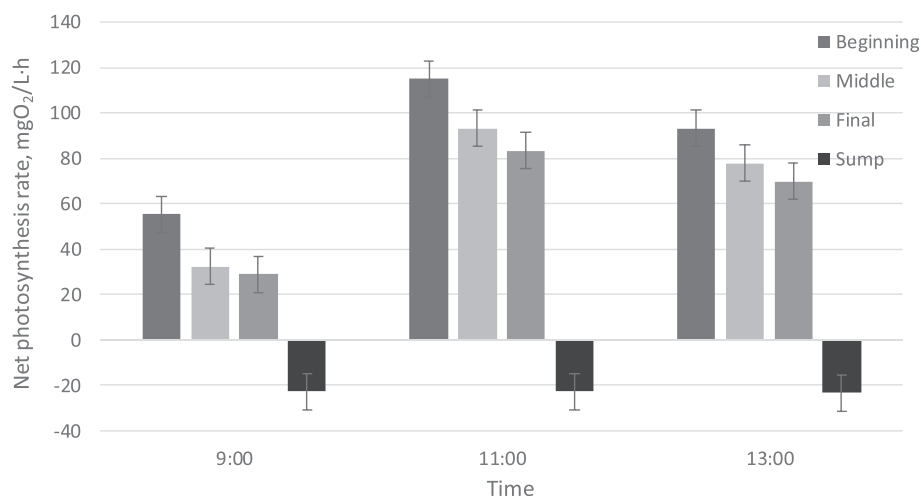


Fig. 3. *In situ* measurements of the photosynthesis rate at different positions in the thin-layer reactor.

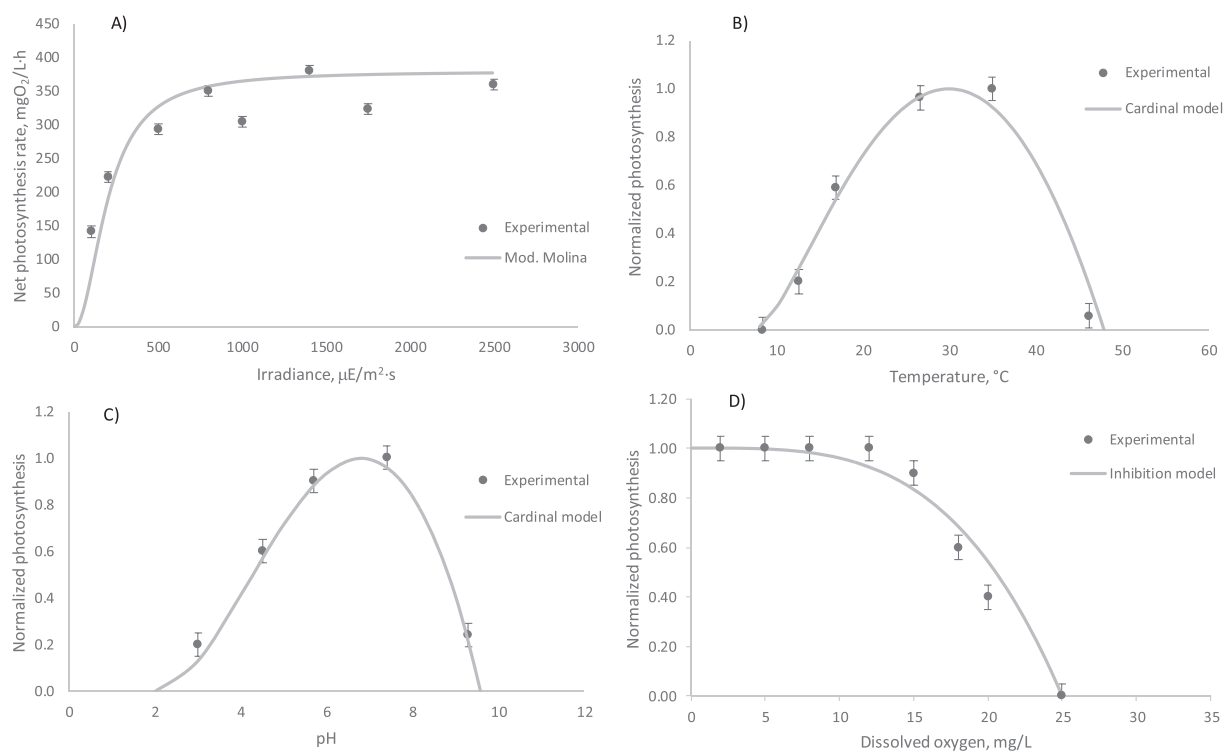


Fig. 4. Offline measurements of the photosynthesis rate versus the irradiance for samples directly taken from the reactor (A). Influence of temperature (B), pH (C) and dissolved oxygen (D) on the normalized photosynthesis rate of *S. almeriensis* at irradiance of $200 \mu\text{E m}^{-2} \text{s}^{-1}$. Lines correspond to the proposed models (Eqs. (3)–(5)).

designed.

Regarding the dissolved oxygen concentration, a much larger variation was observed, both in terms of position and time. The dissolved oxygen concentration clearly increased with the position along the channel length due to oxygen accumulation produced by photosynthesis; the channels' desorption capacity not being enough to remove this oxygen (Fig. 2D). Through the day, the increase in average irradiance also enhanced the production of oxygen, and gradients of dissolved oxygen concentration increased. The mean values of dissolved oxygen concentration ranged from 141 to 197%Sat (Table 1) although values up to 225%Sat were experimentally determined at the end of the channel at 13:00 h, even on a cloudy day. Dissolved oxygen reduces the performance of microalgae cultures if concentration values exceed 250%Sat.; this is because the photosynthesis rate reduces exponentially above this value (Fernández et al., 2012; Pawlowski et al., 2014). The

existence of excessive dissolved oxygen in thin-layer reactors has already been reported, with values up to 23 mg/L being measured (Doucha and Lívanský, 2006; Lívanský and Doucha, 1996).

To determine the influence of these experimental conditions on culture performance, *in situ* measurements of net photosynthesis rates at different reactor positions were carried out. These were taken at the beginning, middle and end of the channel, as well as in the sump (Fig. 3). The data show that the net photosynthesis rate varies based on the position in the reactor and the time (as a result of changes in solar radiation availability over time). In terms of the position, the sump is shown to be a dark volume, with the cells respiring in this section; here, values as low as $-23 \text{ mgO}_2/\text{L-h}$ were measured. Conversely, in the channel, a greater photosynthesis rate is always measured after the bubble column, where the culture is adjusted to the optimal conditions; thus, at the beginning of the solar collector, values from 55 to

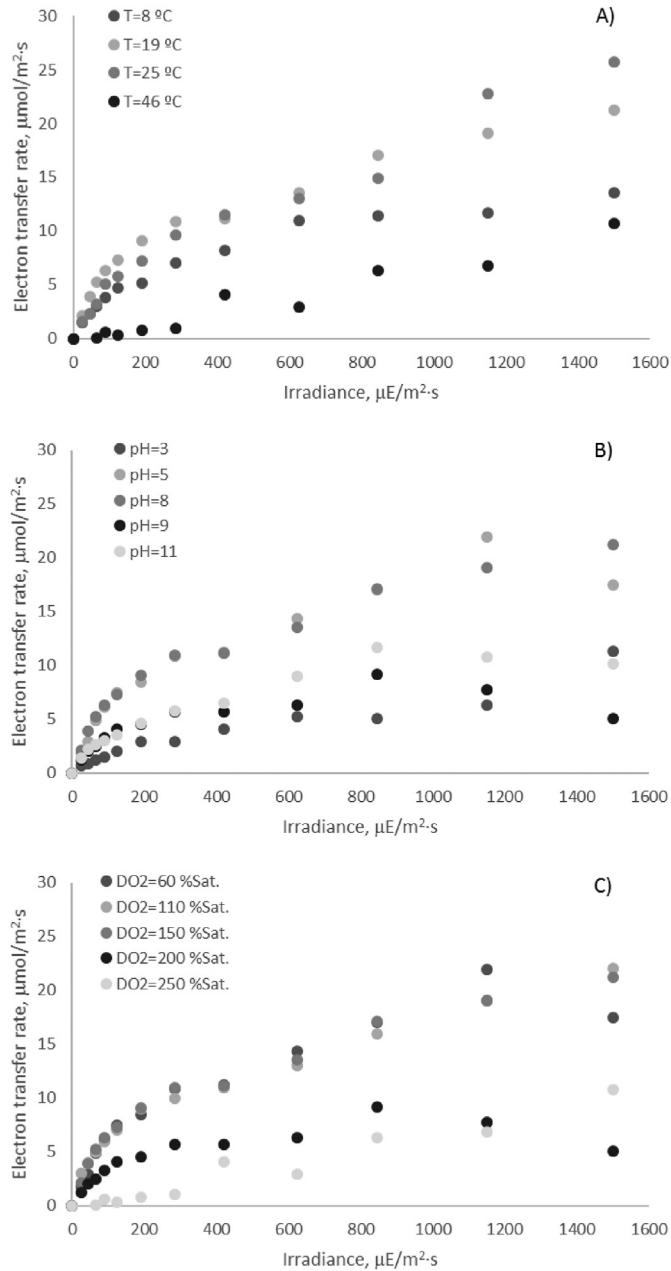


Fig. 5. Influence of temperature (A), pH (B) and dissolved oxygen (C) on the electron transfer rate of *Scenedesmus almeriensis* cells. Data from Chlorophyll-fluorescence measurements.

115 mgO₂/L·h were measured. In the middle of the channel, the net photosynthesis rate reduces, reducing yet further at the end of the channel; this confirms that the modified culture parameters along the channel length create adverse conditions for the photosynthetic process. The values at the end of the channel ranged from 29 to 83 mgO₂/L·h. The hourly variation in the photosynthesis rate agrees with the variation in solar irradiance measured on the reactor surface, and the average irradiance calculated inside the culture; behaviour that we expected to see.

3.2. Offline measurements in the laboratory

To confirm the influence of changing culture conditions on the cell performance offline, measurements were performed in the laboratory that simulated the culture conditions prevailing outdoors. For this, the net photosynthesis rate and chlorophyll-fluorescence methods were

used. Regarding the net photosynthesis rate, experiments were carried out that modified the irradiance to which the cells were exposed, showing the typical light curve response of the photosynthesis rate (Fig. 4A). These measurements were performed under the optimal conditions of temperature (25 °C), pH (8.0) and dissolved oxygen (9 mg/L = 100%Sat.). By fitting the experimental values to the hyperbolic model proposed by Molina et al., (Eq. (2)) (Molina-Grima et al., 1994), the characteristic parameter values of the model were obtained ($PO_{2,max} = 380$ mgO₂/L·h, $I_k = 200$ μE/m²·s, $n = 2$). Therefore, for the entire solar radiation range, we can simulate the curve representing the model. The data show that the model accurately represents the experimental figures; moreover, one can observe that a maximal photosynthesis rate of 350 mgO₂/L·h is achieved at average irradiances of 500 μE/m²·s; above this value the cultures become saturated.

$$PO_2 = \frac{PO_{2,max} \cdot I_{av}^n}{I_k^n + I_{av}^n} \quad (2)$$

To analyse the net photosynthesis rate response to changes in culture parameters (temperature, pH and dissolved oxygen), normalized values were used. To do this, net photosynthesis rate measurements were taken at different temperature, pH and dissolved oxygen values; for each data set, the experimental photosynthesis rate values were divided by the maximal value to help understand and compare the final results. Regarding the temperature, the results show that temperatures below 26 °C, or above 34 °C, significantly reduce the culture performance; at temperatures of 12 °C and 46 °C, the photosynthesis rate becomes almost negligible (Fig. 4B). In the case of pH, a similar trend was observed - the net photosynthesis rate is close to the maximal value from 5.7 to 8.0; outside this range it markedly reduces, nearing zero at pH values of 3 and 10 (Fig. 4C). Regarding the influence of the dissolved oxygen concentration, a different trend was observed - the photosynthesis rate remaining constant at dissolved oxygen concentrations below 15 mg/L (135%Sat.) whereas above 20 mg/L (180% Sat.), it nears zero (Fig. 4D). These results confirm previous studies concerning the effect of culture conditions on *Scenedesmus almeriensis*, which showed the optimal pH to be in the range of 7.0 to 9.0, and the maximal photosynthesis activity to be at a temperature of 35 °C, reducing dramatically at temperatures above this (Costache et al., 2013).

The experimental figures can be fitted to the different models to modelize the influence of culture conditions on cell performance. In the case of temperature and pH, using the cardinal model is recommended (Bernard and Rémond, 2012; Ippoliti et al., 2016a) whereas for dissolved oxygen, using models that consider the inhibition by product is advised (Costache et al., 2013; Ippoliti et al., 2016a).

$$RO_2(T) = \frac{(T - T_{max})(T - T_{min})^2}{(T_{opt} - T_{min})((T_{opt} - T_{min})(T - T_{opt}) - ((T_{opt} - T_{max})(T_{opt} + T_{min} - 2T)))} \quad (3)$$

$$RO_2(pH) = \frac{(pH - pH_{max})(pH - pH_{min})^2}{(pH_{opt} - pH_{min})((pH_{opt} - pH_{min})(pH - pH_{opt}) - ((pH_{opt} - pH_{max})(pH_{opt} + pH_{min} - 2pH)))} \quad (4)$$

$$RO_2(DO_2) = 1 - \left(\frac{DO_2}{DO_{2,max}} \right)^m \quad (5)$$

By fitting the experimental values to these equations, the models' characteristic parameter values were obtained. In terms of the temperature, the maximum and minimum tolerable temperatures were 48 and 7 °C, respectively, while the optimal temperature was 30 °C. For pH, the maximum and minimum tolerable values were 9.6 and 2.0, respectively, whereas the optimal pH was 6.8. In the case of the dissolved oxygen concentration, the maximum dissolved oxygen concentration tolerated by the culture was 25 mg/L (225%Sat.), the proposed model's form parameter having a value of 3.5.

These results are comparable to those obtained when evaluating the

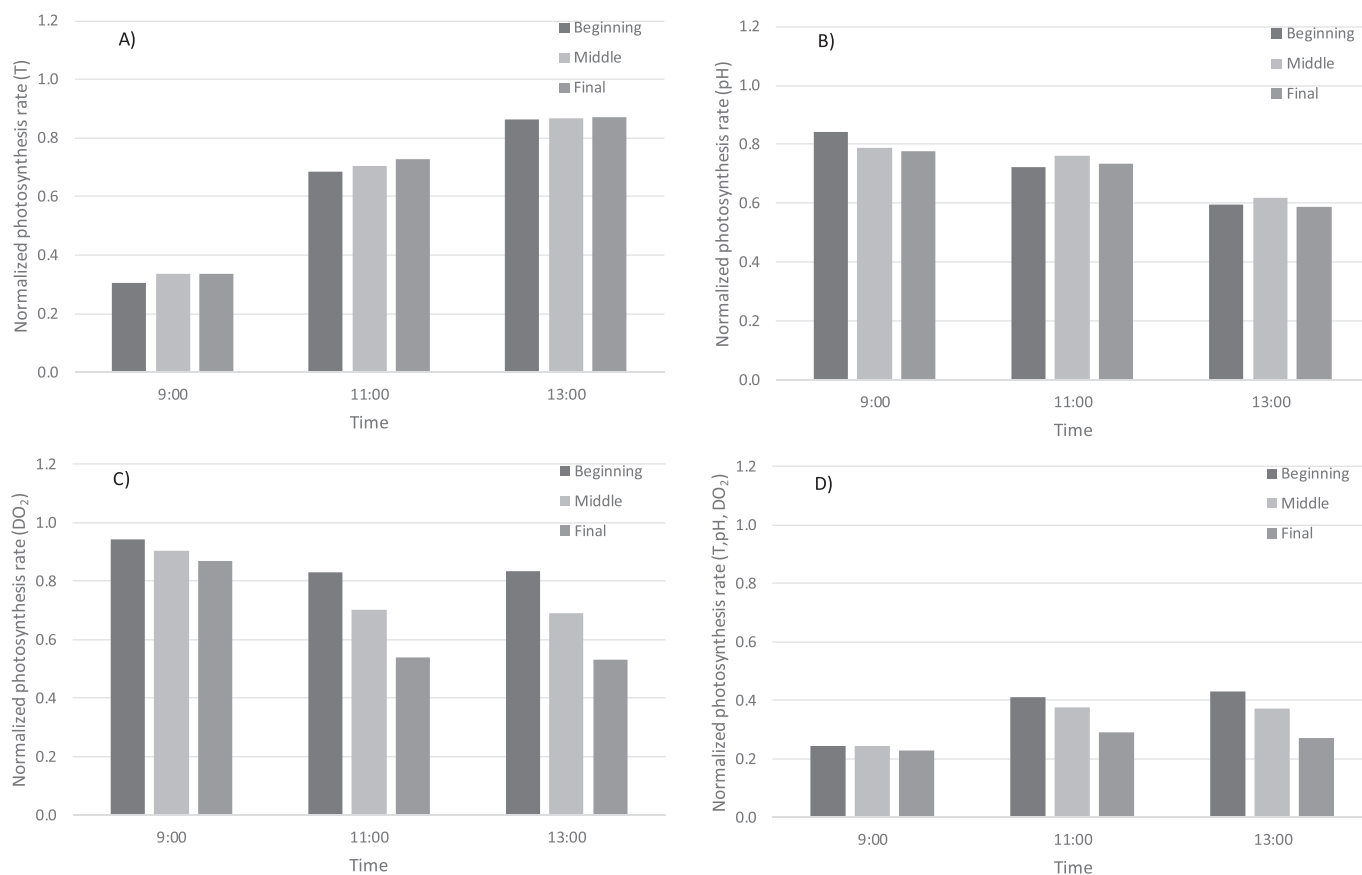


Fig. 6. Variation in the normalized photosynthesis rate at different positions and times in the thin-layer reactor as a function of the prevailing culture conditions. A) Influence of temperature, B) influence of pH, C) influence of dissolved oxygen concentration, D) influence of temperature + pH + dissolved oxygen concentration.

electron transfer rate of the cells in the reactor by taking chlorophyll fluorescence measurements. The data in Fig. 5 show that temperature has a negative effect on the electron transfer rate at values of 8 and 46 °C, with no photo inhibition being observed up to 1500 $\mu\text{E}/\text{m}^2\cdot\text{s}$. In the case of pH, an adverse effect was observed at values below pH 5 and above pH 8; the lowest electron transfer rate being measured at pH 3. Finally, regarding the influence of dissolved oxygen, a similar trend was observed to that of the photosynthesis rate - the electron transfer rate showed a similar trend to that of irradiance at dissolved oxygen concentrations below 150%Sat.; above this value it significantly reduced. Although a relationship between the electron transfer rate and the oxygen production rate can be developed, it is preferable to use the previous models of the photosynthesis rate as a function of the culture conditions to estimate *Scenedesmus almeriensis* cell behaviour under different conditions. The utilization of Chlorophyll-fluorescence measurements to identify adverse culture conditions in thin-layer reactors has already been reported; they are also recommended as a rapid tool for optimizing water depth in these types of reactors (Jerez et al., 2014, 2016).

3.3. Evaluation of productivity losses in the thin-layer reactor

The results reported here demonstrate that inadequate culture conditions occur in thin-layer reactors, both along the channel length and over time. Experimental photosynthesis rate measurements confirm that these inadequate culture conditions reduce the net photosynthesis rate of the *Scenedesmus almeriensis* produced in this type of reactor. Moreover, Chlorophyll-fluorescence measurements confirm this behaviour, allowing us to identify the value limits for the most relevant culture conditions such as temperature, pH and dissolved oxygen. To quantify the loss in productivity caused by inadequate culture

conditions along the channel length and over time, the normalized photosynthesis rates for each of the main variables have been calculated using the obtained models (Fig. 6). The results show that in the early morning, low temperature is the main factor inhibiting *Scenedesmus almeriensis* cell performance, with normalized photosynthesis rate values below 0.4 being measured at 9:00 h, although these increase to 0.87 at noon (Fig. 6A). Conversely, the pH level is adequate in the early morning when the CO₂ demand is low, the normalized photosynthesis rate being 0.84; however, this drops to 0.59 at noon when the CO₂ supply is insufficient to cover the culture demand (Fig. 6B). The dissolved oxygen concentration is the variable showing the greatest variation depending on the position in the channel, with the normalized photosynthesis rate decreasing along the reactor length from 0.94 to 0.87 in the early morning, and from 0.84 to 0.53 at noon (Fig. 6C). When multiplying all these factors together, the overall normalized photosynthesis rate can be calculated. The results show that, in the early morning, the normalized photosynthesis rate remains below 0.24 wherever the position along the channel, increasing up to maximal values of 0.43 at noon at the beginning of the channel but dropping to 0.27 at the end of the channel at this time (Fig. 6D). This behaviour has already been reported in tubular photobioreactors producing T-ISO, with similar normalized photosynthesis rates (Ippoliti et al., 2016b). It has therefore been demonstrated that this methodology is a useful tool for optimizing the design and operation of whichever type of large-scale reactor.

When considering all these factors, the average normalized photosynthesis rate was 0.32, indicating that one could increase the net photosynthesis rate to 68% if the culture conditions inside the reactor were improved. In terms of the net photosynthesis rate, this signifies that the mean measured value of 62 mgO₂/L·h could be increased to 185 mgO₂/L·h under optimal culture conditions. Considering the basic

photosynthesis equation, this means that the maximal achievable productivity is close to 32 g/m²·day, even though the estimated productivity, according to the developed model, was 10.5 g/m²·day; the actual value being measured on the basis of the biomass dry weight and a dilution rate of 11.7 g/m²·day. Accordingly, it has been demonstrated that thin-layer reactors still need to be better characterized and evaluated to achieve robust systems that can perform adequately at the industrial scale. Moreover, the modifications required to achieve full control of control conditions allowing to optimize the biomass productivity must be also analysed from the sustainability point of view, the sustainability of microalgae based processes being recently discussed (Barsanti and Gualtieri, 2018).

4. Conclusions and future prospects

Inadequate culture conditions occur in thin-layer reactors, both with the position along the reactor and over time. Temperature mainly varies along the day, no gradients with the position being observed, whereas large variation of pH and especially of dissolved oxygen concentration occurs both with time and position. The inadequacy of culture conditions was demonstrated to reduce the performance of *Scenedesmus almeriensis* cultures. The methodology used here is of great use for improving the design and performance of whatever reactor. It has been demonstrated that the net photosynthesis rate can be multiplied three-fold if optimized thin-layer reactors are used.

Conflict of interest statement

The authors declare that there are any potential financial or other interests that could be perceived to influence the outcomes of the research.

Acknowledgements

Thanks to the young students who also participated in this work: Rosalía Acien, Paula Blanco, María Casado, María José Ferre, Claudia López, Isabel López, Elena López y Marta Velar. This study was part of the Science IES programme for young students, and it was supported by the Ministry of Economy and Competitiveness (DPI2014-55932-C2-1-R, DPI2017-84259-C2-1-R) and (PURASOL, CTQ2017-84006-C3), along with the European Union's Horizon 2020 Research and Innovation Program under Grant Agreement No. 727874 SABANA. We are most grateful for the practical assistance given by the staff of the "IFAPA" Experimental Station.

References

Acien, F.G., Molina, E., Reis, A., Torzillo, G., Zittelli, G.C., Sepúlveda, C., Masojedek, J., 2017. Photobioreactors for the production of microalgae. In: *Microalgae-Based Biofuels and Bioproducts: From Feedstock Cultivation to End-Products*.
 Barsanti, L., Gualtieri, P., 2018. Is exploitation of microalgae economically and energetically sustainable? *Algal Res.* 31, 107–115.
 Benemann, J., 2013. Microalgae for biofuels and animal feeds. *Energies* 6, 5869–5886.
 Bernard, O., Rémond, B., 2012. Validation of a simple model accounting for light and temperature effect on microalgal growth. *Bioresour. Technol.* 123, 520–527.
 Camacho Rubio, F., Acien Fernandez, F.G., Sánchez Pérez, J.A., García Camacho, F., Molina Grima, E., 1999. Prediction of dissolved oxygen and carbon dioxide

concentration profiles in tubular photobioreactors for microalgal culture. *Biotechnol. Bioeng.* 62 (1), 71–86.
 Costache, T.A.A., Fernández, F.G.A., Acien, F.G., Morales, M.M., Fernández-Sevilla, J.M., Stamatini, I., Molina, E., 2013. Comprehensive model of microalgae photosynthesis rate as a function of culture conditions in photobioreactors. *Appl. Microbiol. Biotechnol.* 97, 7627–7637.
 de Godos, I., Mendoza, J.L., Acien, F.G., Molina, E., Banks, C.J., Heaven, S., Rogalla, F., 2014. Evaluation of carbon dioxide mass transfer in raceway reactors for microalgal culture using flue gases. *Bioresour. Technol.* 153, 307–314.
 Doucha, J., Lívanský, K., 2006. Productivity, CO₂/O₂ exchange and hydraulics in outdoor open high density microalgal (*Chlorella* sp.) photobioreactors operated in a Middle and Southern European climate. 18, 811–826.
 Doucha, J., Lívanský, K., Lívanský, K., 2009. Outdoor open thin-layer microalgal photobioreactor: potential productivity. *J. Appl. Phycol.* 21, 111–117.
 Fernández, I., Acien, F.G., Fernández, J.M., Guzmán, J.L., Magán, J.J., Berenguel, M., 2012. Dynamic model of microalgal production in tubular photobioreactors. *Bioresour. Technol.* 126, 172–181.
 Figueroa, F.L., Jiménez, C., Lubián, L.M., Montero, O., Lebert, M., Häder, D.-P., 1997. Effects of high irradiance and temperature on photosynthesis and photoinhibition in *Nannochloropsis gaditana* Lubián (Eustigmatophyceae). *J. Plant Physiol.* 151, 6–15.
 Gao, X., Kong, B., Vigil, R.D., 2018. Simulation of algal photobioreactors: recent developments and challenges. *Biotechnol. Lett.* 40, 1311–1327.
 Grima, E.M., Camacho, F.G., Pérez, J.A.S., Sevilla, J.M.F., Fernández, F.G.A., Gómez, A.C., 1994. A mathematical model of microalgal growth in light-limited chemostat culture. *J. Chem. Technol. Biotechnol.* 61, 167–173.
 Grobbelaar, J.U., 2010. *Microalgal Biomass Production: Challenges and Realities*.
 Ippoliti, D., Gómez, C., Morales-Amaral, M.M., Pistocchi, R., Fernández-Sevilla, J.M.M., Acien, F.G.G., 2016a. Modeling of photosynthesis and respiration rate for *Isochrysis galbana* (T-Iso) and its influence on the production of this strain. *Bioresour. Technol.* 203, 71–79.
 Ippoliti, D., González, A., Martín, I., Sevilla, J.M.F., Pistocchi, R., Acien, F.G., 2016b. Outdoor production of *Isochrysis lutea* in pilot-scale tubular photobioreactors. *J. Appl. Phycol.* 28, 3159–3166.
 Jerez, C.G., Navarro, E., Malpartida, I., Rico, R.M., Masojedek, J., Abdala, R., Figueroa, F.L., 2014. Hydrodynamics and Photosynthesis Performance of *Chlorella fusca* (Chlorophyta) Grown in a Thin-Layer Cascade (TLC) System. vol. 22. pp. 111–122.
 Jerez, C.G., Malapascua, J.R., Sergejevoá, M., Masojedek, J., Figueroa, F.L., 2016. *Chlorella Fusca* (Chlorophyta) Grown in Thin-Layer Cascades: Estimation of Biomass Productivity by In-Vivo Chlorophyll a Fluorescence Monitoring. vol. 17. pp. 21–30.
 Lívanský, K., Doucha, J., 1996. CO₂ and O₂ gas exchange in outdoor thin-layer high density microalgal cultures. *J. Appl. Phycol.* 8, 353–358.
 Lívanský, K., Doucha, J., Hu, H., Li, Y., 2006. CO₂ partial pressure - pH relationships in the medium and relevance to CO₂ mass balance in outdoor open thin-layer *Arthrospira* (*Spirulina*) cultures. *Arch. fur Hydrobiol.* 165, 365–381.
 Malapascua, J.R.F., Jerez, C.G., Sergejevoá, M., Figueroa, F.L., Masojedek, J., 2014. Photosynthesis Monitoring to Optimize Growth of Microalgal Mass Cultures: Application of Chlorophyll Fluorescence Techniques. vol. 22. pp. 123–140.
 Masojedek, J., Prášil, O., 2010. The Development of Microalgal Biotechnology in the Czech Republic. pp. 1307–1317.
 Masojedek, J., Malapascua, J.R., Kopecký, J., Sergejevoá, M., 2015. Thin-layer systems for mass cultivation of microalgae: Flat panels and sloping cascades. In: *Algal Biorefineries: Volume 2: Products and Refinery Design*. Springer International Publishing, Cham, pp. 237–261.
 Mendoza, J.L., Granados, M.R., de Godos, I., Acien, F.G., Molina, E., Heaven, S., Banks, C.J., 2013. Oxygen transfer and evolution in microalgal culture in open raceways. *Bioresour. Technol.* 137, 188–195.
 Molina-Grima, E., García-Camacho, F., Sánchez-Pérez, J.A., Fernández-Sevilla, J.M., Acien, F.G., Contreras-Gómez, A., 1994. A mathematical model of microalgal growth in light-limited chemostat culture. *J. Chem. Technol. Biotechnol.* 61, 167–173.
 Morales-Amaral, M. del M., Gómez-Serrano, C., Acien, F.G., Fernández-Sevilla, J.M., Molina-Grima, E., 2015a. Outdoor production of *Scenedesmus* sp. in thin-layer and raceway reactors using centrate from anaerobic digestion as the sole nutrient source. *Algal Res.* 12, 99–108.
 Morales-Amaral, M. del M., Gómez-Serrano, C., Acien, F.G., Fernández-Sevilla, J.M., Molina-Grima, E., 2015b. Outdoor production of *Scenedesmus* sp. in thin-layer and raceway reactors using centrate from anaerobic digestion as the sole nutrient source. *Algal Res.* 12, 99–108.
 Pawlowski, A., Mendoza, J.L., Guzmán, J.L., Berenguel, M., Acien, F.G., Dormido, S., 2014. Effective utilization of flue gases in raceway reactor with event-based pH control for microalgae culture. *Bioresour. Technol.* 170, 1–9.

Appendix B

ARTICLES SUBMITTED TO JRC JOURNALS

1
2
3
4
5
6
7
8
9
10
11
12

Photosynthetic performance of *Scenedesmus almeriensis* in thin-layer reactors

L. Alameda-García^{1*}, A. De-Arriba¹, M. Barceló-Villalobos², C. Gómez Serrano¹, F.G. Acién Fernández¹

¹Department of Chemical Engineering, Universidad de Almería, E04120 Almería (Spain)

²Department of Informatics, Universidad de Almería, E04120 Almería (Spain)

*Corresponding author. E-mail address: lidimeda@gmail.es (L. Alameda García)

Keywords:

13
14

Abstract

15 In this work, the photosynthetic performance of *Scenedesmus almeriensis* in a 120 m²
16 thin-layer reactor located inside a greenhouse at the "IFAPA" Research Centre (Almería, Spain)
17 was studied. The objective is to elucidate the main factors determining the performance of
18 microalgae cultures in this type of photobioreactors to be able to propose solutions to maximize
19 it. To achieve this aim, an analysis of the different culture parameters (dissolved oxygen,
20 temperature, pH and irradiance) was carried out and the variation throughout the reactor and
21 throughout the day was studied. Moreover, the oxygen production rate at different positions
22 and times was determined. Finally, the photosynthetic activity in the microalgae was
23 determined through the *in vivo* chlorophyll fluorescence associated with photosystem II in the
24 laboratory to sustain the data collected through the *in situ* measurements. Because dissolved
25 oxygen accumulation was identified as a major problem reducing the performance of the
26 cultures, the mass transfer coefficient (k_La) at the different parts of the reactor such as channel,
27 sump and bubble column was studied. It has been proven that the behaviour of microalgal
28 culture depends directly on the irradiance to which the cells are exposed on the reactor
29 throughout the day. Besides, the culture conditions have a significant influence on the final
30 productivity achieved. The closer these optimal conditions for the microalgae select are, the
31 higher the productivity, rising by 56% if fitting the optimal ones.

32

33 1 INTRODUCTION

34 Over the last decades, microalgae research has achieved an enormous importance due
35 to the wide range of existing applications in the industry. Because of their great biodiversity,
36 their uses range from energy purposes (biofuels) to obtaining high value products with
37 applications in feed and human food, biofertilizers and pharmaceutical and cosmetic industry.
38 In addition, because of the photosynthetic process performed by these microorganisms, other
39 applications, such as CO₂ mitigation and wastewater treatment, can be attributed to them
40 (Fernández et al., 2012). Whatever the process, it must be designed taking into account the
41 specific characteristics of these microorganisms (Acién et al., 2017).

42 To improve the production of microalgae, it is necessary to use photobioreactors
43 properly designed, built and operated in order to satisfy the requirements of the selected
44 microalgae. There are multiple designs and configurations of photobioreactors, but there is no
45 optimal design yet (Acién et al., 2017). Depending on the microalgae used and the desired
46 application of the product obtained, an appropriate culture system to achieve the requirements
47 of the process must be selected. Different systems are used to produce microalgae biomass:
48 open and closed systems. Nowadays, open systems produce thousands of tons of biomass much
49 more economically than closed systems (Benemann, 2013). Therefore, in some industries closed
50 tubular photobioreactors are used, although the most frequently used technology for the
51 cultivation of these microorganisms are raceway ponds. But these systems have drawbacks such
52 as the culture thickness is about 15-30 cm so the penetration of light is limited, which implies a
53 low density of biomass.

54 A promising alternative is the thin-layer cultivation concept pioneered in Třeboň, Czech
55 Republic (Apel et al., 2017; Doucha and Lívanský, 1995). This photobioreactor concept enables
56 the microalgae culture to flow down a slightly sloping channel with a 1-5 cm culture depth using
57 the sun light in a more efficient way, which allows obtaining higher concentrations of biomass.
58 High cell densities of 30-50 g/L after 2-3 weeks have been reported in outdoor cultivation of
59 *Chlorella* and *Scenedesmus* freshwater strains in Czech Republic and Greece (Apel et al., 2017;
60 Doucha and Lívanský, 2006). The short path of light in combination with high cell density and
61 intensive turbulence allows cells to be exposed to intermittent light with short light/dark cycles,
62 thus avoiding the reduction of photosynthetic electron carriers (Masojídek et al., 2011).

63 Unfortunately, the technical information that exists about this type of reactor is scarce
64 and a detailed evaluation of all the reactor parts is not available, which makes the scaling-up of
65 these systems difficult (Apel et al., 2017). Currently, there are still no industries that use thin-
66 layer reactors, so their use is limited to laboratory and pilot scale. Several studies show their
67 greater productivity compared to raceway reactors, but also present problems related to
68 inadequate mass transfer capacities and the existence of gradients of the cultivation conditions
69 which can affect their productivity. In order to accomplish its scaling, its performance must be
70 studied by controlling the culture conditions such as irradiance, pH, temperature and dissolved
71 oxygen both throughout the reactor and throughout the day.

72 In this paper, the photosynthetic performance of *Scenedesmus almeriensis* in a 120 m²
73 thin-layer reactor was studied. The objective is to elucidate the main factors determining the
74 performance of microalgae cultures in this type of photobioreactors to be able to propose
75 solutions to maximize it. To achieve this aim, an analysis of the different culture parameters
76 (dissolved oxygen, temperature, pH and irradiance) was carried out and the variation
77 throughout the reactor and throughout the day was studied. Moreover, the oxygen production

78 rate at different positions and times was determined. Finally, the photosynthetic activity in the
79 microalgae was determined through the *in vivo* chlorophyll fluorescence associated with
80 photosystem II in the laboratory to sustain the data collected through the *in situ* measurements.

81 **2 MATERIALS AND METHODS**

82 **2.1 Microorganism and culture conditions**

83 The microalga *Scenedesmus almeriensis* (CCAP 276/24) is selected because it is a highly
84 productive and fast-growing strain in outdoor reactors. *Scenedesmus* strains are widely reported
85 on for outdoor production because of their tolerance to adverse conditions. It supports
86 temperatures up to 45 °C and pH values of 10; although its optimum conditions are 35 °C and
87 pH 8 (Sánchez et al., 2008).

88 The culture medium used was Mann & Myers, prepared using agricultural fertilizers
89 instead of pure chemicals: 0.18 g/L MgSO₄, 0.14 g/L KH₂PO₄, 0.9 g/L NaNO₃ and 0.015 g/L
90 Karentol. The microalga was produced in a thin-layer reactor, under pH controlled by on-
91 demand injection of pure CO₂.

92 **2.2 Thin-layer reactor design and operating conditions**

93 The thin-layer reactor used is located inside a greenhouse at the "IFAPA" Research
94 Centre facilities (Almería, Spain) (Figure 1). This type of reactor consists of several zones: two
95 channels, 40 m long and 1.5 m wide, slightly inclined to favour the culture flow; a turn that
96 connects the end of the first channel with the beginning of the second one, which is inclined in
97 the opposite direction; a sump in which the culture falls through a cascade from the second
98 channel; and a bubble column through which the culture is recirculated from the sump to the
99 first channel by a low stress centrifugal pump and where the culture is put in contact with air or
100 CO₂ which is injected inside. This bubble column is useful in mixing, oxygen desorption and CO₂
101 absorption. The reactor has a total surface area of 120 m² with a water depth of approximately
102 0.03 m; thus, the total culture volume in this section is 2.55 m³. The sump has an operation
103 volume of 0.62 m³ whereas the bubble column has a volume of 0.23 m³, a height of 2 m and an
104 internal diameter of 0.38 m, making the total culture volume 3.4 m³.

105 The parameters that affect the culture are monitored. The culture's pH is controlled to
106 8.5 by on-demand injection of pure CO₂ with *DAQFactory* software. The gas flow rate of both
107 CO₂ and air entering the bubble column is measured using mass flow meters. The air flow rate
108 in the bubble column is 100 L/min used to avoid dissolved oxygen accumulation.

109 The reactor is operated in continuous mode by harvesting up to 1.0 m³/day of culture,
110 replacing it with fresh medium prepared using freshwater and fertilizers; therefore, the imposed
111 dilution rate is 0.2 day⁻¹. The evaporation is compensated by daily addition of water to maintain
112 the depth of the culture around 3 cm. The culture's temperature was not controlled.

113 **2.3 In situ measurements in the thin-layer reactor**

114 In order to study the existence of culture condition gradients throughout the reactor
115 and throughout the day, measurements of irradiance (Universal Light Meter ULM-500, Walz),
116 pH (HI98190, Hanna Instruments), temperature and dissolved oxygen (HI98198, Hanna
117 Instruments) were made in nine points of the reactor and at three hours during the day. Eight
118 of these points are located 13 meters apart along the channel, while the other one is in the

119 entrance pipe to the bubble column. In addition, because the channel is an area that is exposed
120 to direct sunlight, an additional measurement of dissolved oxygen was made as a function of
121 time to know the oxygen production of the microalga along this zone. These measurements
122 were made at the beginning, middle and end of the channel introducing culture sample and the
123 dissolved oxygen probe in a 40 mL plastic chamber for 5 minutes (Figure 1).

124 Furthermore, unlike the channel, the sump and the bubble column are areas of the
125 reactor in which the culture is in darkness, so the microalga does not perform photosynthesis,
126 but breathes. Thus, to obtain the oxygen consumption in the sump, the same plastic chamber is
127 used but covered with aluminium foil to simulate the growing conditions in this area. Because
128 the residence time of the culture in the bubble column is very short, the measurement of oxygen
129 consumption was not performed because it would not be representative.

130 **2.4 Chlorophyll-fluorescence measurements**

131 A pulse-amplitude-modulation fluorometer (Junior-PAM, Walz) was used to estimate
132 the photosynthetic activity of the microalgae cells using the Rapid Light Curves of Electron
133 Transport Rate. After making the measurements in the reactor, a culture sample was taken in a
134 plastic cup with lid and taken to the laboratory. The fluorescence measurements were made
135 with Junior-PAM fluorometer and Wincontrol 3 computer programme. The microalgae culture
136 sample was incubated in the dark for 15 minutes, to ensure that all the reaction centres were
137 oxidised (open), in three plastic tubes previously wrapped in aluminium foil. After this time of
138 darkness, the fibre was introduced inside the tube, the intensity was modulated to adjust the
139 value of the basal fluorescence (F_t), current fluorescence at steady state in microalgae adapted
140 to light (Jerez and Korbee, 2013), around 210 and the programme was started. It started emitting
141 a saturation pulse to determine the maximum quantum yield (F_v/F_m) and continued emitting
142 increasing irradiances of blue actinic light Three replicates were made in the 3 hours of the day
143 selected to do the experiment.

144 **2.5 Biomass concentration and statistical analysis**

145 For the microalgal biomass concentration quantification, the biomass dry weight was
146 determined. 50 mL culture samples were vacuum filtered through a Whatman GF/F CAT No.
147 1825-090 filter. The filter containing the biomass was taken to the stove where it passes 24
148 hours at 80°C to be weighed again. The difference between the weight of the filter with biomass
149 and the weight of the initial filter with respect to the volume of filtered culture indicates the
150 concentration of biomass in the crop.

151 **2.6 Statistical analysis**

152 To determine if there were significant differences between the variables obtained and
153 the different hours at which the experiments were carried out, analysis of the variance (simple
154 ANOVA) and LSD tests were carried out using the statistical software Statgraphics 18.

155 **3 RESULTS AND DISCUSSION**

156 **3.1 In situ measurements in the thin-layer reactor**

157 The availability of light in outdoor reactors is a function of the solar radiation that exists
158 at that moment. Therefore, the measures obtained will depend to a large extent on this variable.
159 The data show (Figure 2A) that the irradiance on the culture surface varies from 460 to 2,045

160 $\mu\text{E}/\text{m}^2\cdot\text{s}$. Obtaining the highest values at 12:15 h. In general, the irradiance does not follow a
161 clear trend, but the averages obtained from all measurements are quite similar between days.
162 It is observed that at the beginning of the second tray, the radiation decreases every day, mainly
163 due to the arrangement of the reactor inside the greenhouse.

164 Regarding the temperature, representing the measurements that were taken in the
165 different points of the channel (Figure 2B), it is observed that as it advances in the reactor, the
166 temperature values do not vary significantly. Instead, they increase a lot with the time. This is
167 because the culture absorbs infrared radiation from solar radiation. The temperature values
168 obtained are between 16 and 30 °C. In this type of reactors, because the microalgae culture is
169 not exposed to solar radiation for a long period of time, no relevant temperature gradients occur
170 along the 80 m channel. However, as the graphs show, during the day the temperature increases
171 in the culture because the energy that enters is larger than the one that is coming out through
172 evaporation.

173 In terms of the pH, the pH control works by injecting CO_2 into the bubble column when
174 the sensor, which is at the end of the channel, reaches the pH that has been indicated as the set
175 point, in this case 8.5. As noted (Figure 2C), the pH remains close to 8.5 and does not exceed pH
176 9.1. The optimum pH for the microalga *Scenedesmus almeriensis* is 8. As the fixed pH sensor is
177 at the end of the reactor channel, the pH control point is set at 8.5. In this way the pH is expected
178 to remain close to 8 in most of the channel. On the other hand, the data shown in the graphs
179 indicates that the pH control must be optimized to improve the productivity of this microalgae.

180 3.1.1 Dissolved oxygen

181 As far as the measurements of dissolved oxygen along the channel, these were made
182 with measures in percentage of saturation. Therefore, to change this percentage into oxygen
183 concentration in mg/L it is necessary to calculate the saturated dissolved oxygen concentration
184 (DO_2^*) that varies with the temperature according to Eq. (1) (Barceló-Villalobos et al., 2018).

$$185 \quad \text{DO}_2^* = 12.408 - 0.1658 \cdot T(^{\circ}\text{C}) \quad (1)$$

186 Figure 2D represents punctual measurements of oxygen concentration along the
187 channel at different times of the day.

188 As can be observed in the Figure 2D, the concentration of dissolved oxygen increases
189 both along the channel, owing to oxygen accumulation by the microalga as it carries out
190 photosynthesis, as well as with irradiance, mainly due to the fact that an increase in irradiance
191 causes more oxygen production. From these graphs it can also be observed that the slope of the
192 oxygen concentration increases with the irradiance. At values lower than $1,000 \mu\text{E}/\text{m}^2\cdot\text{s}$ the
193 concentration increases approximately 3 mg/L between the beginning and the end of the
194 channel. When the irradiance is higher than $1,000 \mu\text{E}/\text{m}^2\cdot\text{s}$ the concentration increases around
195 8 mg/L.

196 Oxygen concentration at the beginning of the channel at any time of the day, in general,
197 is close to 10 mg/L or even below. This means that the sump and bubble column assembly
198 efficiently consume and desorb the dissolved oxygen that reaches the end of the channel to
199 bring it near saturation at the beginning of the channel. This situation is ideal, since in this way
200 it is avoided that dissolved oxygen is increasingly high at the end of the channel, even exceeding
201 250% sat., which is harmful to the microalgae. The dissolved oxygen values range from 95% sat.
202 to 208%sat. Highest values have been measured at the end of the channel. When these dissolved

203 oxygen values exceed 250%sat., the photosynthetic performance of the microalga is reduced
204 (Fernández et al., 2012). Values up to 23 mg/L in this type of reactors have been obtained
205 (Doucha and Lívanský, 2006).

206

207 To check the effect of the air entering the bubble column, dissolved oxygen
208 measurements were taken along the channel without introducing air into it.

209 In Figure 2E, it is observed that the oxygen concentration continues increasing both
210 along the channel and with the irradiance. When the irradiance is lower than $100 \mu\text{E}/\text{m}^2\cdot\text{s}$, the
211 dissolved oxygen concentration hardly varies along the channel, obtaining a very small slope. By
212 increasing the radiation received by the culture throughout the day, this slope also increases.
213 Comparing Figure 2D with Figure 2E, it is observed that, in this case, the oxygen concentration
214 at the beginning of the channel, at second and third hour, is not close to 10 mg/L, but to values
215 close to 15 mg/L. This value indicates that, by not injecting air into the bubble column, the
216 desorption necessary to reduce, to a value close to saturation, the concentration of dissolved
217 oxygen reaching the channel entrance does not occur.

218 The sump and the bubble column are considered dark areas subsequently, on the one
219 hand, the sump is a container in which the depth of the culture is more than 20 cm and,
220 therefore, most of the microalgae are found in darkness and, on the other hand, the bubble
221 column is an opaque vessel where photosynthesis is not carried out and the residence time of
222 the culture in it is very short. Therefore, the only variable to be controlled in these two parts of
223 the reactor is dissolved oxygen.
224 Figure 3 represents the oxygen concentrations at the end of the channel, in the inlet pipe to the
225 bubble column and at the beginning of the channel at the three hours in which the
226 measurements were taken.

227 As can be seen, the concentration of dissolved oxygen between the end point of the
228 channel and the entrance to the bubble column decreases, this is mainly due to the fact that the
229 culture passes through the sump, which is an area where the microalga is in darkness. In this
230 zone, the reaction of photosynthesis is done in the opposite way, that is, the microalga breathes
231 and, therefore, consumes oxygen. Between the entrance to the bubble column and the entrance
232 to the channel, a greater oxygen decrease is observed than between the previous points. This is
233 because, since breathing is almost non-existent due to the short residence time inside the
234 bubble column, there is a much greater transfer of oxygen from the culture to the atmosphere
235 (desorption) than is produced in the sump. This is mainly due to the fact that in the bubble
236 column a gas stream is introduced in the form of small bubbles, in this case air, in counterflow
237 with the culture.

238 The graphs show that the dissolved oxygen concentration at the initial point of the
239 channel is very close to 10 mg/L and even, occasionally, lower. This shows that with a flow rate
240 of 100 L/min of air in the bubble column, the dissolved oxygen desorption in the culture is
241 adequate at this time of year.

242 **3.2 Mass-transfer characterisation**

243 Because there is an accumulation of oxygen in the reactor, the mass transfer coefficient
244 in each zone of the reactor was calculated. With the measurements taken at each point of the
245 reactor, the following calculations were made in order to obtain the production, oxygen transfer

246 and how they evolve in the different parts of the system. Knowing that the mass balance in the
 247 reactor is:

$$248 \quad O_{2,inlet} + O_{2,produced} = O_{2,outlet} + O_{2,accumulation} \quad (2)$$

249 Assuming that the reactor is in a stationary state, the accumulation term is annulled.
 250 Therefore, the mass oxygen balance is as follows:

$$251 \quad Q_{liq} \cdot DO_{2,inlet} + P_{O_2} - Q_{liq} \cdot DO_{2,outlet} = N_{O_2} \quad (3)$$

252 The parts of which this balance consists are:

253 - Physical oxygen inlet and outlet:

$$254 \quad \text{Physical inlet and outlet} = Q_{liq} \cdot (DO_{2,inlet} - DO_{2,outlet}) \quad (4)$$

$$255 \quad \frac{L}{s} \cdot \frac{mg}{L} [=] \frac{mg}{s}$$

256 - Oxygen production or consumption:

257 By means of the oxygen concentration versus the time measured with the flask, the
 258 oxygen production value is obtained, if positive, or consumption, if negative, in each
 259 zone.

$$260 \quad P_{O_2} = \frac{d DO_2}{dt} \cdot V \quad (5)$$

$$261 \quad \frac{mg}{L \cdot s} \cdot L [=] \frac{mg}{s}$$

262 - Oxygen transfer:

$$263 \quad N_{O_2} = k_L a \cdot F i_{ml} \cdot V \quad (6)$$

$$264 \quad \frac{1}{s} \cdot \frac{mg}{L} \cdot L [=] \frac{mg}{s}$$

265 The logarithmic mean driving force is calculated using the following equation:

$$266 \quad F i_{ml} = \frac{(DO_{2,outlet} - DO_2^*) - (DO_{2,inlet} - DO_2^*)}{Ln \frac{(DO_{2,outlet} - DO_2^*)}{(DO_{2,inlet} - DO_2^*)}} \quad (7)$$

267 In order to calculate the oxygen transfer in each zone of the reactor, it is necessary to
 268 obtain the experimental mass transfer coefficient ($k_L a$), since it is not possible to use the
 269 $k_L a$ associated to raceway reactors obtained by (Mendoza et al., 2013) in this type of
 270 reactors because the culture depth is much lower so the mass transfer must be greater.

$$271 \quad k_L a = \frac{Q_{liq} \cdot (DO_{2,inlet} - DO_{2,outlet}) + \frac{d DO_2}{dt} \cdot V}{F i_{ml} \cdot V} \quad (8)$$

272

273 From the oxygen concentration data versus the time obtained with the flask, oxygen
 274 production data were calculated along the reactor, both at the beginning, middle and end of the
 275 channel and in the sump (Figure 4).

276 On the one hand, the data show that the oxygen production along the channel is
 277 increasing throughout the day, that is, with an increase in irradiance, and it is also maintained
 278 at similar values along the channel at the same hour. It is just at the last hour in which the
 279 experiment is done when a clear decreasing trend from the beginning to the end of the channel
 280 is observed. This is because, at noon, dissolved oxygen at the end of the channel is over 230%
 281 sat. When introducing this culture in the flask to measure the production of oxygen, the
 282 dissolved oxygen values obtained exceed 250% sat. which is harmful for the microalga and,
 283 therefore, its photosynthetic performance decreases (Fernández et al., 2012). These data were
 284 taken in winter and, therefore, did not reached a dissolved oxygen concentration along the
 285 channel greater than 250%, but it is very likely that, in summer, having much more radiation,
 286 these values increase and, therefore, the oxygen production decreases from the beginning to
 287 the middle and at the end of the channel.

288 On the other hand, the oxygen consumption that happens in the sump follows a clear
 289 upward trend throughout the day. This is due to the oxygen concentration in the culture that
 290 reaches the sump. At 9:00 am, when dissolved oxygen in this area is around 115% sat., very small
 291 respiration values are obtained compared to noon, when dissolved oxygen is around 180% sat.
 292 and there is more oxygen that the microalga can consume.

293 Once the logarithmic mean driving force ($F_{i,m}$) is calculated, the experimental values of
 294 the mass transfer coefficient can be obtained. Equation (8) is used to calculate this coefficient.
 295 Therefore, by averaging the values obtained over several days, the mass transfer coefficients in
 296 the different parts of the reactor are:

Zone	$k_{L,a}$, 1/h	NO ₂ average, mg/s
Channel	9.25	21.15
Sump	10.42	18.70
Bubble Column	173.25	1,917.68

297

298 3.3 Chlorophyll-fluorescence measurements

299 From the data obtained with the Junior-PAM fluorometer, the electron transport rate
 300 (ETR) representing the transit of electrons through the photosynthetic transport chain is
 301 calculated (Eq.9).

$$302 \quad ETR = QY \cdot I \cdot F(II) \cdot A' \quad (9)$$

303 Being: QY the effective quantum yield, I the actinic light intensity, F(II) the fraction of
 304 light absorbed by chlorophyll associated with photosystem II, which is assumed to be 0.5 for
 305 chlorophyllides (Suggett et al., 2004) and A' the culture absorptance.

306 The absorptance, which is the fraction of light actually captured by a sample, was
 307 estimated by making the absorption spectrum of the culture from 400 to 750 nm in a
 308 spectrophotometer. Subsequently, the average of these absorbances (Abs) was carried out and
 309 the following formula was applied:

$$310 \quad A' = 1 - 10^{-Abs} \quad (10)$$

311 With the QY measurements obtained at different light intensities the ETR curve was
312 constructed. From this curve the photosynthetic efficiency (α_{ETR}) was calculated, which indicates
313 the initial slope of the ETR curve versus I, the maximum ETR (ETR_{max}), which represents the
314 maximum photosynthetic activity that the culture can have, and the ETR curve saturation
315 intensity versus I (I_k) using the Eilers & Peeters model (1988).

316 The ETR curves (Figure 5) show that the values of the electron transport rate are higher
317 throughout the day. This indicates that the culture is more productive as the day progresses
318 (increase in external irradiance), which agrees with the results obtained in Figure 4.

319 Taking the different days in which, the photosynthetic measurements were made as
320 replicas, a statistical study was carried out to verify if there are significant differences in the data
321 obtained (Figure 6).

322 The optimal quantum yield values (Fv/Fm) do not show significant differences at
323 different times of the day, representing the same degree of photosynthetic stress throughout
324 the day. The Fv/Fm values are between 0.512 and 0.588, these are close to 0.7 which would be
325 the maximum value corresponding to cells in perfect conditions.

326 ETR_{max} values fluctuate between 69.816 and 131.206 ($\mu\text{mol e}^-/\text{m}^2\cdot\text{s}$). An increase is
327 observed throughout the day, that is, as the irradiance is higher. It was possible to find
328 statistically significant differences between 9:00 and 12:15. The highest values were recorded
329 at noon.

330 The initial slope, α , has values that range from 0.294 to 0.452 [$(\mu\text{mol e}^-/\text{m}^2\cdot\text{s})/(\mu\text{E}/\text{m}^2\cdot\text{s})$].
331 The results of the variance analysis show that there are no significant differences throughout
332 the day and, therefore, as can be seen in Figure 5, the initial slopes of the different ETR curves
333 are very similar.

334 In terms of the saturation intensity, I_k , the values fluctuate between 180.669 and
335 311.212 ($\mu\text{E}/\text{m}^2\cdot\text{s}$). The statistical analysis does not present significant differences during the
336 day.

337 **4 CONCLUSIONS**

338 In this paper it has been demonstrated that there are inadequate cultivation conditions
339 that present gradients throughout the day and throughout the reactor, which entails a reduction
340 in the photosynthetic performance of the *Scenedesmus almeriensis* culture. The pH control is
341 also an important factor that determines the efficiency of these systems and, especially, the
342 efficiency of the use of CO_2 (Lívanský and Doucha, 1996). Therefore, it is important to carefully
343 design and optimize the pH control in thin-layer reactors.

344 One of the main factors that caused a reduction in the culture yield the dissolved oxygen
345 concentration must also be controlled by a good bubble column design and an adequate air flow
346 to desorb the necessary amount of oxygen so that when the culture is introduced again at the
347 beginning of the channel it has an oxygen concentration as close as saturation.

348 The average data of $k_L a$, indicate that the mass transfer in the channel and the sump is
349 minimal compared to the one existing in the bubble column. Therefore, a design and a suitable
350 air flow in the bubble column is essential to increase the productivity of the culture in this type
351 of reactors.

352 5 REFERENCES

- 353 Acién, F.G., Molina, E., Reis, A., Torzillo, G., Zittelli, G.C., Sepúlveda, C., Masojídek, J., 2017.
354 Photobioreactors for the production of microalgae, in: *Microalgae-Based Biofuels and*
355 *Bioproducts*. Woodhead Publishing, pp. 1–44. [https://doi.org/10.1016/B978-0-08-101023-](https://doi.org/10.1016/B978-0-08-101023-5.00001-7)
356 [5.00001-7](https://doi.org/10.1016/B978-0-08-101023-5.00001-7)
- 357 Apel, A.C., Pfaffinger, C.E., Basedahl, N., Mittwollen, N., Göbel, J., Sauter, J., Brück, T., Weuster-
358 Botz, D., 2017. Open thin-layer cascade reactors for saline microalgae production
359 evaluated in a physically simulated Mediterranean summer climate. *Algal Res.* 25, 381–
360 390. <https://doi.org/10.1016/j.algal.2017.06.004>
- 361 Barceló-Villalobos, M., Gómez Serrano, C Sánchez Zurano, A., García, Alameda, L., Esteve
362 Maldonado, S., Acién Fernández, F.G., 2019. Variation of culture parameters in pilot scale
363 thin-layer reactor and its influence on the performance of *Scenedesmus almeriensis*
364 culture. *Bioresour. Technol. Reports* 6, 190–197.
365 <https://doi.org/10.1016/j.biteb.2019.03.007>
- 366 Barceló-Villalobos, M., Guzmán Sánchez, J.L., Martín Cara, I., Sánchez Molina, J.A., Acién
367 Fernández, F.G., 2018. Analysis of mass transfer capacity in raceway reactors. *Algal Res.*
368 35, 91–97. <https://doi.org/10.1016/j.algal.2018.08.017>
- 369 Benemann, J., 2013. Microalgae for biofuels and animal feeds. *Energies* 6, 5869–5886.
370 <https://doi.org/10.3390/en6115869>
- 371 de Marchin, T., Ercicum, M., Franck, F., 2015. Photosynthesis of *Scenedesmus obliquus* in
372 outdoor open thin-layer cascade system in high and low CO₂ in Belgium. *J. Biotechnol.* 215,
373 2–12. <https://doi.org/10.1016/J.JBIOTECH.2015.06.429>
- 374 Doucha, J., Lívanský, K., 2006. Productivity, CO₂/O₂ exchange and hydraulics in outdoor open
375 high density microalgal (*Chlorella* sp.) photobioreactors operated in a Middle and Southern
376 European climate 18, 811–826. <https://doi.org/10.1007/s10811-006-9100-4>
- 377 Doucha, J., Lívanský, K., 1995. Novel outdoor thin-layer high density microalgal culture system:
378 productivity and operational parameters. *Gate Res.* 106, 129–147.
- 379 Fernández, I., Acién, F.G., Fernández, J.M., Guzmán, J.L., Magán, J.J., Berenguel, M., 2012.
380 Dynamic model of microalgal production in tubular photobioreactors. *Bioresour. Technol.*
381 126, 172–181. <https://doi.org/10.1016/J.BIORTECH.2012.08.087>
- 382 Jerez, C.G., Korbee, N., 2013. Use of in vivo chlorophyll fluorescence to estimate photosynthetic
383 activity and biomass productivity in microalgae grown in different culture systems *Uso de*
384 *la fluorescencia de la clorofila in vivo para estimar la actividad fotosintética y productividad*
385 *d. Lat. Am. J. Aquat. Res.* 41, 801–819.
- 386 Lívanský, K., Doucha, J., 1996. CO₂ and O₂ gas exchange in outdoor thin-layer high density
387 microalgal cultures. *J. Appl. Phycol.* <https://doi.org/10.1007/BF02178578>
- 388 Masojídek, J., Kopecký, J., Giannelli, L., Torzillo, G., 2011. Productivity correlated to
389 photobiochemical performance of *Chlorella* mass cultures grown outdoors in thin-layer
390 cascades. *J. Ind. Microbiol. Biotechnol.* <https://doi.org/10.1007/s10295-010-0774-x>
- 391 Mendoza, J.L., Granados, M.R., de Godos, I., Acién, F.G., Molina, E., Heaven, S., Banks, C.J., 2013.

- 392 Oxygen transfer and evolution in microalgal culture in open raceways. *Bioresour. Technol.*
393 137, 188–195. <https://doi.org/10.1016/j.biortech.2013.03.127>
- 394 Sánchez, J.F., Fernández, J.M., Ación, F.G., Rueda, A., Pérez-Parra, J., Molina, E., 2008. Influence
395 of culture conditions on the productivity and lutein content of the new strain *Scenedesmus*
396 *almeriensis*. *Process Biochem.* 43, 398–405.
397 <https://doi.org/10.1016/J.PROCBIO.2008.01.004>
- 398 Suggett, D.J., Macintyre, H.L., Geider, R.J., 2004. Evaluation of biophysical and optical
399 determinations of light absorption by photosystem II in phytoplankton. *Limnol. Oceanogr.*
400 *Methods*. <https://doi.org/10.4319/lom.2004.2.316>
- 401
- 402

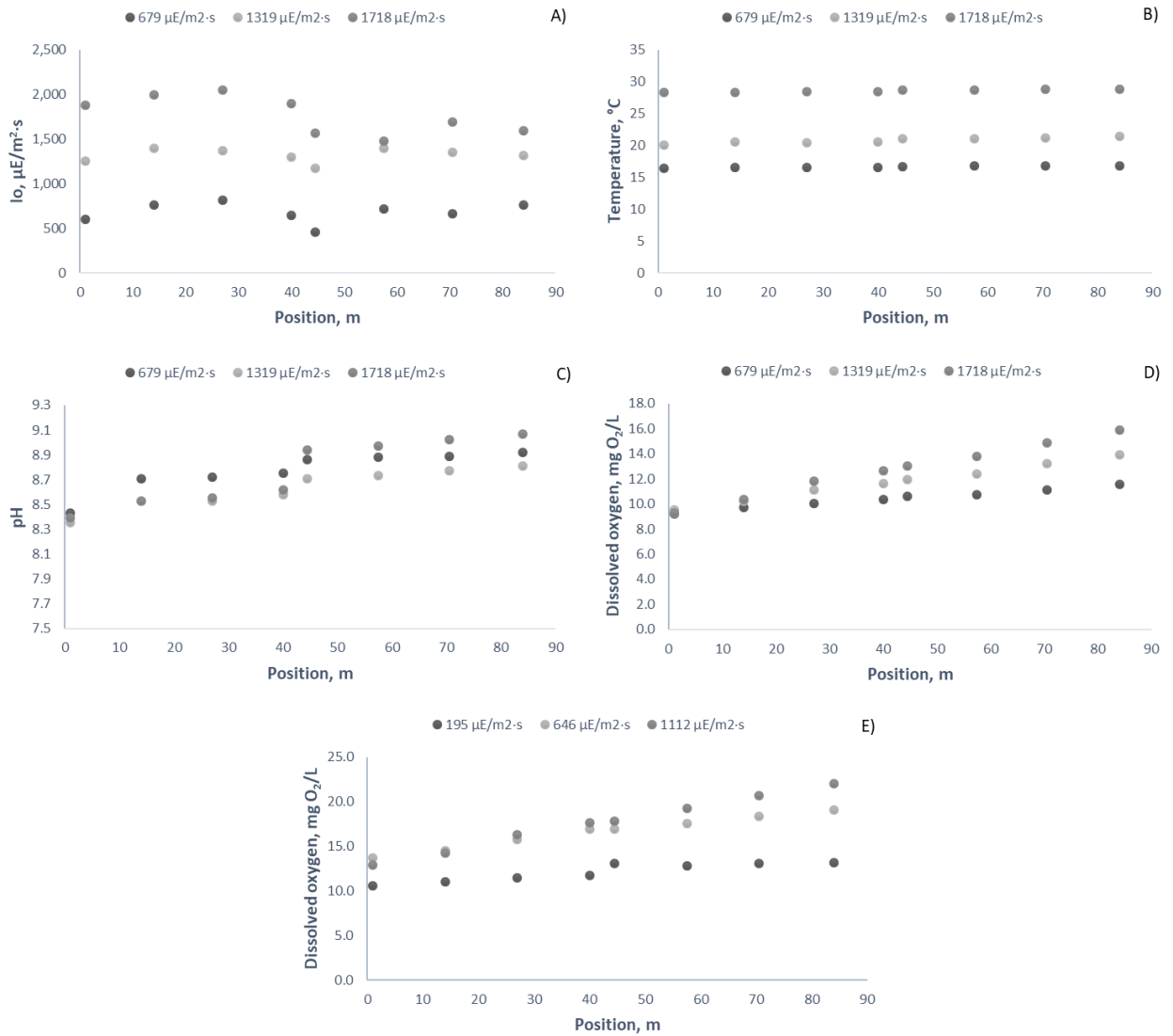


403

404

405

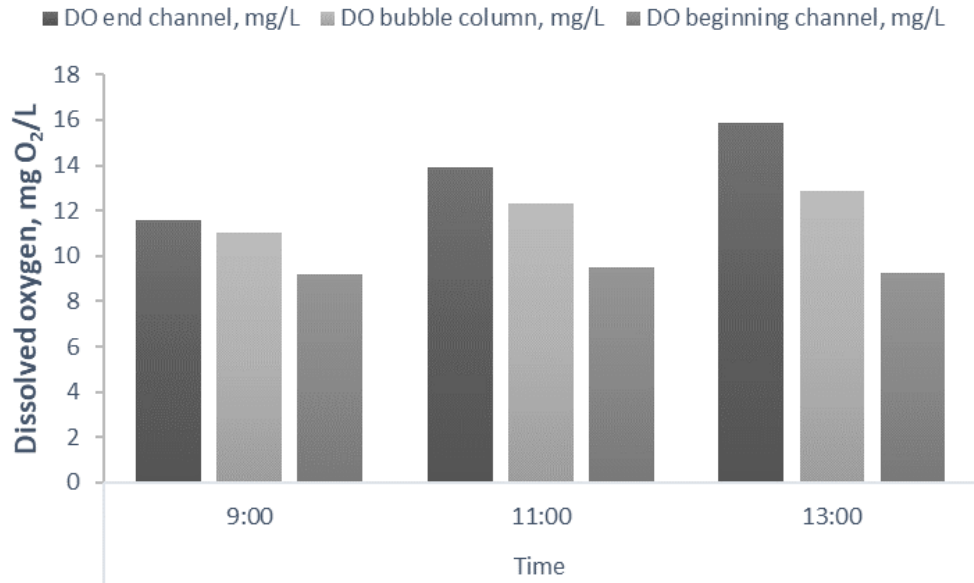
Figure 1.- Images of the thin-layer reactor located at the IFAPA Research Center (Almería, Spain) (Up) and the plastic chamber used to determine the oxygen production and consumption at the different positions (Below).



406

407
408

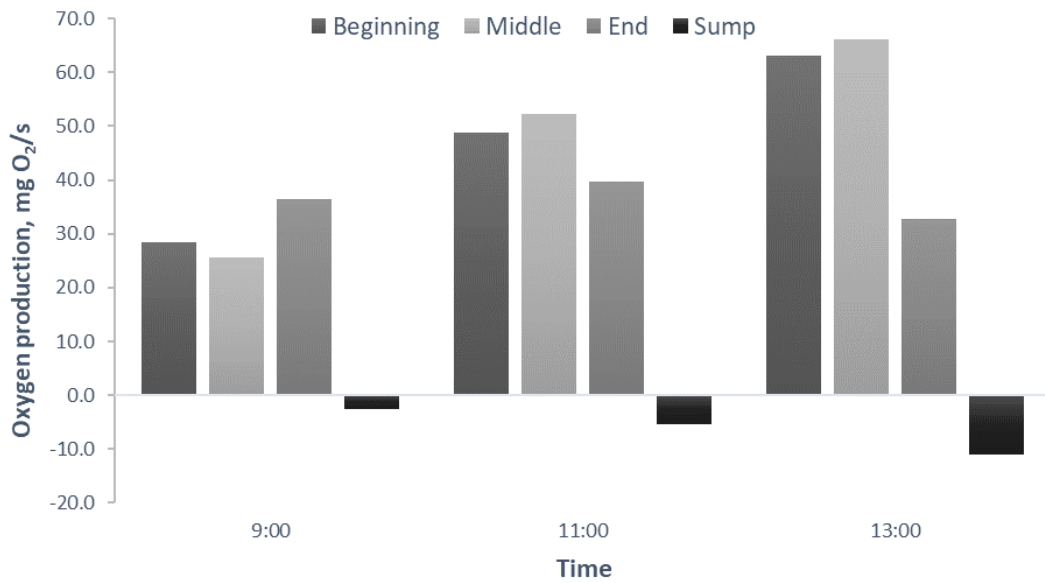
Figure 2.- Variation in culture parameters (irradiance, temperature, pH and dissolved oxygen) with the position and time of day in the thin-layer reactor operated in continuous mode at 0.2 day^{-1} at the IFAPA research centre.



409

410
411

Figure 3.- Variation of dissolved oxygen concentration at the end of the channel, in the inlet pipe to the bubble column and at the beginning of the channel.

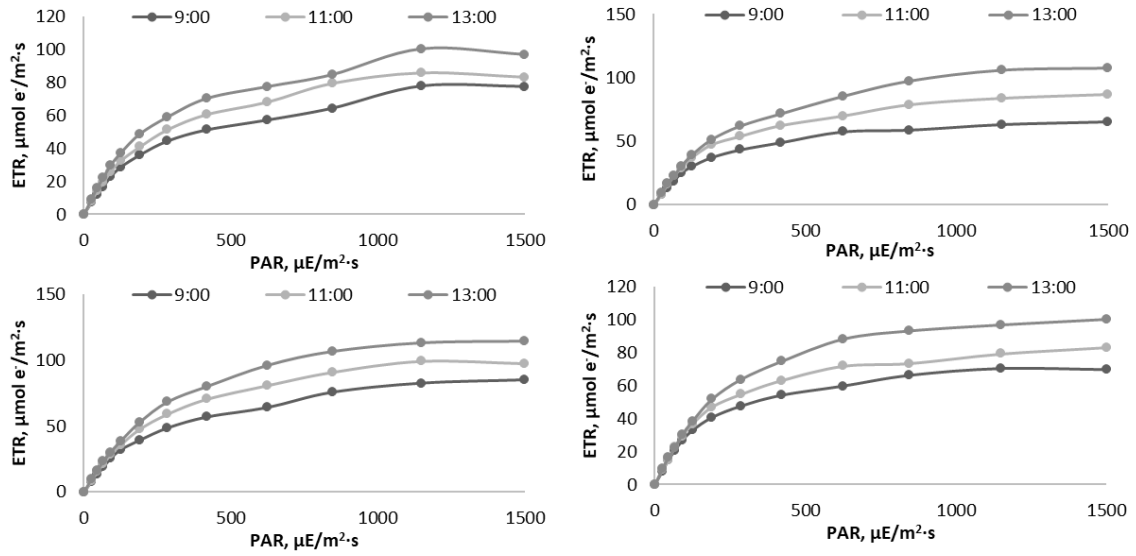


412

413
414

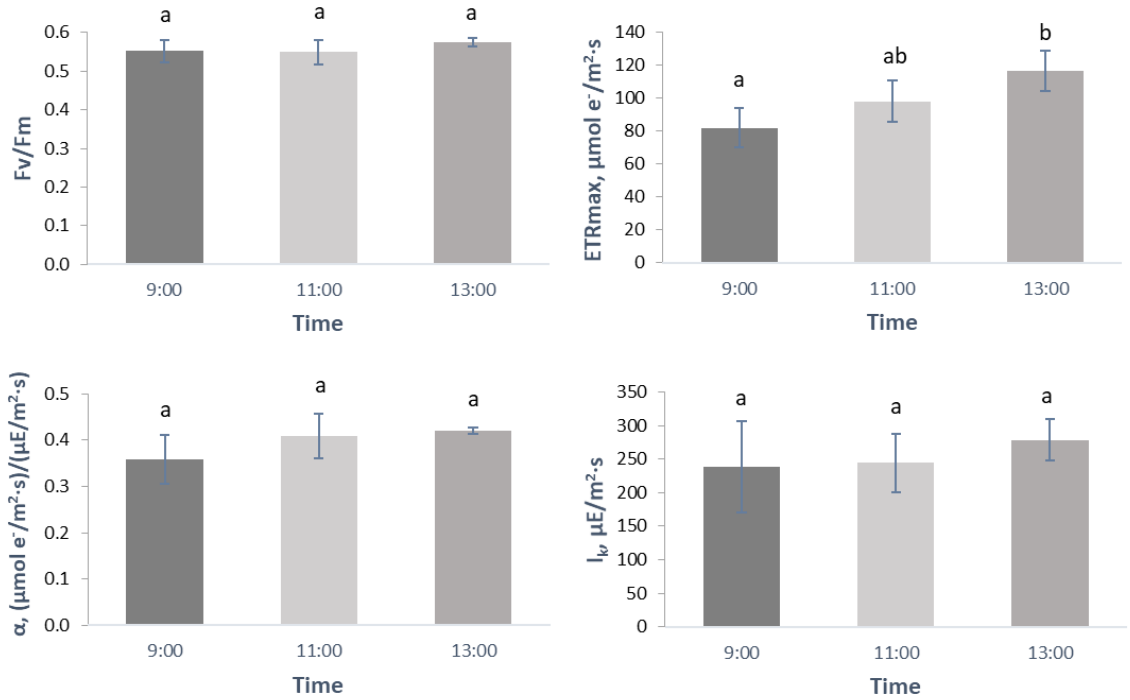
Figure 4.- In situ measurements of the oxygen production and consumption at different positions in the thin-layer reactor.

415



416
417
418

Figure 5.- Electron transfer rate curves of *Scenedesmus almeriensis* cells from Chlorophyll-fluorescence measurements.



419
420
421
422
423
424
425
426

Figure 6.- Statistical results associated with the different photosynthetic parameters.

32 **1 INTRODUCTION**

33 Basically, two approaches to phototrophic microalgae production are used: one applies to
34 cultivation in closed or semi-closed vessels – photobioreactors (PBRs, e.g. transparent tubes,
35 columns or panels), while the other involves open reservoirs (mixed ponds, raceways or
36 cascades) with direct contact of the microalgal culture with the environment (for a recent
37 review, see Acién et al., 2017). Cultivation systems have been developed since the 1950s. At
38 present large-scale cultivation units have been often used to produce microalgae biomass for
39 specific purposes determining which system is the most suitable.

40 There is no universal all-purpose unit and improved design and operational conditions have
41 been essential to optimise culture in order to produce biomass at competitive cost (Chisti, 2012;
42 Mendoza et al., 2013a). One of the most important advantages of open cultivation systems is
43 their simple and low cost construction. This fact nominate them for biomass production in an
44 industrial scale (Chisti, 2007). On the other hand, there are still some drawbacks to be solved to
45 make this technology competitive. The most crucial variable for phototrophic growth is light
46 availability. The amount of photon energy received by each cell is a combination of several
47 factors: irradiance intensity, cell density, length of optical path (thickness of culture layer), rate
48 of mixing as well as cultivation unit design (Masojídek et al., 2015).

49 Shallow systems like sloping cascades are highly efficient for biomass production (Masojídek et
50 al. 2011). Thin-layer cascades (TLCs) have been used for the first time for microalgae cultivation
51 at the Institute of Microbiology in Třeboň (Czech Republic) in the 1960s (Šetlík et al., 1970). The
52 unique feature of these TLCs is the low depth of microalgae culture as to maximize light
53 utilization efficiency that results in high areal productivity and biomass density. One of the major
54 advantages of TLCs is the efficient mixing of microalgae culture, inducing short light-dark cycles
55 of cells due to short light path (Richmond 2003, Masojídek et al. 2015).

56 Outdoor cultivation units are subject to daily variations in culture conditions that influence their
57 production yield (Camacho-Rubio et al., 1999; Fernández et al., 2014; Mendoza et al., 2013b).
58 The use of optimal culture conditions can increase the production and quality of the biomass
59 (Barceló-villalobos, M; Gómez Serrano, C; Sánchez Zurano, A; Alameda García, L; Esteve
60 Maldonado, S; Peña, J; Acién Fernández, 2019). Thus, pH, dissolved oxygen concentration (DOC),
61 temperature and incident light (I_0) variables should be controlled under their optimal values to
62 ensure the maximal productivity of these systems.

63 Microalgae growth is predominantly a function of light availability. Average irradiance concept
64 has firstly been introduced by Molina (Molina et al., 1994). It has been used to analyse the

65 continuous irradiance inside the culture. It refers to the light intensity at a given point inside the
66 cultivation unit, which depends on the light path length (p), biomass concentration (C), and on
67 the biomass absorption coefficient (K_a). One disadvantage of this concept is that it does not take
68 into consideration the light/dark cycle pattern. Recently, the effect of the frequency of light
69 intermittency on the photosynthetic response of microalgae under varying light has been
70 evaluated (Fernández-Sevilla et al., 2018).

71 The light path is basically divided into two zones: light and dark zone. Microalgae carry on
72 photosynthesis when exposed in the light zone while they operate respiration in the dark zone.
73 It is more realistic for industrial cultivation to study the microalgae growth during light/dark
74 cycling than in continuous illumination (Barceló-Villalobos et al., 2019a).

75 Two types of cycles could take place into photobioreactors: short and long. Short cycles mean
76 short residence time as well as fast mixing in the culture layer. On the other hand, long cycles
77 mean slower cycles, which implies a high dark volume. As much longer is the culture in light
78 zone, as higher photosynthesis takes place. Thus, dark volume should be minimized to reduce
79 respiration process and increase photosynthesis.

80 This article focuses the influence of DOC and temperature variations along three different thin-
81 layer cascades to analyse their limitation for biomass productivity. Moreover, light/dark cycling
82 of cells in culture layer has also been analysed in order to improve the knowledge of oxygen
83 production (PO_2 , mg/gb h) as it influences photosynthesis.

84

85 **2 MATERIAL AND METHODS**

86 **2.1 Microorganism and culture conditions**

87 The microalga *Chlorella spp.*, from the culture collection of the Laboratory of Algal Biotechnology
88 at the Institute of Microbiology (Třeboň, Czech Republic) was used. The cultures were grown
89 photoautotrophically in a mineral medium in a fed-batch regime for 15 days. The
90 photobioreactors were operated in parallel in batch mode, data at the same days from the three
91 different photobioreactors being used.

92

93 **2.2 Thin-layer cascades**

94 Three different thin-layer cascades with an area of 24, 90 and 224 m² respectively, all of them
95 at the same water depth of 6 mm, have been evaluated at the “Algatech” Experimental Station
96 (Třebon, Czech Republic) (Figure 1, Table 1). The module usually consists of two (or more) sloped

97 platforms (divided into longitudinal lanes) where the lower end of the upper platform is
 98 connected by a trough to the beginning of the lower platform that is declined in the opposite
 99 direction. The units are made of glass plates or stainless steel, supported by scaffolding. Each
 100 TLCs consists of several parts: retention tank with CO₂ supply and aeration, cultivation surface,
 101 pump, measurement and control sensors, and supporting construction.

102 The operation cycle starts in a retention tank from where the microalgae suspension is pumped
 103 via a return pipe (riser) to the upper part of the cultivation area (photostage) where it is
 104 distributed by a perforated tube, flows from the top to the bottom over sloping platforms and
 105 ends back in the retention tank (degasser). This cycle takes 90–120 s depending on the pumping
 106 speed. Pure CO₂ is supplied directly into the suspension in the riser. At night or during rainfall
 107 the culture is stored in the retention tank under air bubbling. The system is designed to minimize
 108 the dark volume of the microalgae suspension which can be as low as 10%.

109 Sensors (pH, DOC, temperature and water depth) are mounted in the degasser and in the
 110 connecting trough. The culture can be harvested via a three-way valve. The whole system is
 111 controlled by a data acquisition software.

112
 113

Table 1. Technical parameters of three thin-layer cascade units (TLCs)

	Small TLC	Medium TLC	Large TLC
Surface, m ²	24	90	225
Water depth, m	0.006	0.006	0.006
Light volume, L	144	540	1350
Dark volume, L	56	60	850
Total Volume, L	200	600	2200
Dark/Total Volume	0.28	0.10	0.39
Q Liq, L/s	3	10	12
Time light, s	48	54	113
Time dark, s	19	6	71

114

115 **2.3 In situ measurements in the cascades**

116 The gradients of the variables – DOC and temperature in the culture were measured at 18 points
 117 along the three TLCs (Small=24 m², Medium=90 m², Large=220 m²) (Figure 2). Measurements
 118 were performed using a portable oximeter (HI98198, Hanna, Czech Republic). Measurements
 119 were carried out at various times during the daylight period (9:00, 11:00, 13:00 and 15:00 h) to
 120 determine the variation in gradients. A total of 50 measurements were analysed for each
 121 variable (DOC and temperature).

122

123 **2.4 Oxygen mass balance analysis**

124 The oxygen mass balance was estimated to analyse the influence of the existing culture
125 conditions on the oxygen production rate of each TLC. Thus, the DOC was measured at various
126 positions along the loop at each TLC. The oxygen produced by cultures is desorbed to the
127 atmosphere as a function of the conditions in the unit. Therefore, for whatever section of the
128 TLC the following balance can be defined (*Equation 1*).

$$O_{2,inlet} + O_{2,produced} = O_{2,outlet} + O_{2,accumulation} \quad \text{Equation 1}$$

129 $O_{2\text{ inlet}}$ refers to the oxygen produced at the beginning of the loop, $O_{2\text{ produced}}$ refers to the oxygen
130 produced by the microalgae during the photosynthesis process, $O_{2\text{ outlet}}$ refers to oxygen
131 produced at the end of the loop and $O_{2\text{ accumulation}}$ refers to the oxygen accumulated along the
132 day.

133 At each time measurements were taken to obtain enough information to determine the overall
134 oxygen mass balance. From this balance the net oxygen production rate was calculated
135 (*Equation 2-Equation 4*) as a function of the oxygen desorbed to the atmosphere, NO_2 , it being
136 a function of mass transfer coefficient (k_{lal}) of 0.9 h^{-1} (Alameda-García, L. et al., under review).

$$PO_{2,produced} = PO_{2,net} + NO_2 \quad \text{Equation 2}$$

$$PO_{2,net} = \frac{(O_{2,end} - O_{2,initial})}{Section} \times Q_{liq} \quad \text{Equation 3}$$

$$NO_2 = F_{iml} \times K_{lal} \quad \text{Equation 4}$$

137

138 **2.5 Statistical analysis**

139 The oxygen production rate ($\text{mg } O_2/\text{gb h}$) was modelled and correlated by descriptive statistics
140 (correlation, R^2) in total of 15 days of assays. A total of 50 measurements were analysed for each
141 variable (DOC and temperature). The Statistica v.7 program was used to perform the statistical
142 analysis.

143

144 **3 RESULT AND DISCUSSION**

145 **3.1 Overall performance of TLCs**

146 The mean values of daily culture variables are showed in Table 2. It shows that the irradiance on
147 the TLCs surface (light intensity, I_0) is similar at the three thin-layer cascade units. It varies over
148 time ranging from 872 to 1580 $\mu\text{mol photons}/\text{m}^2\cdot\text{s}$; the maximal value being obtained at 11:00

149 h, as the TLCs are located in central Europe. Based on these values, the average irradiance to
150 which the cells were exposed in the TLC varied from 761 to 1400 $\mu\text{mol photons/m}^2\cdot\text{s}$ within the
151 period of trial (for 15 days).

152 The DOC and temperature were measured through the day and along the TLC at three different
153 TLCs (Figure 2). The culture temperature increases due to the absorption of infrared solar
154 radiation; the larger is the area exposed to the sunlight, the greater is the increase in
155 temperature (Barceló-Villalobos et al., 2019).

156 Regarding DOC, it increases significantly along the TLC throughout the day at the small and
157 medium TLCs with peaks up to 400% Sat at 11:00 h. The DOC figures were ranging from 120 to
158 400% Sat (Figure 2). It means that at some daytimes the channels' desorption capacity was not
159 sufficient to remove oxygen and keep DOC which is considered physiologically acceptable. The
160 existence of excessive DOC in TLCs has already been reported, with values up to 23 mg/L being
161 measured (Lívanský and Doucha, 1996). It was shown that photosynthesis can be downregulated
162 when DOC accumulation is over 250% Sat. (Fernández et al., 2012; Mendoza et al., 2013b;
163 Pawlowski et al., 2014). Thus, DOC influence on the culture performance should be taken into
164 consideration to optimize the oxygen production model.

165 Thus, the improvement of mass transfer capacity is a way how to reduce DO accumulation in
166 open TLCs (Barceló-Villalobos et al., 2018). Mass transfer coefficient has to be increased in order
167 to maintain high photosynthetic rate. Nevertheless, the measurements at the large TLC were
168 quite stable, with physiologically acceptable DO accumulation up to 200% Sat. Thus, it indicated
169 that mass transfer capacity in this unit is sufficient and promote efficient degassing.

170 Regarding temperature, the results showed that there were not as great changes during the day
171 (Figure 3). It ranges between 24 and 29 °C which is suitable temperature for *Chlorella* R-117
172 (Masojídek et al., 2011). Thus, in this case, temperature is not a variable that influence on the
173 culture performance. Here it is important to note that the trials were carried out at very similar
174 culture temperatures. These trials were carried out in August when ambient temperature
175 maxima at midday were around 30 °C. The culture is exposed to solar radiation only for one third
176 of the circulation cycle. Thus, it is cooled in the reservoir which is close to the ground and mostly
177 by self-cooling due to evaporation in thin culture layer (Table 1).

178 Regarding average irradiance (I_{av}), there are significant differences between the three
179 TLCs. Small TLC ranged from 761 to 1400 $\mu\text{mol photons/m}^2\text{ s}$, in the medium TLC it ranged from
180 825 to 1140 $\mu\text{mol photons/m}^2\text{ s}$ and the large TLC ranged from 732 to 1093 $\mu\text{mol photons/m}^2\text{ s}$.
181 Such differences were caused by the time and volume of the culture spent in dark volume of
182 reservoir, pump and tubing (Figure 1, Table 1). Biomass concentrations (g/L) of the cultures were

183 determined once per day in the morning and the mean values were about 28, 37 and 40 g/L in
184 the small, medium and large TLCs, respectively (Table 3). Regarding photosynthetic oxygen
185 production, Table 3 shows that the small and medium TLCs had higher values, as compared to
186 the large TLC. If it is taken into consideration the technical parameters shown in Table 1 Table
187 1, it seems that the photosynthetic production may be inversely related to the dark volume of
188 the culture. As much higher is the volume in darkness, as lower is the productivity as it is shown
189 for the large TLCs (Table 1 vs. Table 3). On the other hand, the high volume exposed to light may
190 indicate the higher photosynthetic productivity, as it is shown for the small and medium TLCs
191 (Table 3). Here, it is interesting to correlate the photosynthetic productivity with the values of
192 DOC in individual TLCs. Although the small TLC showed highest DOC, it had a high photosynthetic
193 activity. For example, mean DOC was found 307 %Sat while mean photosynthesis rate was 291
194 g O₂/m²d, which is very similar to the mean photosynthetic oxygen production found at the
195 medium unit (301 g O₂/m²d, 268%Sat.). Both, small and medium units obtained a PO₂ higher
196 than in the large TLCs where DOC was significantly lower (compare Figure 2, Table 2 and Table
197 3). The results reveal that DOC is not as crucial for photosynthetic productivity as higher figures
198 can be achieved even at DOC much higher than 250 %Sat if the flow of the culture is fast which
199 causes efficient degassing and fast light/dark cell cycling (intermittent light) (Masojidek et al.,
200 2015). Thus, the design and set-up of the TLC seems to be important to overcome short build-
201 up of DOC which may not suppress high culture productivity.

202 **3.2 Oxygen mass balance analysis**

203 To ensure DOC of the optimal values, it is important to improve the TLC design as well as the
204 operational conditions, especially the mass transfer capacity (Barceló-Villalobos et al., 2018). It
205 was concluded that the handling of mass transfer capacity of raceway ponds to maintain the
206 DOC below inhibitory values is a challenge (Barceló-Villalobos et al., 2018). The same is valid for
207 TLCs. Higher mass transfer coefficient (klal) was found in TLC channel compared to raceway
208 ponds loop (Alameda-García et al. unpublished results, in review). This value (9 h⁻¹), was used to
209 analyse the mass transfer capacity in the three TLCs located at Centre Algatech. Calculated
210 values showed that the mass transfer capacity of each TLC was below 4% of total oxygen
211 production (PO₂ produced, mg/gb h) (Figure 4). Thus, it is possible to assume that the net oxygen
212 production is equal to the generated oxygen production (Equation 5).

$$PO_{2,produced} = PO_{2,net} \quad \text{Equation 5}$$

213

214 **3.3 Modelling oxygen production**

215 The influence of culture conditions to the performance of *Chlorella* was modelled as
216 photosynthesis rate (PO_2 , mg/gb h) according to the experimental DO measurements. Oxygen
217 production (PO_2) was modelled according to DOC and temperature variables. DOC effect was
218 included into the model described by Costache et al. (2013). As a result, there is a high reduction
219 of the oxygen production (PO_2 , mg/gb h) (Figure 5). On the other hand, the temperature cardinal
220 model was used to analyse the temperature effect on oxygen production (Ippoliti et al., 2016).
221 It has been demonstrated that temperature values are not harmful, in this case, the values are
222 close to the optimal values (Figure 5). In contrast, if we include the effect of temperature and
223 optimal DOC variables into the oxygen production model (Modelled PO_2 , Iav, T, Optimal DO_2
224 model), it is not enough to validate the experimental values of oxygen production (Figure 6).
225 A previous work (Barceló-Villalobos et al., 2019a) demonstrated that the light penetration into
226 the culture depends on the location of the microalgae cell in the culture depth. Thus, light/dark
227 time and volume should be taken into consideration to better understand and model the
228 photosynthesis rate (mg O_2 /gb h) according to the design of the reactor.
229 The different sections of the TLCs have different light/dark behaviour. For instance, bubble
230 column and sink/sump/reservoir sections should be considered as dark volumes. On the other
231 hand, loop section should be considered as light volume. Moreover, culture depth and flow
232 speed also influence into the light/dark cycling. Thus, the culture spends some time in light or
233 dark zone. It depends on the residence time at each section of the reactor. In case of large dark
234 time, the culture might be in respiration process due to the dark photosynthesis phase.

235 As mentioned above three TLCs of different size were analysed in this work (Figure 1, Table 1).
236 A small TLC with a total volume of 200 L (dark volume of 56 L and light volume of 144 L), the
237 medium TLC with a total volume of 600 L (dark volume of 60 L and light volume of 540 L) and
238 the large TLC with a total volume of 2200 L (dark volume of 850 L and light volume of 1350 L).

239 The cultures were exposed to solar radiation along the photostage for 48, 54 and 113 sec in the
240 small, medium and large TLCs, respectively (Table 1). Photosynthetic productivity might be
241 increased by improving the light/dark cycles in TLCs as demonstrated in the previous
242 experiments (Barceló-Villalobos et al., 2019a; Fernández-Sevilla et al., 2018). On the other hand,
243 if the culture spent some time in the dark sections – 19, 6 and 71 sec at the small, medium and
244 large TLCs, respectively, (Table 1). As longer is this time, as lower is the productivity of the system
245 – 291, 301 and 263 g O_2 /m² d at the small, medium and large TLCs respectively (Table 3).
246 Furthermore, there exists a significant influence of biomass concentration on the productivity

247 of the system that should be considered to analyse how the biomass concentrations affects to
 248 the light path penetrance as well as to the light/dark volume.

249 In this work, we propose to include irradiance as a variable called an average integrated
 250 irradiance (*IavInt*), where the light/dark time is included (Equation 6). That is because the light
 251 time and dark time affect the process of photosynthesis and respiration respectively. Moreover,
 252 light frequency was incorporated into the model with optimal conditions of DOC by the inclusion
 253 of the average irradiance integration concept (*IavInt*) (Modeled PO₂ (*IavInt*, T, Optimal DO₂
 254 Model),Equation 7).

255 Results demonstrated that experimental data fit the PO₂ *IavInt* model in a 81% of the cases
 256 ($R^2=0.8115$) (Figure 7); that is better compared to PO₂ *Iav* model ($R^2=0.7947$) which take into
 257 consideration average irradiance (*Iav*) concept. Both results are good if we consider that the
 258 three TLCs are operated outdoors and exposed to environmental conditions.

259 As a result (Figure 6, Figure 7), the modelled data reach much better results compare to *Iav*
 260 concept. It is shown that light/dark frequency is optimal for the medium thin-layer cascade
 261 reactor (540 L light volume and 60L dark volume).

262 This work demonstrates that it should be taken into consideration the influence of the light/dark
 263 time and volume ratio regarding to the design and operation conditions of the reactor to achieve
 264 as maximum production of the system as possible.

265

$$PO_{2,(IavInt)} = \frac{PO_{2max} \times IavInt^n}{I_k^n + IavInt^n} \quad \text{Equation 6}$$

where, *IavInt*

$$= \frac{Iav \times t \text{ light}}{t \text{ light} + t \text{ dark}}$$

$$PO_{2,(IavInt,Optimal DO_2)} = \frac{PO_{2max} \times IavInt^n}{I_k^n + IavInt^n} \times \left(1 - \left(\frac{DO_2}{DO_{2,max}}\right)^m\right) \quad \text{Equation 7}$$

266 4 CONCLUSIONS

267 DOC and temperature variables were analysed in photostage of the three TLCs during the
 268 daylight cycle. The results confirm that there were not temperature gradients along the TLCs.
 269 On the other hand, DOC increased along the cultivation area; reaching values up to 400%Sat.

270 Furthermore, the mass transfer capacity of the system was also determined, being lower than
271 4% at all reactors.

272 The inclusion of optimal DOC into the average irradiance model (PO₂ lav model) is not enough
273 to explain the experimental data obtained (Experimental PO₂). Thus, the influence of light/dark
274 cycling into the performance of thin-layer cascade reactors was analysed and modelled. It is a
275 powerful tool for the knowledge and improvement of TLC design and operation.

276

277 **Conflict of interest statement**

278 The authors declare that there are no potential financial or other interests that could be
279 perceived to influence the outcomes of the research.

280

281 **Acknowledgements**

282 This study was supported by the Ministry of Economy and Competitiveness (DPI2014-55932-C2-
283 1-R, DPI2017-84259-C2-1-R) and (PURASOL, CTQ2017-84006-C3), along with the European
284 Union's Horizon 2020 Research and Innovation Program under Grant Agreement No. 727874
285 SABANA. The research activity of Centre Algatech was funded by National Sustainability
286 Programme of the Ministry of Education, Youth and Sports (project Algatech Plus LO1416).

287

288 **References**

- 289 Alameda-García, L.; De-Arriba, A.; Barceló-Villalobos, M.; Gómez Serrano, C.; Ación Fernández,
290 F.G., n.d. Photosynthetic performance of *Scenedesmus almeriensis* in thin-layer reactors.
- 291 Barceló-villalobos, M; Gómez Serrano, C; Sánchez Zurano, A; Alameda García, L; Esteve
292 Maldonado, S; Peña, J; Ación Fernández, F.G., 2019. Variations of culture parameters in a
293 pilot-scale thin-layer reactor and their influence on the performance of *Scenedesmus*
294 *almeriensis* culture. *Bioresour. Technol. Reports* 6, 190–197.
295 <https://doi.org/10.1016/j.biteb.2019.03.007>
- 296 Barceló-Villalobos, M., Guzmán Sánchez, J.L., Martín Cara, I., Sánchez Molina, J.A., Ación
297 Fernández, F.G., 2018. Analysis of mass transfer capacity in raceway reactors. *Algal Res.*
298 35, 91–97. <https://doi.org/10.1016/j.algal.2018.08.017>
- 299 Barceló-Villalobos, M., Olmo, P.F., Guzmán, J.L., Fernández-Sevilla, J.M., Fernández, F.G.A.,
300 2019. Evaluation of photosynthetic light integration by microalgae in a pilot-scale raceway
301 reactor. *Bioresour. Technol.* <https://doi.org/10.1016/j.biortech.2019.02.032>
- 302 Camacho-Rubio, F., Ación, F.G., Sánchez-Pérez, J.A., García-Camacho, F., Molina-Grima, E., 1999.
303 Prediction of dissolved oxygen and carbon dioxide concentration profiles in tubular
304 photobioreactors for microalgal culture. *Biotechnol. Bioeng.* 62, 71–86.

305 [https://doi.org/10.1002/\(SICI\)1097-0290\(19990105\)62:1<71::AID-BIT9>3.0.CO;2-T](https://doi.org/10.1002/(SICI)1097-0290(19990105)62:1<71::AID-BIT9>3.0.CO;2-T)

306 Chisti, Y., 2012. Microalgal biotechnology: Potential and production, in: Raceways-Based
307 Production of Algal Crude Oil. C. Posten & C. Walter, de Gruyter, Berlin, pp. 113–146.

308 Chisti, Y., 2007. Biodiesel from microalgae. *Biotechnol. Adv.* 25(3), 294–306.

309 Costache, T.A.A., Fernández, F.G.A., Acien, F.G., Morales, M.M., Fernández-Sevilla, J.M.,
310 Stamatini, I., Molina, E., 2013. Comprehensive model of microalgae photosynthesis rate as
311 a function of culture conditions in photobioreactors. *Appl. Microbiol. Biotechnol.* 97, 7627–
312 7637. <https://doi.org/10.1007/s00253-013-5035-2>

313 Fernández-Sevilla, J.M., Brindley, C., Jiménez-Ruiz, N., Acien, F.G., 2018. A simple equation to
314 quantify the effect of frequency of light/dark cycles on the photosynthetic response of
315 microalgae under intermittent light. *Algal Res.* 35, 479–487.
316 <https://doi.org/10.1016/j.algal.2018.09.026>

317 Fernández, I., Acien, F.G., Berenguel, M., Guzmán, J.L., Andrade, G.A., Pagano, D.J., 2014. A
318 lumped parameter chemical-physical model for tubular photobioreactors. *Chem. Eng. Sci.*
319 112, 116–129. <https://doi.org/10.1016/j.ces.2014.03.020>

320 Fernández, I., Acien, F.G., Fernández, J.M., Guzmán, J.L., Magán, J.J., Berenguel, M., 2012.
321 Dynamic model of microalgal production in tubular photobioreactors. *Bioresour. Technol.*
322 126, 172–181. <https://doi.org/10.1016/j.biortech.2012.08.087>

323 Grivalský T, Ranglová K, Câmara Manoel JA, Lakatos GE, Lhotský R, Masojídek J (2019)
324 Development of thin-layer cascades for microalgae cultivation: milestones (review) *Folia*
325 *Microbiologica* 64, 603–614

326 Ippoliti, D., Gómez, C., del Mar Morales-Amaral, M., Pistocchi, R., Fernández-Sevilla, J.M., Acien,
327 F.G., 2016. Modeling of photosynthesis and respiration rate for *Isochrysis galbana* (T-Iso)
328 and its influence on the production of this strain. *Bioresour. Technol.* 203, 71–79.
329 <https://doi.org/10.1016/j.biortech.2015.12.050>

330 Lívanský, K., Doucha, J., 1996. CO₂ and O₂ gas exchange in outdoor thin-layer high density
331 microalgal cultures. *J. Appl. Phycol* 8, 353–358.

332 Masojídek J., Sergejevová M., Malapascua J.R., K.J., 2015. Thin-Layer Systems for Mass
333 Cultivation of Microalgae: Flat Panels and Sloping Cascades, in: Prokop A., Bajpai R., Z.M.
334 (eds) (Ed.), *Algal Biorefineries*. Cham, pp. 237–261.

335 Masojídek, J., Kopecký, J., Giannelli, L., Torzillo, G., 2011. Productivity correlated to
336 photobiochemical performance of *Chlorella* mass cultures grown outdoors in thin-layer
337 cascades. *J. Ind. Microbiol. Biotechnol.* 38, 307–317. [https://doi.org/10.1007/s10295-010-](https://doi.org/10.1007/s10295-010-0774-x)
338 [0774-x](https://doi.org/10.1007/s10295-010-0774-x)

339 Mendoza, J.L., Granados, M.R., de Godos, I., Acien, F.G., Molina, E., Banks, C., Heaven, S., 2013a.

340 Fluid-dynamic characterization of real-scale raceway reactors for microalgae production.
341 Biomass and Bioenergy 54, 267–275. <https://doi.org/10.1016/j.biombioe.2013.03.017>
342 Mendoza, J.L., Granados, M.R., de Godos, I., Ación, F.G., Molina, E., Heaven, S., Banks, C.J.,
343 2013b. Oxygen transfer and evolution in microalgal culture in open raceways. Bioresour.
344 Technol. 137, 188–195. <https://doi.org/10.1016/j.biortech.2013.03.127>
345 Molina Grima, E., García Camacho, F., Sánchez Pérez, J.A., Fernández Sevilla, J., Ación
346 Fernández, F., Contreras Gómez, A., 1994. A mathematical model of microalgal growth in
347 light-limited chemostat culture. J. Chem. Technol. Biotechnol.
348 <https://doi.org/10.1002/jctb.280610212>
349 Pawlowski, A., Fernández, I., Guzmán, J.L.L., Berenguel, M., Ación, F.G.G., Normey-Rico, J.E.E.,
350 2014. Event-based predictive control of pH in tubular photobioreactors. Comput. Chem.
351 Eng. 65, 28–39. <https://doi.org/10.1016/j.compchemeng.2014.03.001>
352 Šetlík, I., Šust, V., Málek, I., 1970. Dual purpose open circulation units for large scale culture of
353 algae in temperate zones. I. Basic design considerations and scheme of a pilot plant. Algal
354 Stud 1:111–164
355 Richmond A (2013) Biological principles of mass cultivation of photoautotrophic microalgae. In:
356 Richmond A, Hu Q (eds) Handbook of microalgal culture: applied phycology and
357 biotechnology. Blackwell Science, p 171-204
358
359
360
361
362
363
364

365

366

367

Figure captions



368

Figure 1. Areal view of the thin layer cascades (small A= 200 L/24 m²; medium B = 600 L/90 m²; large C – three units, each 2200 L/224 m²) located at Centre Algatech in Třeboň (Czech Republic) (detailed description in Masojídek et al. 2011, 2015, Grivalský et al. 2019)

369

370
371
372
373
374
375
376
377
378
379
380
381
382
383
384
385
386
387
388
389
390
391
392
393
394
395
396
397
398
399

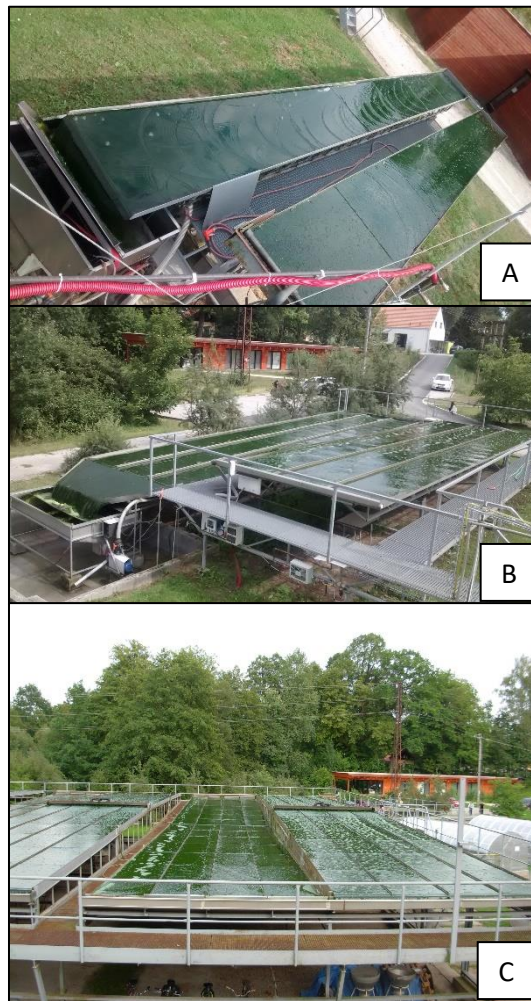


Figure 2. View of the thin layer reactors (A=200 L, B=600 L, C=2200 L) located at the "Algatech" Experimental Station in Trebon (Czech Republic). Pictures from August 2018.

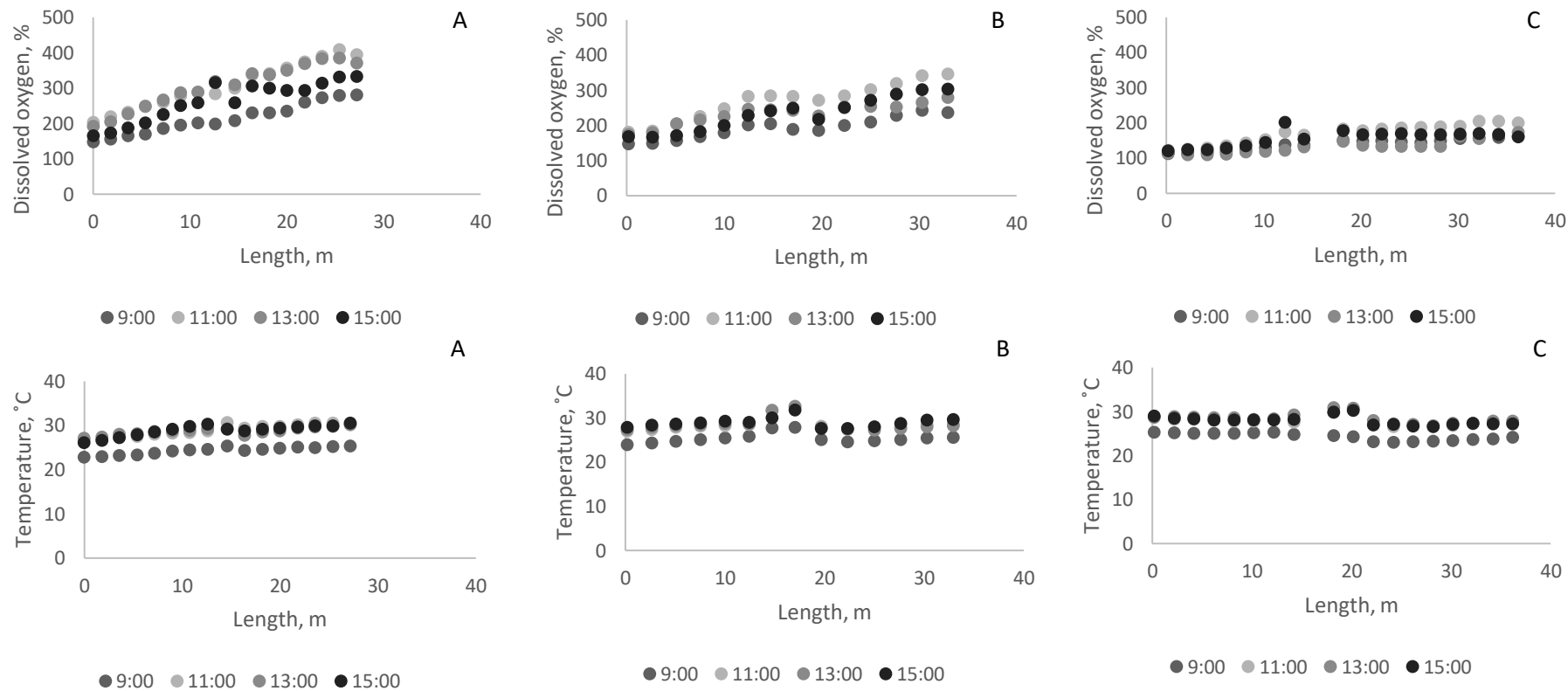


Figure 3. Variation of culture parameters (Dissolved oxygen and temperature) with the position and time of the day (9:00, 11:00, 13:00 and 15:00 h) in three thin-layer reactors (A=200 L, B=600 L and C=2200 L) operated in batch mode and located in Třeboň (Czech Republic).

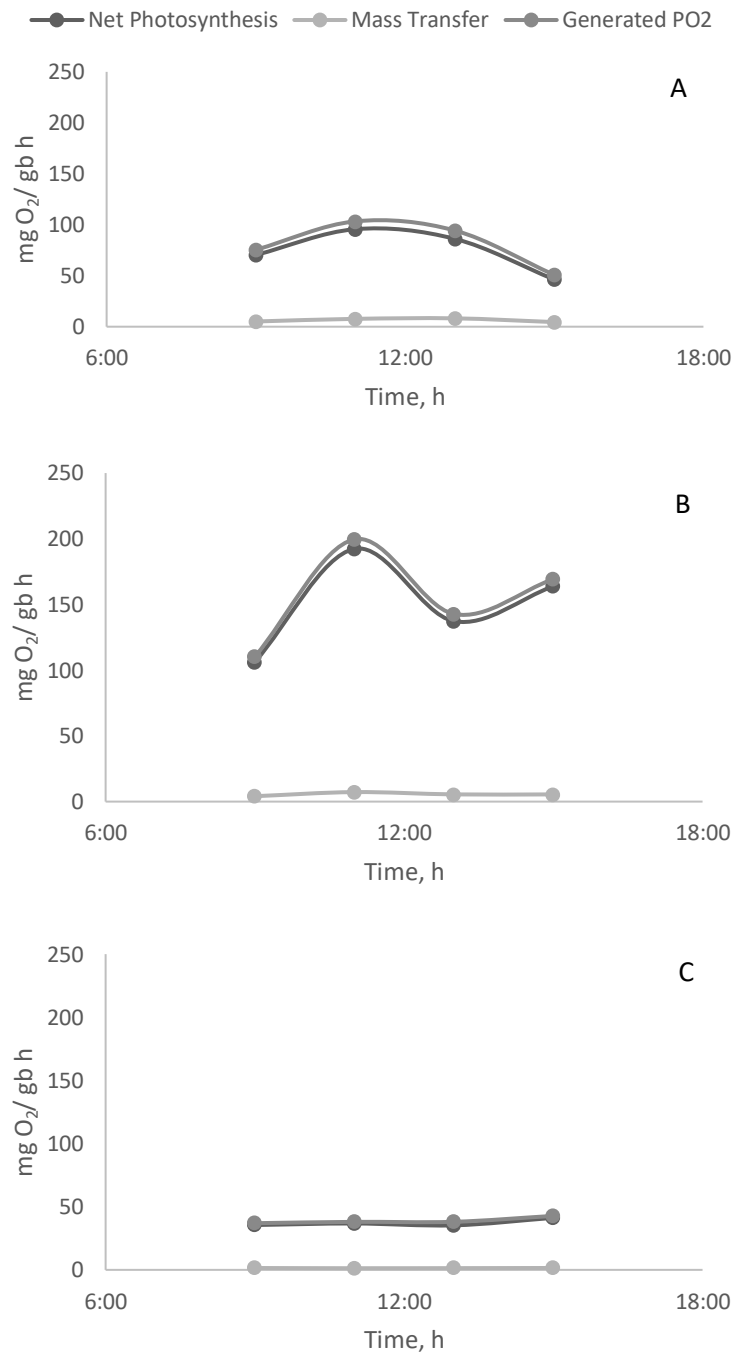


Figure 4. Oxygen mass balance analysis at three thin-layer cascade reactors (A=Small, B=Medium, C=Large).

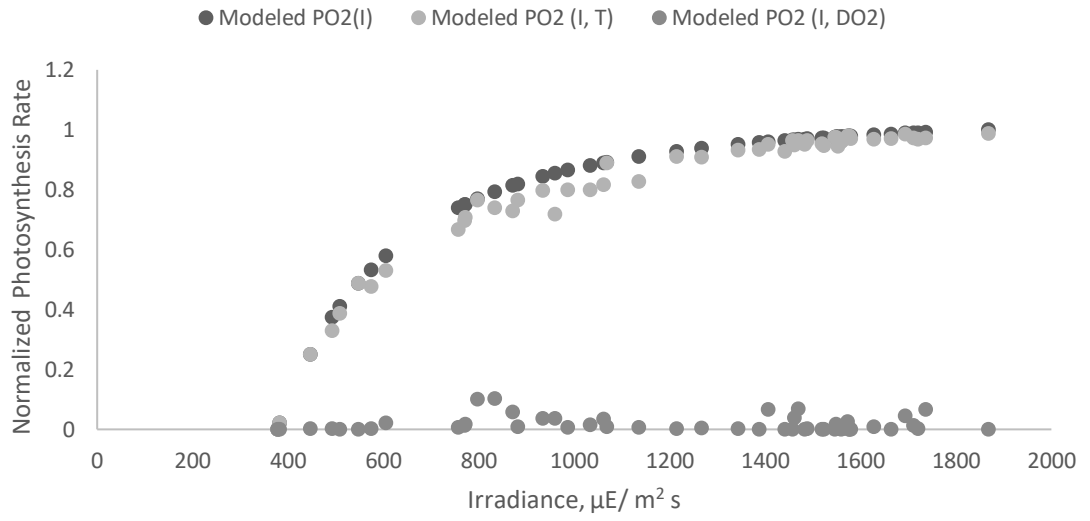


Figure 5. Comparison of oxygen production model (PO2 (I)) by including temperature or dissolved oxygen concentration (DOC) effect.

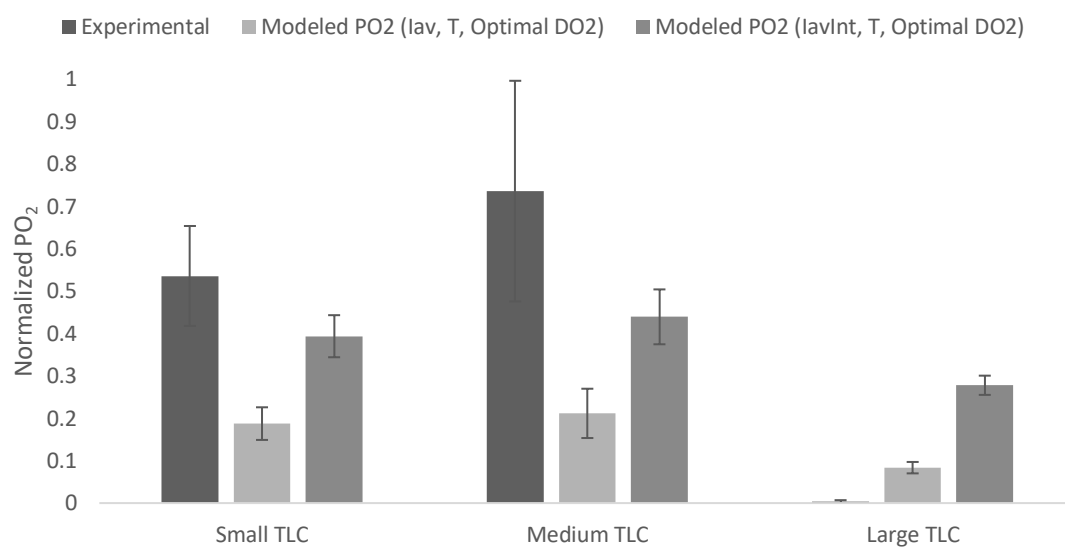


Figure 6. Comparison of experimental data respect to: modeled PO₂ (lav, T, Optimal DO₂) and modeled PO₂ (lavInt, T, Optimal DO₂) at three different thin-layer cascade reactors (Small, Medium and Large).

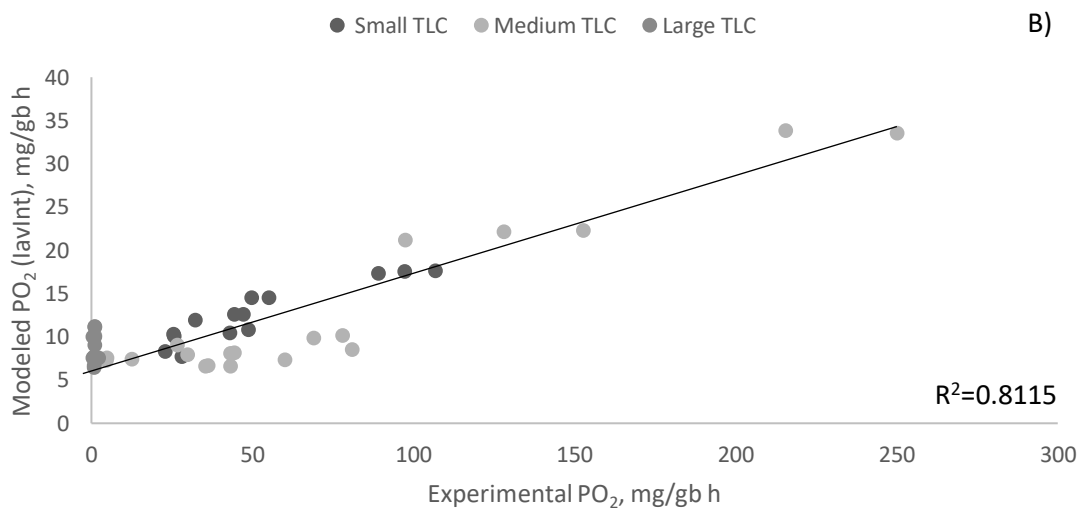
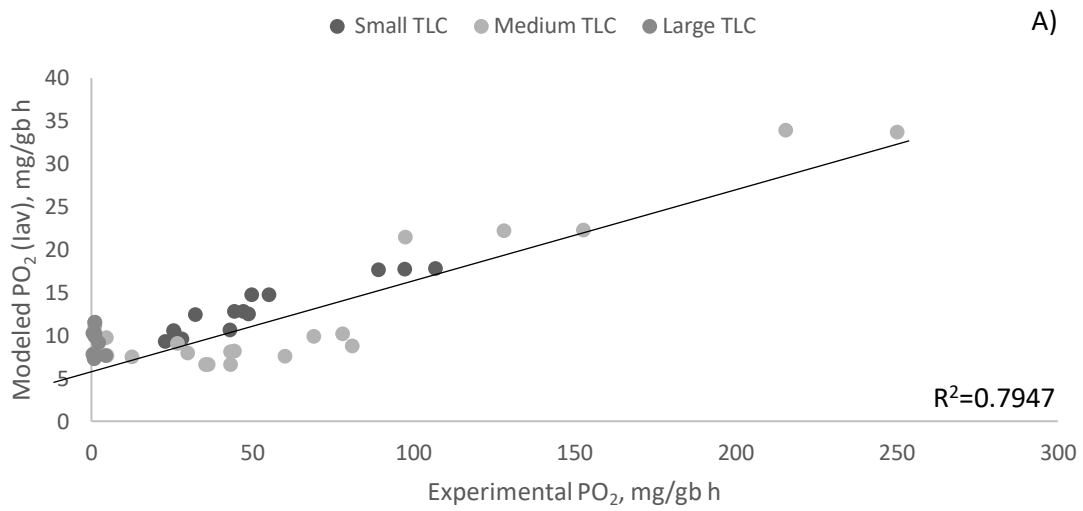


Figure 7. Validation of experimental data by using two models: (A) Modeled PO₂ (lav) and (B) Modeled PO₂ (lavInt) at three thin-layer cascade reactors.

Table captions

Table 2. Mean \pm SE values of hourly variation in light intensity, average irradiance, integrated average irradiance, temperature and DOC.

Small TLC					
Time	Light Intensity I_0 $\mu\text{mol photons/m}^2 \text{ s}$	Average Irradiance $\mu\text{mol photons/m}^2 \text{ s}$	I_{av} Integrated $\mu\text{mol photons/m}^2 \text{ s}$	Temperature $^{\circ}\text{C}$	Dissolved Oxygen Sat. %
9	872 \pm 194.1	761 \pm 163	498 \pm 106.7	24 \pm 0.4	214 \pm 4.3
11	1580 \pm 30	1400 \pm 40	917 \pm 26.1	29 \pm 1.4	307 \pm 24.3
13	1329 \pm 389	1185 \pm 360	776 \pm 235.3	29 \pm 2.5	305 \pm 43.5
15	1179 \pm 270	1047 \pm 243.2	685 \pm 159.2	29 \pm 2.0	263 \pm 33
Medium TLC					
Time	Light Intensity I_0 $\mu\text{mol photons/m}^2 \text{ s}$	Average Irradiance $\mu\text{mol photons/m}^2 \text{ s}$	I_{av} Integrated $\mu\text{mol photons/m}^2 \text{ s}$	Temperature $^{\circ}\text{C}$	Dissolved Oxygen Sat. %
9	1011 \pm 43.8	867 \pm 20.3	780 \pm 18.3	26 \pm 1.1	188 \pm 10.8
11	1317 \pm 163.4	1140 \pm 150	1026 \pm 134.6	29 \pm 1.1	268 \pm 8.4
13	1398 \pm 213	1124 \pm 251.1	898 \pm 209.8	29 \pm 1.6	239 \pm 21.7
15	1072 \pm 182.2	825 \pm 168.7	815 \pm 138	28 \pm 1.4	167 \pm 13.3
Large TLC					
Time	Light Intensity I_0 $\mu\text{mol photons/m}^2$	Average Irradiance $\mu\text{mol photons/m}^2 \text{ s}$	I_{av} Integrated $\mu\text{mol photons/m}^2 \text{ s}$	Temperature $^{\circ}\text{C}$	Dissolved Oxygen Sat. %
9	900 \pm 29	732 \pm 40.1	462 \pm 22.0	24 \pm 0.7	140 \pm 10.7
11	1302 \pm 263.3	1093 \pm 199.5	670 \pm 122.4	28 \pm 0.5	180 \pm 11.2
13	1169 \pm 324	975 \pm 269	598 \pm 165.3	28 \pm 0.4	155 \pm 23.0
15	1216 \pm 266	1026 \pm 259	630 \pm 159.1	28 \pm 1.5	155 \pm 13.06

1
2
3
4
5
6
7
8
9
10
11
12
13
14
15
16
17
18
19
20
21
22

Table 3. Mean values of biomass concentration (g/L) and photosynthesis rate (PO₂) at three thin-layer cascade (TLC) units.

TLC unit	Biomass concentration g/L	PO ₂ gO ₂ /L h	PO ₂ mg O ₂ /gb h	PO ₂ g/m ² d
Small	28.2	1.3	51.0	290.6
Medium	36.7	1.9	78.2	300.9
Large	40.1	1.1	1.4	263.5

1 **A feedback control strategy for the air injection flow at raceway reactors**

2 M. Barceló-Villalobos¹, A. Hoyo¹, E. Miranda¹, J.L. Guzmán ¹, F.G. Acién Fernández²

3 ¹ Department of Informatics, University of Almería, ceiA3, CIESOL, E04120 Almería, Spain

4 ² Department of Chemical Engineering, University of Almería, Almería, Spain

7 **Abstract**

8 Microalgae industry is growing worldwide despite production technology has not been greatly
9 improved in the last years. Raceway reactors are still the most extended technology for
10 microalgae production. However, these reactors have some drawbacks, one of them being it
11 low mass transfer capacity, it is determining the existence of dissolved oxygen accumulation
12 that reduces the performance of these systems (Barceló-Villalobos et al., 2018; Mendoza et al.,
13 2013). To overpass this problem, it is imperative to improve the photobioreactor design as well
14 as the operational conditions, especially the mass transfer capacity. Thus, it is possible to
15 maintain the dissolved oxygen below the defined set point by using advanced control strategies.
16 In this work, it is demonstrated as the mass transfer capacity of raceway reactors can be
17 improved to avoid that dissolved oxygen accumulation overpass the inhibitory value, by using
18 adequate control systems capable to manipulate the time and flow at which the air is supplied.
19 Air supply required is calculated as a function of dissolved oxygen concentration into the culture
20 but also of the oxygen production rate in the entire reactor as a function of dissolved oxygen
21 concentration along the channel. The effect of the control strategy proposed on the air flow
22 required is analysed.

24 Keywords: Microalgae, raceway, oxygen accumulation, control strategy

34 1. INTRODUCTION

35 Microalgae industry is growing worldwide despite this technology still having some drawbacks
36 that need to be solved to make it economically profitable. In general, there are two types of
37 reactors: open and close. The close ones have been widely studied due to its high productivity,
38 but on the other hand, they have a high cost construction and production.

39

40 Regarding open reactors, two types are widely been used: raceway and thin-layer reactors. The
41 first ones are characterized by a paddlewheel to maintain the culture in constantly movement
42 and usually works at a water depth of 15 cm. On the other hand, the second ones include a
43 column and usually works at a culture depth ranged from 0.006m-0.04 m (Acién et al., 2017).

44

45 Previous works demonstrated that one of the problems that microalgae cultivation must deal
46 with, is the accumulation of dissolved oxygen into the culture (Mendoza et al., 2013; Pawlowski
47 et al., 2015). That it is because it could affect to photosynthesis efficiency. Previous works
48 demonstrated that photosynthesis rate decay when the dissolved oxygen concentration is over
49 250 %Sat., which is taking place during most of central hours of the day when the higher solar
50 radiation is available. It has been demonstrated that the biomass productivity increases up to
51 double when there is an adequate oxygen removal to maintain the dissolved oxygen
52 concentration below 200 %Sat. compare to the productivity obtained when there is no oxygen
53 removal (de Godos et al., 2014). To overpass this problem, it is imperative to improve the
54 photobioreactor design as well as the operational conditions. In this sense, previous works
55 demonstrated that it is possible to control dissolved oxygen accumulation by improving the mass
56 transfer capacity (Barceló-Villalobos et al., 2018). The mass transfer capacity of a reactor can be
57 optimized by installing sumps and make air/CO₂ injections through it. Usually, air injections are
58 supplied at a constant rate, which allows to minimize the dissolved oxygen accumulation
59 problem. However, the air flow is manually operated. To solve this problem, control strategies
60 could be a solution to automatize air gas injections properly for 24 hours / 365 days a year.

61

62 Advanced control strategies have been worldwide used to obtain models that reflects properly
63 the dynamics of the system. There are many models, from those based on steady-state
64 relationships (Rotatore et al., 1995) or lineal approximations (Berenguel et al., 2004; García
65 Sánchez et al., 2003) to those based non-lineal empirical features or first principles models. The
66 control system designs must take into consideration the dynamics of the system. Different
67 control strategies have been used in microalgae industrial development. For instance, an event-

68 based control has been used to control a raceway reactor (Pawlowski et al., 2016). This type of
69 control is especially useful in bioprocess, as has been confirmed in previous works (Beschi et al.,
70 2014). This type of control allows to adapt the system to the dynamic process of the system.
71 This is one of the most important difference compared to the classical feedback control.
72 Previous works demonstrated that the use of event-based control could improve the biomass
73 production as well as reduce the effort in controlling the effective use of CO₂ (Pawlowski et al.,
74 2016).

75

76 In the present work, a combination of control strategy and the empirical model developed in
77 Barceló-Villalobos et al., 2018 is proposed. Thus, dissolved oxygen accumulation issue could be
78 solved automatically according to the culture conditions. The effect of the control strategy
79 proposed in the present work on the air flow required is analysed, in addition to its effect on the
80 dissolved oxygen accumulation of the reactor.

81

82 **2. MATERIAL AND METHODS**

83 **2.1 Photobioreactor description**

84 The raceway reactor used in this thesis is located at "IFAPA" Research Centre (Almería,
85 Spain) (Figure 1). The reactor consists of two 40 m long channels (0.46 m high × 1 m wide), both
86 connected by 180° bends at each end, with a 0.59 m³ sump (0.65 m long × 0.90 m wide × 1 m
87 deep) located 1 m along one of the channels. A paddlewheel system was used to recirculate the
88 culture through the reactor at a regular velocity of 0.2 m·s⁻¹, although this could be increased up
89 to 0.8 m·s⁻¹ by manipulating the frequency inverter of the engine. The pH, temperature and
90 dissolved oxygen in the culture were measured using appropriate probes (5083 T and 5120,
91 Crison Instruments, Barcelona, Spain), connected to an MM44 control-transmitter unit (Crison
92 Instruments, Spain), and data acquisition software (Labview, National Instruments, USA)
93 providing complete monitoring and control of the system. A proportional air valve (CAMOZZI,
94 Brescia, Italy) was used in order to adequately minimize and control the air injections. The
95 culture pH was maintained at 8.0 by on-demand CO₂ injections whereas temperature was not
96 controlled.

97 The raceway reactor was inoculated and operated in batch mode for one week, after
98 which it was operated in continuous mode a culture depth of 0.14 m at a dilution rate of 0.2 d⁻¹.
99 Only samples from stable conditions were used. Evaporation inside the reactor was
100 compensated for by the daily addition of fresh medium.

101
102
103
104
105
106
107
108
109
110



Figure 1. General view of the open raceway reactor at IFAPA Experimental Station

112

113 2.2 Experimental mass transfer model

114 It has been reported that it is possible to improve mass transfer capacity in raceway reactors by
115 using an empirical mathematical model. The mass transfer model (Equation 4, Equation 5,
116 Equation 6) has been developed by using a large set of experimental data all over a year (Barceló-
117 Villalobos et al., 2018). It uses the gas flow inputs to improve the mass transfer coefficient (klal,
118 s⁻¹). Moreover, Fernández et al., (2016) model has been improved by including mass transfer
119 capacity as follow:

120

$$PO_{2,max} = K_{lal} \times [(O_2) - (O_2^*)] \quad \text{Equation 1}$$

$$K_{lal} = 10379 \times U_{gr}^{0.9123} \quad \text{Equation 2}$$

$$U_{gr} = \frac{G_{flow}}{A} \quad \text{Equation 3}$$

121

122 where PO₂ max is the maximal oxygen production rate (g m⁻² h⁻¹) online calculated from
123 the dissolved oxygen concentration measurements, and O₂* is the oxygen in equilibrium with
124 the atmosphere (9 mg L⁻¹). From these equations, it is possible to know which is the on-line gas
125 inflow necessary to ensure optimal mass transfer coefficient (Klal); so then, to maintain the
126 dissolved oxygen concentration below the limit value.

127 Fernández et al., (2016) modified model has been used in simulation to demonstrate the
128 adequacy of dissolved oxygen accumulation over the set-point imposed, as well as to control
129 the mass transfer coefficient according to the requirements of the system. It is greatly
130 advantageous for optimal control of the system, to measure this coefficient (Klal) during the
131 reactor operation.

132 The simulation performed indicates how is the variation of different parameters
133 (dissolved oxygen, gas inflow ($L \text{ min}^{-1}$), mass transfer coefficient (s^{-1}) at different control
134 conditions (no control, control using a fixed mass transfer coefficient, control using a variable
135 mass transfer coefficient) and at different set-points of dissolved oxygen (180, 220, 250 %Sat);
136 all the simulations have been made at solar irradiance higher than 300 W m^{-2} .

137

138 **2.3 Control strategy**

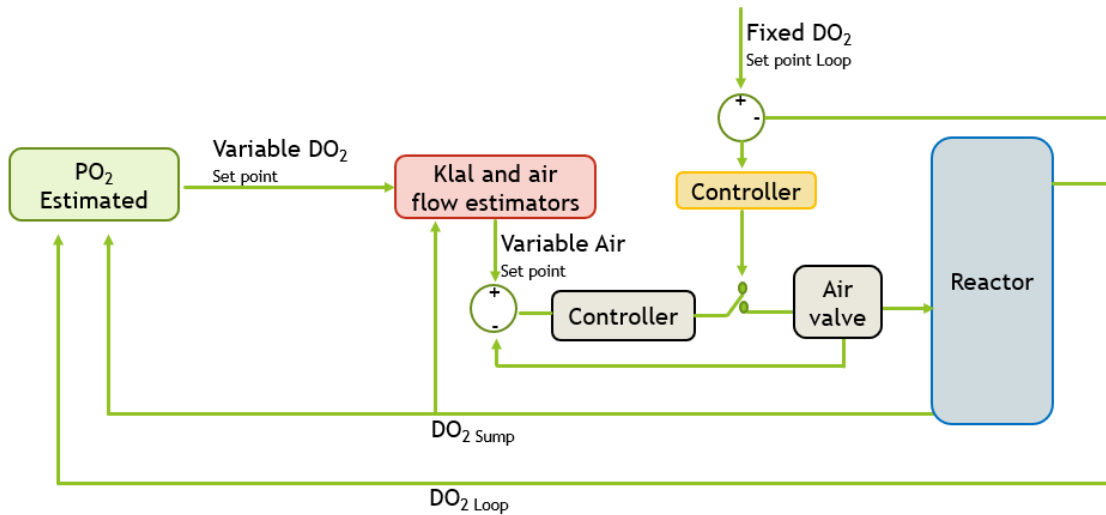
139 A feedback control strategy with a set-point generator was developed in this project to regulate
140 the air injection flow. This control approach allows to control the dissolved oxygen accumulation
141 into the reactor by improving the mass transfer coefficient (Kl). The control strategies that
142 have been developed until now, use a fixed air injection flow through the day. This project
143 demonstrates that it is possible to save air injections actions by using a feedback control
144 strategy, as well as, to reduce the dissolved oxygen accumulation into the reactor until values
145 lower than the optimal dissolved oxygen imposed (usually below 250% Sat.).

146 The control strategy proposed (*Figure 2*) includes two different possibilities. The first one is to
147 set a fixed set-point for the DO_2 (that usually works at 250% Sat) and the controller opens or
148 closes the air valve to regulate the DO_2 by using a fixed air injection flow. This first option is the
149 classical control approach to regulate the DO_2 . On the other hand, in the second option the DO_2
150 set-point is estimated by using an on-line oxygen production estimation (PO_2 estimated;
151 Equation 4) and is the contribution of this work. Now, the set-point value is calculated by using
152 the liquid flow (Q_{Liq}), the dissolved oxygen measurement at the loop (DO_{2Loop}) and at the sump
153 (DO_{2Sump}). The estimation should be equal to the dissolved oxygen desorption (NO_2 , Equation
154 5) to ensure lower values of dissolved oxygen than the Fixed DO_{2set} -point.

$$PO_2 \text{ estimated} = Q_{Liq} \times (DO_{2Loop} - DO_{2Sump}) \quad \text{Equation 4}$$

$$NO_2 = PO_2 \text{ estimated} \quad \text{Equation 5}$$

155



156

157

Figure 2. Feedback control strategy proposed to ensure optimal dissolved oxygen (DO₂) accumulation into the system.

158

159

Then, the next step was to calculate the estimated mass transfer coefficient (K_l estimated) which is calculated at every minute (Equation 6, Equation 7). Once the estimated K_l value is obtained, an air flow set-point (L/min) is calculated at every minute by using the empirical model developed in Barceló-Villalobos et al., (2018) (Equation 8 - Equation 10). So, this air gas is injected into the system by using the proportional valve. The air flow set-point is used as a reference for a cascade control applied to the proportional air valve (Åström, et al., 2006). This cascade control acts by regulating the voltage input of the air valve to ensure a precise and constant air flow output.

167

$$NO_2 = K_{l_{estimated}} \cdot (DO_{2_{Sump}} - O_2^*) \times V \quad \text{Equation 6}$$

$$K_{l_{estimated}} = \frac{(PO_{2_{estimated}} - PO_{2_{set-point}})}{(DO_{2_{Sump}} - O_2^*) \times V} \quad \text{Equation 7}$$

$$U_{gr} = \frac{\text{Gas injection}}{\text{Sump area}} \quad \text{Equation 8}$$

$$\text{Log } U_{gr} = \frac{(\text{log } K_{l_{estimated}} \times 3600) - (\text{log } 10379)}{0.9123} \quad \text{Equation 9}$$

$$\text{Gas injection} = e^{(\text{Log } U_{gr} \times \text{Sump area} \times 3600)} \quad \text{Equation 10}$$

168

169

The feedback control strategy proposed has been validated, in simulation by using the Fernández et al., (2016) model.

171

172

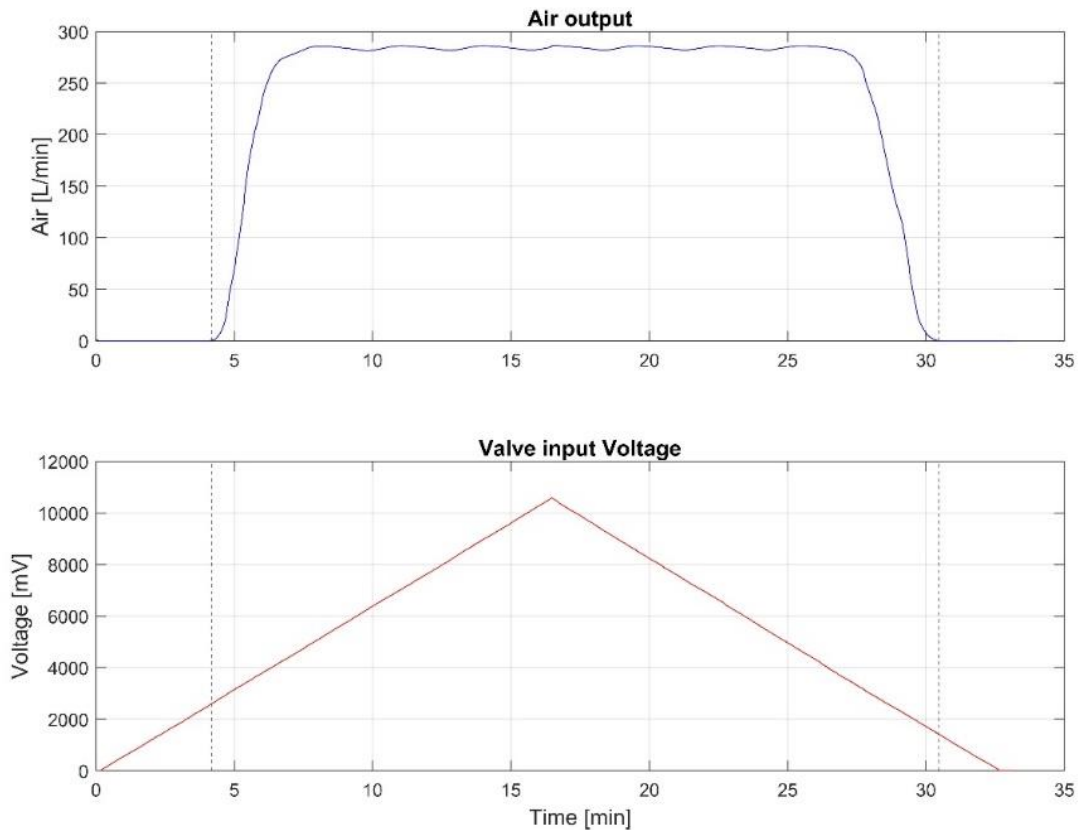
173

174 **3. RESULTS AND DISCUSSION**

175

176 **3.1 Proportional air valve characterization**

177 To perform adequate air control over a desired set-point, it is necessary to develop a control
178 loop for the valve such as shown in Figure 2. This control will allow a precise air injection
179 depending on the needs of the system. The input range varies between 0 and 10000 (mV), while
180 the flow rate ranges between 0 and 280 (L/min) approximately. The valve is not proportional in
181 the entire input range, in addition to presenting dead zone and a diverse behavior with respect
182 to the increase or decrease of flow. Therefore, two types of open loop test have been carried
183 out to characterize the valve, by means of ramp input and step input.



184

185

Figure 3. Air valve characterization test with ramp input (mV)

186 On the one hand, Figure 3 shows a ramp input test, for up and down flows, to determine the
187 voltage input that corresponds to the dead zone and the maximum flow, both for an increasing
188 and decreasing flow. In this case, a dead zone of 2700 mV in rise and 1600 mV in descent has
189 been determined. The maximum flow is reached with an input of 4700 mV.

190

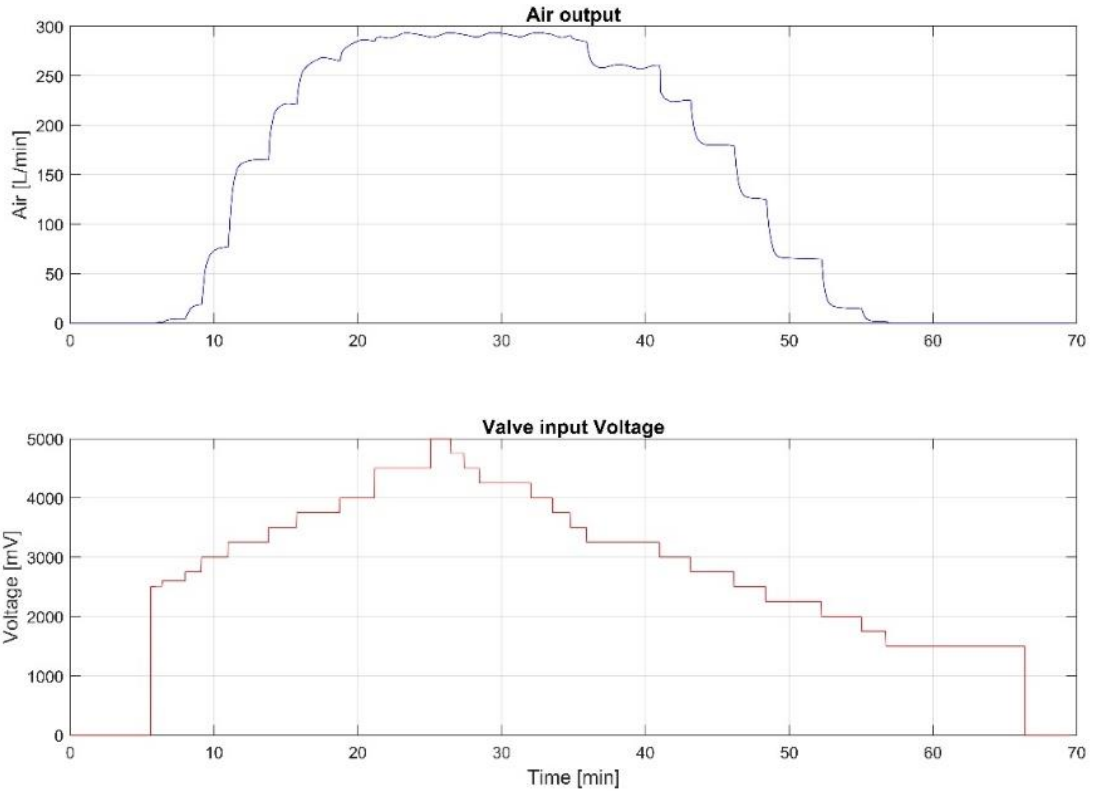


Figure 4. Air valve open loop step test (mV)

191

192

193

194 On the other hand, different dynamics from step inputs have been observed, such as shown in
 195 Figure 4. It is observed that the dynamics is not linear, with a greater amplitude at intermediate
 196 areas of flow, around 120 (L/min). An operating point between 50 and 250 of flow has been
 197 considered.

198 The proportional air valve is a non-linear system and presents a variable dynamic, as can be seen
 199 on the open loop test performed with step inputs shown in Figure 4. Due to the valve dynamic,
 200 it is necessary to model the system in different areas or points of operation. Therefore, the
 201 characteristics parameters of the transfer functions referring to three zones have been
 202 obtained, separating the increase in flow from the decrease in flow. Thus, the modeling areas
 203 selected based on the flow have been those that range from 0 to 80 for the first, 80 to 200 for
 204 the second and from 200 to 280 (L/min) for the third. The static gains (k_i) and time constants
 205 (τ_i) obtained are the following:

Flow zone $\left(\frac{L}{min}\right)$	Increase in flow		Decrease in flow	
	Static gain $\left(\frac{L}{mV min}\right)$	Time constant (s)	Static gain $\left(\frac{L}{mV min}\right)$	Time constant (s)
0 - 80	0.24	17.52	0.20	14.53
80 - 200	0.35	16.96	0.23	16.85
200 - 280	0.18	20.81	0.18	14.82

206
 207 The models obtained at different operating points and the great nonlinearity of the system
 208 allows to implement gain scheduling control as the main control strategy. Gain scheduling is a
 209 method for the control of nonlinear system. It is formed by a set of linear controllers derived for
 210 a corresponding set of plants linearized. Each controller provides satisfactory control for a
 211 different operating point of the system. The controller used is PI control algorithm.

212
 213 The Proportional-Integral-Derivative (PID) controllers are the most commonly used controller in
 214 industrial applications, due to its simplicity, stability and rapid response. This type of controller
 215 is closed loop system, which takes into consideration the process variable as a feedback and
 216 compare it with a established set-point. The error resulting from the comparison is treated by the
 217 proportional, integral and derivative actions which PID is composed, generating an input signal
 218 to the system. Other control configurations arise from the combination of actions, such as the
 219 Proportional-Integral (PI) or the Proportional-Derivative (PD) (Åström, et al., 2006).

220
 221 The simplicity of the models (first order) and the lack of delay, simplify the controller design.
 222 That is why the zero pole cancellation method has been selected (Åström, et al., 2006) to obtain
 223 PI controllers in each section. The time constant in the closed loop is 0.9 times the open loop.

224

	<i>Increase controllers</i>			<i>Decrease controllers</i>	
	Kp	Ti		Kp	Ti
1	4.62	17.52	4	5.55	14.53
2	3.17	16.96	5	4.83	16.85
3	6.17	20.81	6	6.17	14.82

225
 226 Once all the controllers are obtained, they are implemented in the photobioreactor. Figure 5
 227 shows a closed loop test of reference tracking in different setpoint. It can be observed that it
 228 behaves as desired. In this way, the control of cascade internal loop ensures that it will follow
 229 the air reference settled on the external loop.

230

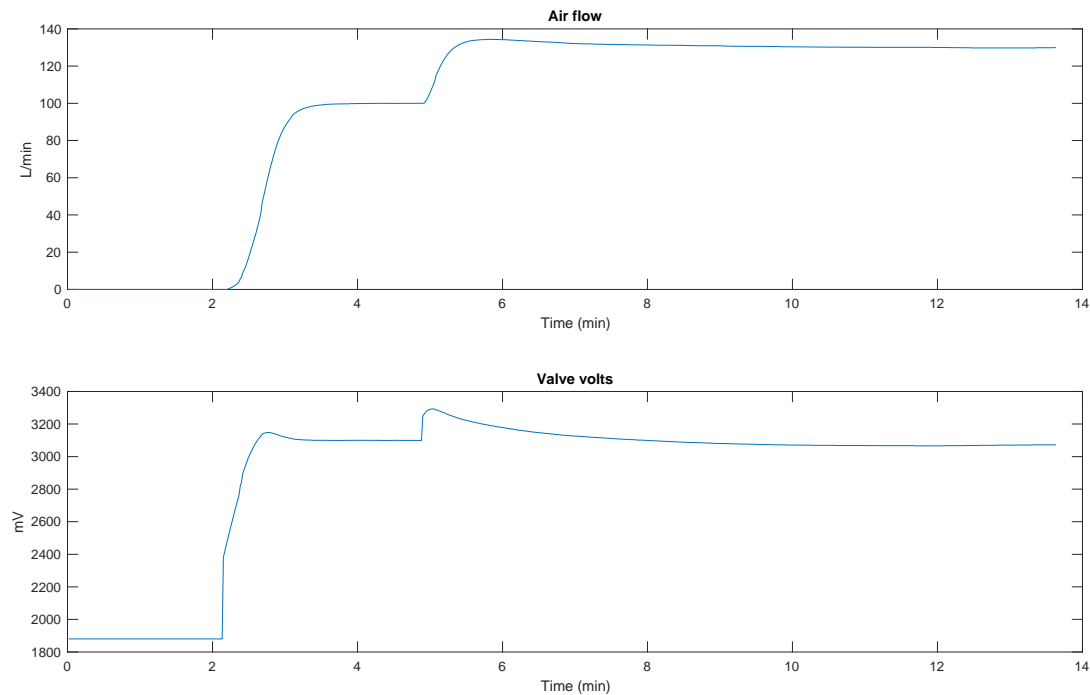


Figure 5. Valve closed loop test on the real system

231
232

233

234 3.2 Simulation approach

235 In this article, it is shown that it is possible to reduce the number of gas inflow
 236 actuations, as well as, to maintain the dissolved oxygen concentration below the defined set
 237 point by using a feedforward control strategy. Furthermore, results shown that for the same
 238 oxygen dissolved set-point, less gas flow injections are required in case of using feedforward
 239 control strategy. Moreover, results also shown that when the dissolved oxygen reference goes
 240 down respect to the initial reference (250% Sat), the necessary gas flow is higher, and although
 241 this fact can increase the overall operation cost, it can also maximize the biomass production by
 242 avoiding the existence of photorespiration processes.

243 Different results have been obtained from the simulation approach:

244 (1) The optimization of mass transfer coefficient ($K_l a$, s^{-1}) allows to properly control
 245 dissolved oxygen accumulation until the set-point imposed (250% Sat.) (Figure 6).

246 (2) It is demonstrated that the mass transfer coefficient ($K_l a$, s^{-1}) can be controlled as a
 247 fixed or a variable parameter. The present work shows that it should be controlled in a variable
 248 manner to optimize the air gas injections into the system (Figure 7).

249 (3) Furthermore, regarding air gas injections (L/min), it is possible to control it by a fixed
 250 and/or a variable manner (Figure 8).

251 (4) It is also demonstrated that it is possible to adjust the dissolved oxygen set-point to
 252 different values, depends on the requirements of the strain used in the reactor. As much higher

253 is the value of dissolved oxygen set-point the lower mass transfer coefficient ($klal$) is required;
254 thus, lower amount of gas injections is required (Figure 9).

255 (5) Different mass transfer coefficients ($Klal, s^{-1}$) should be used, depends on the
256 dissolved oxygen set-point (Figure 10). As lower is the dissolved oxygen set-point, the higher
257 amount of dissolved oxygen should be desorp to the atmosphere, which means that a higher
258 value of mass transfer coefficient ($klal$) should be imposed.

259 (6) A variable control of mass transfer coefficient allows to control and save gas
260 injections and use it efficiently. As lower is the dissolved oxygen set-point imposed, as higher is
261 the amount of gas injections (L/min) that should be inject; which means, increasing of the
262 production costs of the system (Figure 11).

263

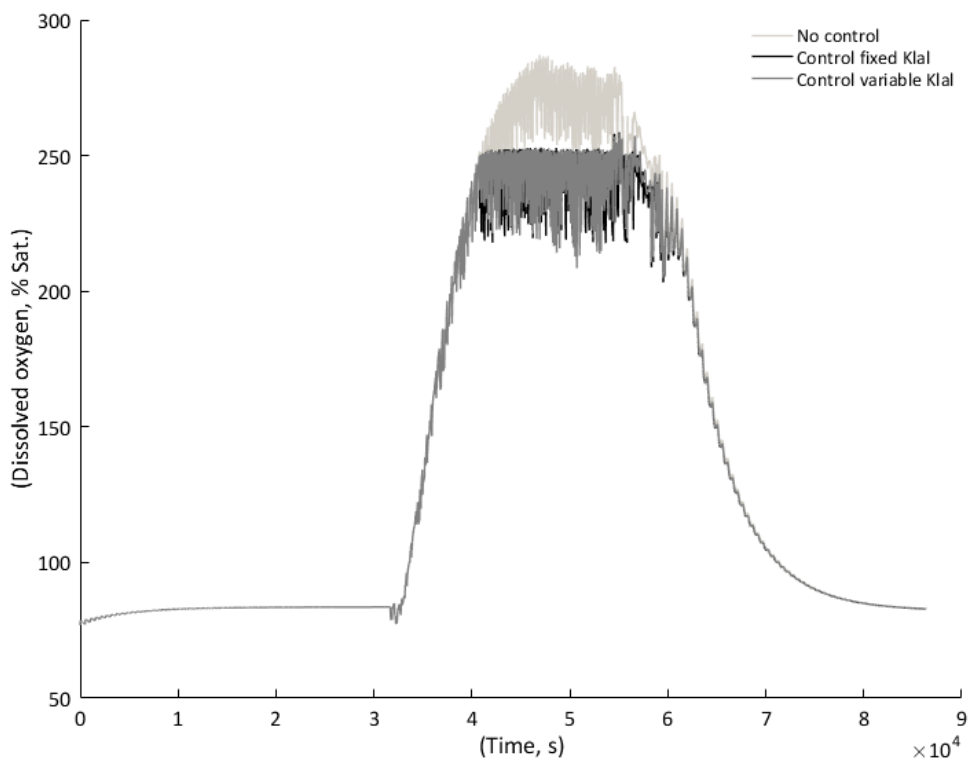


Figure 6. Simulation of dissolved oxygen accumulation into the culture at different control conditions

264

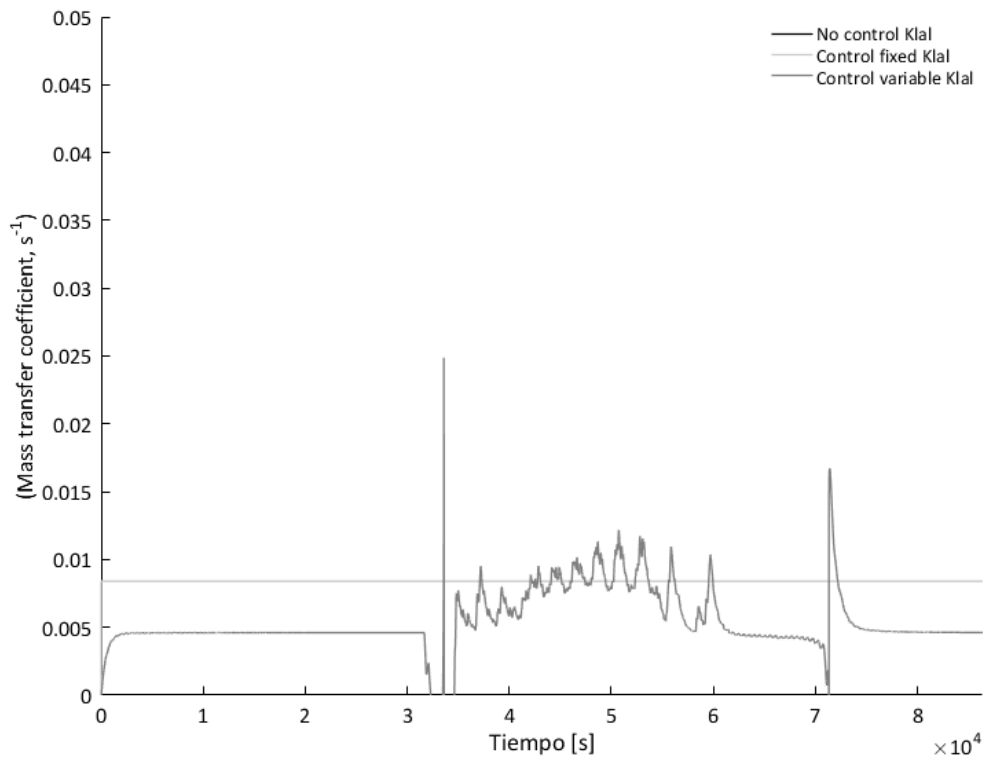


Figure 7. Simulation of mass transfer coefficient (s^{-1}) performance along the day at different control conditions

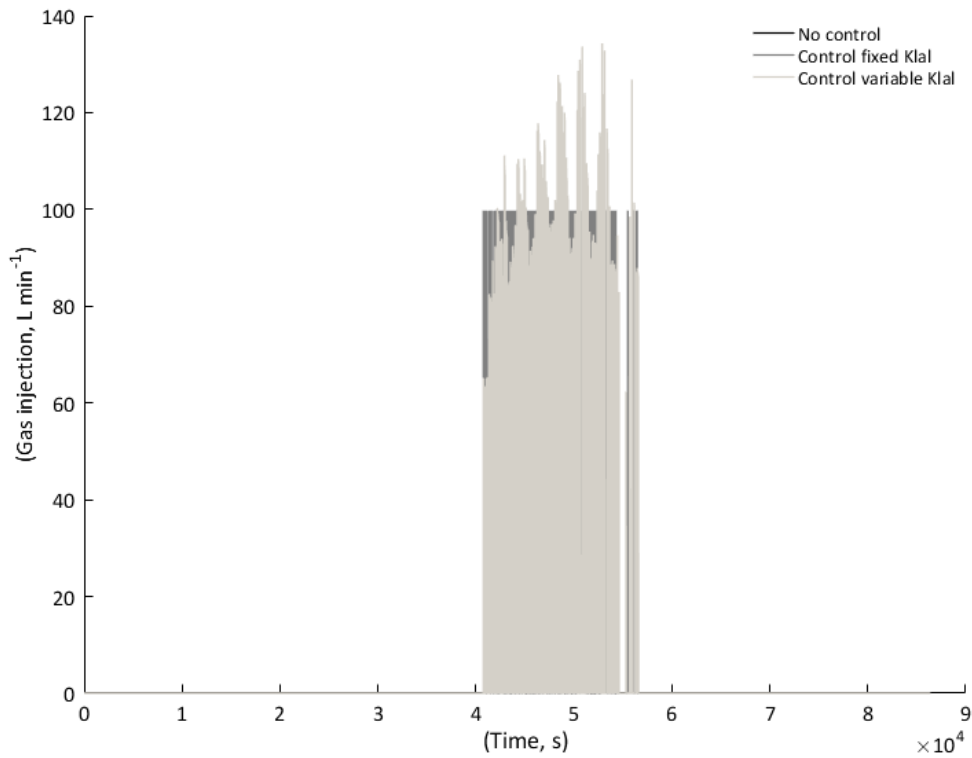


Figure 8. Simulation of air gas injection (L/min) into the culture at different control conditions

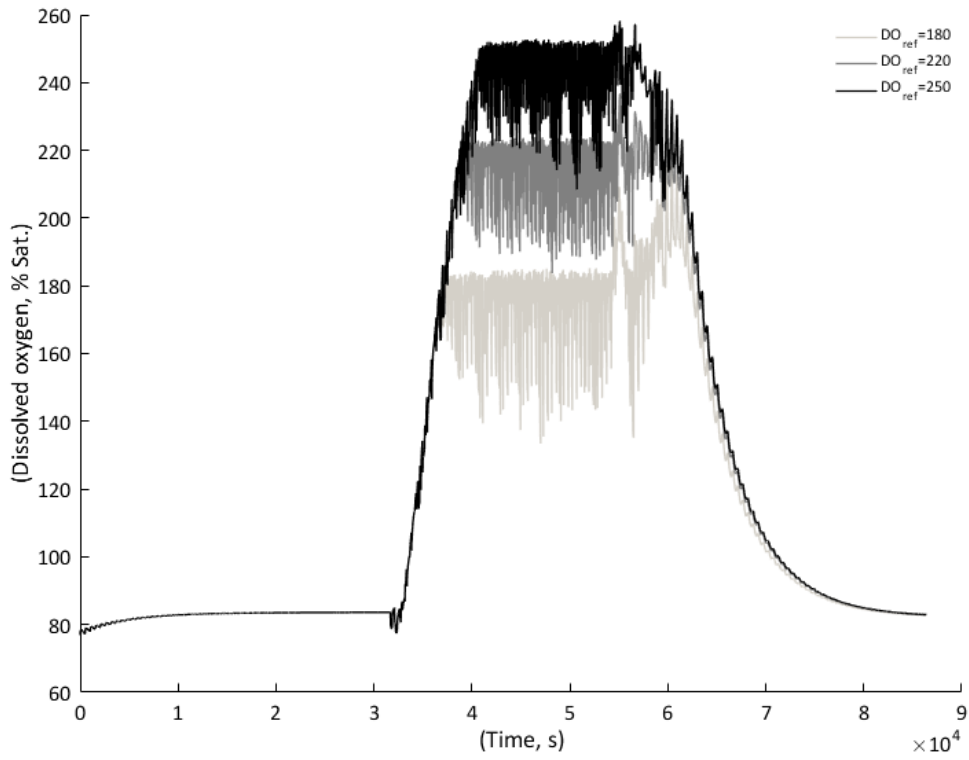


Figure 9. Simulation of dissolved oxygen accumulation control (% Sat.) into the culture, at different set-points

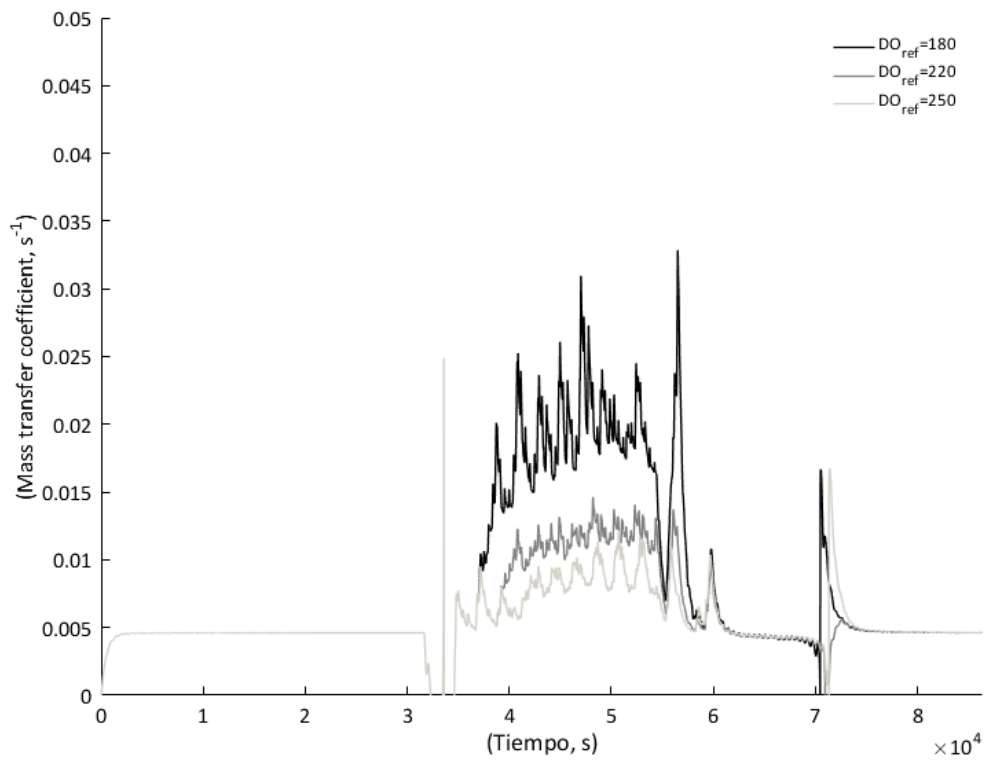


Figure 10. Simulation of mass transfer coefficient (s-1) performance at different dissolved oxygen set-points

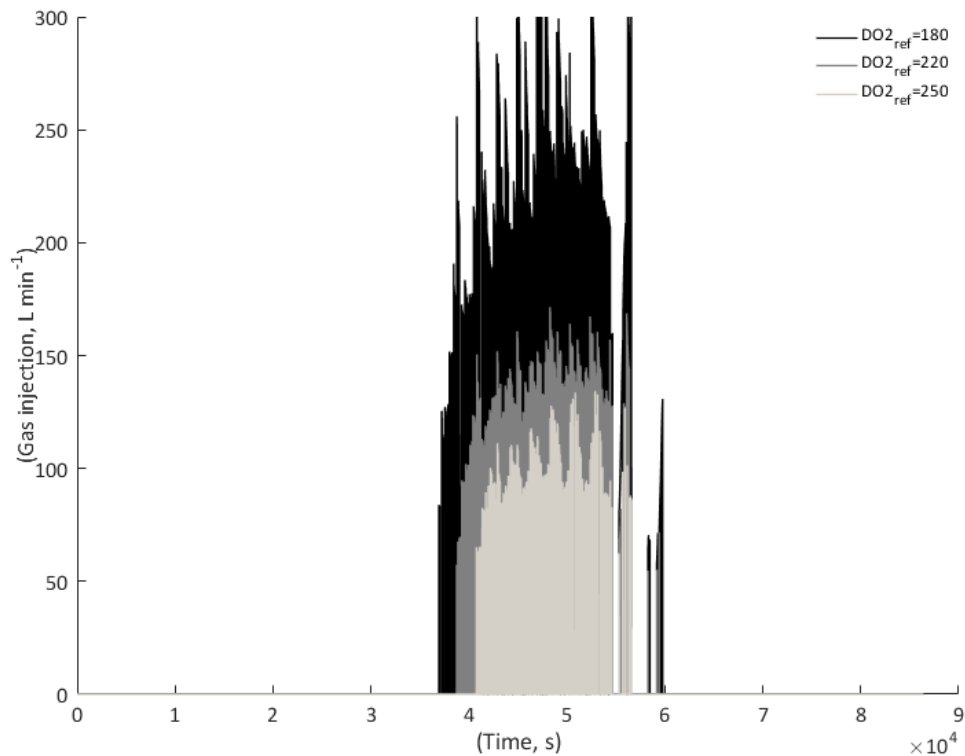


Figure 11. Simulation of air gas injection (L/min) into the culture at different dissolved oxygen set-points

270

271 4. CONCLUSIONS

272 A feedback control strategy was used as a solution to the dissolved accumulation drawback that
 273 the microalgae reactors already have. The results confirm that it is possible to reduce the
 274 number of gas inflow actuations, as well as, to maintain the dissolved oxygen concentration
 275 below the defined set point by using the feedforward control strategy proposed. Furthermore,
 276 results shown that for the same oxygen dissolved set-point, less gas flow injections are required
 277 in case of using feedforward control strategy. The air gas was injected into the system by using
 278 the proportional valve, in order to adequately minimize and control the air injections. Results
 279 shown that this proportional valve is a non-linear system and presents a variable dynamic.
 280 Moreover, it has a dead zone which should be taken into consideration regarding to dynamic
 281 modelling of real systems.

282

283 Acknowledgements

284 This study was supported financially by the Ministry of Economy and Competitiveness (DPI2014-
 285 55932-C2-1-R, DPI2017-84259-C2-1-R) and (EDARSOL, CTQ2014-57293-C3-1-R), and the

286 European Union's Horizon 2020 Research and Innovation Program under Grant Agreement No.
287 727874 SABANA. We are most grateful for the practical assistance given by the staff of the IFAPA
288 Experimental Station (Almería, Spain).

289

290 REFERENCES

291 Acién, F.G., Molina, E., Reis, A., Torzillo, G., Zittelli, G.C., Sepúlveda, C., Masojídek, J., 2017.
292 Photobioreactors for the production of microalgae, *Microalgae-Based Biofuels and*
293 *Bioproducts: From Feedstock Cultivation to End-Products*. [https://doi.org/10.1016/B978-](https://doi.org/10.1016/B978-0-08-101023-5.00001-7)
294 [0-08-101023-5.00001-7](https://doi.org/10.1016/B978-0-08-101023-5.00001-7)

295 Åström, K.J.; Hägglund, T., 2006. *Advanced PID Control*, ISA. ed.

296 Barceló-Villalobos, M., Guzmán Sánchez, J.L., Martín Cara, I., Sánchez Molina, J.A., Acién
297 Fernández, F.G., 2018. Analysis of mass transfer capacity in raceway reactors. *Algal Res.*
298 *35*, 91–97. <https://doi.org/10.1016/j.algal.2018.08.017>

299 Berenguel, M., Rodríguez, F., Acién, F.G., García, J.L., 2004. Model predictive control of pH in
300 tubular photobioreactors. *J. Process Control* *14*, 377–387.
301 <https://doi.org/10.1016/j.jprocont.2003.07.001>

302 Beschi, M., Pawlowski, A., Guzmán, J.L., Berenguel, M., and Visioli, A., 2014. Symmetric send-on-
303 delta PI control of a greenhouse system., in: *Proceedings of the 19th IFAC World Congress*.
304 Cape Town, South Africa.

305 de Godos, I., Mendoza, J.L., Acién, F.G., Molina, E., Banks, C.J., Heaven, S., Rogalla, F., 2014.
306 Evaluation of carbon dioxide mass transfer in raceway reactors for microalgae culture using
307 flue gases. *Bioresour. Technol.* *153*, 307–314.
308 <https://doi.org/10.1016/j.biortech.2013.11.087>

309 Fernández, I., Acién, F.G., Guzmán, J.L., Berenguel, M., Mendoza, J.L., 2016. Dynamic model of
310 an industrial raceway reactor for microalgae production. *Algal Res.* *17*, 67–78.
311 <https://doi.org/10.1016/j.algal.2016.04.021>

312 García Sánchez, J.L., Berenguel, M., Rodríguez, F., Fernández Sevilla, J.M., Brindley Alias, C.,
313 Acién Fernández, F.G., 2003. Minimization of Carbon Losses in Pilot-Scale Outdoor
314 Photobioreactors by Model-Based Predictive Control. *Biotechnol. Bioeng.* *84*, 533–543.
315 <https://doi.org/10.1002/bit.10819>

316 Mendoza, J.L., Granados, M.R., de Godos, I., Acién, F.G., Molina, E., Banks, C., Heaven, S., 2013.
317 Fluid-dynamic characterization of real-scale raceway reactors for microalgae production.
318 *Biomass and Bioenergy* *54*, 267–275. <https://doi.org/10.1016/j.biombioe.2013.03.017>

319 Pawlowski, A., Fernández, I., Guzmán, J.L., Berenguel, M., Acién, F.G., Dormido, S., 2016. Event-
320 based selective control strategy for raceway reactor: A simulation study. *IFAC-*
321 *PapersOnLine* *49*, 478–483. <https://doi.org/10.1016/j.ifacol.2016.07.388>

322 Pawlowski, A., Mendoza, J.L., Guzmán, J.L., Berenguel, M., Acién, F.G., Dormido, S., 2015.
323 Selective pH and dissolved oxygen control strategy for a raceway reactor within an event-
324 based approach. *Control Eng. Pract.* *44*, 209–218.
325 <https://doi.org/10.1016/j.conengprac.2015.08.004>

326 Rotatore, C., Colman, B., Kuzma, M., 1995. the Active Uptake of Carbon-Dioxide By the Marine
327 Diatoms *Phaeodactylum-Tricornutum* and *Cyclotella* Sp. *Plant Cell Environ.* *18*, 913–918.

328 <https://doi.org/10.1111/j.1365-3040.1995.tb00600.x>

329

330

331